APL-TDR 64-77

# KINETICS AND DIFFUSION STUDY OF THE PARA-ORTHO SHIFT OF HYDROGEN

TECHNICAL DOCUMENTARY REPORT NO. APL-TDR-64-77

September 1964



AF Aero Propulsion Laboratory
Research and Technology Division
Air Force Systems Command
Wright-Patterson Air Force Base, Ohio

Project No. 1(10-3048) Task No. 30193

(Prepared under Contract No. AF 33(616)7654 by the University of Colorado, Department of Chemical Engineering, Boulder, Colorado. P. L. Barrick (Principal Investigator), L. F. Brown, and H. L. Hutchinson, authors)

CLEARINGHOUSE FOR FEDERAL SCIENTIFIC AND TECHNICAL INFORMATION CFSTI
DOCUMENT MANAGEMENT BRANCH 410.11

LIMITATIONS IN REPRODUCTION QUALITY

ACCESSION # AD606495

☑ 1. WE REGRET THAT LEGIBILITY OF THIS DOCUMENT IS IN PART UNSATISFACTORY. REPRODUCTION HAS BEEN MADE FROM BEST AVAILABLE COPY.

☐ 2. A PORTION OF THE ORIGINAL DOCUMENT CONTAINS FINE DETAIL WHICH MAY MAKE READING OF PHOTOCOPY DIFFICULT.

☐ 3. THE ORIGINAL DOCUMENT CONTAINS COLOR, BUT DISTRIBUTION COPIES ARE AVAILABLE IN BLACK-AND-WHITE REPRODUCTION ONLY.

☐ 4. THE INITIAL DISTRIBUTION COPIES CONTAIN COLOR WHICH WILL BE SHOWN IN BLACK-AND-WHITE WHEN IT IS NECESSARY TO REPRINT.

☐ 5. LIMITED SUPPLY ON HAND: WHEN EXHAUSTED, DOCUMENT WILL BE AVAILABLE IN MICROFICHE ONLY.

☐ 6. LIMITED SUPPLY ON HAND: WHEN EXHAUSTED DOCUMENT WILL NOT BE AVAILABLE.

☐ 7. DOCUMENT IS AVAILABLE IN MICROFICHE ONLY.

☐ 8. DOCUMENT AVAILABLE ON LOAN FROM CFSTI ( TT DOCUMENTS ONLY).

☐ 9.

PROCESSOR: ral

TSL-107-10/64

# KINETICS AND DIFFUSION STUDY OF THE PARA-ORTHO SHIFT OF HYDROGEN

TECHNICAL DOCUMENTARY REPORT NO. APL-TDR-64-77

September 1964

AF Aero Propulsion Laboratory
Research and Technology Division
Air Force Systems Command
Wright-Patterson Air Force Base, Ohio

Project No. 1(10-3048) Task No. 30193

(Prepared under Contract No. AF 33(616)7654 by the University of Colorado, Department of Chemical Engineering, Boulder, Colorado. P. L. Barrick (Principal Investigator), L. F. Brown, and H. L. Hutchinson, authors)

## NOTICES

When Government drawings, specifications, or other data are used for any purpose other than in connection with a definitely related Government procurement operation, the United States Government thereby incurs no responsibility nor any obligation whatsoever; and the fact that the Government may have formulated, furnished, or in any way supplied the said drawings, specifications, or other data, is not to be regarded by implication or otherwise as in any manner licensing the holder or any other person or corporation, or conveying any rights or permission to manufacture, use, or sell any patented invention that may in any way be related thereto.

Qualified requesters may obtain copies of this report from the Defense Documentation Center (DDC), (formerly ASTIA), Cameron Station, Bldg. 5, 5010 Duke Street, Alexandria, Virginia, 22314.

This report has been released to the Office of Technical Services, U.S. Department of Commerce, Washington 25, D. C., for sale to the general public.

Copies of this report should not be returned to the Research and Technology Division, Wright-Patterson Air Force Base, Ohio, unless return is required by security considerations, contractual obligations, or notice on a specific document.

C

## FOREWORD

This report was prepared by the Department of Chemical Engineering, University of Colorado, Boulder, Colorado, on Air Force Contract No. AF 33(616)-7654 under Task No. 30193 of Project No. 1 (10-3048). The contract efforts were accomplished under cognizance of the AF Aero-Propulsion Laboratory, Research and Technology Division, Wright-Patterson Air Force Base, Ohio. The technical work was directed by Messrs. J. Lawler, P. R. Pitts and H. R. Lander.

This final report covers work conducted from November 1960 through December 1963.

The work discussed in this report was supervised by Dr. P. L. Barrick, Professor, Department of Chemical Engineering. The assistance of Mr. D. D. Geddes, Mr. J. L. Von Wald, Mr. R. L. Cruse, Mr. F. T. Finch, and Dr. D. Gini, who performed some of the experimental work, is gratefully acknowledged. The authors express their appreciation to Mr. D. L. Page, who gave help in design and construction of the equipment, and also helped with the experimental operations. Special thanks are due to Mr. D. H. Weitzel of the National Bureau of Standards, for consultation during the course of the investigation, and to Mr. J. R. Purcell, of Apogee Development Corp., for his assistance in the solution of instrumental problems.

## ABSTRACT

A broad investigation has been carried out into factors affecting the rate of the para-orthohydrogen shift reaction, when promoted by the ferric oxide gel catalyst. The investigation included studies of:

(a) the kinetics of the reaction

It was concluded that when diffusion effects are absent, the rate of the reaction may be expressed by:

$$r = \frac{k(c_p - c_{pe})}{1 + k' c_p}$$

where r is the rate of conversion, $c_p$ is the concentration of parahydrogen, $c_{pe}$ is the equilibrium concentration, and k and k' are constants.

(b) the effects of diffusion within the catalyst particle

These effects are small, apparently because of high internal diffusion rates. The most probable mechanism of transport within the catalyst particle is surface migration.

(c) the relation between catalyst surface area and activity

Higher surface area catalysts appear generally more active, but no direct correlation exists between catalyst activity and surface area.

(d) the effects of diffusion external to the catalyst particles

It is shown both theoretically and experimentally that interparticle diffusion has no discernible effect on the reaction rate within normal operating conditions.

(e) technique of preparation and activation of the catalyst

Improved activation procedures are shown to produce a catalyst with more than double the highest activity previously reported for ferric oxide gel catalysts.


This technical documentary report has been reviewed and is approved.

Marc P. Dunnam

MARC P. DUNNAM
Chief, Technical Support Division
AF Aero Propulsion Laboratory

TABLE OF CONTENTS

SECTION PAGE

LIST OF FIGURES

LIST OF TABLES

# SECTION I

## GENERAL INTRODUCTION

This report presents the results of a broad investigation into the various factors affecting the rate of the catalyzed para-orthohydrogen shift reaction. This report is divided into five sections. Each section after the introduction treats a different phase of the investigation, and with bibliography, nomenclature and appendixes is complete in itself. Any preceding sections need not be read for an understanding of an individual section.

The study of the para-orthohydrogen shift is of value in the use of liquid hydrogen. The conversion of parahydrogen to orthohydrogen is endothermic, and as a result can be used as a heat sink in any type of space craft that uses liquid hydrogen as fuel. A possible application for this ability to absorb heat is the use of liquid hydrogen as a coolant in a condenser for liquid oxygen on board a space craft.

The study of the para-ortho shift of hydrogen is of value from another aspect. When manufacturing liquid hydrogen, it is economically essential to convert the hydrogen obtained at normal temperatures to almost pure parahydrogen during the liquefaction process. The more efficiently this can be done, the cheaper it will be to produce liquid hydrogen. The only practical method of accomplishing this at the present time is by converting the orthohydrogen to parahydrogen catalytically. The capability of the catalyst for the conversion of ortho to parahydrogen plus the knowledge required for efficient design of reactors are thus necessary factors in the production of cheap liquid hydrogen. Studies of the mechanism of the catalytic reaction can lead to more powerful catalysts and better design data, as is shown by the investigation carried out at the University of Colorado and the results of which are presented in this report.

In analytical treatments of gas-phase chemical reactions that take place on the interior surfaces of porous catalysts, it is customary to divide the complete process into seven steps. These steps, which are mentioned in numerous references (e.g., 1), are:

1. The diffusion of the reactant from the bulk gas phase to the exterior surface of the porous catalyst.

2. The diffusion of the reactant within the catalyst pores from the exterior surface of the catalyst to the site where the reaction takes place.

3. The adsorption of the reactant on the solid surface of the catalyst.

4. The chemical change of the reactant into the product on the solid surface of the catalyst.

5. The desorption of the product from the solid surface of the catalyst into the gas phase in the interior of the catalyst pellet.

6. The diffusion of the product within the catalyst pellet from the reaction site to the exterior surface of the pellet.

7. The diffusion of the product from the exterior surface of the catalyst pellet into the bulk phase of the gas passing through the chemical reactor.

All of these steps were studied in various phases of this investigation. A brief description of these different phases of the investigation and how the individual steps are treated is presented in the following paragraphs.

Section II--The Kinetics of the Para to Orthohydrogen Reaction

In Section II of this report are presented the results of the study of the overall surface kinetics. The overall kinetics of the surface reaction depend on the third, fourth, and fifth steps--the adsorption of the reactants on the catalyst surface, the actual conversion of the reactant to the product on the surface, and the desorption of the product from the surface.

This section reports how the conversion of parahydrogen to orthohydrogen was studied over a temperature range of 40°K. to 80°K., and over a pressure range of 42 psia to 1012 psia. It is shown that attempts to correlate the data over the entire range of conditions that were studied by assuming first-order, three-halves order, second order, or third order reversible reactions are unsuccessful. However, an excellent fit to the data is obtained from the rate expression:

$$r = \frac{k(c_p - c_{pe})}{1 + k'c_p}$$

in which

$r$ = rate of consumption of parahydrogen

$c_p$ = gas-phase concentration of parahydrogen

$c_{pe}$ = equilibrium gas-phase concentration of parahydrogen at reaction temperature

$k$ and $k'$ = reaction rate constants

The derivation of this expression is presented, based on the third, fourth, and fifth steps of a catalyzed reaction. From the dependence of the reaction rate constants on concentration, temperature, and pressure, it is shown that the rate-controlling step is the reaction on the catalyst surface.

Section III-Effects of Diffusion Rates and Catalyst Surface Area on Catalyst Activity

The effects of diffusion rates within the catalyst particle--steps two and six listed above--and the effects of catalyst surface area on the activity of the catalyst are studied in Section III of this report. This section shows that intra-particle diffusion apparently has only a small inhibiting effect on the rate of reaction when the ferric oxide gel catalyst is used. It is also concluded that surface migration is the principal mode of the transport of reactant and product, rather than diffusion in the gas phase within the catalyst particle.

This section shows that the higher surface area catalysts generally have higher activities. Since the surface area measured by common nitrogen adsorption techniques is not an accurate indication of the total surface area of substances with many fine pores, such as the ferric oxide gel catalyst, it should not be expected that the activity would be directly proportional to the surface area measured in this fashion.

Section IV--Effects of Interparticle Diffusion on the Kinetics of the Ortho-Para Hydrogen Shift over the Ferric Oxide Gel Catalyst

The fourth section of this report concerns the importance of interparticle mass transfer--the first and seventh steps listed above--in the para-ortho hydrogen reaction. The available correlations for mass transfer through the boundary layer surrounding granules in a fixed bed predict that diffusion through this boundary layer should have a negligible effect on the reaction rate under normal reaction conditions. Correlations for longitudinal diffusion also predict that this second type of diffusion should have

a negligible effect on the reaction rate. In support of these correlations, this section shows that there is no evidence of any type of interparticle diffusion affecting the reaction rate within the range studied. It is also shown in this section that the expression for the rate of the reaction developed in Section II for the conversion of parahydrogen to orthohydrogen is equally valid for the conversion of orthohydrogen to parahydrogen.

Section V--The Activity of the Ferric Oxide Gel Catalyst--Its Dependence on Preparation, Composition, and Method of Activation

All of the above studies were carried out using the hydrous ferric oxide catalyst developed by Weitzel and Loebenstein (2). The fifth section of this report shows how the activity of this catalyst is dependent upon the method of preparation, the composition of the solutions which are used in the preparation, and the techniques of activation. Previous papers concerning this catalyst in the literature report difficulty in reproducing catalysts of high activity. This section shows how catalysts of consistently high activity may be obtained by proper methods of preparation. Some different compositions and techniques of preparation are also explored, which point the direction in which further improvements may be expected.

This section also reports a study of different activation procedures, which indicate that there are three critical factors in the activation of the catalyst--the temperature of activation, the time of activation, and the rate of temperature rise during the activation. By new methods of activation developed from this study, a catalyst with an activity more than double that previously reported may be obtained.

## REFERENCES

1. Hougen, O. A., and K. M. Watson, "Chemical Processes Principles," Vol. III, "Kinetics and Catalysis," Wiley, 1947, p. 906.

2. Weitzel, D. H., and W. V. Loebenstein, U. S. Patent 2,943,917, July 5, 1960.

## SECTION II

## KINETICS OF THE PARA- TO ORTHOHYDROGEN REACTION

### II. 1 Introduction

This section of the final report covers the kinetics study of the reaction

$$\text{parahydrogen} \rightleftarrows \text{orthohydrogen} \qquad \text{(A)}$$

that was made in partial fulfillment of Contract AF 33(616)-7654.

Since the discovery of the two forms of molecular hydrogen, called ortho- and parahydrogen, there has been much interest in the rate of conversion of the two forms, especially in the realm of the catalyzed reaction. Much has been published on the reaction and a wide variety of catalysts has been used (e.g. 3,4,5,6,10,12,16,24,25,26,27,28,30).

Most of the investigations have been carried out over a limited range of temperatures and pressures, e.g. 60-76°K, 20-350 psia (10,16,25,26,27,28). Usually the reaction

$$\text{orthohydrogen} \rightleftarrows \text{parahydrogen} \qquad \text{(B)}$$

has been found to follow first order kinetics reasonably well (4,5,6,16,25, 26,27,28).

The purpose of this investigation was to obtain kinetic data for the catalyzed para-orthohydrogen shift reaction over a wide range of pressures and temperatures and to obtain a correlation for the data. The data were obtained in a flow reactor, which was constructed to provide temperature and pressure control over the desired ranges. Pressures of 30, 200, 400, 600, 800, and 1000 psig with temperatures of 40, 50, 60, 70, and 80°K at each pressure were the operating conditions maintained in the reactor to obtain the data. The catalyst was a hydrous ferric oxide gel with an activity of about 1600 $min^{-1}$.

There seems to have been some inconsistency in earlier reporting of the data. For example most investigators have assumed that reaction (B) is first order (4,5,6,8,9,12,21,22,24,25). Others have tried to show that the reaction (A) is also first order (16,26). But there has been some doubt about this last assumption (2,26). The data of Weitzel et. al., do not support the fact that (A) is first order (26). If (A) is first order, then (B) should be also, because the principle of microscopic reversibility states that for a reversible

reaction which proceeds by a series of steps, the steps should be the same in either direction (although occurring in reverse sequence for the reverse reaction) and further, if one of the steps is slower than the others, it should be the slow step regardless of the direction of the reaction. Thus, the kinetic expression should be of the same form for both the forward and reverse reactions. It was hoped that the study described by this section of the report would clear up these difficulties, while at the same time providing design data for catalytic reactors which use the para-orthohydrogen shift reaction.

The para-orthohydrogen shift reaction is important because it is potentially a source of low temperature refrigeration. Reaction (A) is an endothermic reaction and thus needs heat to sustain it. By taking this heat from its surroundings, the reaction can cool the surroundings. The range of temperatures at which the reaction operates are becoming increasingly useful to industrial and military applications.

## II. 2 Experimental Apparatus

In order to obtain the data, a reactor was needed whose temperature could be controlled accurately and which would remain as isothermal as possible. Also needed were a source of parahydrogen feed and a system to analyze the gas for parahydrogen content. Since a flow reactor was to be used, it was required that the system have components to control and measure the flow as accurately as possible. Also the pressure had to be regulated, both in the chamber and in the analyzing section. The analyzer that was used was a thermal conductivity analyzer of the type described by Purcell and Keeler (20). To prevent errors in detection, the hydrogen stream was purified before it entered the flow system.

A schematic view of the apparatus is shown in Fig. II-1. Room temperature (normal) hydrogen was fed to a purifying coil containing silica gel at 76°K, where any moisture and other impurities were removed. The stream was then split; one side went through a "normalizing" unit, which converted the stream to room-temperature i.e. 75% orthohydrogen composition, and then to the ortho-parahydrogen analyzer to be used as reference gas. The other side was the sample and first passed into a catalyst chamber which was immersed in liquid hydrogen. This provided a source of para hydrogen feed. The chamber was large enough to provide parahydrogen at high flow rates-up to 14 liters/min. (measured at room temperature.)

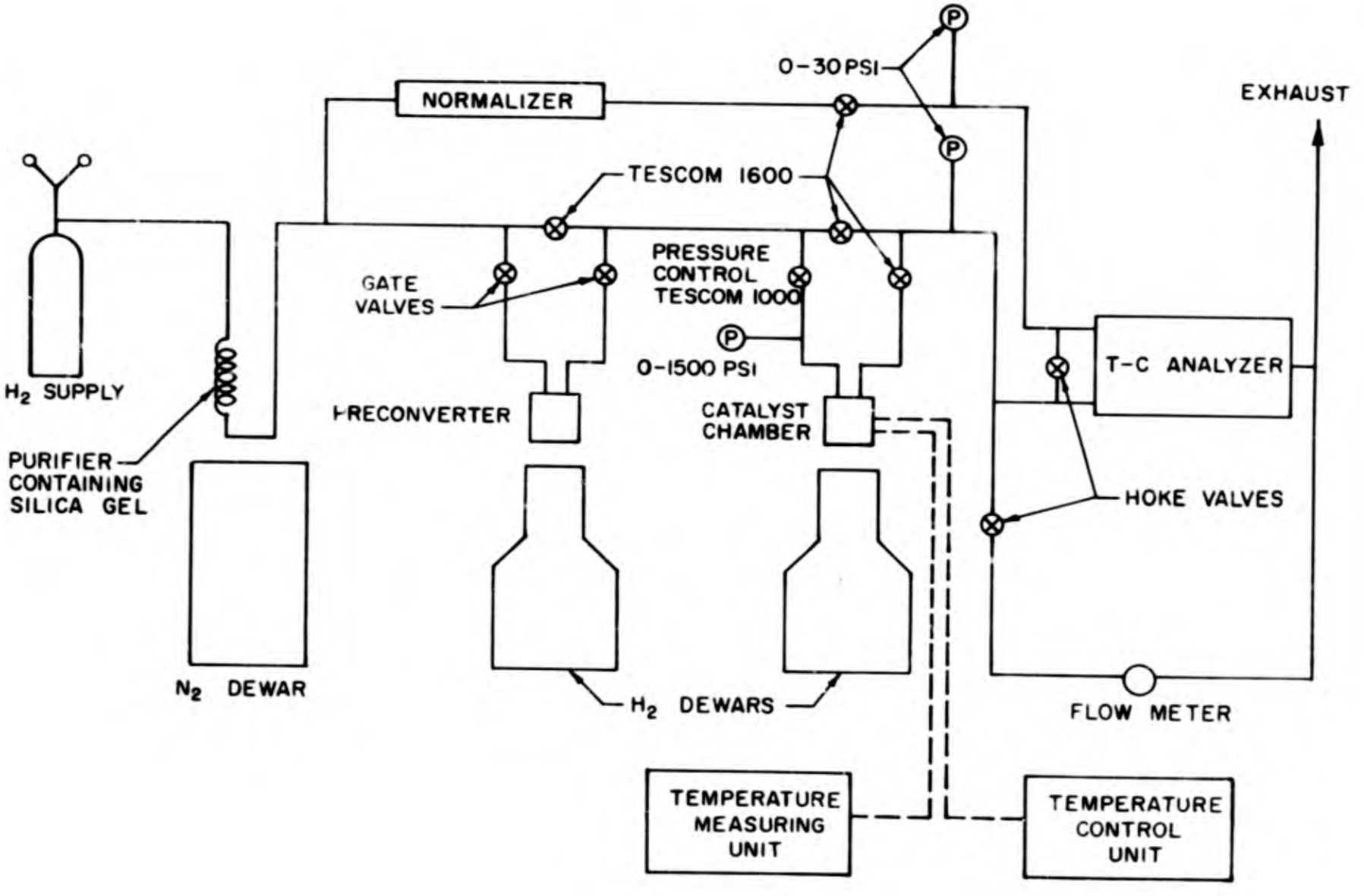


SCHEMATIC OF SYSTEM FOR STUDYING KINETICS OF THE PARA-TO-ORTHO HYDROGEN REACTION

Figure II - 1

This stream passed through a pressure regulating valve, into the reactor. Here the temperature was controlled to within ± 0.1°K by a continuous controller. After being partially converted, the hydrogen passed out and was split again, part flowing through a wet-test gas flow meter, and a small part through the analyzer, where its ortho-para composition was measured. All the hydrogen was then vented to the outside.

A schematic diagram of the reactor unit is shown in Fig. II-2. The hydrogen entered at 20°K after having passed through a tube immersed in liquid hydrogen. It passed through a preliminary heat exchanger, where it cooled the leaving gas, and then spiraled about the outside of the catalyst bed. The spiral tubes were enclosed with solder so that the reactor resembled a solid cylinder of copper and solder. This heavy metal cylinder became a heat sink which tended to maintain an isothermal condition in the reactor.

At the bottom of the reactor, the hydrogen entered the catalyst bed where it underwent conversion. It left the system through the warm side of the preliminary heat exchanger and went to the analyzer. A resistance thermometer was mounted at the top and another near the bottom of the reactor. The purpose of the thermometers was to check the isothermality of the reactor, although they actually measured a temperature that was the average of the heater temperature and the outside temperature of the metal block that comprised the reactor.

Outside of the thermometers were the two heaters that provided temperature control. One of these, the inner heater, was automatically controlled to maintain the temperature at the required level while the outer one was manually controlled and helped to stabilize the temperature.

A stainless steel cylinder enclosed the entire reactor assembly. A low pressure helium atmosphere was maintained inside the cylinder during the runs. This provided an insulation layer between the reactor and the liquid hydrogen bath in which it was immersed. The temperature was controlled by heating the reactor to the desired level and releasing the excess heat to the liquid hydrogen bath.

A run was begun by closing off the reactor and the flow meter and allowing essentially pure parahydrogen to circulate through the analyzer. This step allowed the range on the recorder to be set. A data point was generated by setting the controller to the desired temperature, opening the valves to the

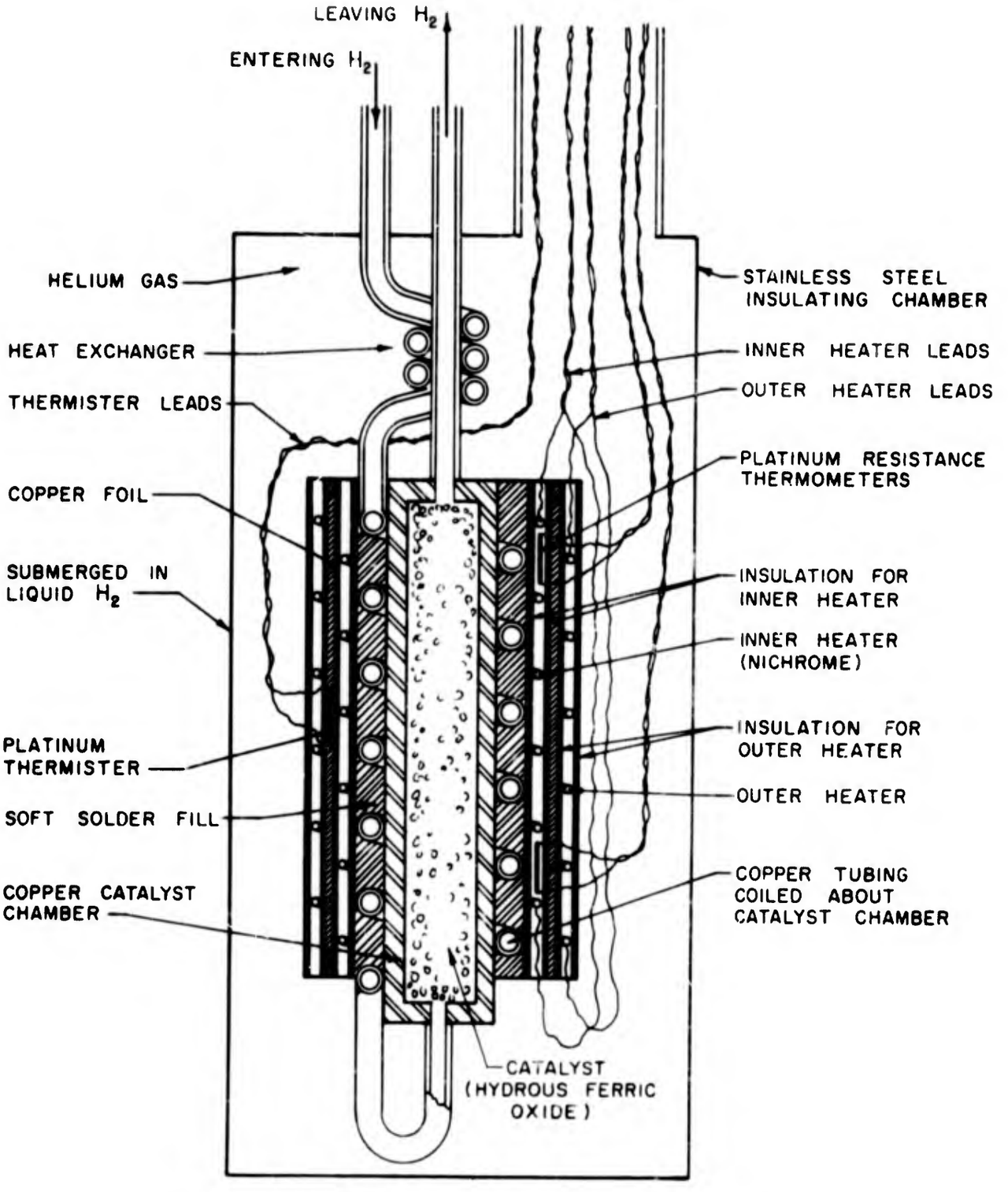


(NOT TO SCALE)

SCHEMATIC DIAGRAM OF CHAMBER UNIT CONTAINING CATALYTIC REACTOR

Figure II 2

reactor, and adjusting the flow to the desired value. When the flow, temperature, and conversion had reached steady state, the temperatures were recorded, the flow measured, and the recorder reading noted. At the conclusion of these readings, the flow to the reactor and meter was stopped. This was done in order to check the range on the recorder. The temperature control setting was adjusted from point to point so that the average of the top and bottom temperatures remained constant.

The barometric pressure and wet-test meter temperature were recorded. This enabled the vapor pressure of water to be taken into consideration when calculating the volume of gas which passed through the meter. The flow rate was measured by the noting of the volume of gas which passed through the meter in 1.0 minute.

The catalyst that was used in the runs was a hydrous ferric oxide gel manufactured by Cryogenic Engineering Company. It was batch number 339-6 and is described more fully in Section III of this report.

## II. 3 Results

A total of 31 runs were made--six operating pressures from 42 to 1012 psia with five different temperature runs, from 40 to 80°K, at each pressure, plus a run at 112 psia and 80°K. It was felt that this range would give a comprehensive coverage of the operating conditions most likely to be encountered for this reaction.

The data, which are given by Hutchinson (14), are presented as a series of space velocity curves in Figs. II-3-8. Conversion as a function of space velocity for given pressures and temperatures may be taken directly from these curves. The values of $x_e$ used in the calculation of the rate constants were obtained from these graphs.

In the preliminary attempts to correlate the data, many rate expressions were tried prior to finding the successful one. The next few paragraphs will summarize these and explain why they were abandoned.

The procedure that was used consisted of the following steps:

A) A rate expression was chosen, and substituted into Eq. II-1, which is the basic equation for a flow reactor as given by, for example, Levenspiel (17). The equation was then integrated.

$$-rdV_r = Fc_H dx \qquad \text{(II-1)}$$

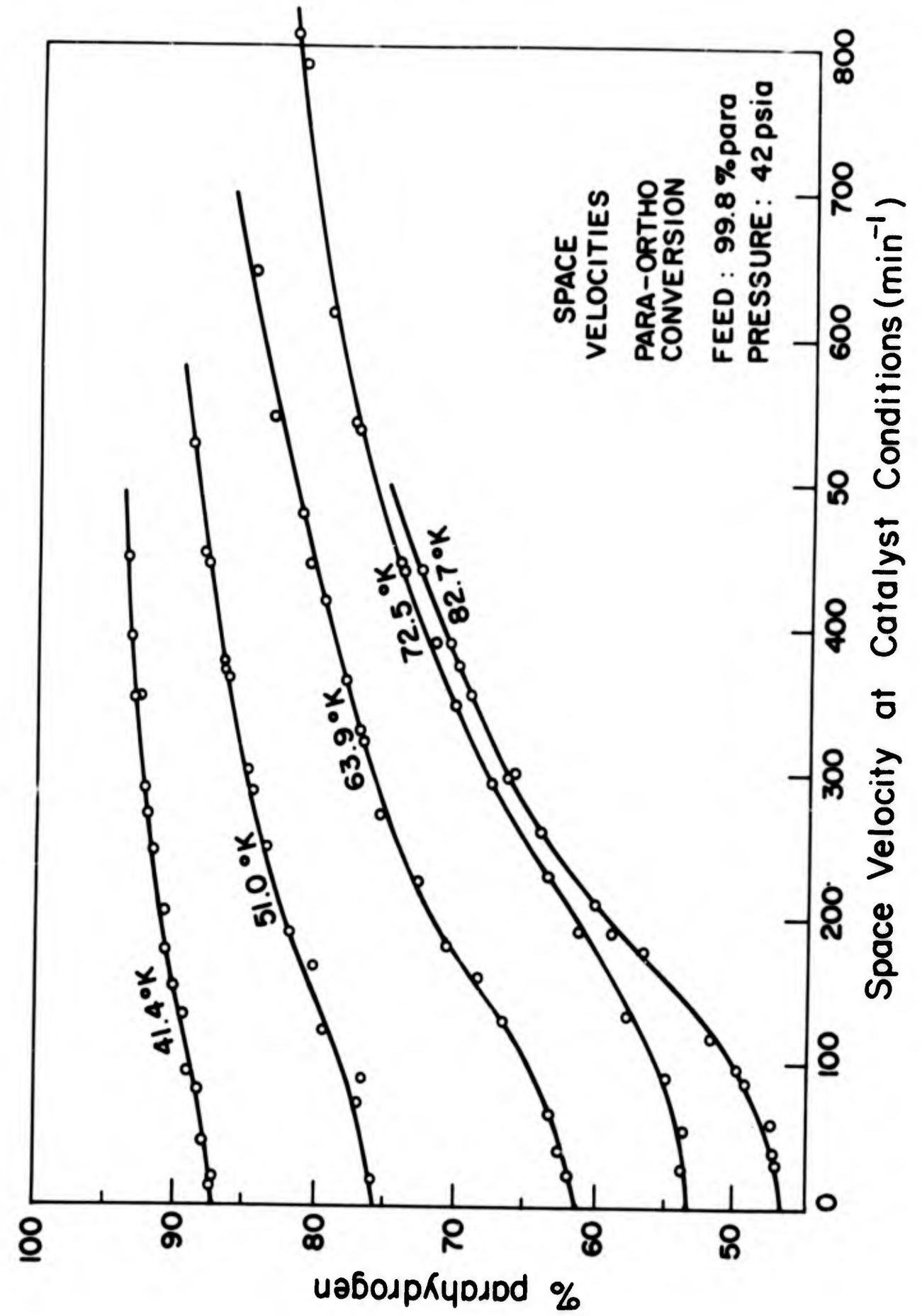
% parahydrogen
100
90
80
70
60
50
0
100
200
300
400
50
600
700
800
Space Velocity at Catalyst Conditions (min⁻¹)
41.4°K
51.0°K
63.9°K
72.5°K
82.7°K
SPACE VELOCITIES
PARA-ORTHO CONVERSION
FEED: 99.8 %para
PRESSURE: 42 psia

Figure II 3

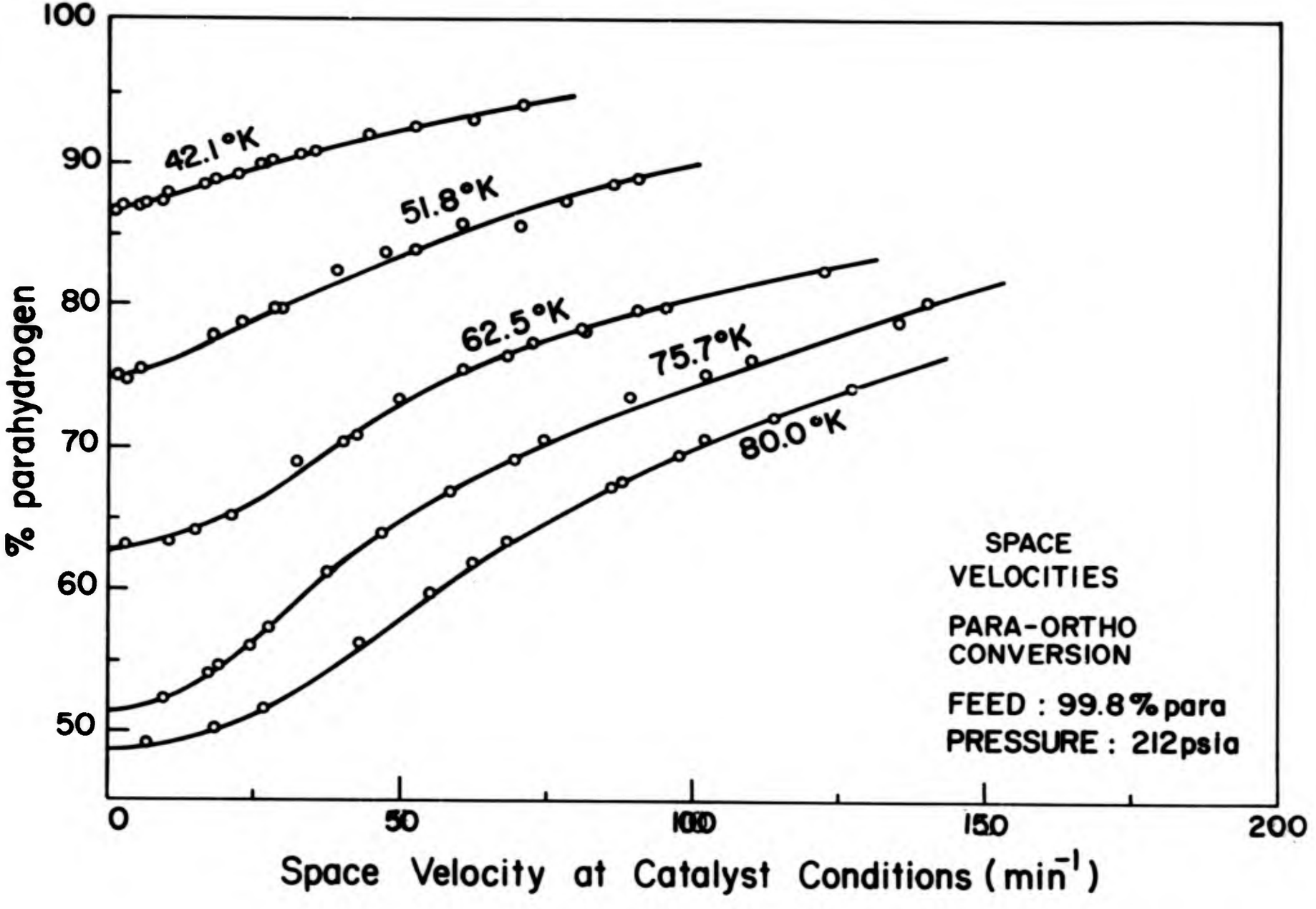
100
90
80
70
60
50
% parahydrogen
42.1°K
51.8°K
62.5°K
75.7°K
80.0°K
SPACE
VELOCITIES
PARA-ORTHO
CONVERSION
FEED : 99.8% para
PRESSURE : 212psia
0
50
100
150
200
Space Velocity at Catalyst Conditions (min⁻¹)

Figure II 4

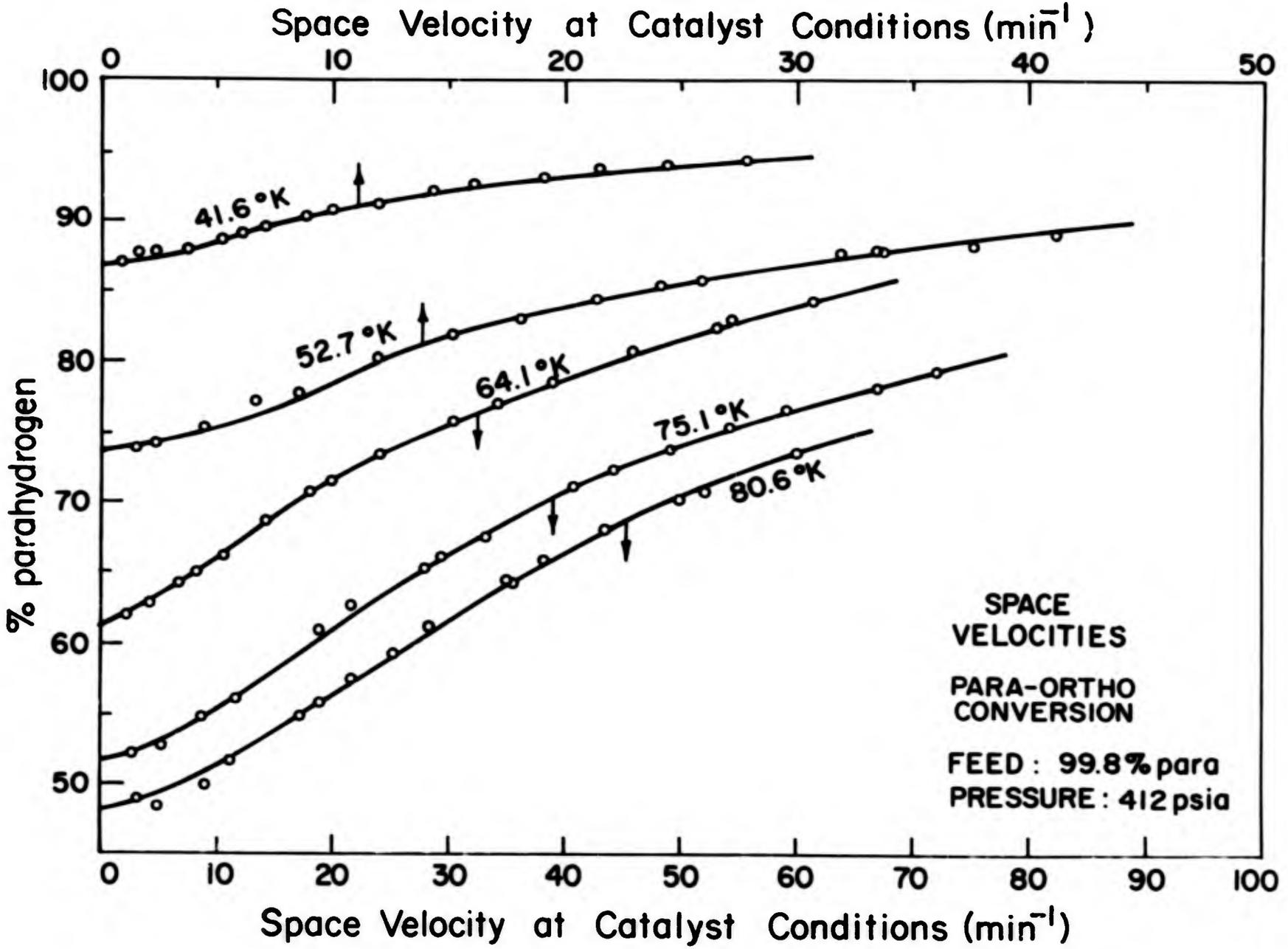
Space Velocity at Catalyst Conditions (min⁻¹)
0
10
20
30
40
50
100
90
80
70
60
50
% parahydrogen
41.6 °K
52.7 °K
64.1 °K
75.1 °K
80.6 °K
SPACE VELOCITIES
PARA-ORTHO CONVERSION
FEED : 99.8% para
PRESSURE : 412 psia
0
10
20
30
40
50
60
70
80
90
100
Space Velocity at Catalyst Conditions (min⁻¹)

Figure II 5

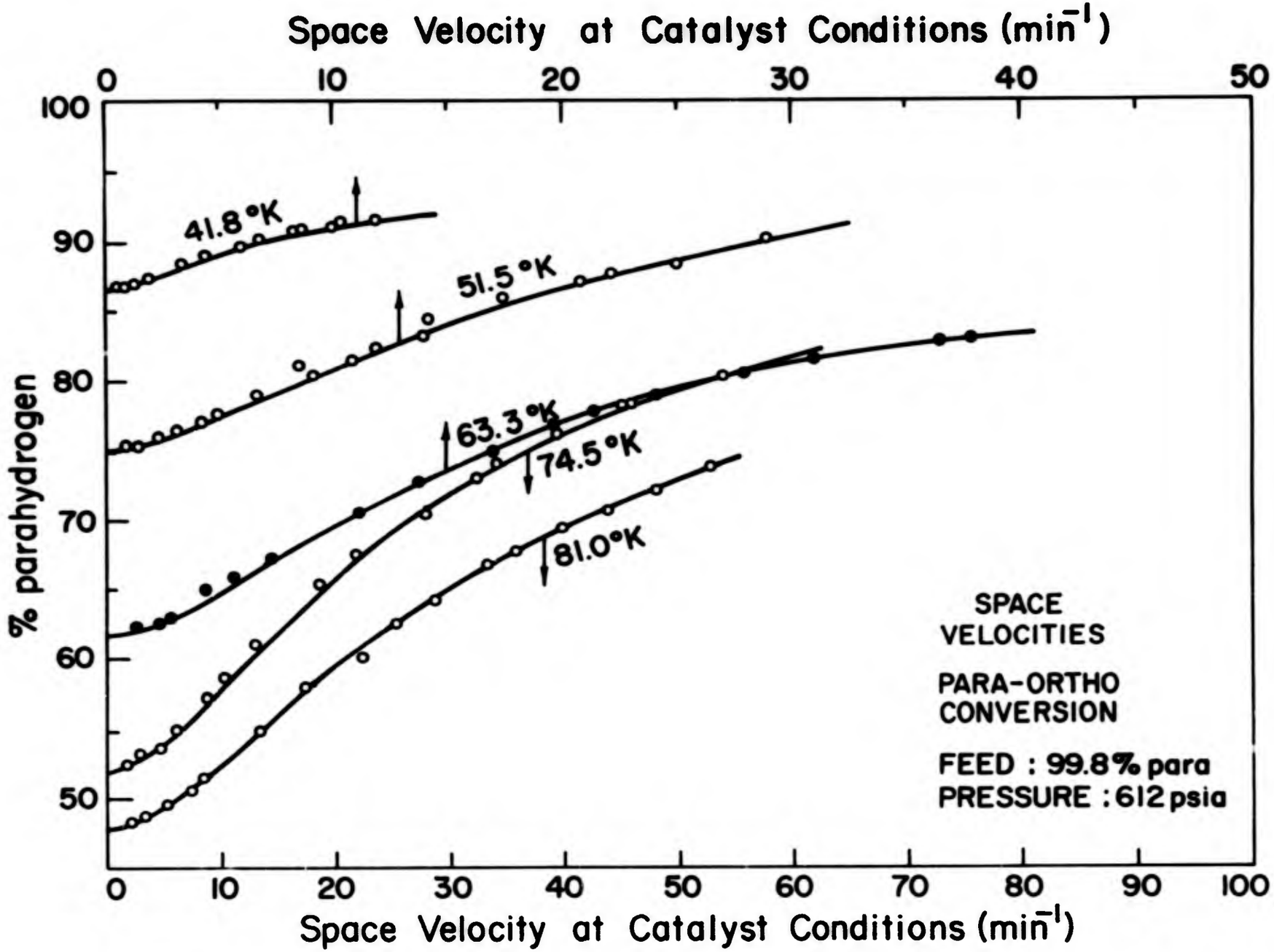
Space Velocity at Catalyst Conditions (min⁻¹)
0
10
20
30
40
50
100
90
80
70
60
50
% parahydrogen
41.8°K
51.5°K
63.3°K
74.5°K
81.0°K
SPACE
VELOCITIES
PARA-ORTHO
CONVERSION
FEED : 99.8% para
PRESSURE : 612 psia
0
10
20
30
40
50
60
70
80
90
100
Space Velocity at Catalyst Conditions (min⁻¹)

Figure II 6

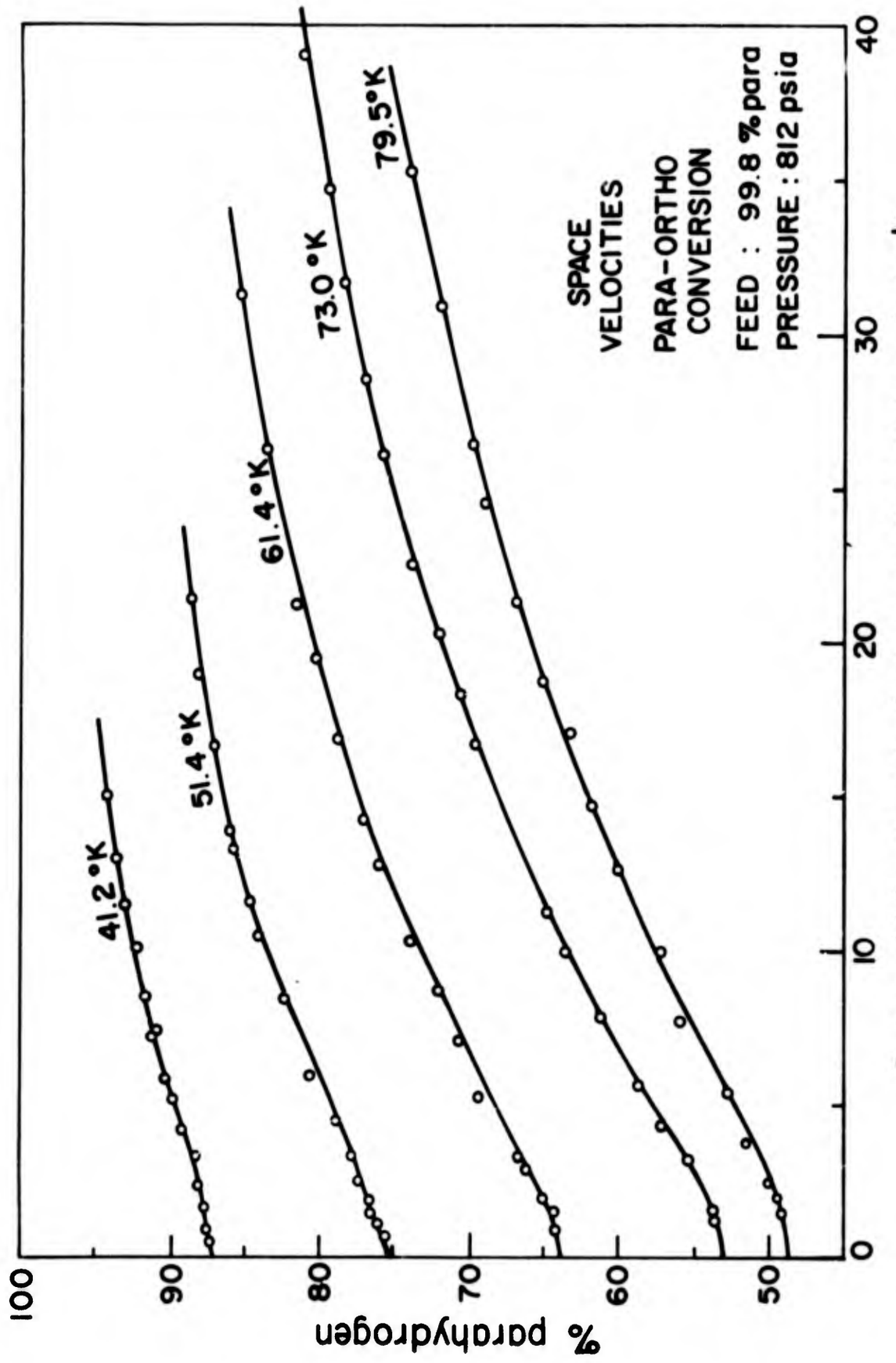
% parahydrogen
100
90
80
70
60
50
0
10
20
30
40
Space Velocity at Catalyst Conditions (min⁻¹)
41.2°K
51.4°K
61.4°K
73.0°K
79.5°K
SPACE VELOCITIES
PARA-ORTHO CONVERSION
FEED : 99.8 % para
PRESSURE : 812 psia

Figure II 7

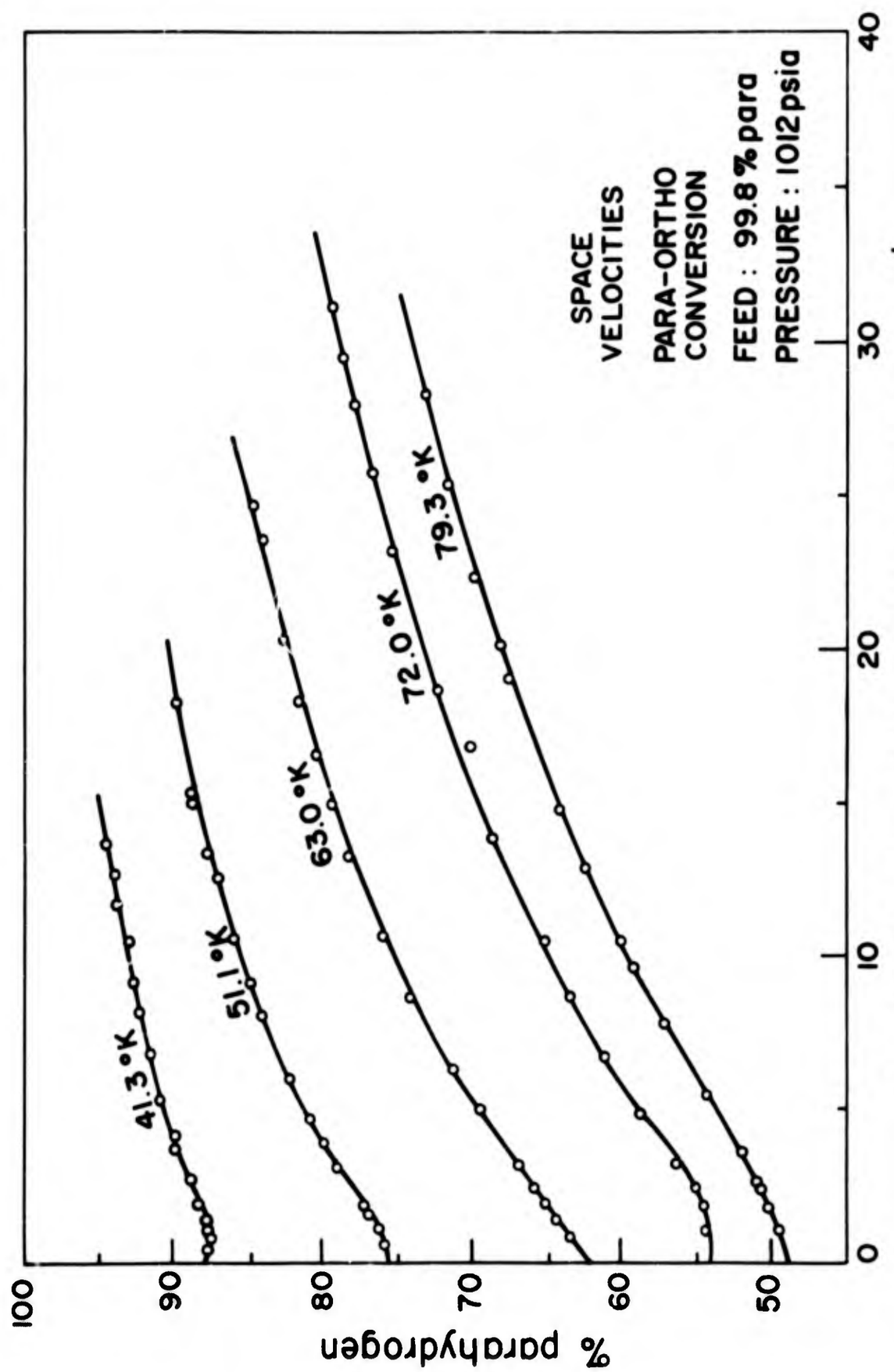
% parahydrogen
100
90
80
70
60
50
0
10
20
30
40
Space Velocity at Catalyst Conditions (min⁻¹)
41.3°K
51.1°K
63.0°K
72.0°K
79.3°K
SPACE VELOCITIES
PARA-ORTHO CONVERSION
FEED : 99.8% para
PRESSURE : 1012 psia

Figure II 8

where

$-r$ = Rate of disappearance of parahydrogen, g-moles /(min) ($cm^3$ catalyst).

$V_r$ = Volume of catalyst, $cm^3$.

$F$ = Feed rate, $cm^3$/min.

$c_H$ = Total hydrogen concentration, g-moles/$cm^3$.

$x$ = Mole fraction parahydrogen.

B) The integrated equation was rearranged into a form in which an expression containing $\tau$ could be plotted vs. an expression containing x such that a straight line would result if the assumed expression were correct.

where

$\tau$ = Space time, min. = Amount of time for one reactor volume of feed gas to pass through the reactor.

C) The expressions in Part (B) were calculated from the data and the necessary plot was constructed.

D) It was noted whether or not the data yielded a straight line.

E) The procedure was repeated for several runs in order to see if an equally good plot was obtained.

F) If the data from all the runs fit the curve equally well, then the assumed rate expression was accepted as correct.

In general, it was not too difficult to find a rate expression which described the data from one or two individual runs very well. But in all cases presented here, as the pressure and/or temperature were changed, the data began to deviate from the curve and so the expression was abandoned. Following is a summary of the rate expressions that were tried, with a few representative examples of the plots that were prepared.

First Order Reaction

Since the ortho → para reaction had been presented as being first order, it seemed natural that the reverse reaction should have been first order, so first order kinetics was the first expression tried. The first order rate expression (in terms of mole fractions) is

$$r = kx - k_{-} (1 - x) \qquad \text{(II-2)}$$

where

$k, k_{-}$ = First order rate constants, $min^{-1}$.

Eq. (II-2) may be rearranged by using that fact that at equilibrium r = 0 and $kx_e = k_{-} (1 - x_e)$ to

$$r = k_r (x - x_e) \qquad \text{(II-3)}$$

Substitution of Eq. (II-3) into Eq. (II-1) and integration of the resulting equation yields

$$- k_r \tau = \ln (x - x_e) - \ln (x_o - x_e) \qquad \text{(II-4)}$$

From Eq. (II-4) it can be seen that a plot of $\ln (x - x_e)$ vs. $\tau$ should yield a straight line for first order kinetics. Figs. II-9, II-10, and II-11 show plots that were made for 1st order kinetics. It was noted that Fig. II-10 showed a fair approximation to first order kinetics. As the temperature went down, however, the deviation became greater, as is evidenced by Fig. II-9. It was noted that the straight lines in Fig. II-9 do not quite pass though the calculated intercept and that there is a slight but noticeable curvature in the data. This curvature was more pronounced at a pressure of 212 psia as evidenced by Fig. II-11. From these and similar plots it was concluded that a more fruitful approach would be to try a higher order. However, first order rate constants can be obtained for 80°K and 32 psia and this may explain why previous investigators found the reaction to be first order, as they were operating at about this temperature and pressure.

3/2 Order Kinetics

The next expression tried was suggested by Blake (2), who had previously tried a 3/2 order mechanism and found good agreement at 76°K and 22 psia. The rate expression is

$$r = kx^{3/2} - k_{-} x^{1/2} (1 - x) \qquad \text{(II-5)}$$

Again, using the equilibrium conditions, this expression may be reduced to the form

$$r = k_r x^{1/2} (x - x_e) \qquad \text{(II-6)}$$

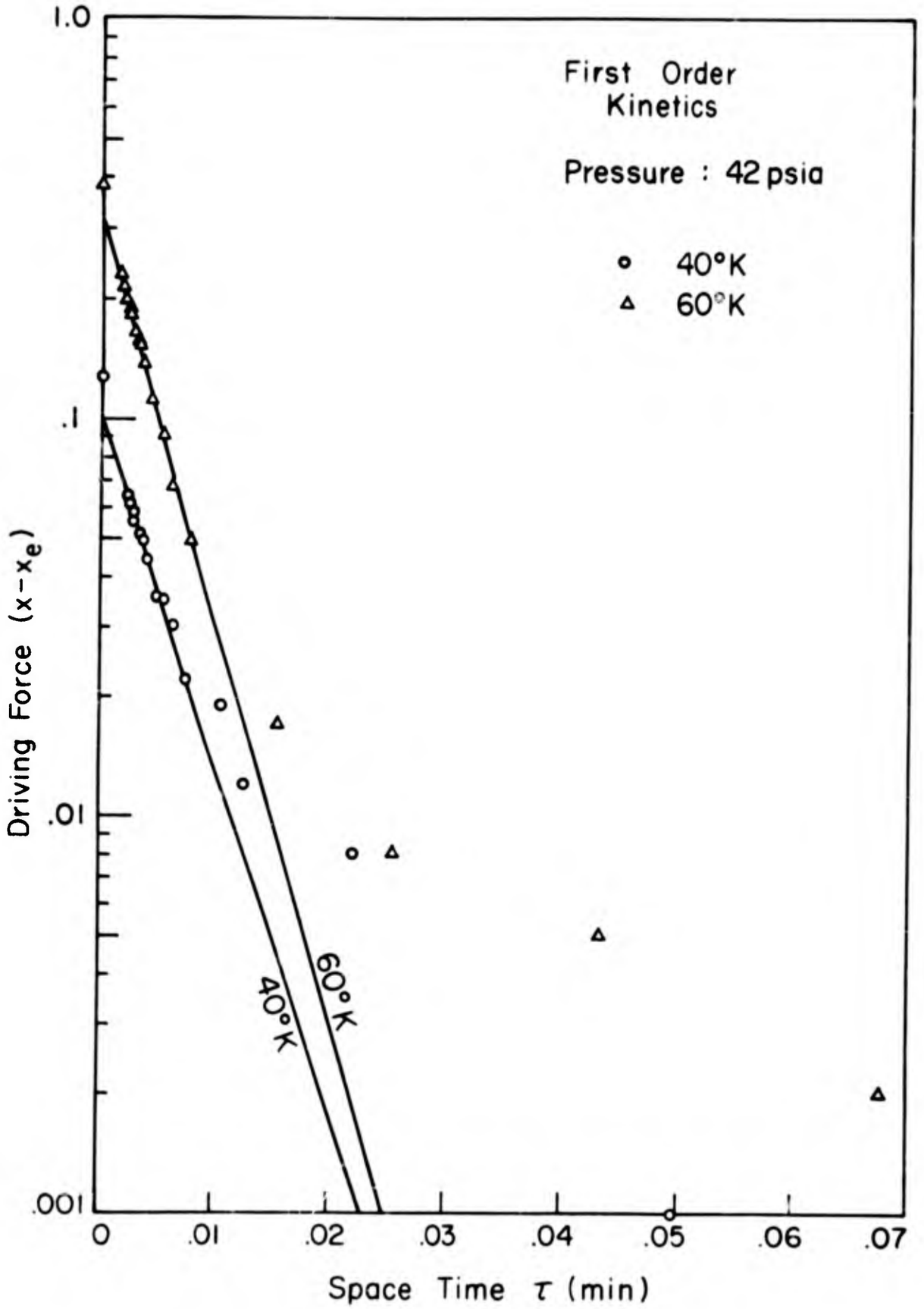
First Order
Kinetics
Pressure : 42 psia
40°K
60°K
1.0
.1
.01
.001
Driving Force (x-xe)
0
.01
.02
.03
.04
.05
.06
.07
Space Time τ (min)
60°K
40°K

Figure II 9

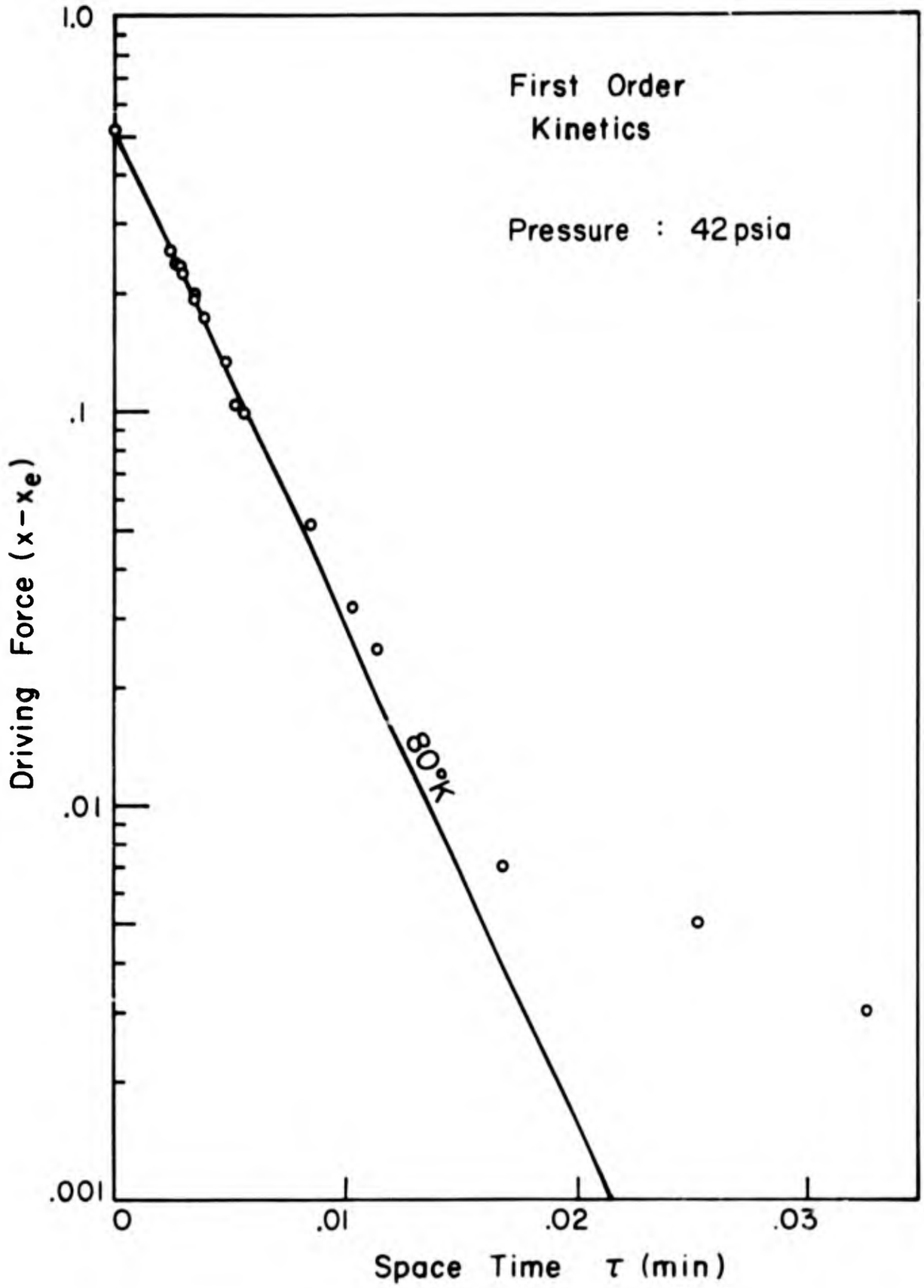
First Order
Kinetics
Pressure : 42 psia
80°K
1.0
.1
.01
.001
0
.01
.02
.03
Driving Force (x - xe)
Space Time τ (min)

Figure II 10

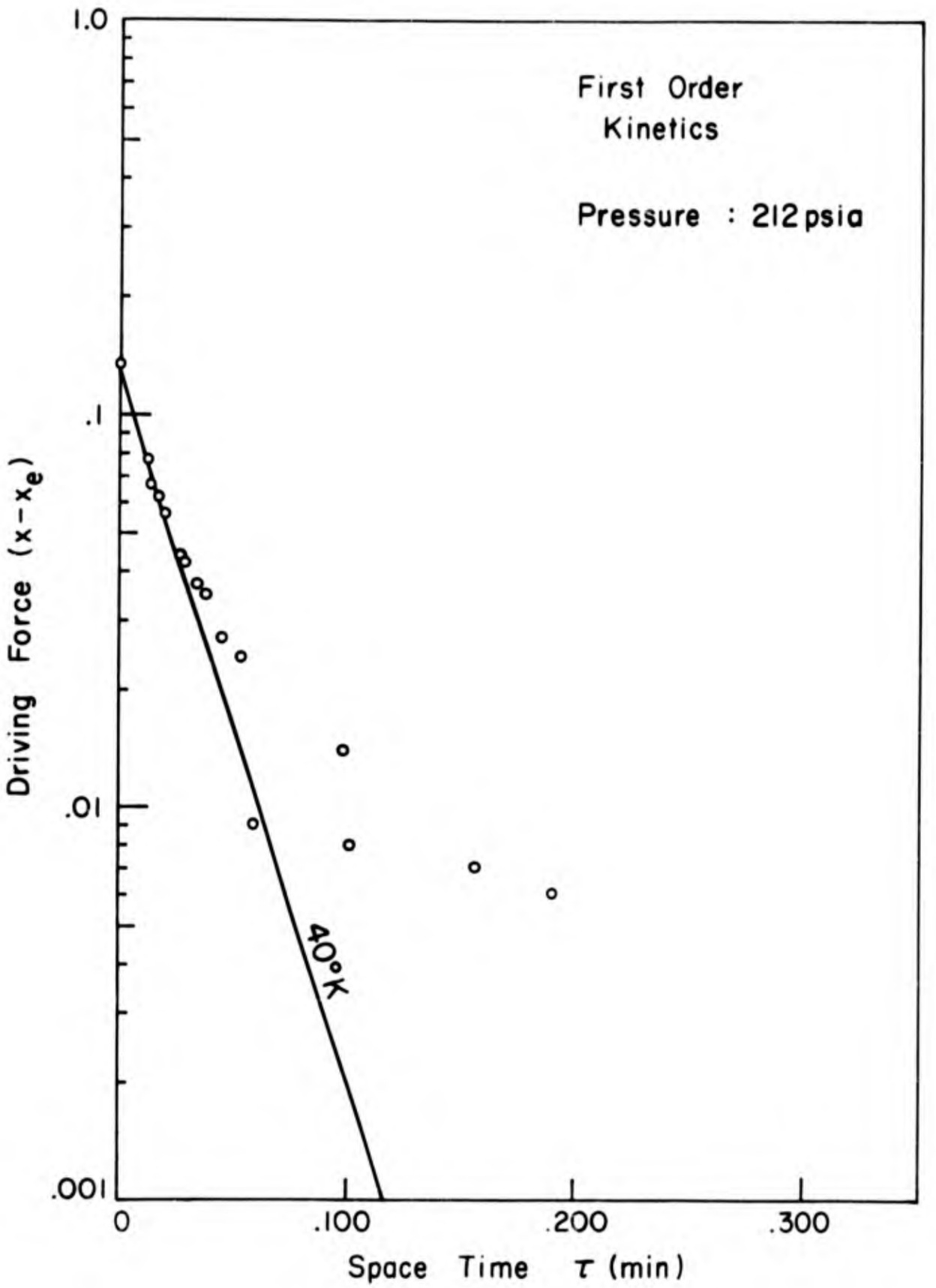
1.0
.1
.01
.001
Driving Force $(x-x_e)$
First Order
Kinetics
Pressure : 212 psia
40°K
0
.100
.200
.300
Space Time $\tau$ (min)

Figure II 11

Combination of Eq. (II-6) with Eq. (II-1) and integration yields

$$-k_r\tau = \ln \frac{\sqrt{x} - \sqrt{x_e}}{\sqrt{x} + \sqrt{x_e}} - \ln \frac{\sqrt{x_o} - \sqrt{x_e}}{\sqrt{x_o} + \sqrt{x_o}} \qquad \text{(II-7)}$$

Thus, a plot of $\ln [(\sqrt{x} - \sqrt{x_e})/(\sqrt{x} + \sqrt{x_e})]$ vs. $\tau$ should yield a straight line if Eq. (II-5) is the correct rate expression. Figs. II-12-14 show a few of the plots that were made illustrating this expression. It was evident that there was still some deviation at the lower temperatures, as shown by Fig. II-12, and higher pressures, as shown by Fig. II-14. However, around 80°K and lower pressures, the data were in very good agreement with the mechanism. Since there appeared to be no general agreement, however, it was decided to look still further and see if a better correlation could be obtained.

## Second Order Kinetics

The next step was to try a higher order, so a second order expression was postulated. The rate expression is

$$r = kx^2 - k_{-}x\,(1 - x) \qquad \text{(II-8)}$$

which, by treatment analogous to the above, reduces to

$$r = k_r x\,(x - x_e) \qquad \text{(II-9)}$$

Combination of Eq. (II-9) with Eq. (II-1) and integration yields

$$-k_r\tau = \ln \frac{x - x_e}{x} - \ln \frac{x_o - x_e}{x_o} \qquad \text{(II-10)}$$

Here, a straight line on a plot of $\tau$ vs. $\ln [(x - x_e)/x]$ would show agreement. Again, some runs showed remarkable agreement with the second order rate expression, but again there wasn't general agreement. Figs. II-15-19 illustrate a few of the plots for a second order reaction. About this time it began to be apparent that merely trying higher and higher order was a fruitless approach, but in the hope that something might be gained, the next step was tried.

## Third Order Kinetics

A rate expression for third order kinetics is

$$r = kx^3 - k_{-}x^2 (1 - x) \qquad \text{(II-11)}$$

which may be reduced, as above to

$$r = k_r x^2 (x - x_e) \qquad \text{(II-12)}$$

The integrated form of Eq. (II-12) is

$$-k_r\tau = \frac{1}{xx_e} + \frac{1}{x_e^2} \ln \frac{x - x_e}{x} - \frac{1}{x_o x_e} - \frac{1}{x_e^2} \ln \frac{x_o - x_e}{x_o} \qquad \text{(II-13)}$$

The coordinates of the plot would thus be $\tau$ vs. $(1/xx_e) + (1/x_e^2) \ln[(x - x_e)/x]$. Figs. II-20-22 show typical plots made for the third order expression. Again, the same effects were noted: the kinetics of some runs was well correlated by the third order expression while others were not. At this point it was decided to try a different approach, as fourth order was the next step and it is quite difficult to postulate a mechanism for fourth order. It became apparent that a trend in orders appeared to run somewhat as Fig. A indicates. Table II-I gives a summary of the reaction orders which were tried and those which appear to correlate the data for some of the runs. It would be quite difficult to derive a mechanism to explain a trend such as this so the search for higher orders was abandoned, as it was felt that little useful information could be derived from this approach.

It should be noted that, in principle, mechanisms can be postulated which lead to the above rate expressions. (See, for example, Hougen and Watson (13)). On the other hand, it is extremely difficult, if not impossible, to postulate a mechanism for the "empirical driving forces" which are presented in the following part of the discussion.

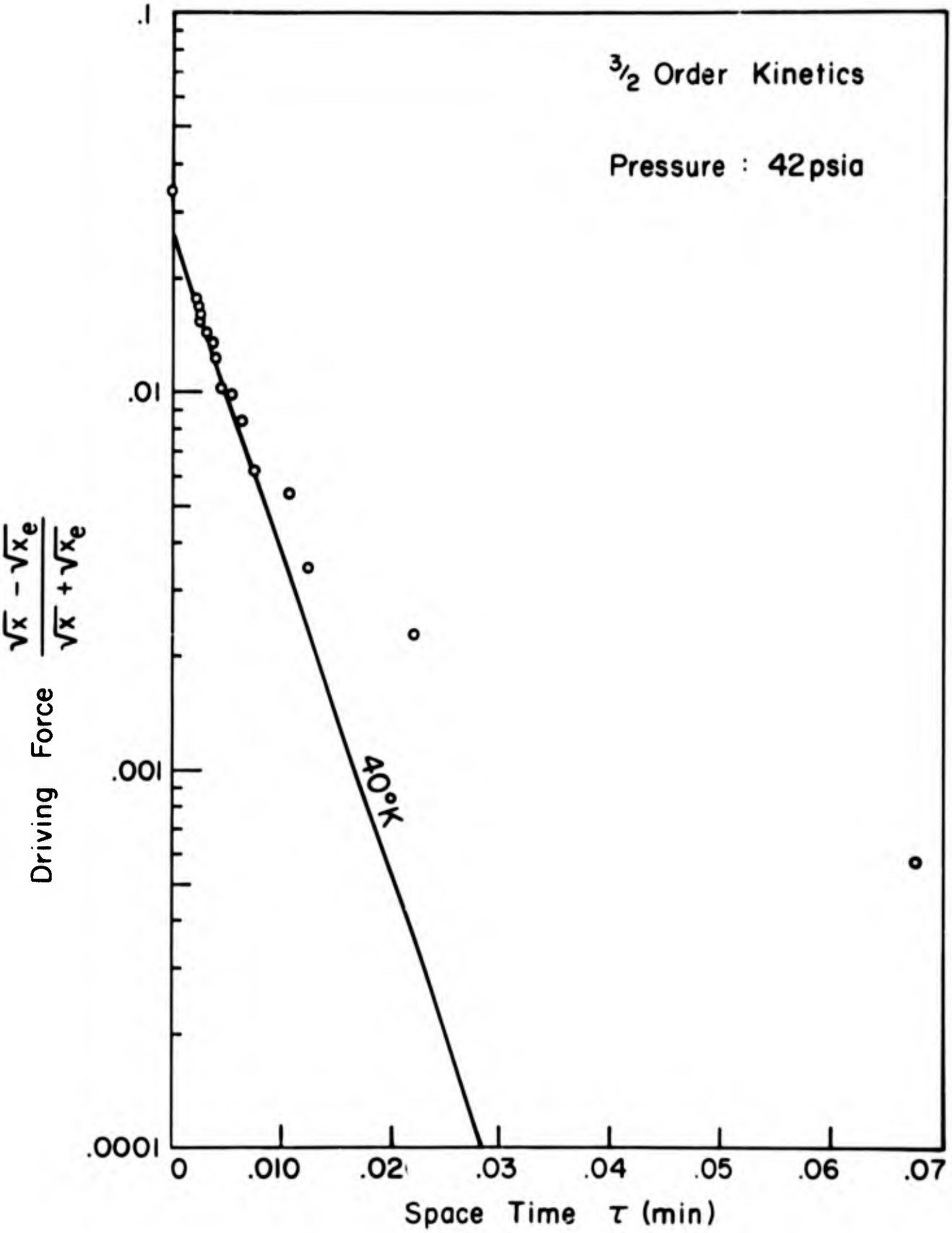
3/2 Order Kinetics
Pressure : 42psia
40°K
.1
.01
.001
.0001
0
.010
.02
.03
.04
.05
.06
.07
Space Time τ (min)
Driving Force $\frac{\sqrt{x} - \sqrt{x_e}}{\sqrt{x} + \sqrt{x_e}}$

Figure II 12

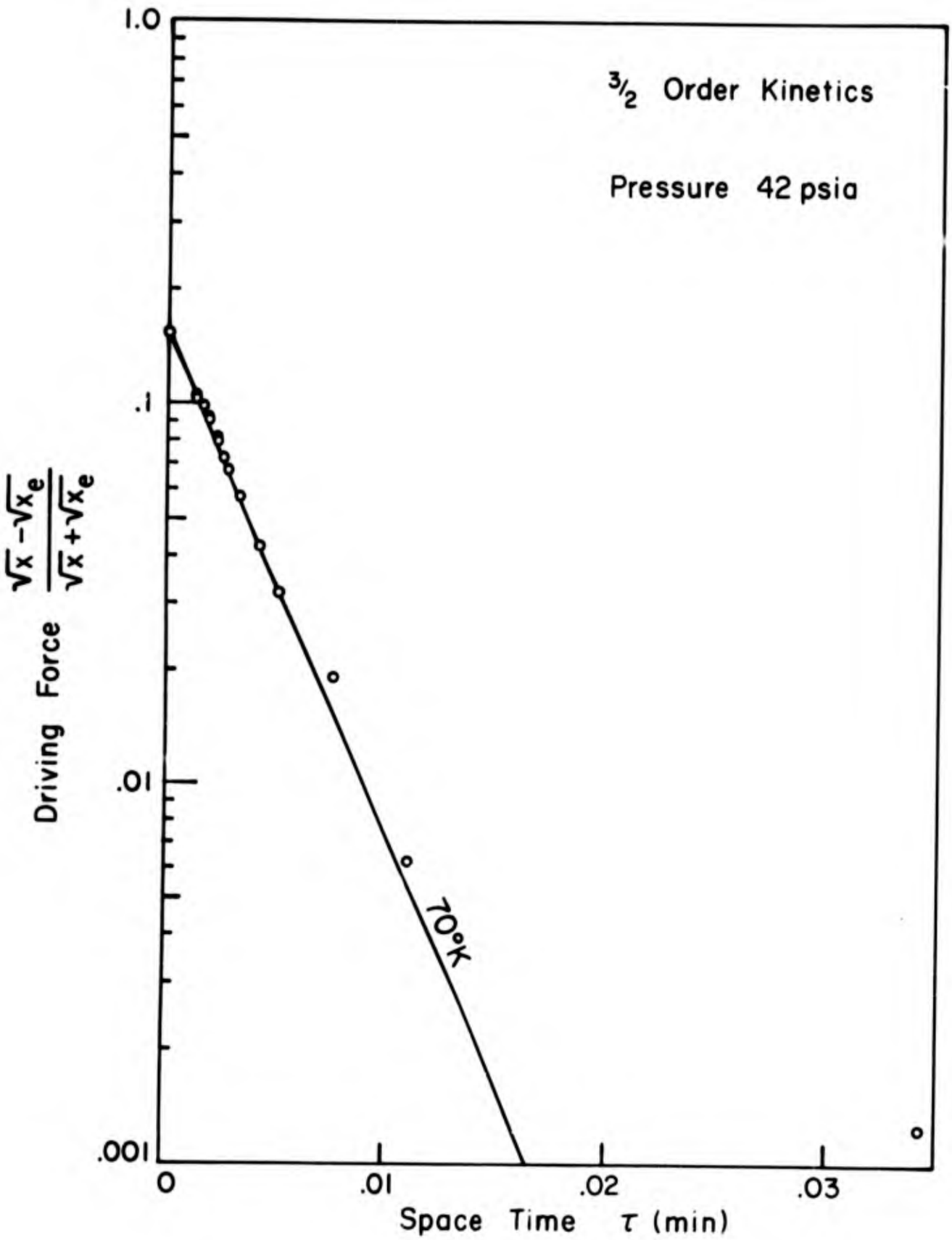
1.0
.1
.01
.001
0
.01
.02
.03
3/2 Order Kinetics
Pressure 42 psia
70°K
Driving Force $\frac{\sqrt{x}-\sqrt{x_e}}{\sqrt{x}+\sqrt{x_e}}$
Space Time τ (min)

Figure II 13

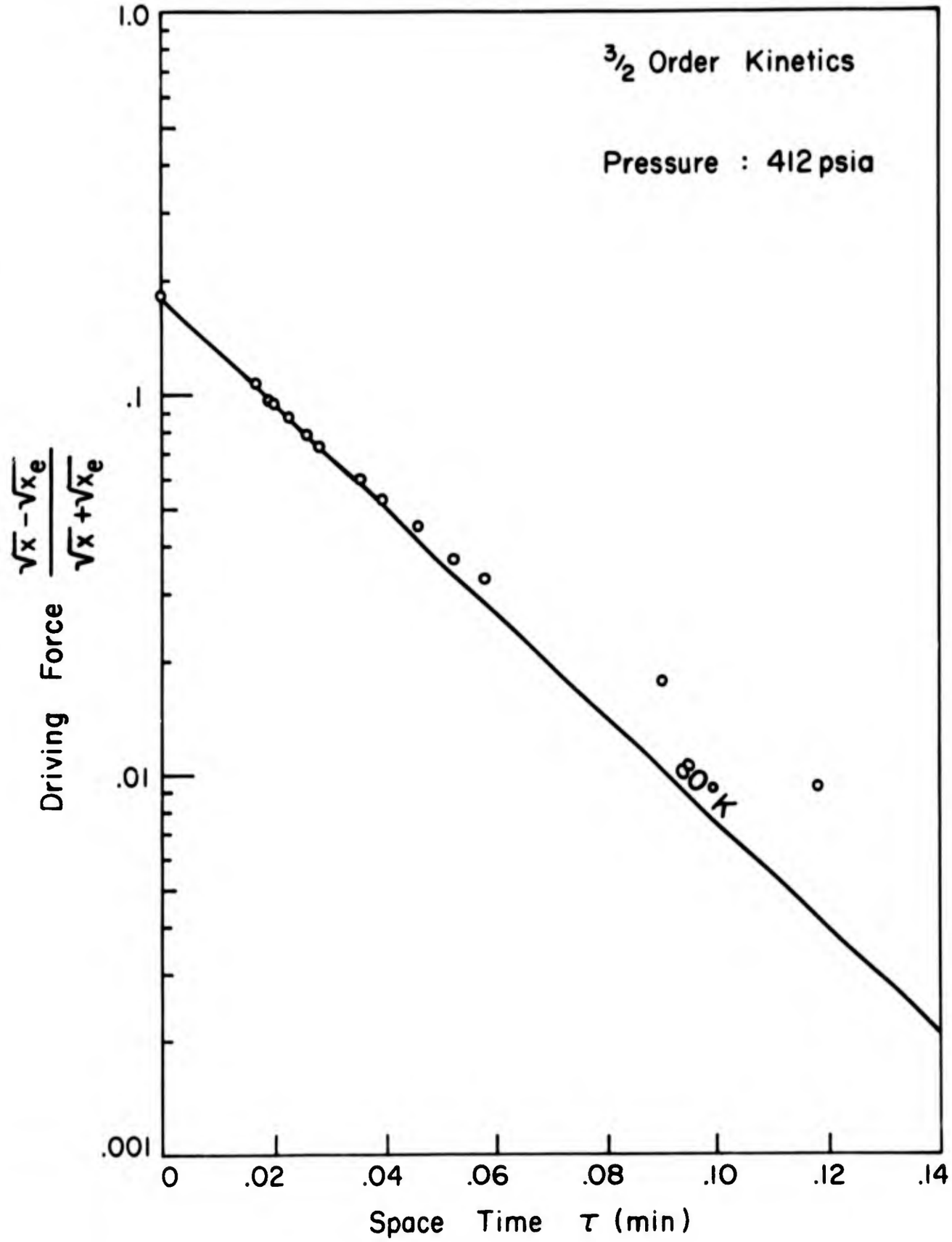
3/2 Order Kinetics
Pressure : 412 psia
80°K
Driving Force $\frac{\sqrt{x}-\sqrt{x_e}}{\sqrt{x}+\sqrt{x_e}}$
1.0
.1
.01
.001
0
.02
.04
.06
.08
.10
.12
.14
Space Time τ (min)

Figure II 14

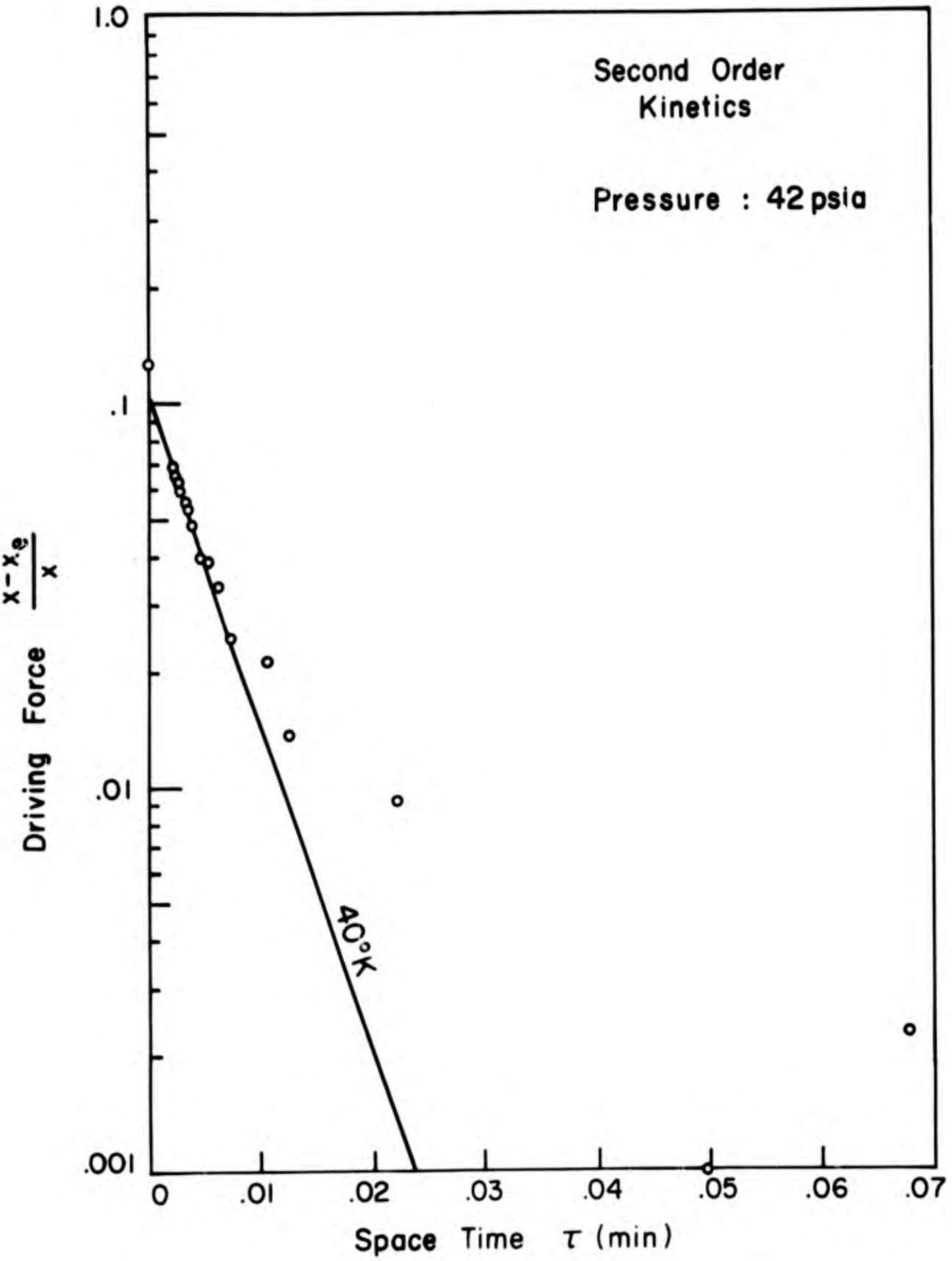
Second Order
Kinetics
Pressure : 42 psia
1.0
.1
.01
.001
Driving Force $\frac{x-x_e}{x}$
40°K
0
.01
.02
.03
.04
.05
.06
.07
Space Time τ (min)

Figure II 15

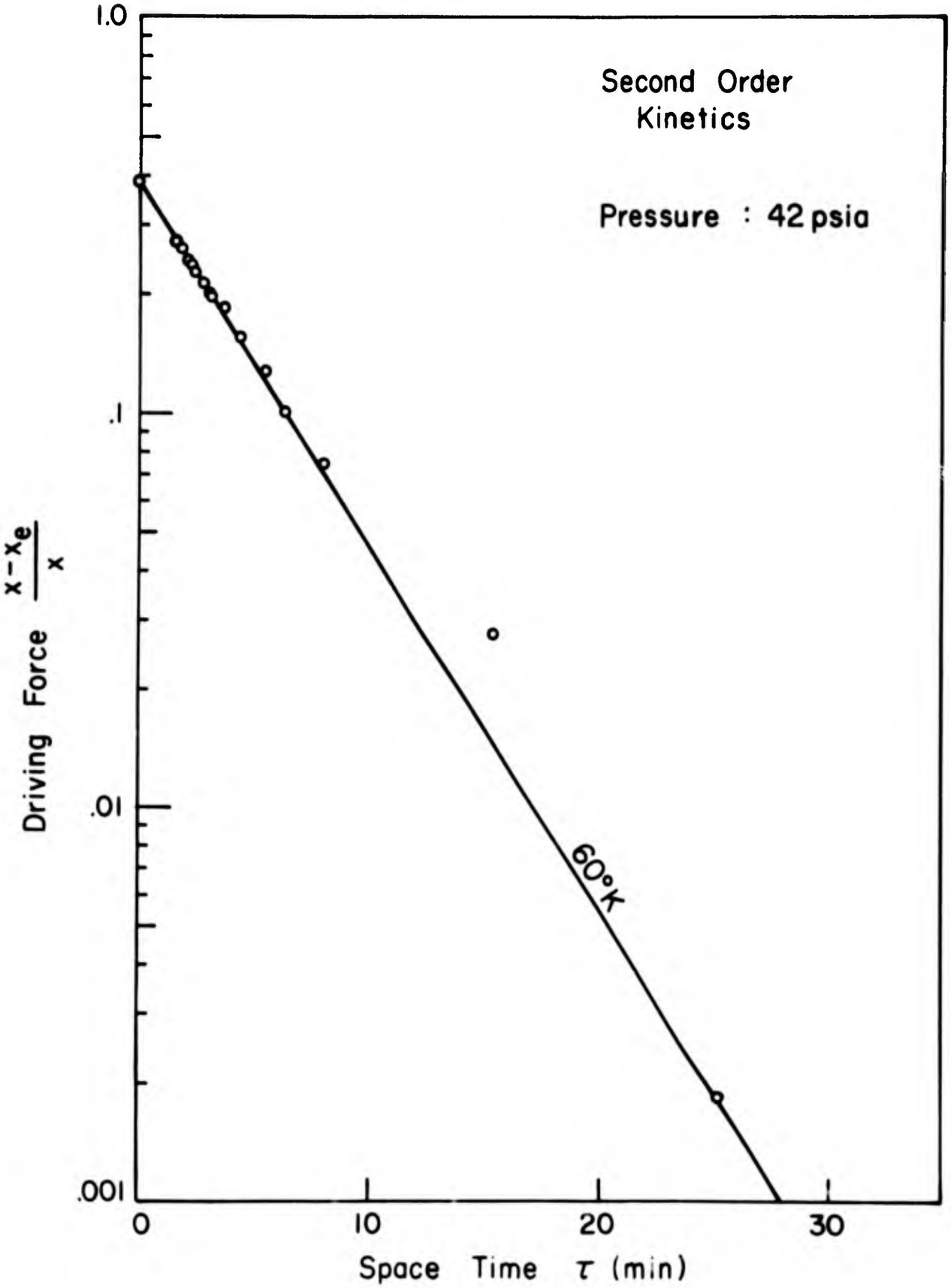
1.0
.1
.01
.001
Second Order
Kinetics
Pressure : 42 psia
60°K
Driving Force $\frac{x-x_e}{x}$
0
10
20
30
Space Time $\tau$ (min)

Figure II 16

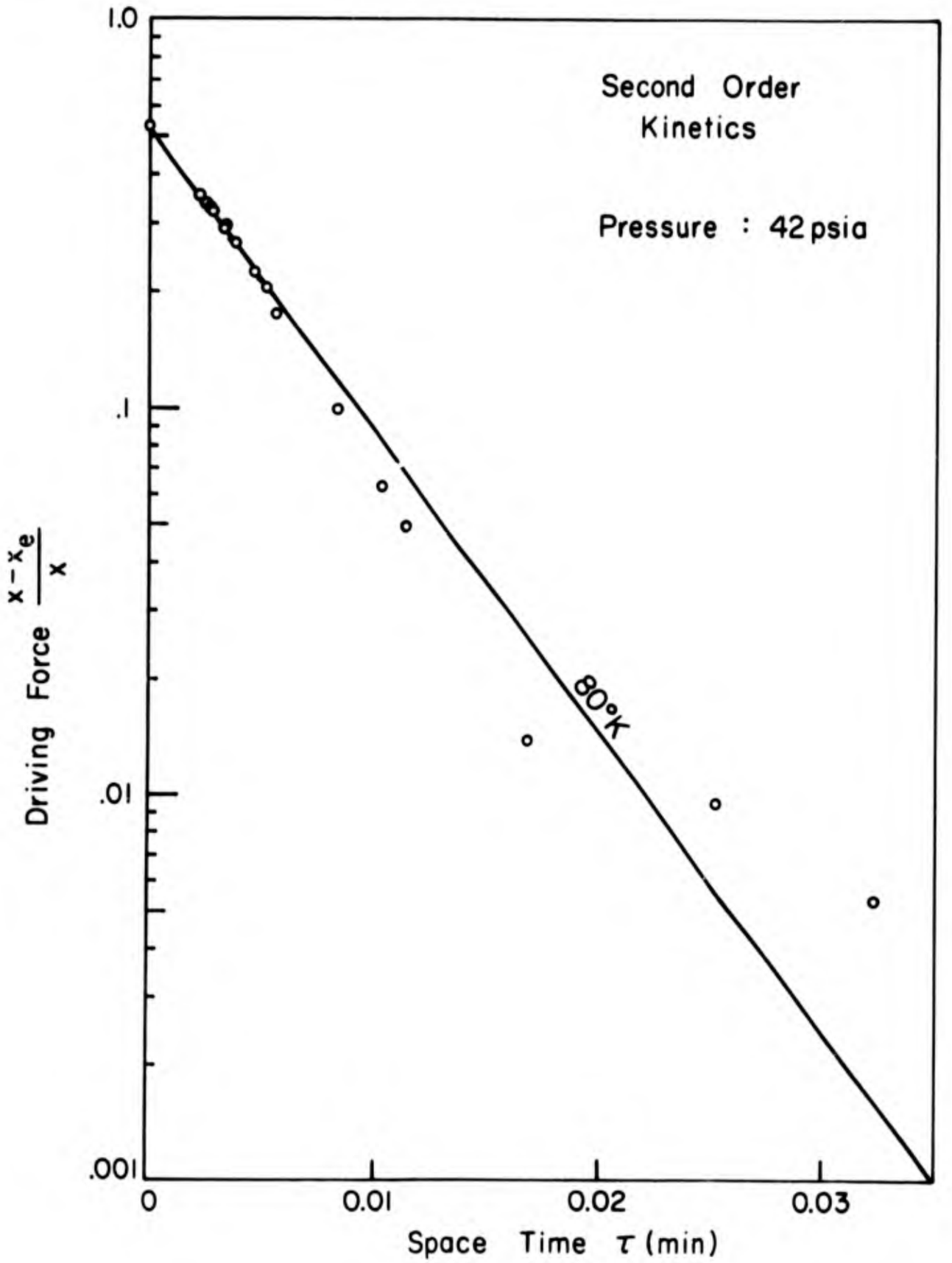
Second Order
Kinetics
Pressure : 42 psia
80°K
1.0
.1
.01
.001
0
0.01
0.02
0.03
Driving Force $\frac{x-x_e}{x}$
Space Time $\tau$ (min)

Figure II 17

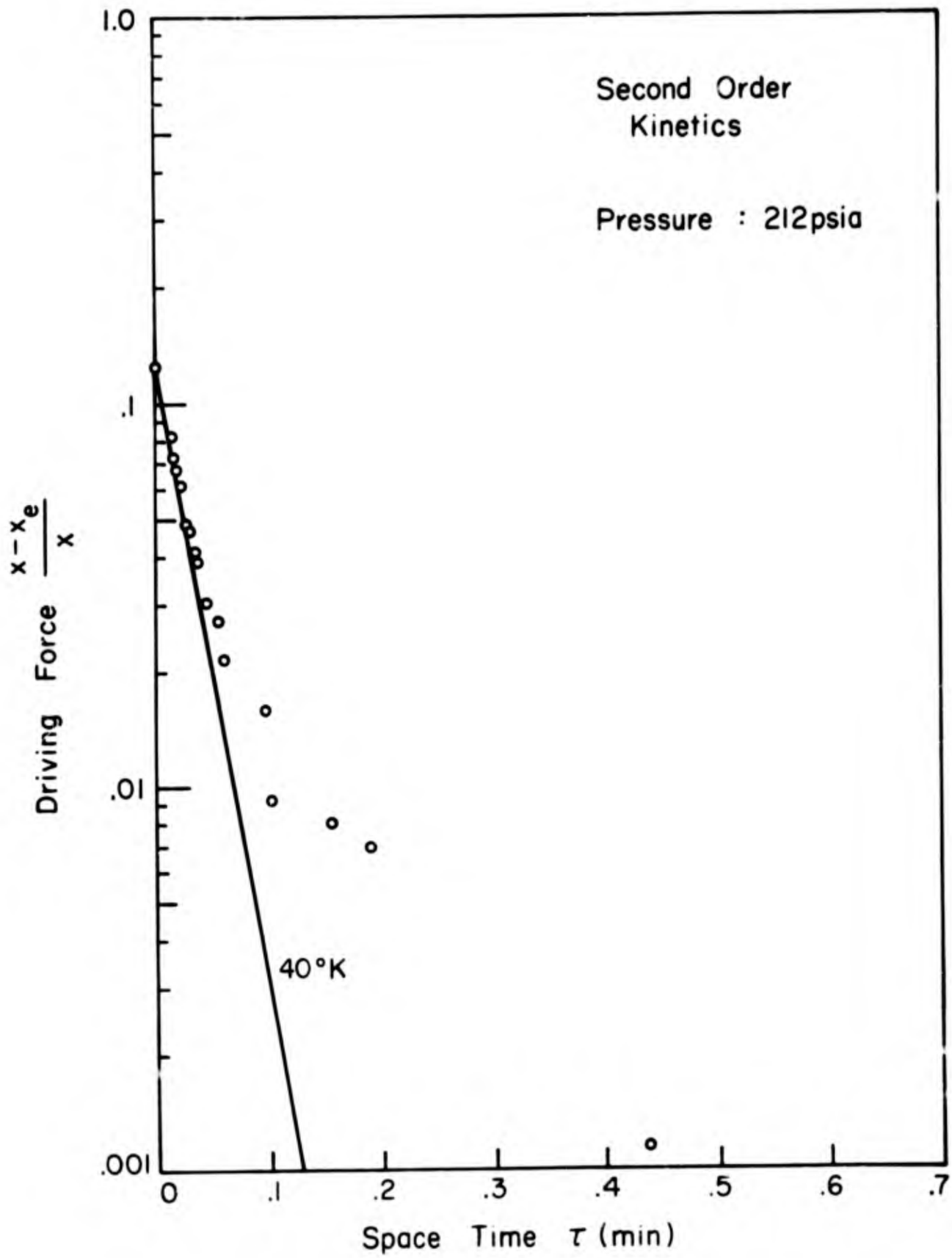
1.0
.1
.01
.001
Second Order
Kinetics
Pressure : 212psia
40°K
Driving Force $\frac{x-x_e}{x}$
0
.1
.2
.3
.4
.5
.6
.7
Space Time $\tau$ (min)

Figure II 18

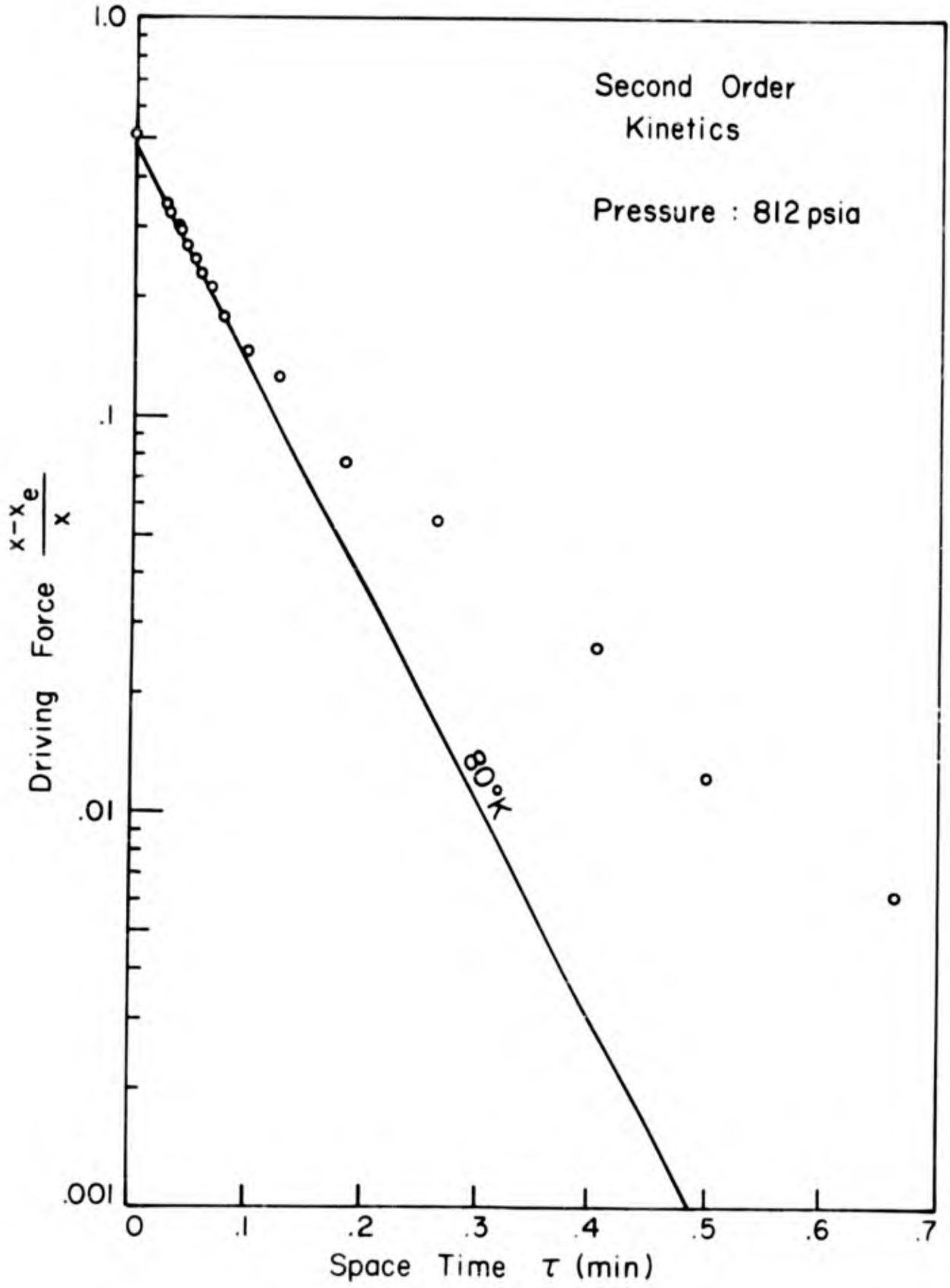
Second Order
Kinetics
Pressure : 812 psia
80°K
Driving Force $\frac{x-x_e}{x}$
1.0
.1
.01
.001
0
.1
.2
.3
.4
.5
.6
.7
Space Time τ (min)

Figure II 19

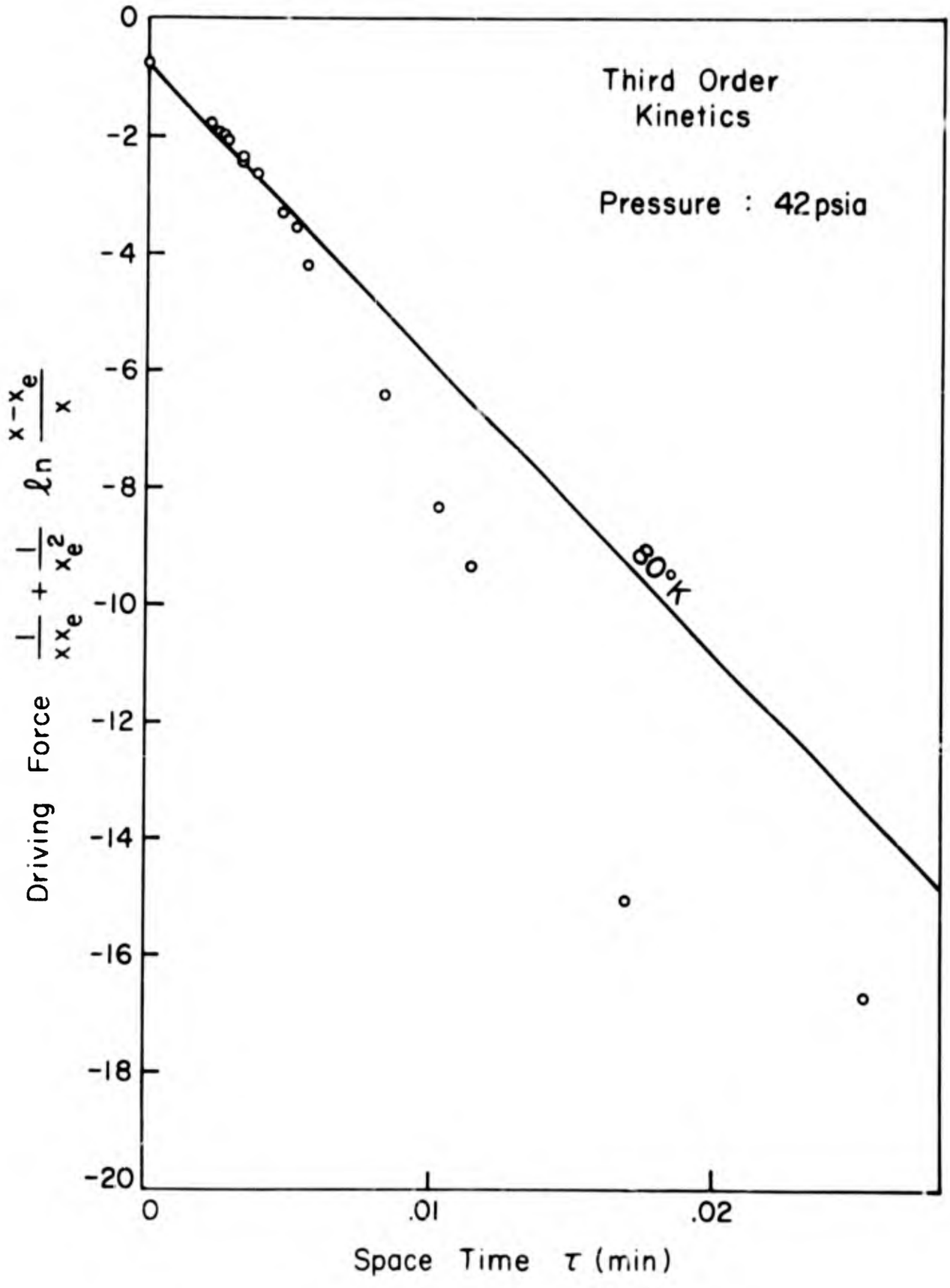
Third Order
Kinetics
Pressure : 42psia
80°K
Driving Force $\frac{1}{x x_e} + \frac{1}{x_e^2} \ln \frac{x - x_e}{x}$
Space Time $\tau$ (min)
0
-2
-4
-6
-8
-10
-12
-14
-16
-18
-20
0
.01
.02

Figure II 20

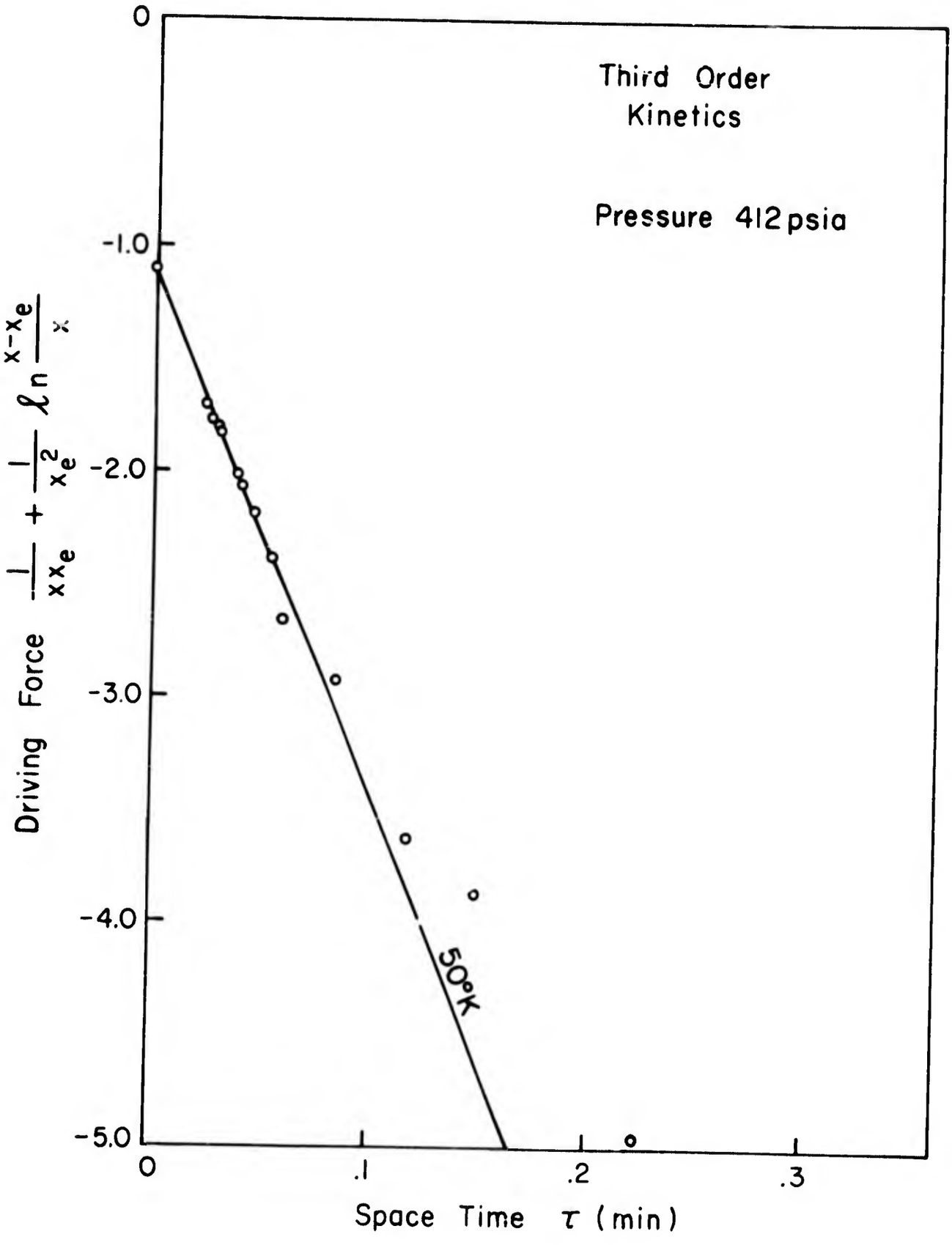
Third Order
Kinetics
Pressure 412 psia
50°K
Driving Force $\frac{1}{xx_e} + \frac{1}{x_e^2} \ln \frac{x-x_e}{x}$
Space Time $\tau$ (min)
0
-1.0
-2.0
-3.0
-4.0
-5.0
0
.1
.2
.3

Figure II 21

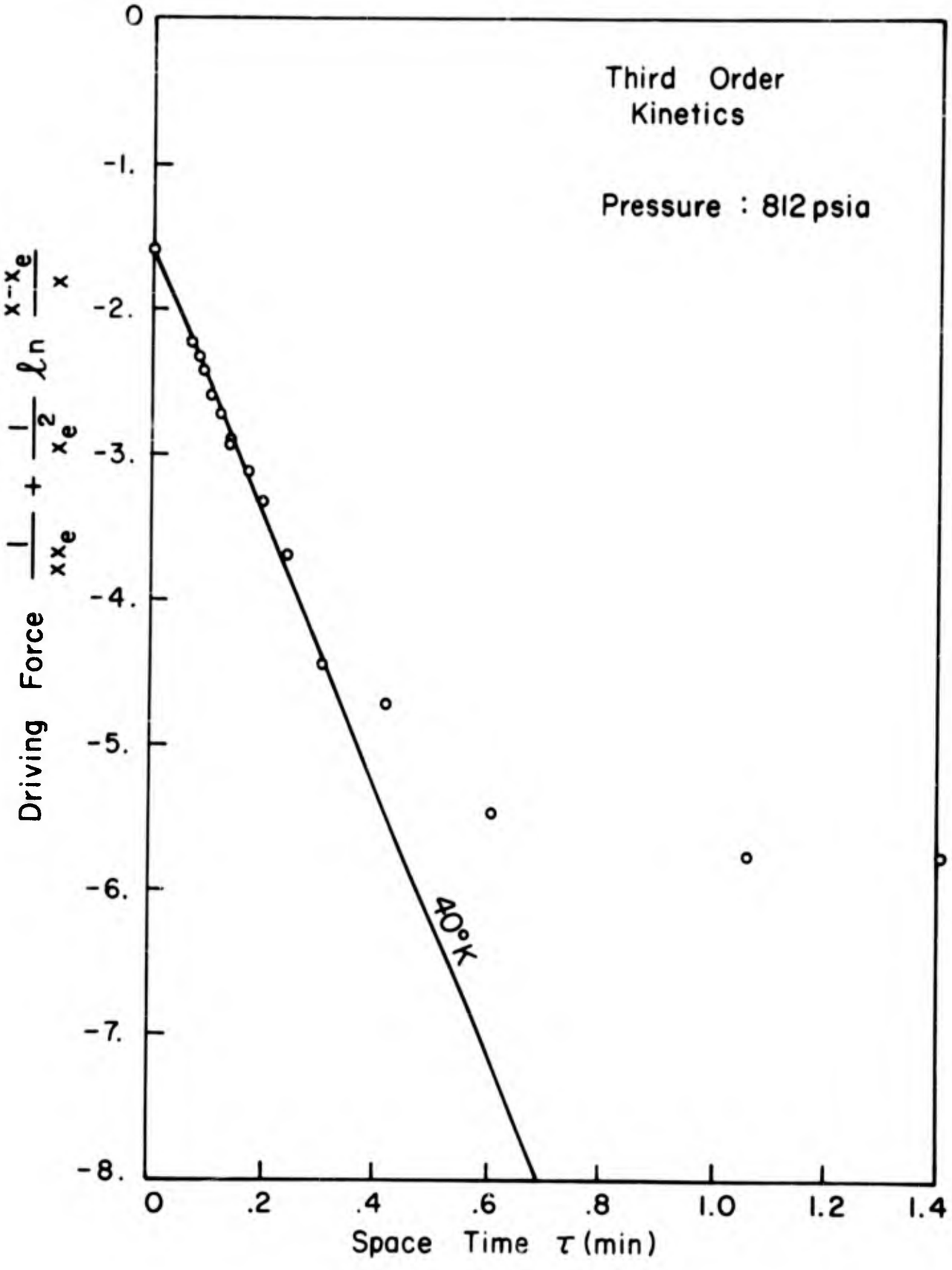
Third Order
Kinetics
Pressure : 812 psia
40°K
Driving Force $\frac{1}{xx_e} + \frac{1}{x_e^2} \ln \frac{x-x_e}{x}$
Space Time $\tau$ (min)
0
-1.
-2.
-3.
-4.
-5.
-6.
-7.
-8.
0
.2
.4
.6
.8
1.0
1.2
1.4

Figure II 22

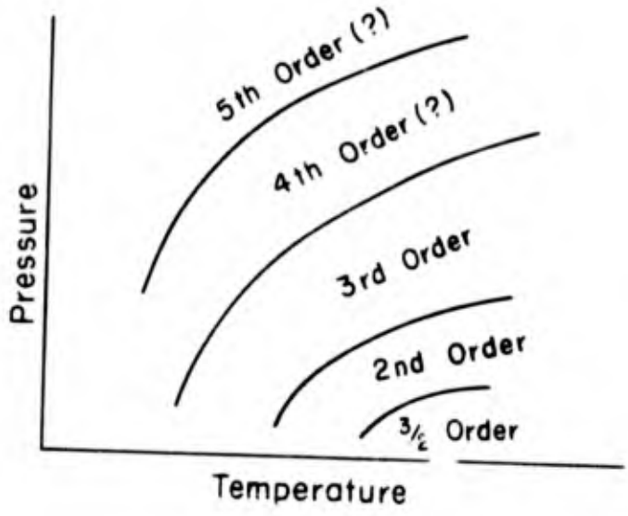


Figure A
Empirical Orders

It was next decided that, since the data were primarily intended for design usuage, perhaps an empirical rate expression might correlate the data. There were two rate expressions tried. These were

$$r = k\,(x - x_e)^{3/2} \tag{II-14}$$

$$r = k\,(x - x_e)^{n} \qquad n \neq 1 \tag{II-15}$$

If eq. (II-14) is integrated, the expression is

$$\frac{k}{2}\,\tau = (x - x_e)^{-1/2} - (x_o - x_e)^{-1/2} \tag{II-16}$$

Figs. II-23 and II-24 show typical plots of $\tau$ vs. $(x - x_e)^{-1/2}$. The correlation here was fair, but was not felt to be adequate. If Eq. (II-15) is integrated, the form is

$$-(-n+1)\,k\tau = (x - x_e)^{-n+1} - (x_o - x_e)^{-n+1} \tag{II-17}$$

If $\tau$ is plotted vs. $(x - x_e)$ on log-log coordinates, the resulting slope is $-(-n + 1)$. This plot was made and a least squares straight line drawn. Fig. II-25 is a typical plot of the data with the least squares line drawn. This showed no correlation of the type of Eq. (II-15), so the empirical approach was abandoned.

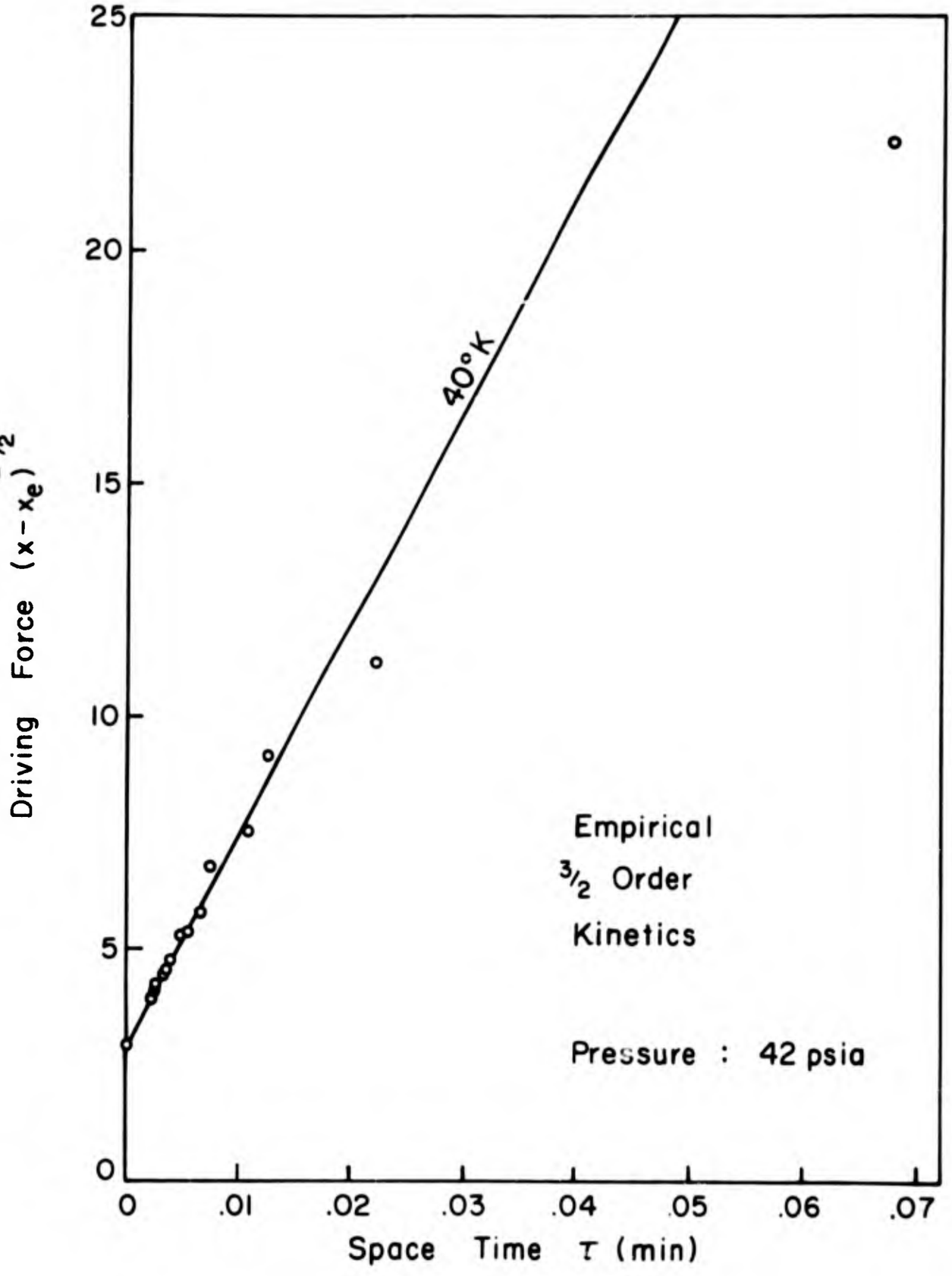
25
20
15
10
5
0
0
.01
.02
.03
.04
.05
.06
.07
Driving Force $(x - x_e)^{-1/2}$
Space Time $\tau$ (min)
40°K
Empirical
3/2 Order
Kinetics
Pressure : 42 psia

Figure II 23

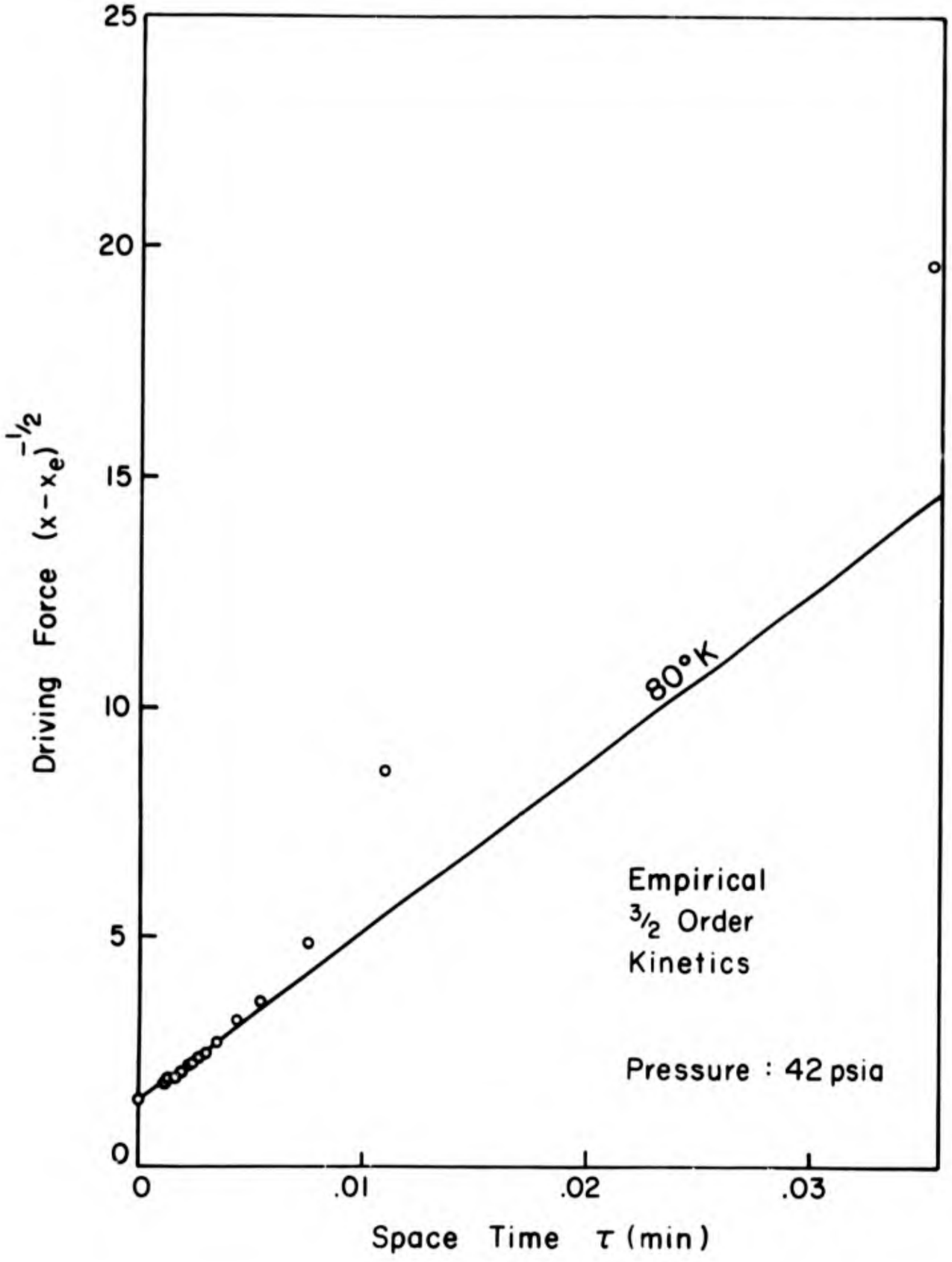
25
20
15
10
5
0
0
.01
.02
.03
Driving Force $(x-x_e)^{-1/2}$
Space Time $\tau$ (min)
80°K
Empirical
3/2 Order
Kinetics
Pressure : 42 psia

Figure II 24

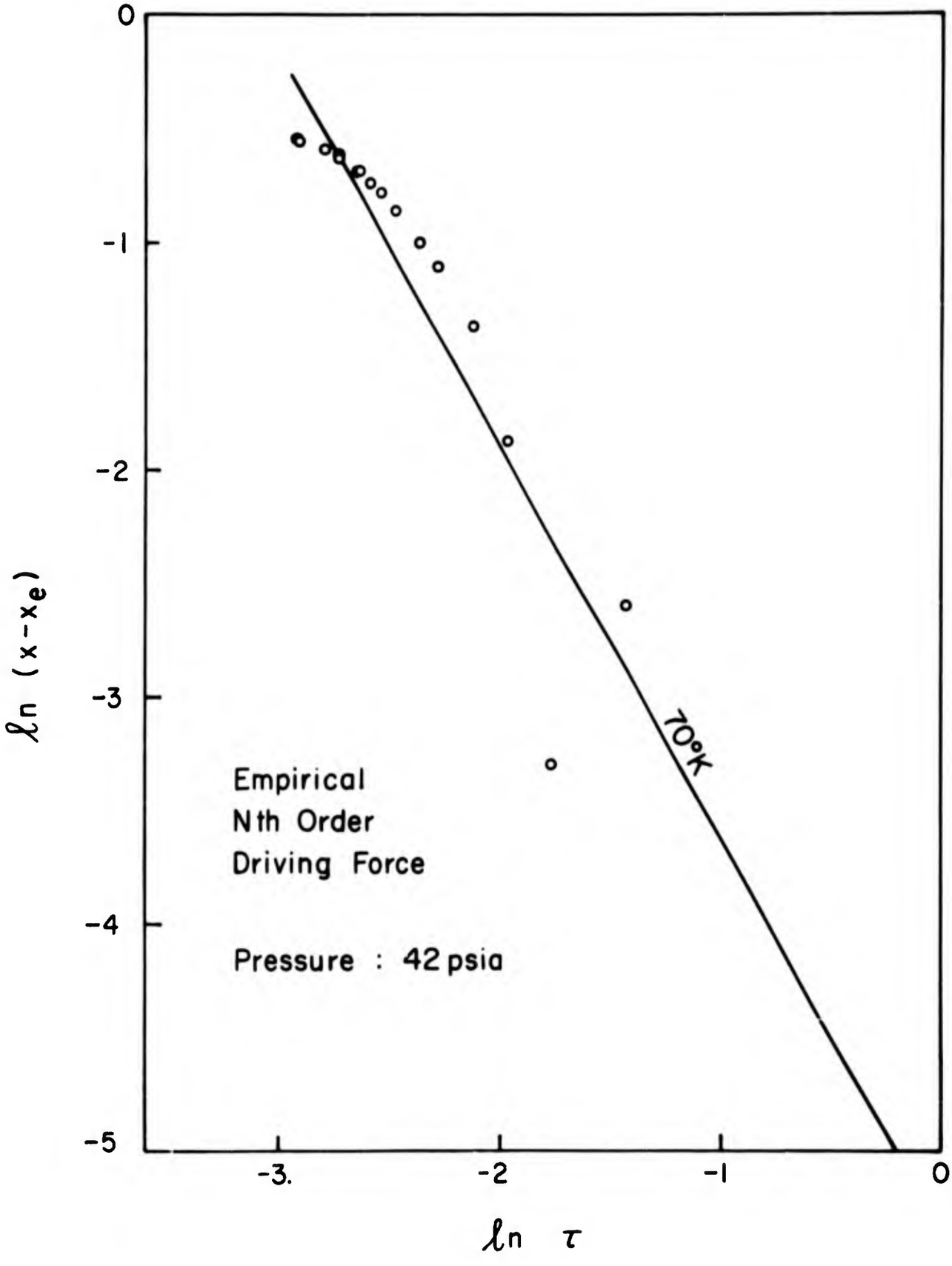
0
-1
-2
-3
-4
-5
-3.
-2
-1
0
ln (x-xe)
ln τ
70°K
Empirical
Nth Order
Driving Force
Pressure : 42 psia

Figure II 25

A summary of the different rate expressions that have been listed thus far is presented in Table II-I. A survey of the success of these various expressions in correlating the data from different operating conditions is also presented in this table.

## Rate Law

It was found that the data were satisfactorily correlated by the rate law given by Eq. (II-18).

$$r = \frac{k(c_p - c_{pe})}{1 + k'c_p} \qquad \text{(II-18)}$$

in which $c_p$ is the parahydrogen concentration. The integrated form of this rate law is presented in Eq. (II-19), which illustrates how the data were plotted to obtain the rate constants.

$$\frac{\ln \left(\frac{x - x_e}{x_o - x_e}\right)}{(x - x_o)} = \frac{-k}{1 + k'c_H x_e} \cdot \frac{\tau}{(x - x_o)} - \frac{k'c_H}{1 + k'c_H x_e} \qquad \text{(II-19)}$$

Here, it can be seen that a plot of $\ln [(x - x_e)/(x_o - x_e)]/(x - x_o)$ vs. $\tau/(x - x_o)$ should give a straight line of slope $- k/(1 + k' c_H x_e)$ and intercept $- k'c_H/(1 + k'c_H x_e)$. This enables k and k' to be determined.

Table II-II summarizes the values of the rate constants which were obtained from the data. The plots of Eq. (II-19), using the data from the different runs, are presented in Fig. II-29-59.

The rate constants were treated in a semi-empirical manner to determine their pressure and temperature dependence. The rate constant k was plotted on Arrhenius plots. These plots of ln k vs. 1/T were found to fit a straight line fairly well for each pressure. These lines are shown for all runs by Fig. II-26. The activation energy $E^{\ddagger}$ and frequency factor A in the Arrhenius equation were determined from the slopes and intercepts of these lines. The activation energy was found to be nearly constant. Its value ranged from

Table II-I

Summary of Reaction Orders Tried for Correlation

| Run | | Correlation of Order | | | | |
|---|---|---|---|---|---|---|
| Press (psia) | Temp (°K) | 1st | 3/2 | 2nd | 3rd | 3/2 emp. |
| 42 | 40 | none | none | poor | poor | fair |
| " | 50 | none | | good | | none |
| " | 60 | none | poor | good | | poor |
| " | 70 | none | good | none | | none |
| " | 80 | poor | good | none | none | |
| 212 | 40 | none | | poor | none | |
| " | 50 | | | good | | |
| " | 60 | | | good | | |
| " | 70 | | none | good | | |
| " | 80 | | good | none | | |
| 412 | 40 | | | none | none | |
| " | 50 | | | none | good | |
| " | 60 | | | none | | |
| " | 80 | | none | good | none | |
| 612 | 40 | | | none | none | |
| " | 50 | | | | none | |
| " | 60 | | | | fair | |
| " | 70 | | | | good | |

Table II-I (continued)

| Run | | Correlation of Order | | | | |
|---|---|---|---|---|---|---|
| Press (psia) | Temp (°K) | 1st | 3/2 | 2nd | 3rd | 3/2 emp. |
| 612 | 80 | | | none | none | |
| 812 | 40 | | | | none | |
| | 50 | | | | none | |
| | 80 | | | none | none | |
| 1012 | 80 | | | none | none | |

TABLE II-II

Rate constants k and k'

| Constant | Temp (°K) | 42 (psia) | 212 (psia) | 412 (psia) | 612 (psia) | 812 (psia) | 1012 (psia) |
|---|---|---|---|---|---|---|---|
| k * | 40 | 27.9 | 5.84 | 1.69 | 0.745 | 1.37 | 1.095 |
| k' | 40 | 1032 | 153.8 | 55.7 | 40.1 | 32.4 | 30.5 |
| k | 50 | 82.5 | 13.4 | 4.16 | 2.78 | 2.60 | 2.07 |
| k' | 50 | 1110 | 201.4 | 97.3 | 63.1 | 43.7 | 37.9 |
| k | 60 | 133.7 | 20.1 | 11.1 | 5.07 | 4.32 | 3.42 |
| k' | 60 | 1089 | 259 | 112 | 85.7 | 60.5 | 50.4 |
| k | 70 | 192.8 | 27.1 | 18.2 | 9.97 | 6.16 | 5.02 |
| k' | 70 | 1090 | 287 | 122 | 94.7 | 76.0 | 65.3 |
| k | 80 | 202 | 39.0 | 22.4 | 13.7 | 8.45 | 6.74 |
| k' | 80 | 937 | 320 | 126.7 | 112 | 87.8 | 72.5 |

* Units:

k ($min^{-1}$).

k' ($cm^3$ g $mole^{-1}$).

280 cal/mole to 350 cal/mole, with no observable trends. The average value was taken. This gave $E^{\neq} = 317$ cal/mole.

The frequency factors were plotted vs. pressure on log-log coordinates (see Fig. II-27). The plot was linear, a fact which meant that k was proportional to $\Pi^n$. n was found to have a value -1.06. The proportionality constant was 86,500, if $\Pi$ has units of psia. The rate constant k can thus be calculated from the relation

$$k = 86{,}500\ \Pi^{-1.06} \exp\ [-159/T] \qquad \text{(II-20)}$$

where

$n$ = rate constant, $min^{-1}$.

$\Pi$ = total pressure, psia.

$T$ = temperature, °K.

The constant k' was then treated and it was found to be negative. At first, k' was tried for an Arrhenius law correlation. It was found that k' was not well correlated by the Arrhenius law, as the activation energy seemed to be a linear function of pressure at high pressures and became zero at low pressures.

Further treatment yielded the fact that, to a very good degree of approximation, k' was inversely proportional to the hydrogen concentration. A plot of $1/k'$ vs. $c_H$ yielded a straight line, of slope -1.18 (See Fig. II-28). The relationship between k' and $c_H$ is

$$k' = -\frac{0.85}{c_H} \qquad \text{(II-21)}$$

While there is still some deviation of the data from the rate law, particularly at the higher pressures, the form of the rate law given by Eq. (II-18) was found to correlate all the data better than any other form.

## II. 4 Discussion

Since the reaction takes place on a catalytic surface, it is envisioned to occur in a series of steps. These are:

I) Diffusion of reactant from the bulk of the gas to the pore mouth.

II) Diffusion of reactant through the pores to the active sites.

III) Adsorption of reactant onto the catalytic surface.

IV) Chemical conversion of reactant to product on the surface.

V) Desorption of product from the surface.

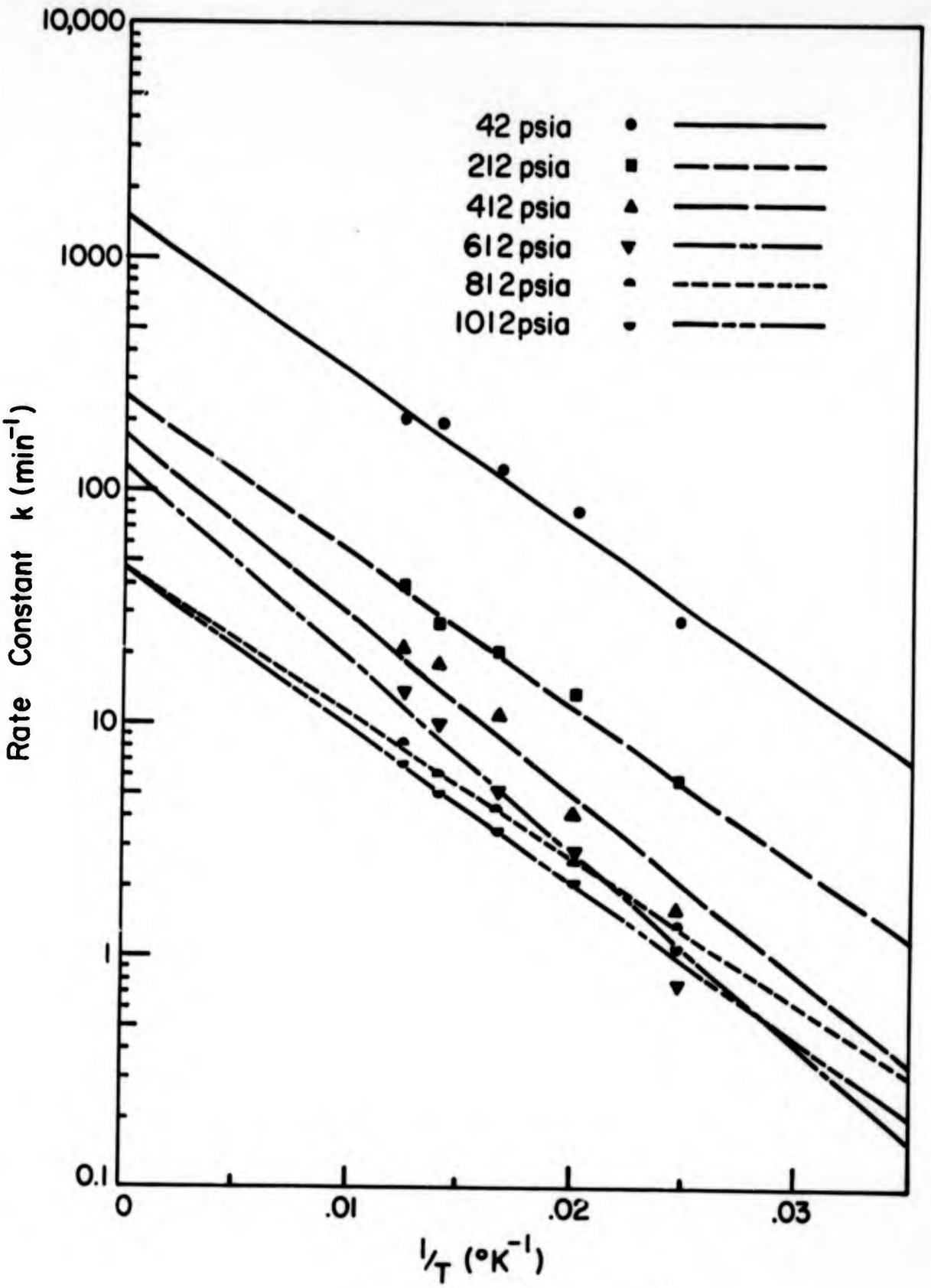


Figure II 26

EFFECT OF TEMPERATURE ON k'

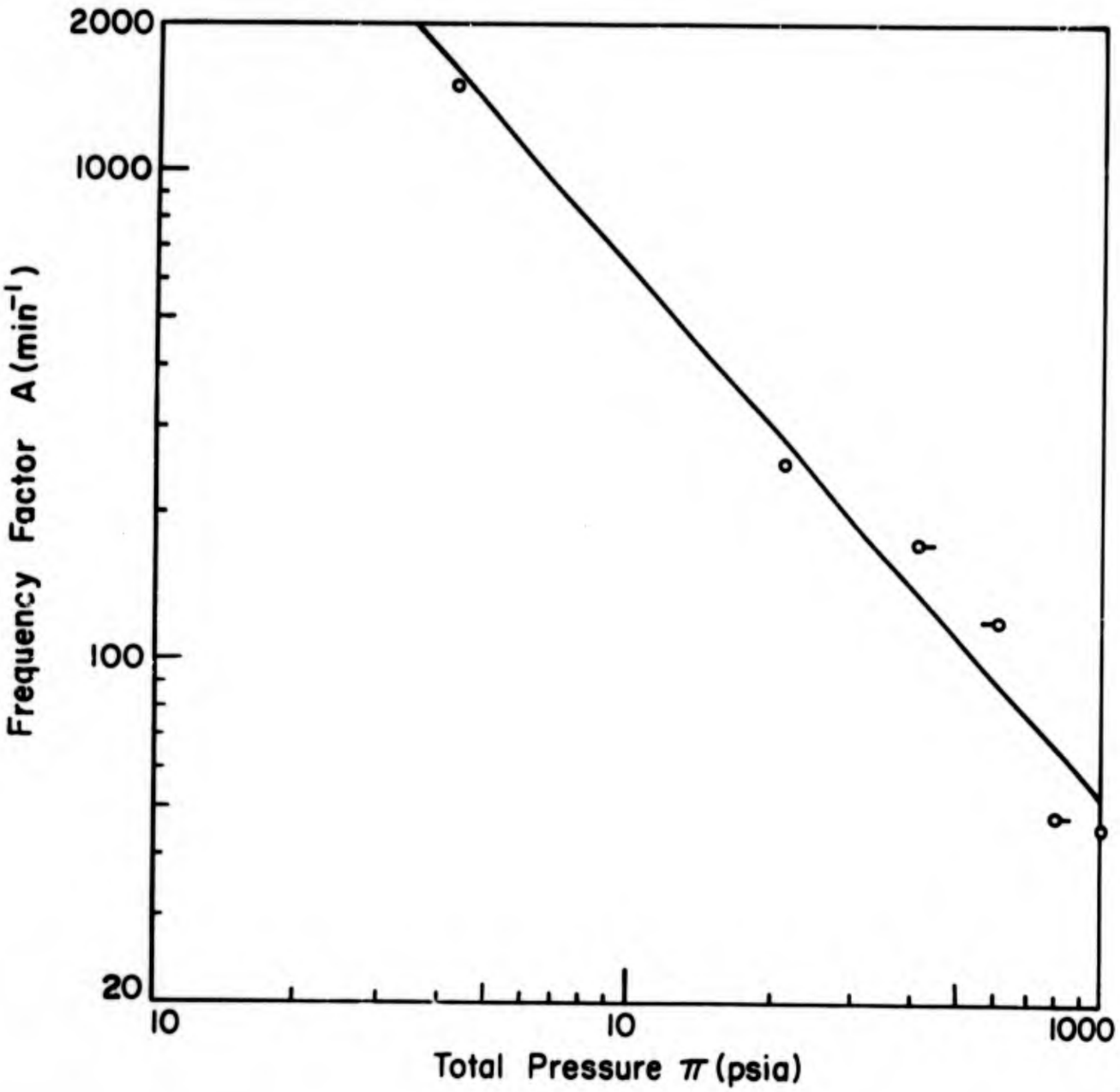


Figure II 27

EFFECT OF PRESSURE ON "A"

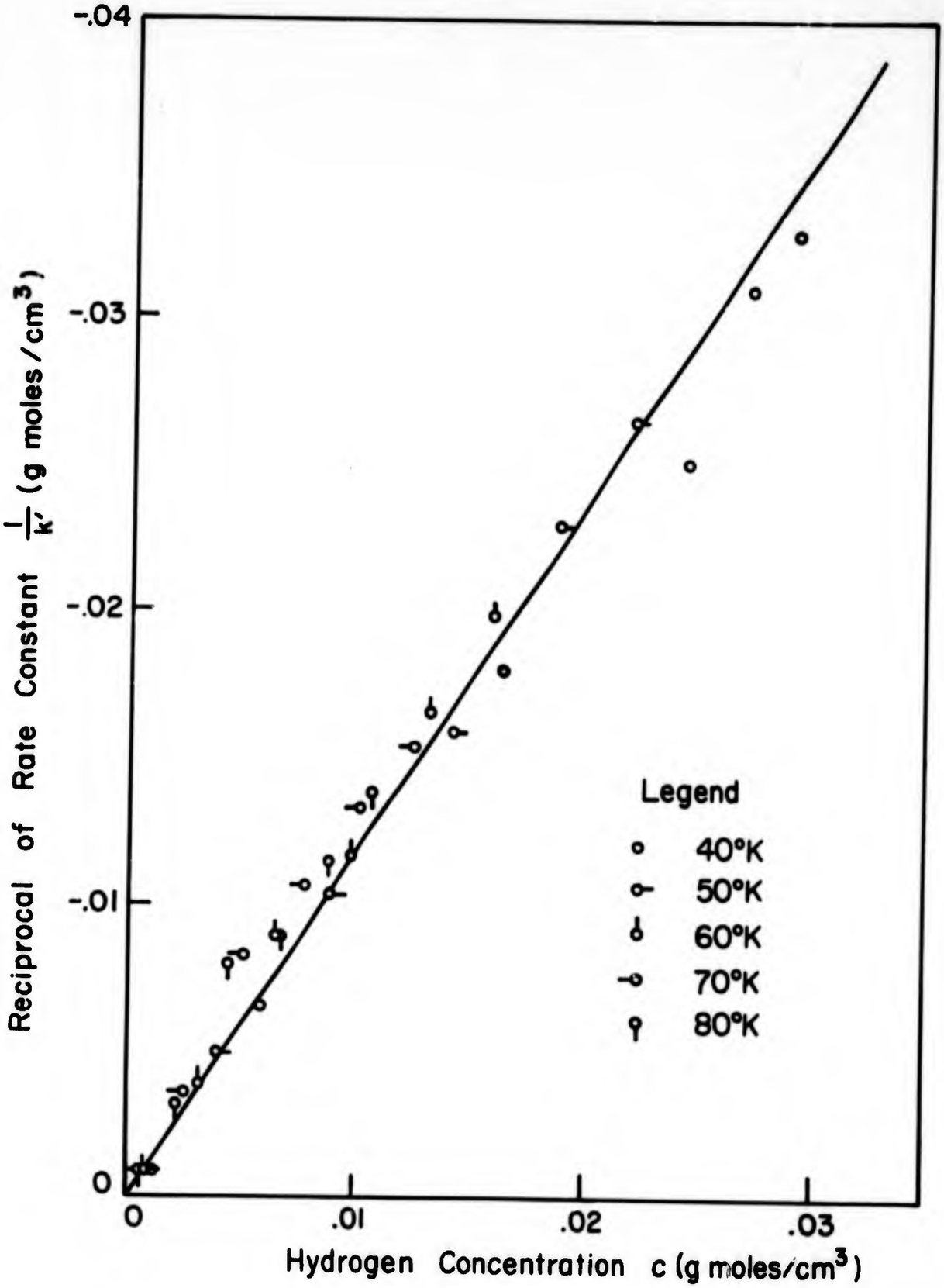


Figure II 28

EFFECT OF PRESSURE ON k'

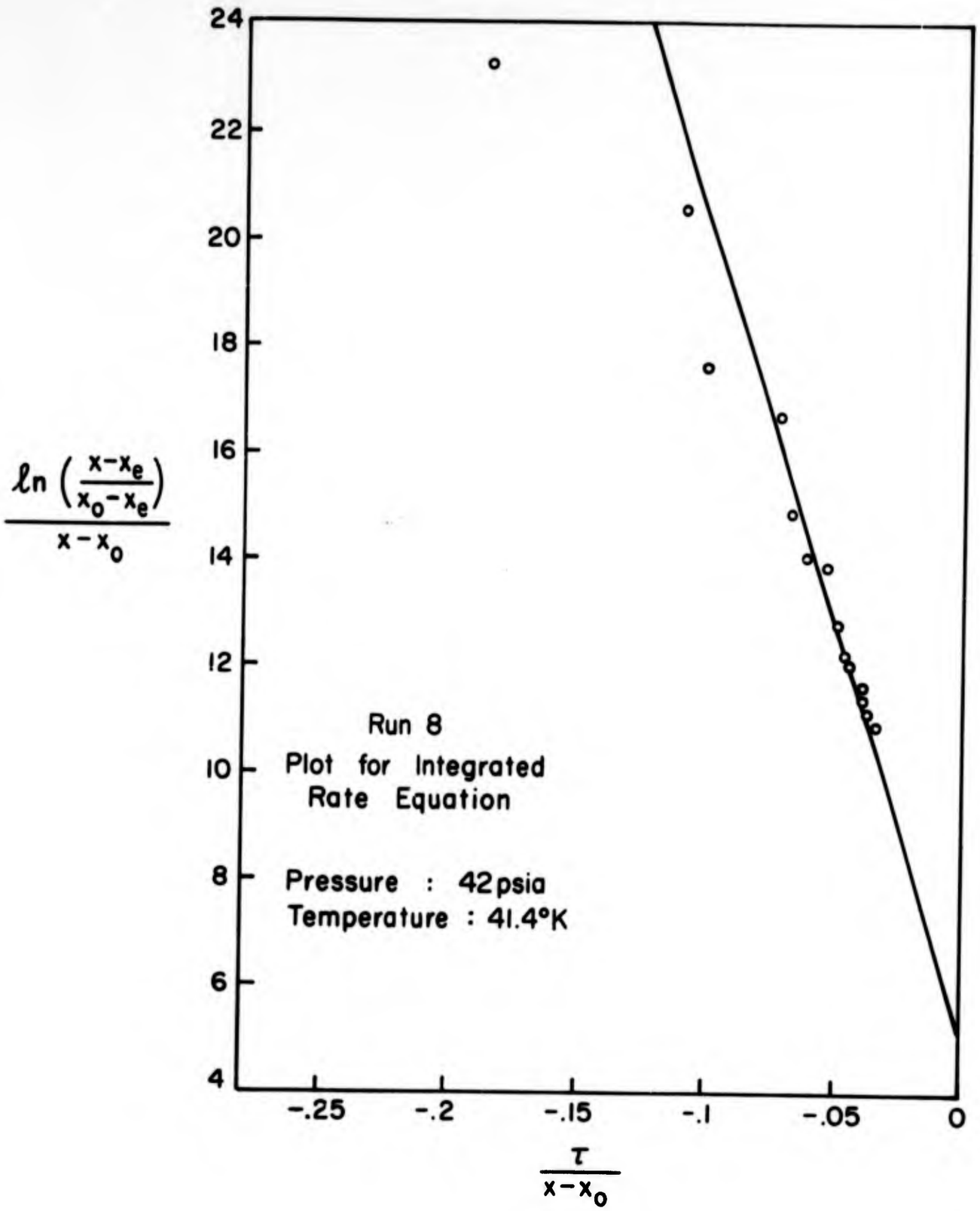
$\frac{\ell n \left(\frac{x-x_e}{x_0-x_e}\right)}{x-x_0}$
24
22
20
18
16
14
12
10
8
6
4
Run 8
Plot for Integrated
Rate Equation
Pressure : 42psia
Temperature : 41.4°K
-.25
-.2
-.15
-.1
-.05
0
$\frac{\tau}{x-x_0}$

Figure II 29

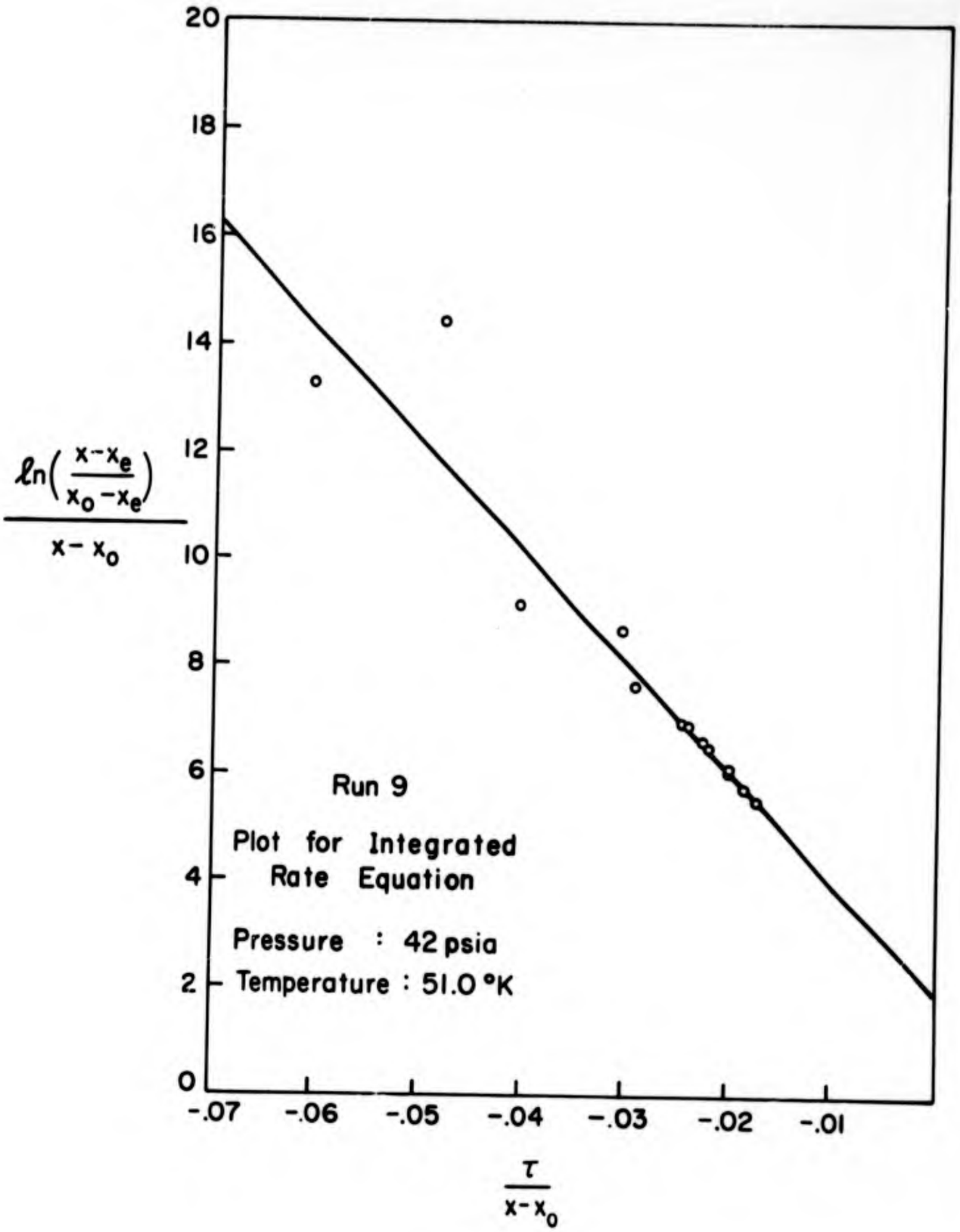
20
18
16
14
12
10
8
6
4
2
0
$\frac{\ell n\left(\frac{x-x_e}{x_0-x_e}\right)}{x-x_0}$
Run 9
Plot for Integrated
Rate Equation
Pressure : 42 psia
Temperature : 51.0 °K
-.07
-.06
-.05
-.04
-.03
-.02
-.01
$\frac{\tau}{x-x_0}$

Figure II 30

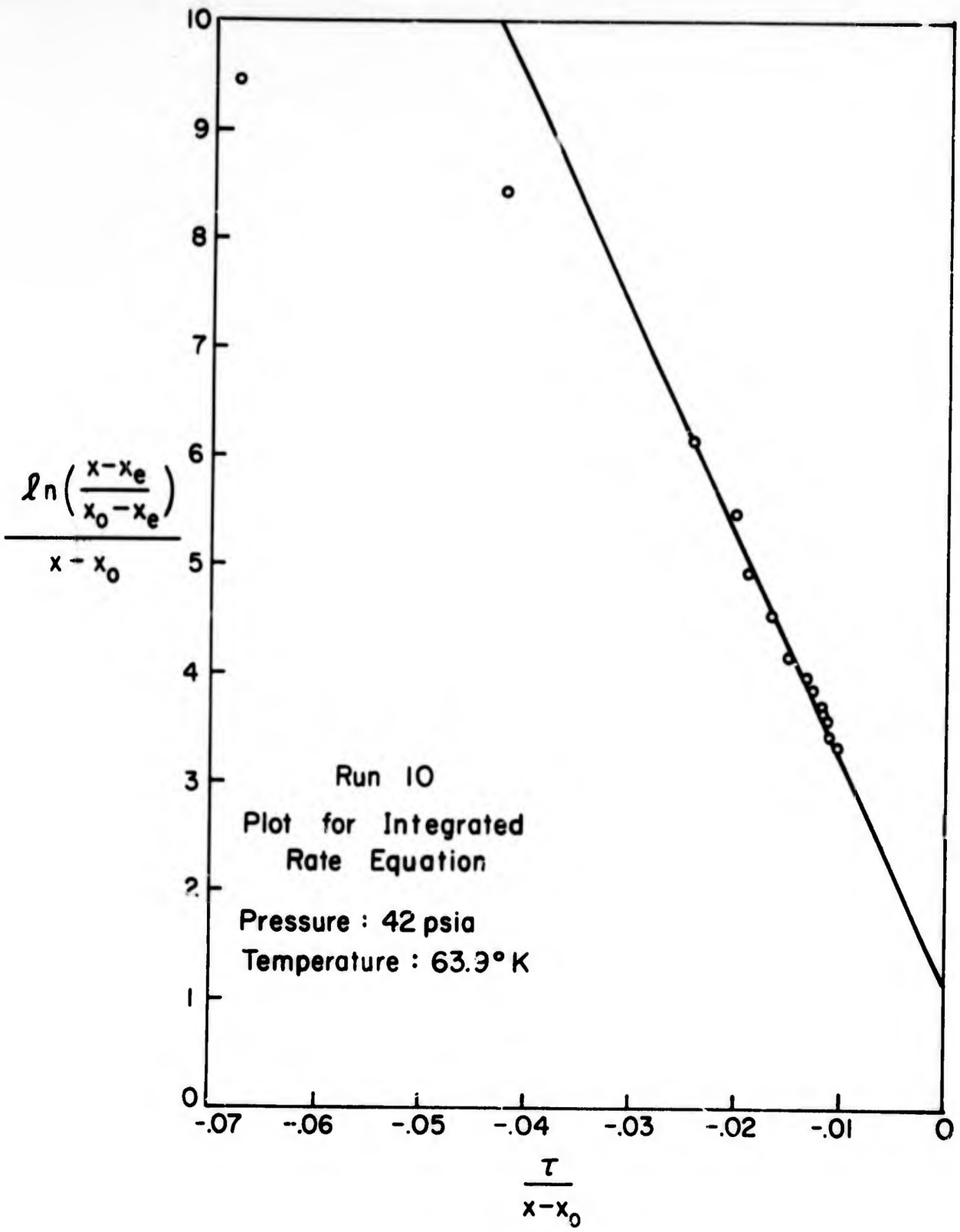
10
9
8
7
6
5
4
3
2
1
0
$\ell n\left(\frac{x-x_e}{x_0-x_e}\right)$
$x - x_0$
Run 10
Plot for Integrated
Rate Equation
Pressure : 42 psia
Temperature : 63.9° K
-.07
-.06
-.05
-.04
-.03
-.02
-.01
0
$\frac{\tau}{x-x_0}$

Figure II 31

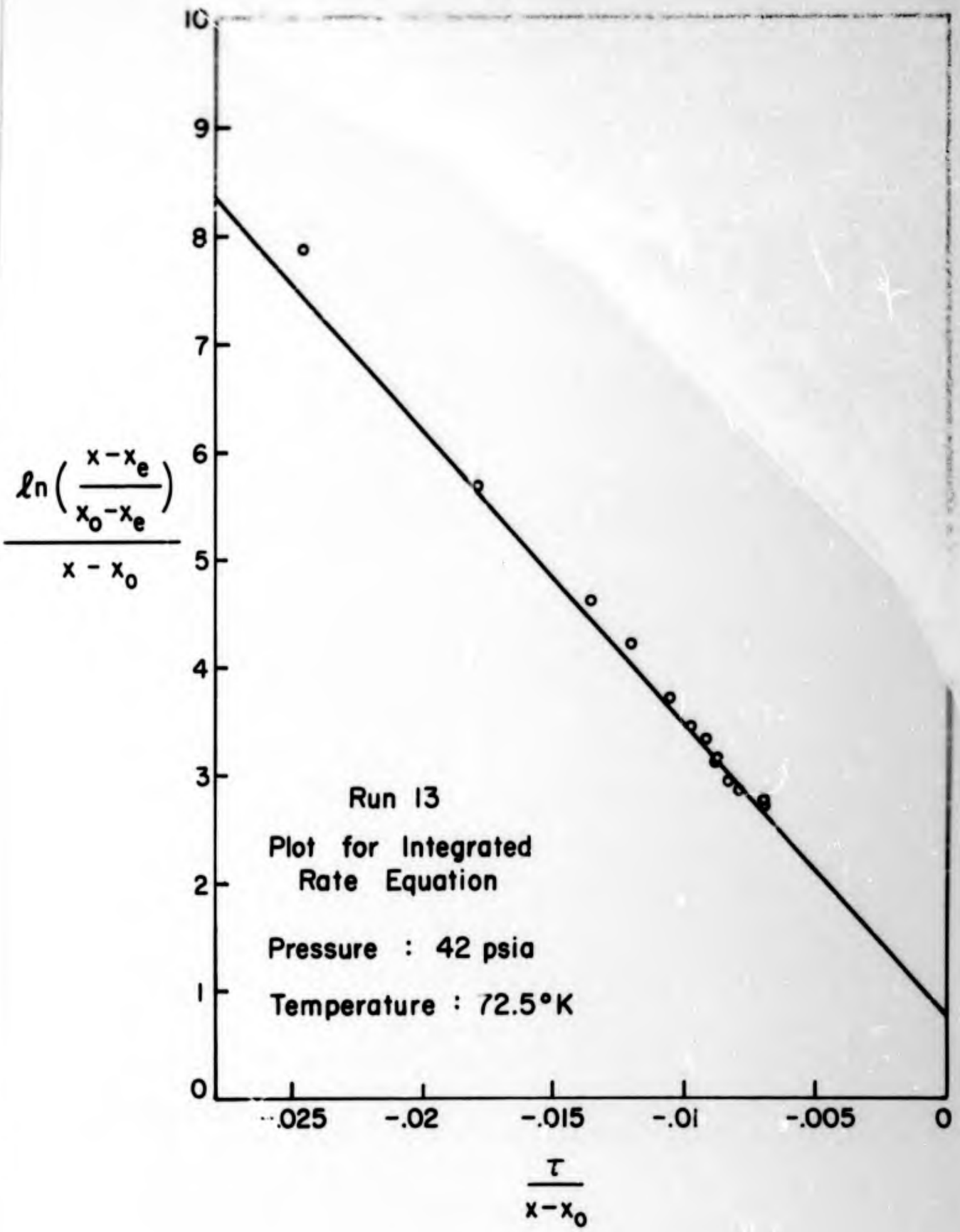
10
9
8
7
6
5
4
3
2
1
0
$\ell n\left(\frac{x-x_e}{x_0-x_e}\right)$
$x - x_0$
Run 13
Plot for Integrated
Rate Equation
Pressure : 42 psia
Temperature : 72.5°K
-.025
-.02
-.015
-.01
-.005
0
$\frac{\tau}{x-x_0}$

Figure II 32

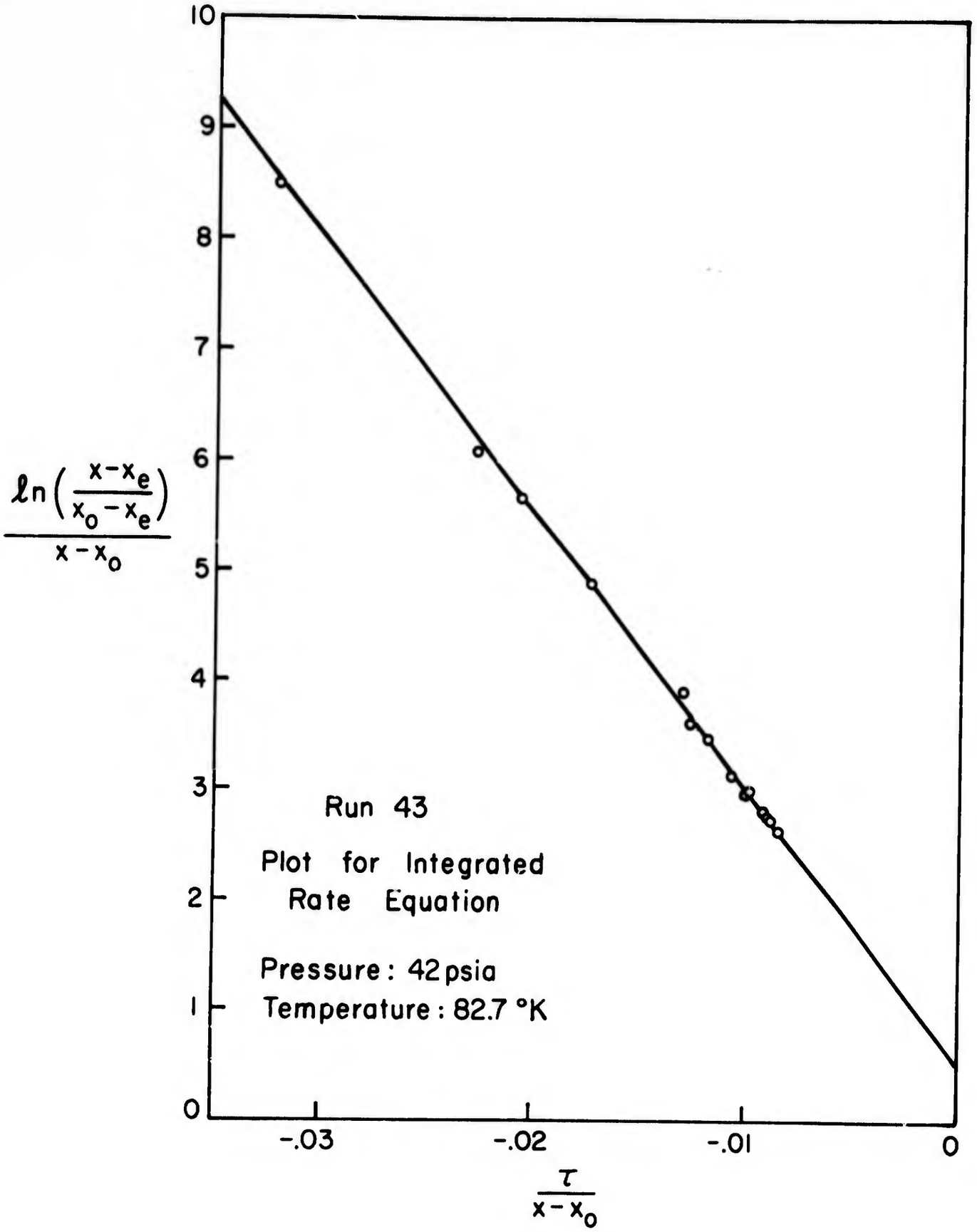
$\frac{\ell n\left(\frac{x-x_e}{x_o-x_e}\right)}{x-x_o}$
10
9
8
7
6
5
4
3
2
1
0
Run 43
Plot for Integrated
Rate Equation
Pressure : 42 psia
Temperature : 82.7 °K
-.03
-.02
-.01
0
$\frac{\tau}{x-x_o}$

Figure II 33

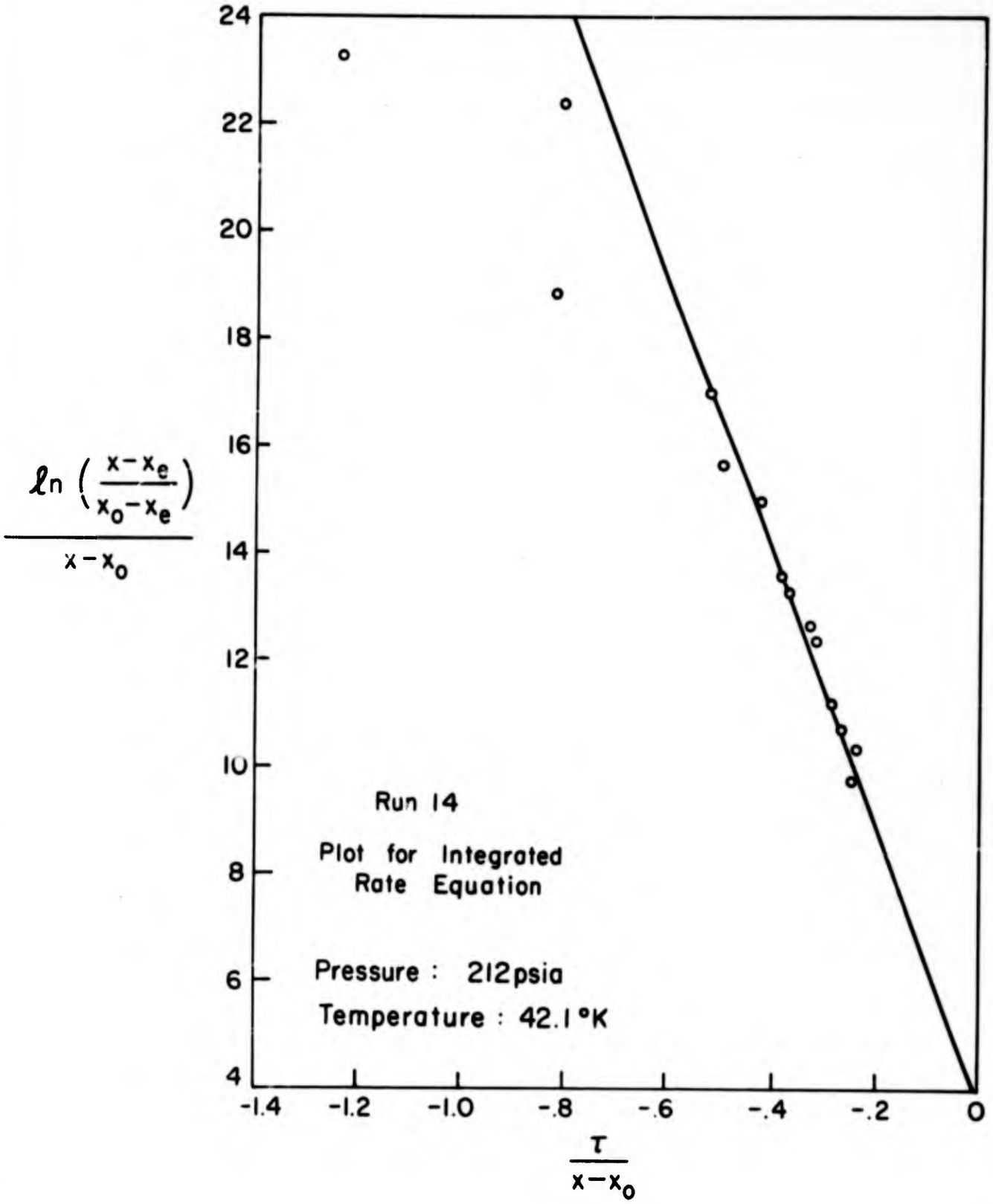
24
22
20
18
16
14
12
10
8
6
4
-1.4
-1.2
-1.0
-.8
-.6
-.4
-.2
0
$\frac{\ln\left(\frac{x-x_e}{x_0-x_e}\right)}{x-x_0}$
$\frac{\tau}{x-x_0}$
Run 14
Plot for Integrated Rate Equation
Pressure : 212psia
Temperature : 42.1 °K

Figure II 34

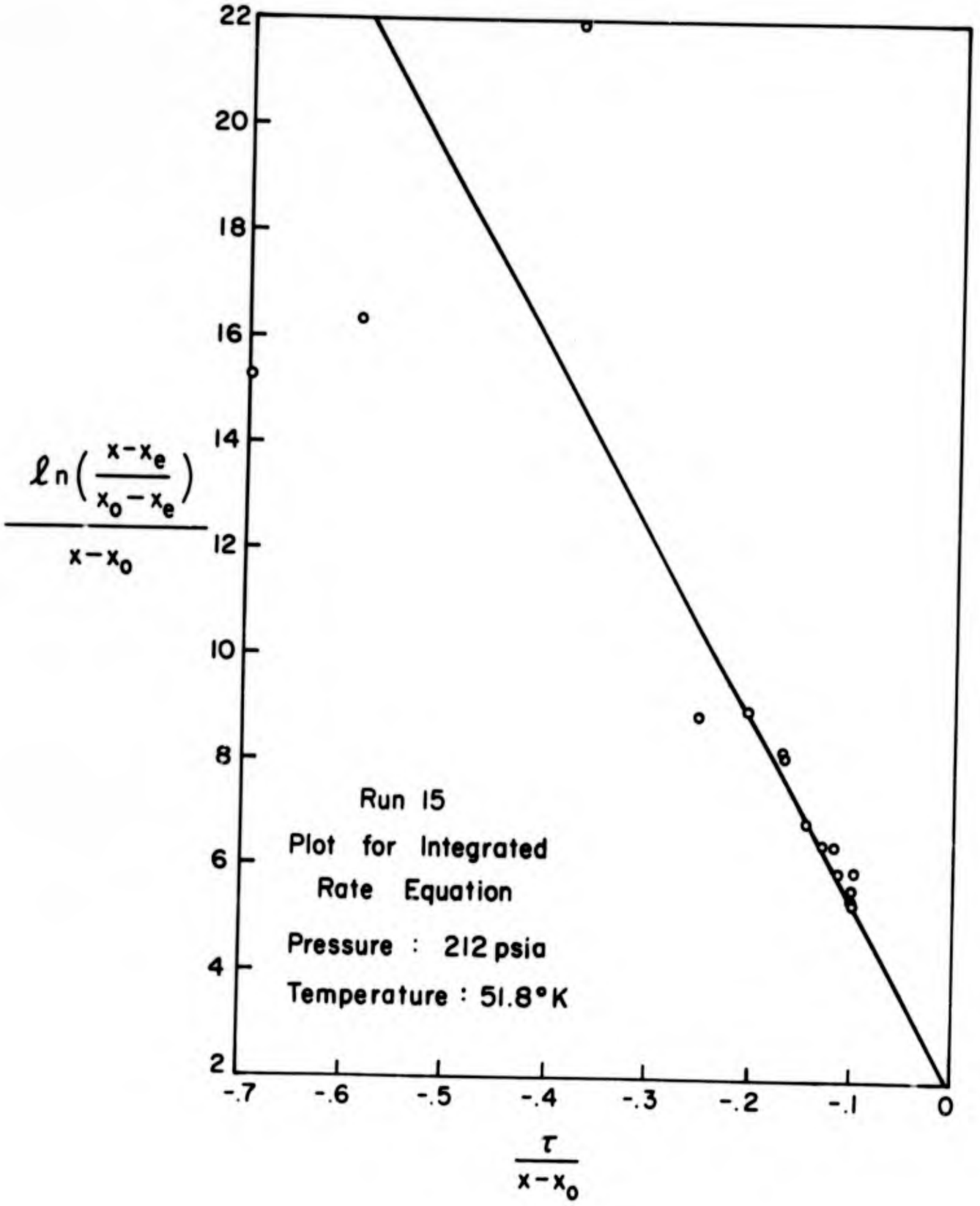
22
20
18
16
14
12
10
8
6
4
2
-.7
-.6
-.5
-.4
-.3
-.2
-.1
0
$\frac{\ell n\left(\frac{x-x_e}{x_0-x_e}\right)}{x-x_0}$
$\frac{\tau}{x-x_0}$
Run 15
Plot for Integrated
Rate Equation
Pressure : 212 psia
Temperature : 51.8°K

Figure II 35

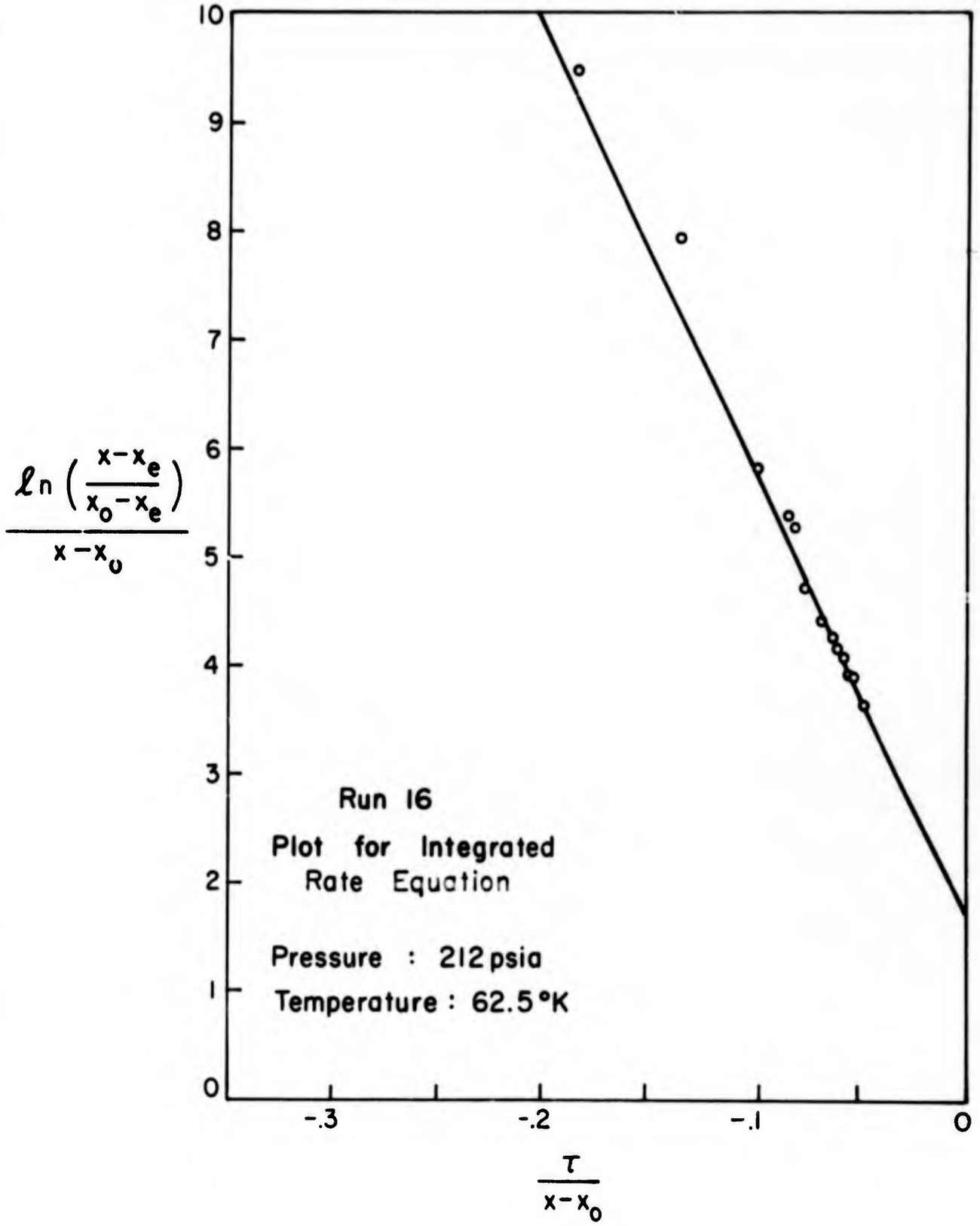
10
9
8
7
6
5
4
3
2
1
0
-.3
-.2
-.1
0
Run 16
Plot for Integrated
Rate Equation
Pressure : 212 psia
Temperature : 62.5 °K
$\frac{\ell n \left( \frac{x-x_e}{x_0-x_e} \right)}{x-x_0}$
$\frac{\tau}{x-x_0}$

Figure II 36

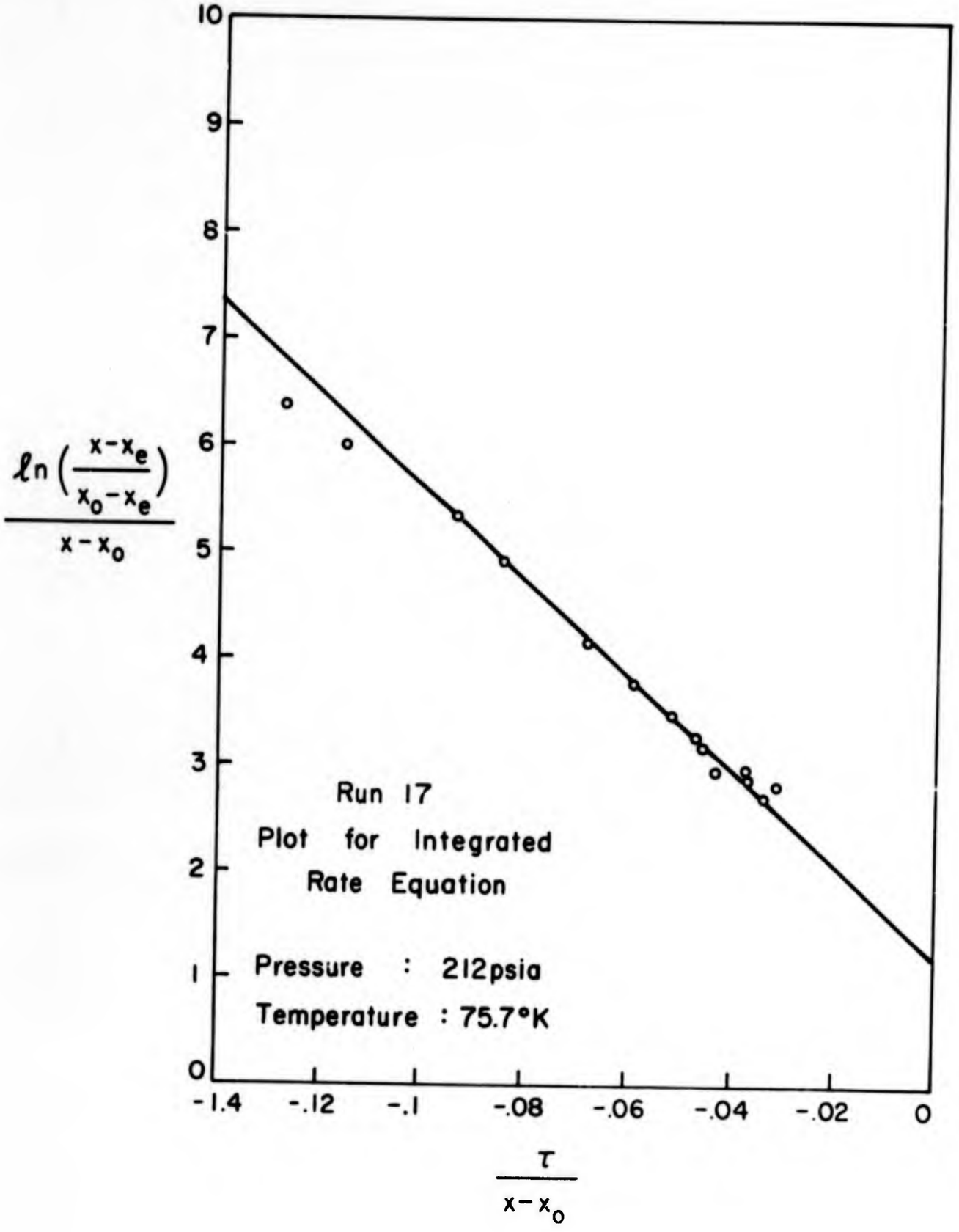
10
9
8
7
6
5
4
3
2
1
0
$\ln\left(\frac{x-x_e}{x_0-x_e}\right)$
$x-x_0$
Run 17
Plot for Integrated
Rate Equation
Pressure : 212psia
Temperature : 75.7°K
-1.4
-.12
-.1
-.08
-.06
-.04
-.02
0
$\frac{\tau}{x-x_0}$

Figure II 37

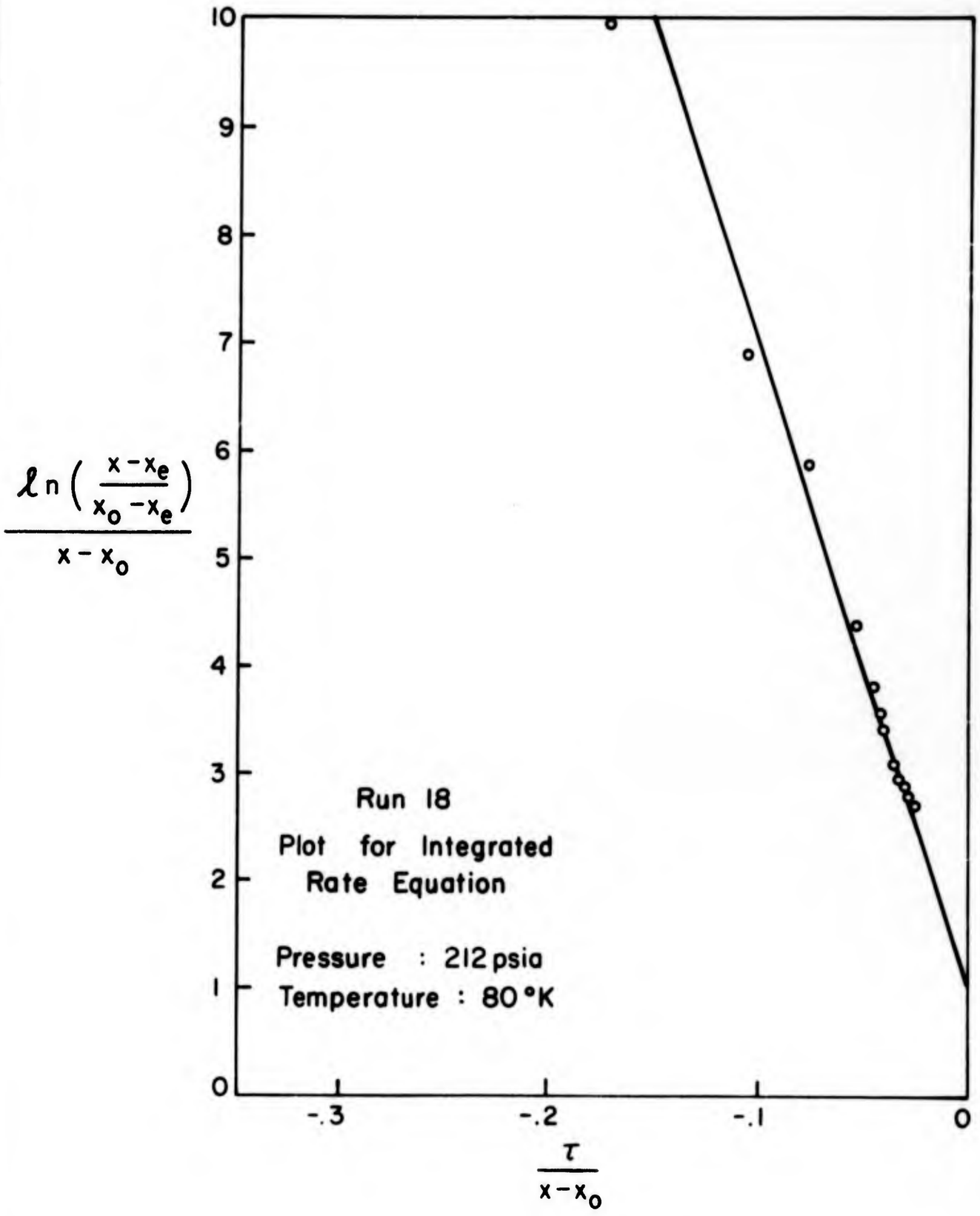
$\frac{\ell n\left(\frac{x-x_e}{x_o-x_e}\right)}{x-x_o}$
10
9
8
7
6
5
4
3
2
1
0
Run 18
Plot for Integrated
Rate Equation
Pressure : 212 psia
Temperature : 80 °K
-.3
-.2
-.1
0
$\frac{\tau}{x-x_o}$

Figure II 38

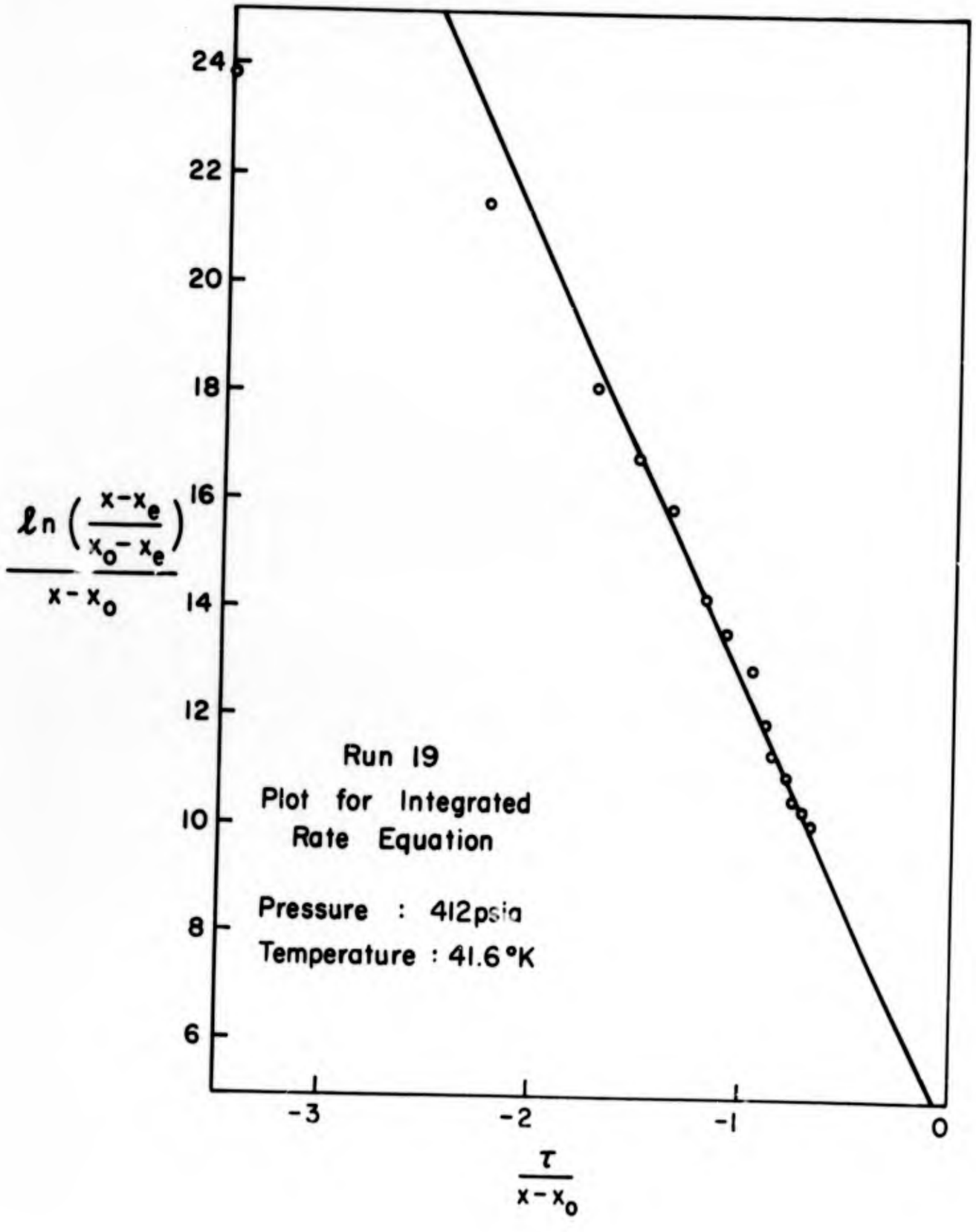
24
22
20
18
16
14
12
10
8
6
$\frac{\ell n\left(\frac{x-x_e}{x_o-x_e}\right)}{x-x_o}$
Run 19
Plot for Integrated
Rate Equation
Pressure : 412psia
Temperature : 41.6°K
-3
-2
-1
0
$\frac{\tau}{x-x_o}$

Figure II 39

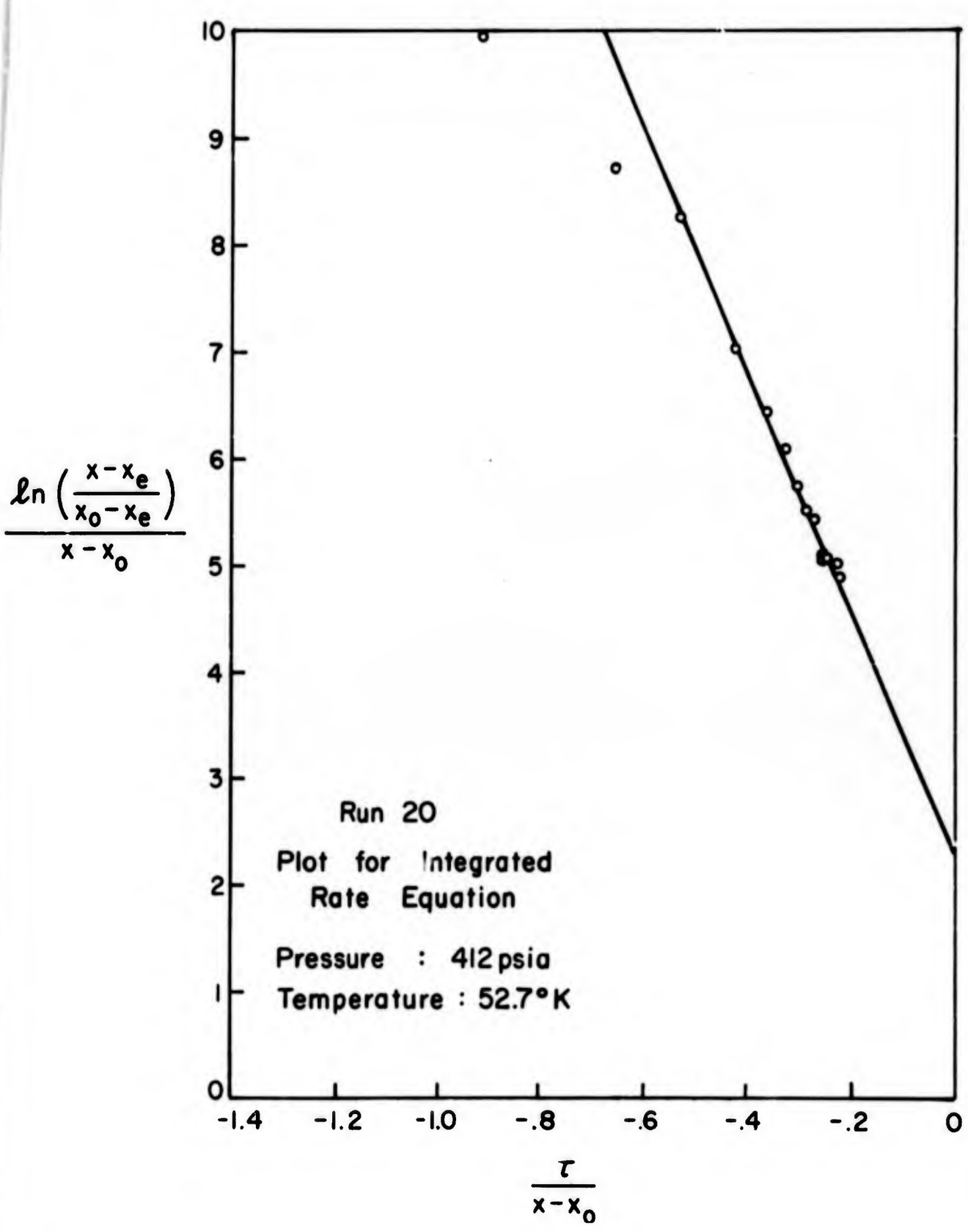
$\frac{\ell n \left(\frac{x-x_e}{x_0-x_e}\right)}{x-x_0}$
10
9
8
7
6
5
4
3
2
1
0
-1.4
-1.2
-1.0
-.8
-.6
-.4
-.2
0
$\frac{\tau}{x-x_0}$
Run 20
Plot for Integrated Rate Equation
Pressure : 412 psia
Temperature : 52.7°K

Figure II 40

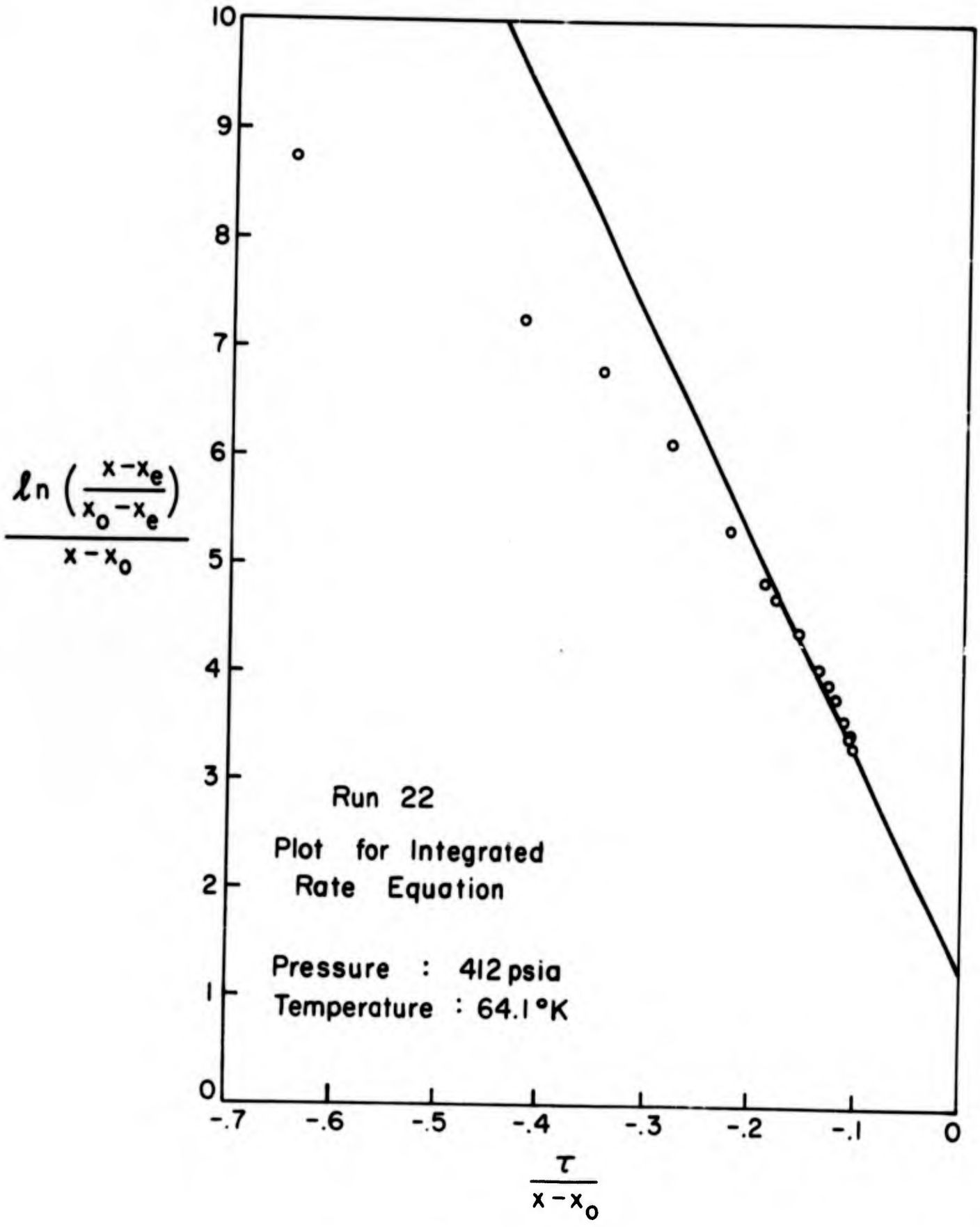
$\frac{\ln\left(\frac{x-x_e}{x_o-x_e}\right)}{x-x_o}$
10
9
8
7
6
5
4
3
2
1
0
Run 22
Plot for Integrated
Rate Equation
Pressure : 412 psia
Temperature : 64.1 °K
-.7
-.6
-.5
-.4
-.3
-.2
-.1
0
$\frac{\tau}{x-x_o}$

Figure II 41

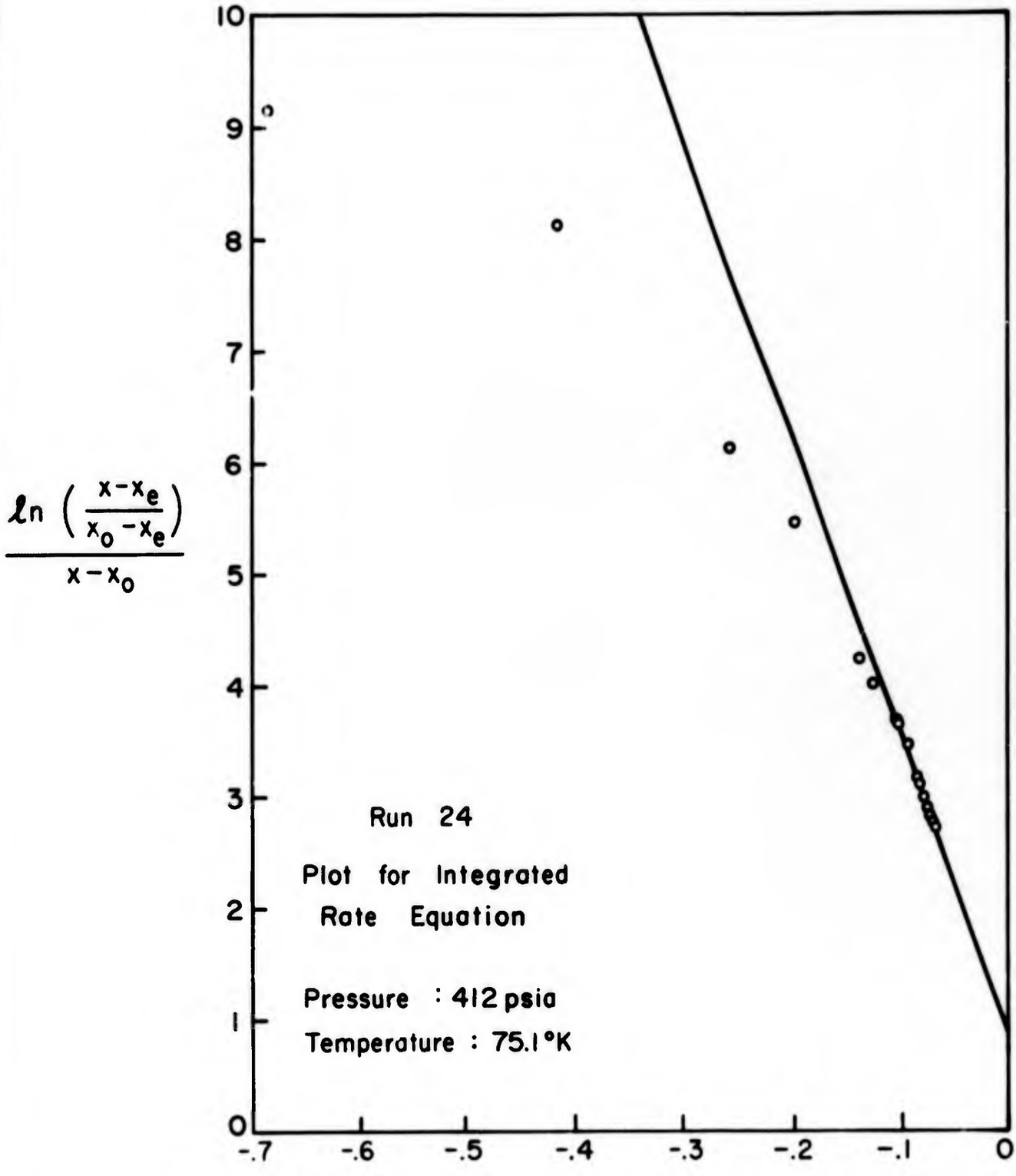
$\frac{\ln\left(\frac{x-x_e}{x_0-x_e}\right)}{x-x_0}$
10
9
8
7
6
5
4
3
2
1
0
-.7
-.6
-.5
-.4
-.3
-.2
-.1
0
Run 24
Plot for Integrated
Rate Equation
Pressure : 412 psia
Temperature : 75.1°K

Figure II 42

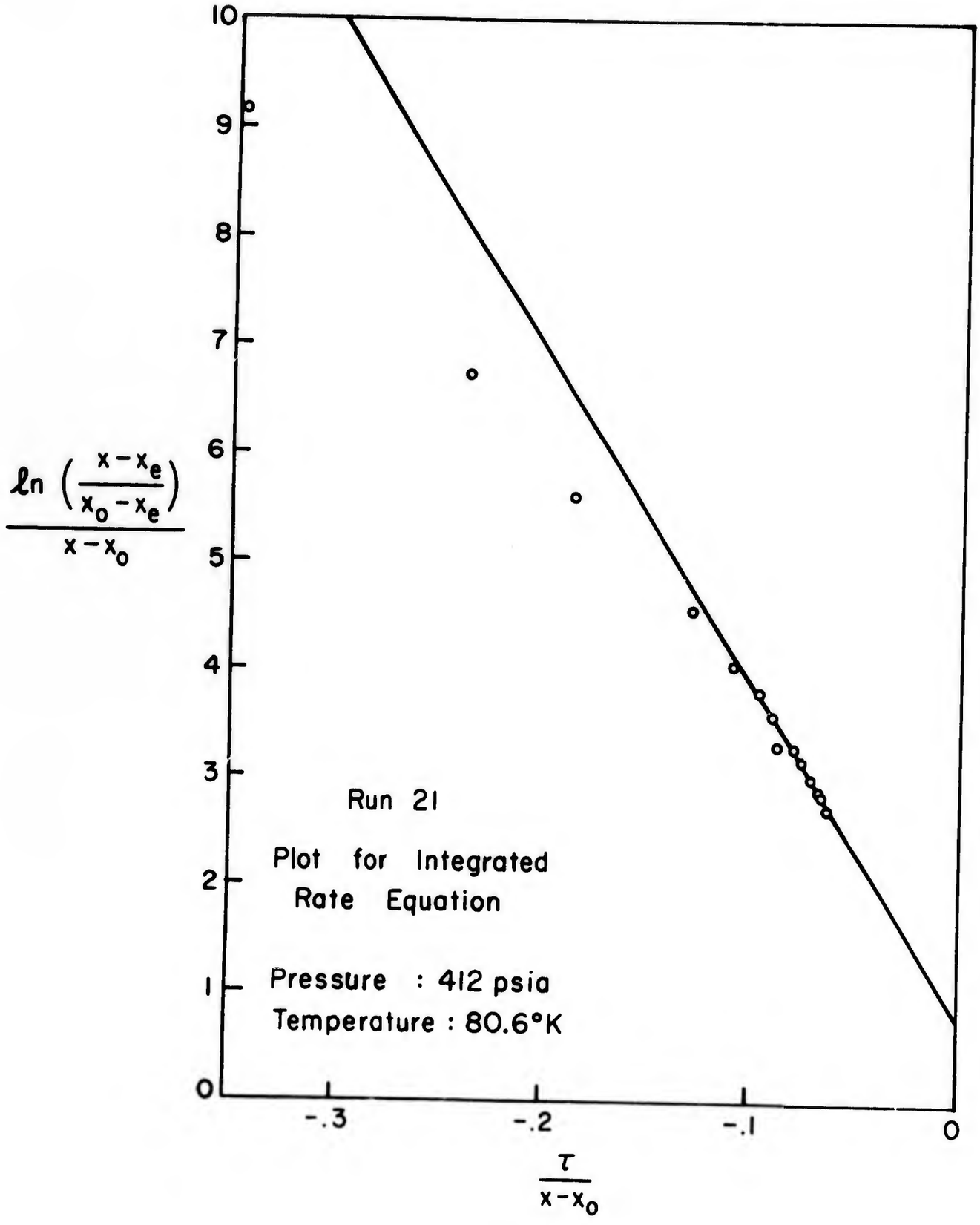
10
9
8
7
6
5
4
3
2
1
0
$\ln\left(\frac{x-x_e}{x_0-x_e}\right)$
$x-x_0$
Run 21
Plot for Integrated
Rate Equation
Pressure : 412 psia
Temperature : 80.6°K
-.3
-.2
-.1
0
$\frac{\tau}{x-x_0}$

Figure II 43

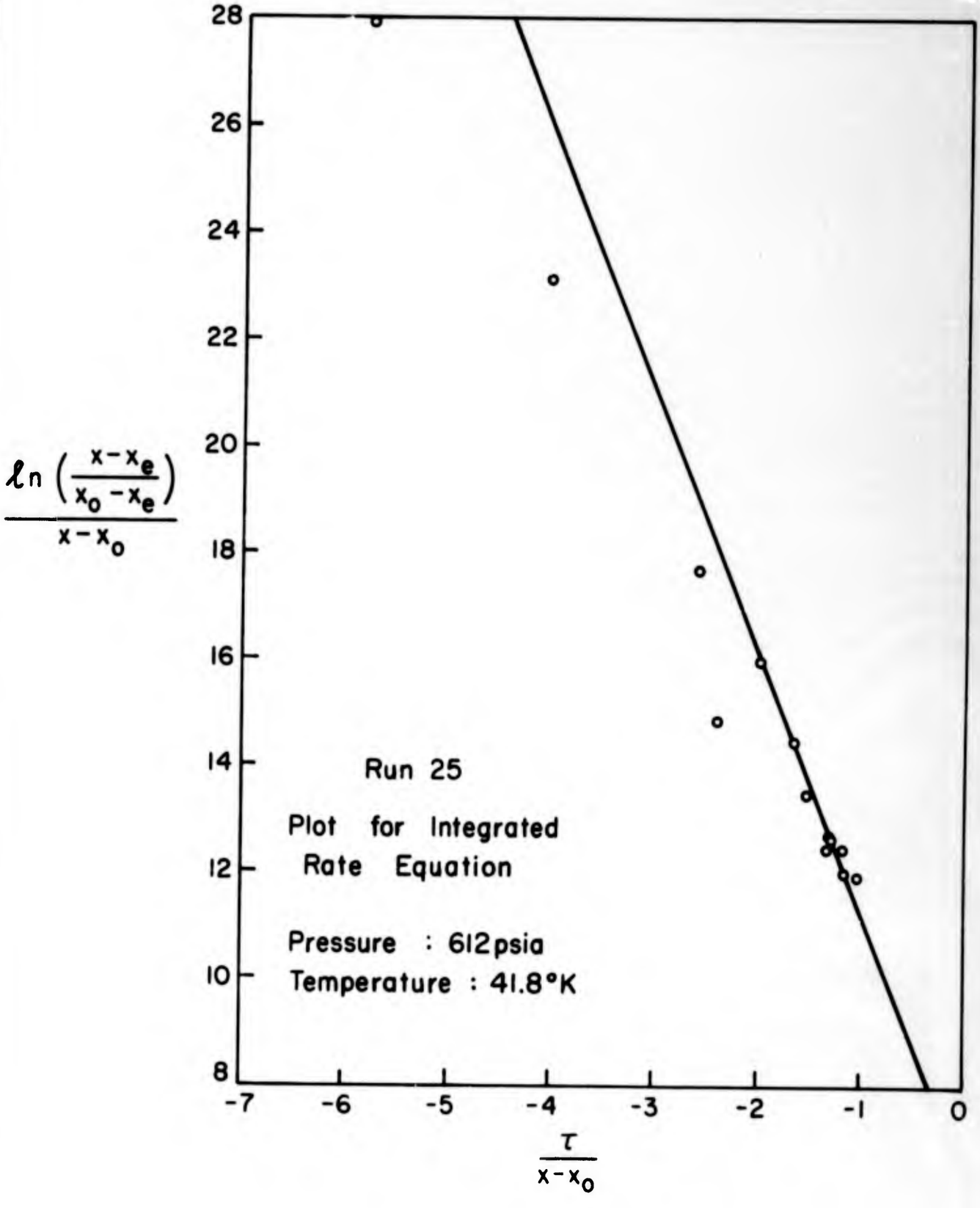
28
26
24
22
20
18
16
14
12
10
8
-7
-6
-5
-4
-3
-2
-1
0
Run 25
Plot for Integrated
Rate Equation
Pressure : 612psia
Temperature : 41.8°K
$\ln\left(\frac{x-x_e}{x_0-x_e}\right)$
$x-x_0$
$\frac{\tau}{x-x_0}$

Figure II 44

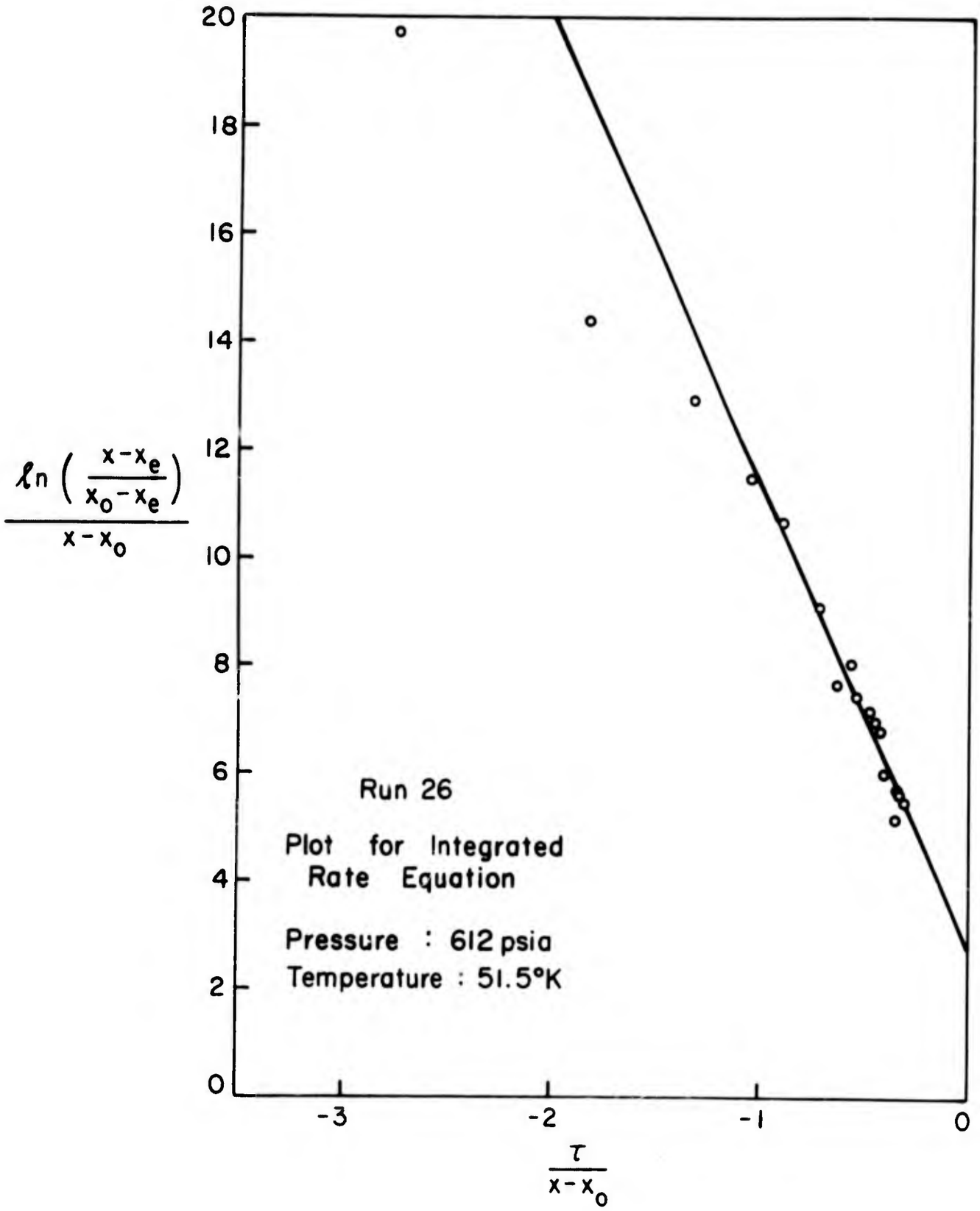
$\frac{\ell n \left( \frac{x-x_e}{x_0-x_e} \right)}{x-x_0}$
20
18
16
14
12
10
8
6
4
2
0
-3
-2
-1
0
$\frac{\tau}{x-x_0}$
Run 26
Plot for Integrated Rate Equation
Pressure : 612 psia
Temperature : 51.5°K

Figure II 45

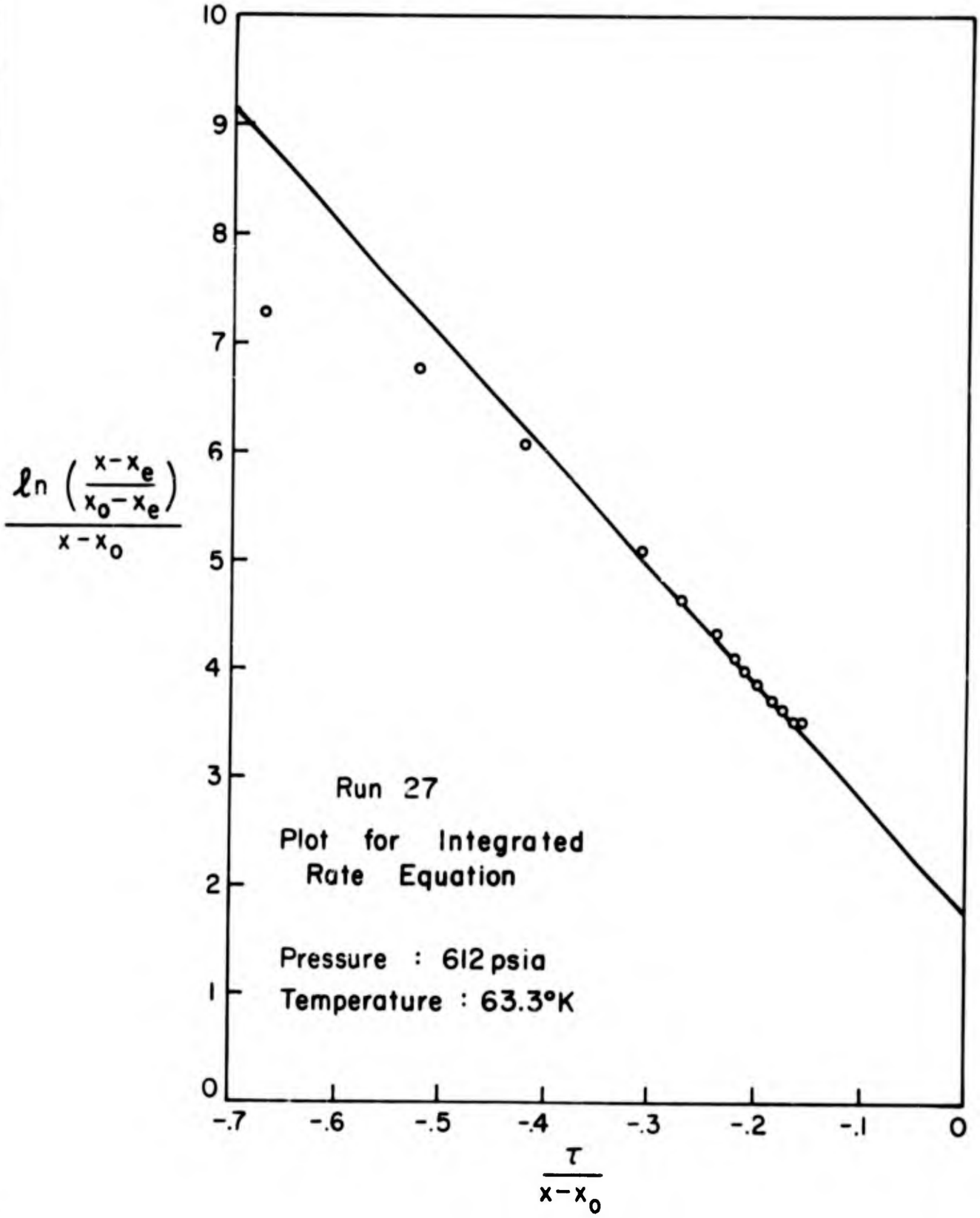
10
9
8
7
6
5
4
3
2
1
0
-.7
-.6
-.5
-.4
-.3
-.2
-.1
0
$\ell n \left(\frac{x-x_e}{x_o-x_e}\right)$
$x-x_o$
$\frac{\tau}{x-x_o}$
Run 27
Plot for Integrated Rate Equation
Pressure : 612 psia
Temperature : 63.3°K

Figure II 46

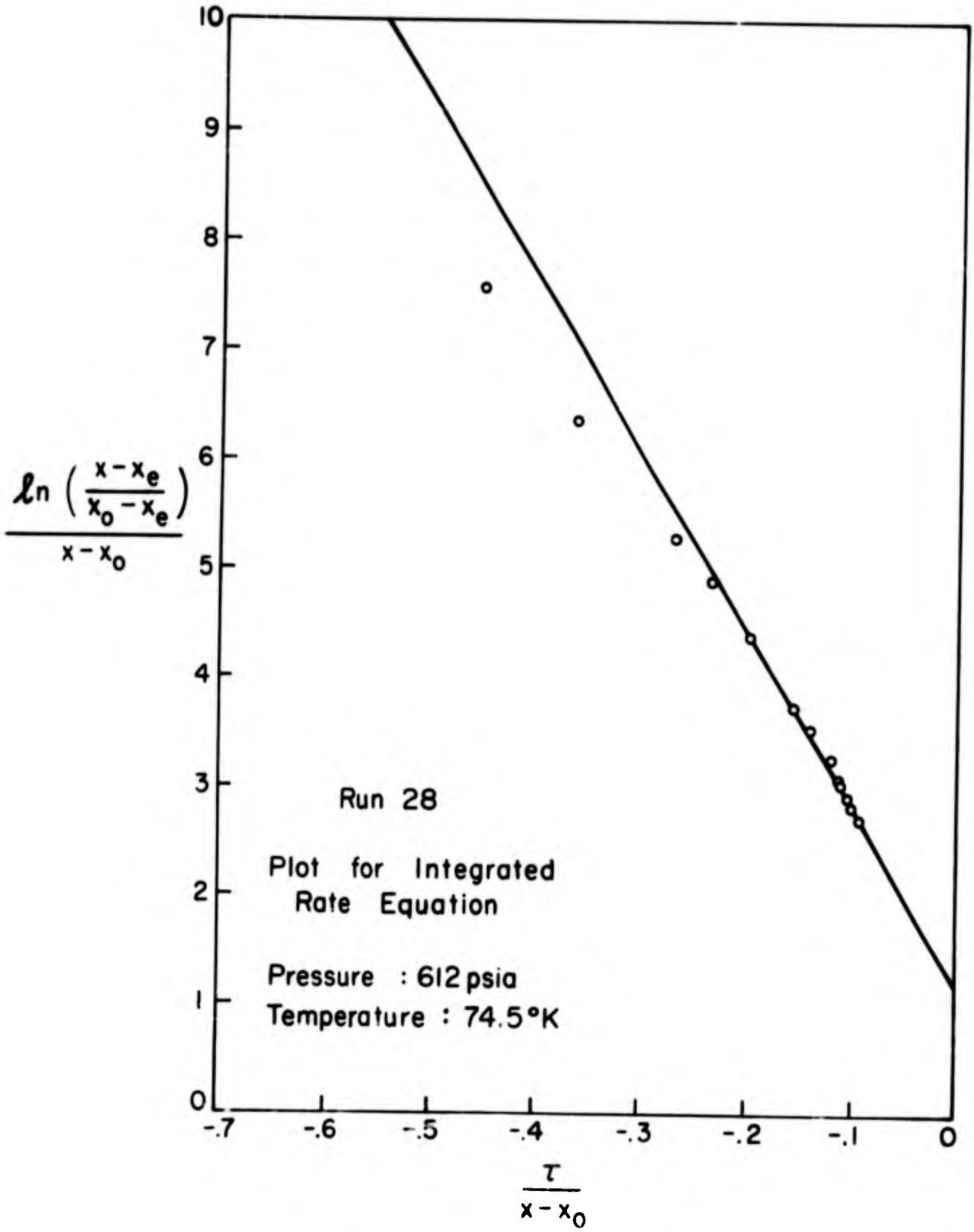
10
9
8
7
6
5
4
3
2
1
0
-.7
-.6
-.5
-.4
-.3
-.2
-.1
0
$\frac{\ell n \left(\frac{x-x_e}{x_o-x_e}\right)}{x-x_o}$
$\frac{\tau}{x-x_o}$
Run 28
Plot for Integrated Rate Equation
Pressure : 612 psia
Temperature : 74.5°K

Figure II 47

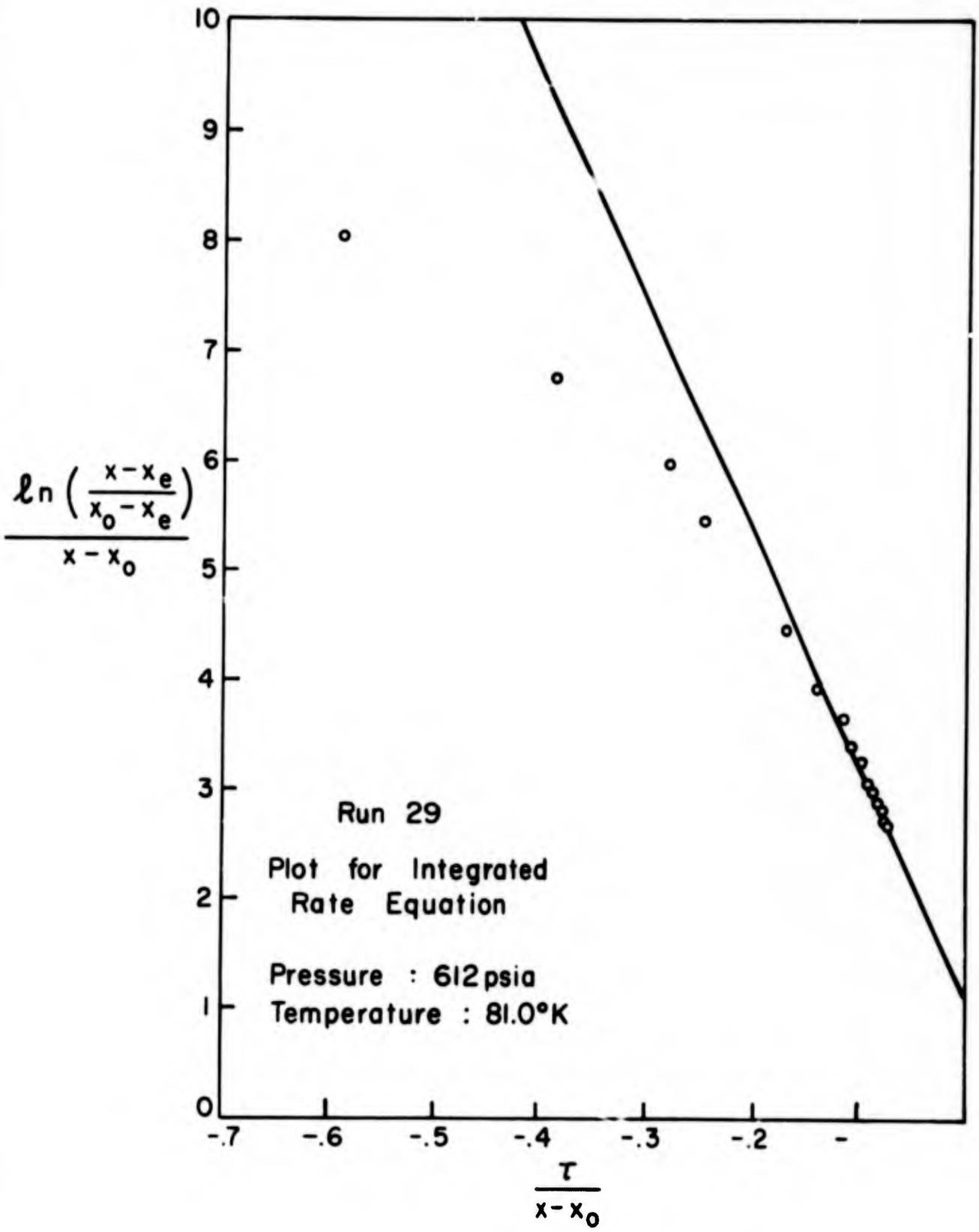
10
9
8
7
6
5
4
3
2
1
0
$\ell n \left( \frac{x - x_e}{x_o - x_e} \right)$
$x - x_o$
Run 29
Plot for Integrated
Rate Equation
Pressure : 612 psia
Temperature : 81.0°K
-.7
-.6
-.5
-.4
-.3
-.2
-
$\frac{\tau}{x - x_o}$

Figure II 48

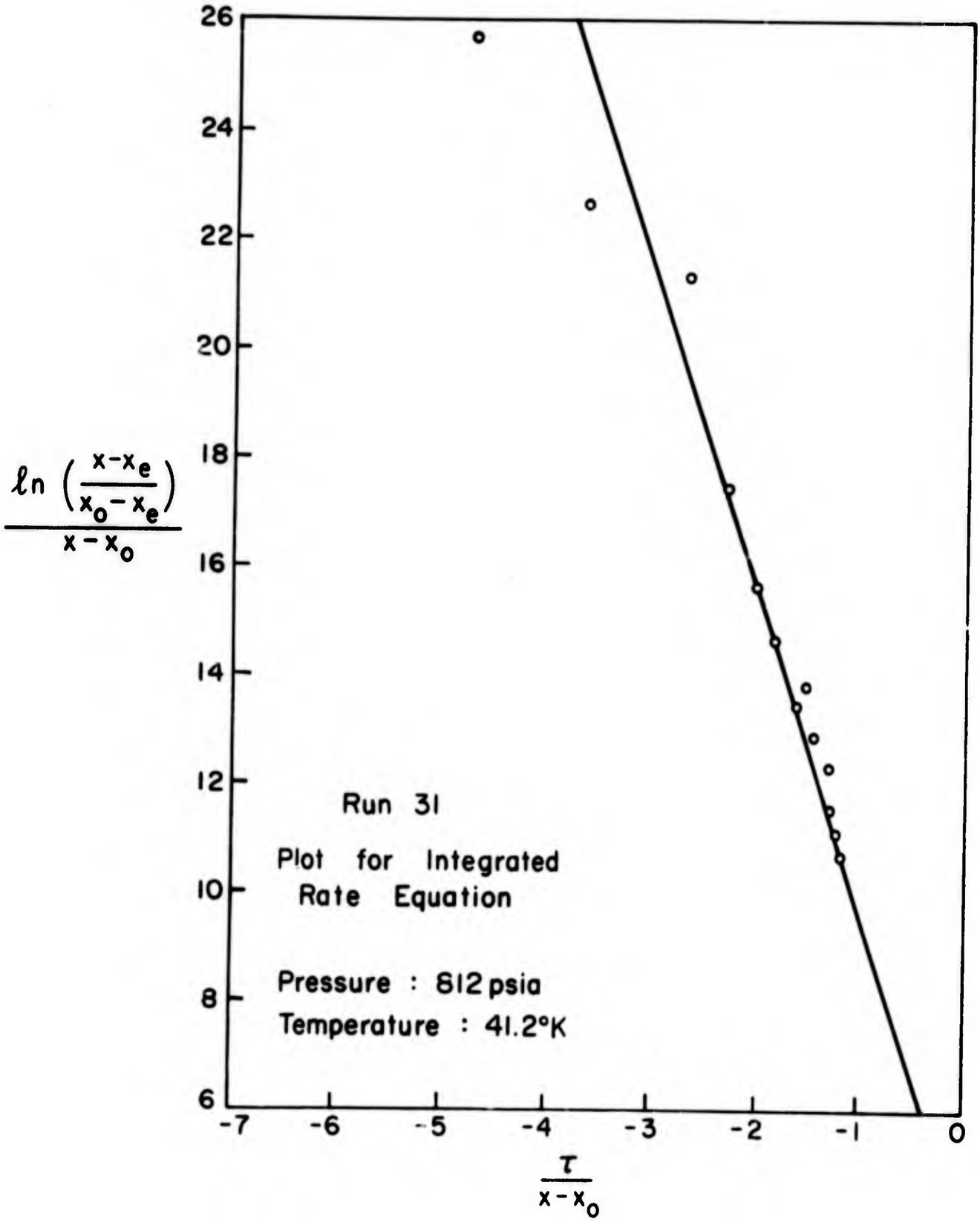
$\frac{\ell n \left(\frac{x-x_e}{x_o-x_e}\right)}{x-x_o}$
26
24
22
20
18
16
14
12
10
8
6
-7
-6
-5
-4
-3
-2
-1
0
$\frac{\tau}{x-x_o}$
Run 31
Plot for Integrated Rate Equation
Pressure : 812 psia
Temperature : 41.2°K

Figure II 49

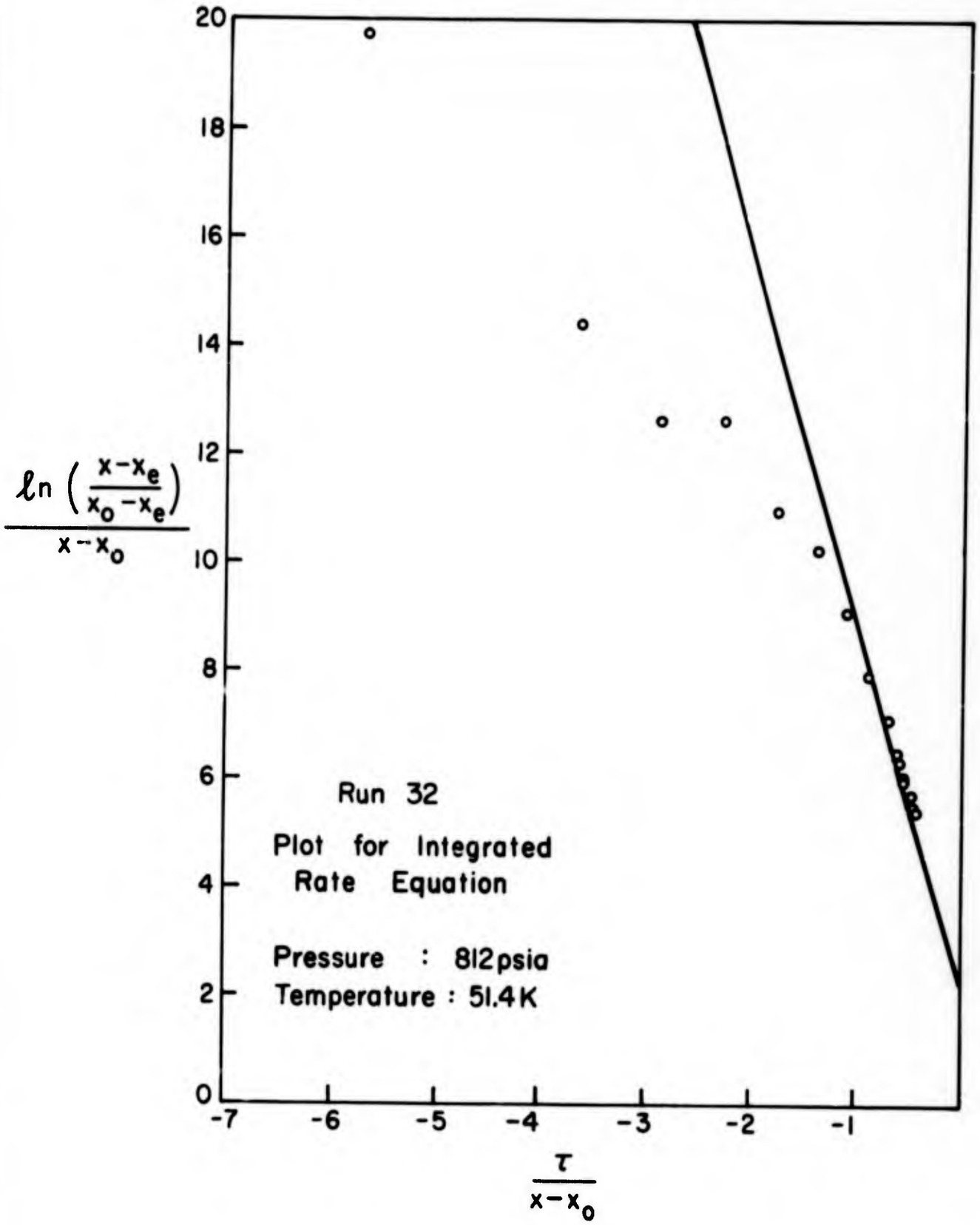
20
18
16
14
12
10
8
6
4
2
0
-7
-6
-5
-4
-3
-2
-1
$\ln\left(\frac{x-x_e}{x_o-x_e}\right)$ / $x-x_o$
$\frac{\tau}{x-x_o}$
Run 32
Plot for Integrated Rate Equation
Pressure : 812psia
Temperature : 51.4K

Figure II 50

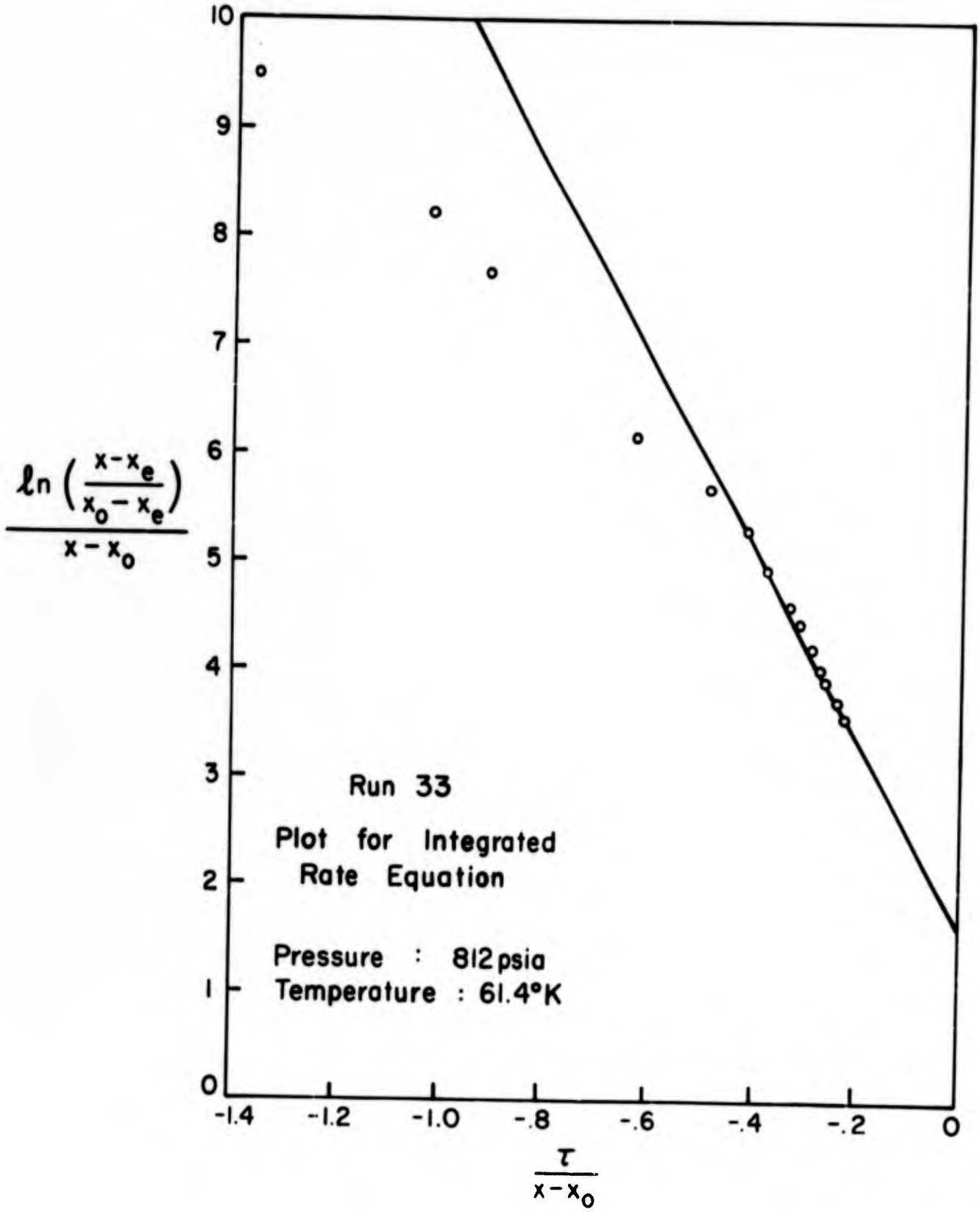
$\frac{\ln\left(\frac{x-x_e}{x_0-x_e}\right)}{x-x_0}$
10
9
8
7
6
5
4
3
2
1
0
Run 33
Plot for Integrated
Rate Equation
Pressure : 812 psia
Temperature : 61.4°K
-1.4
-1.2
-1.0
-.8
-.6
-.4
-.2
0
$\frac{\tau}{x-x_0}$

Figure II 51

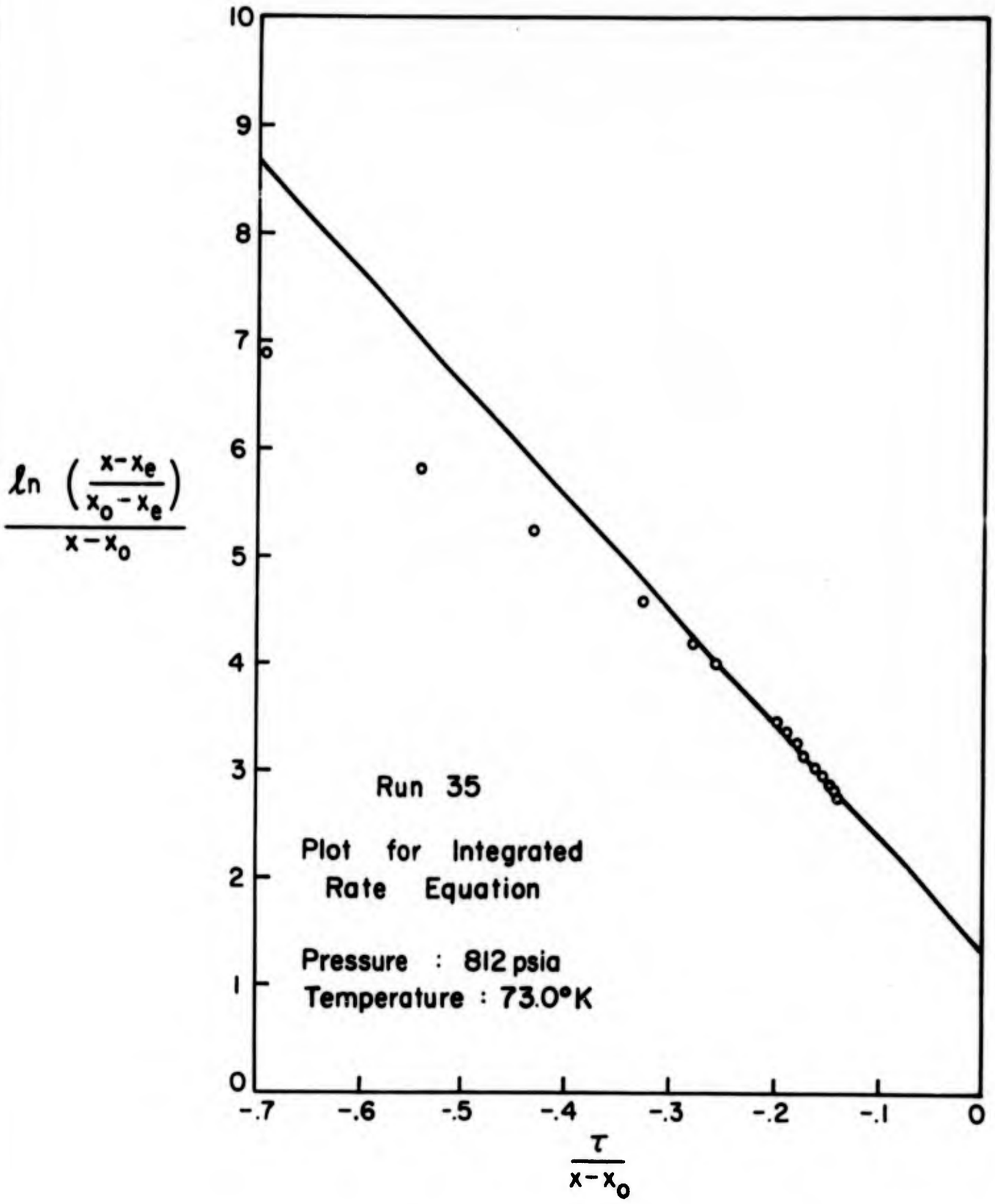
$\frac{\ln\left(\frac{x-x_e}{x_0-x_e}\right)}{x-x_0}$
10
9
8
7
6
5
4
3
2
1
0
-.7
-.6
-.5
-.4
-.3
-.2
-.1
0
$\frac{\tau}{x-x_0}$
Run 35
Plot for Integrated Rate Equation
Pressure : 812 psia
Temperature : 73.0°K

Figure II 52

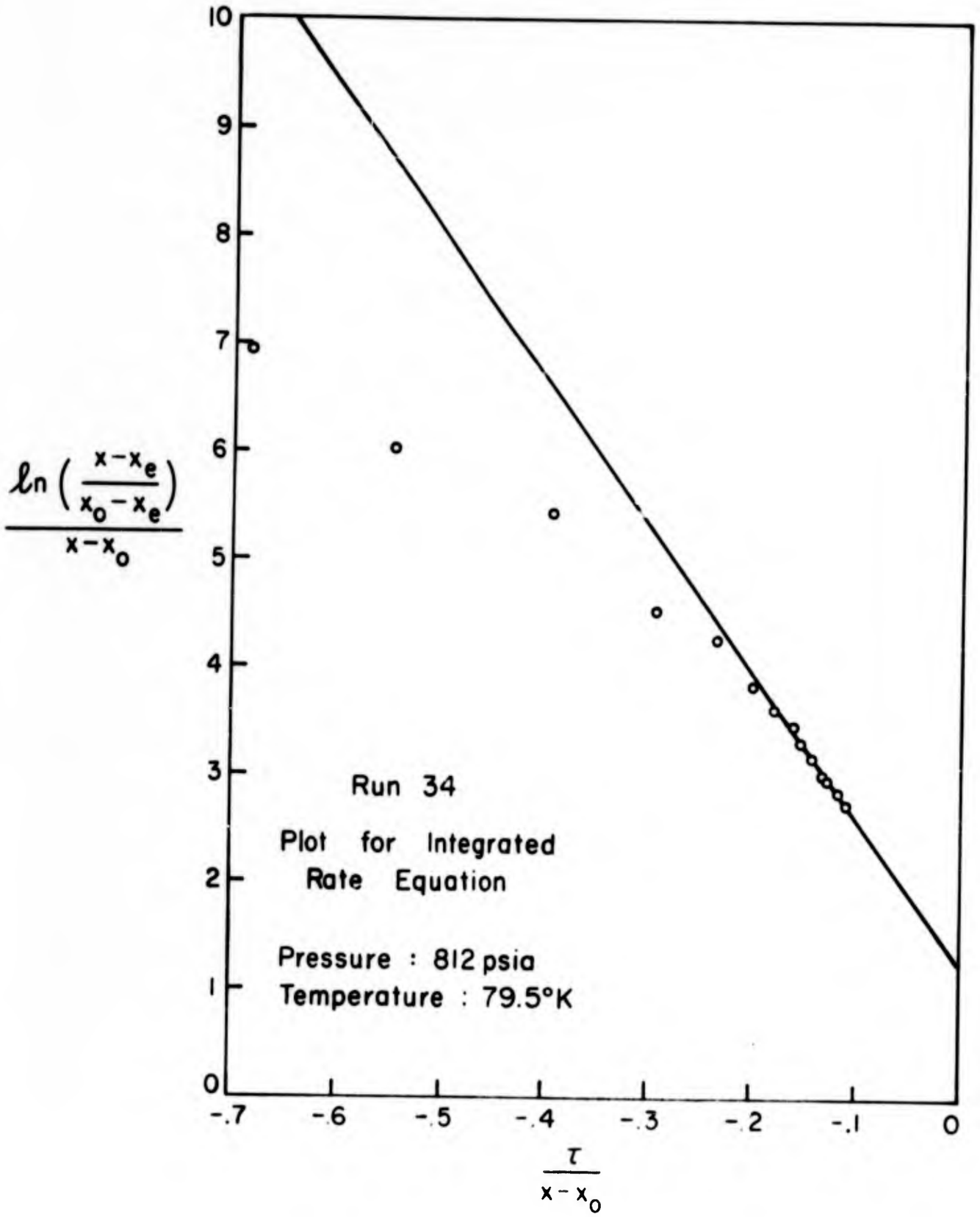
$\frac{\ln\left(\frac{x-x_e}{x_o-x_e}\right)}{x-x_o}$
10
9
8
7
6
5
4
3
2
1
0
-.7
-.6
-.5
-.4
-.3
-.2
-.1
0
$\frac{\tau}{x-x_o}$
Run 34
Plot for Integrated
Rate Equation
Pressure : 812 psia
Temperature : 79.5°K

Figure II 53

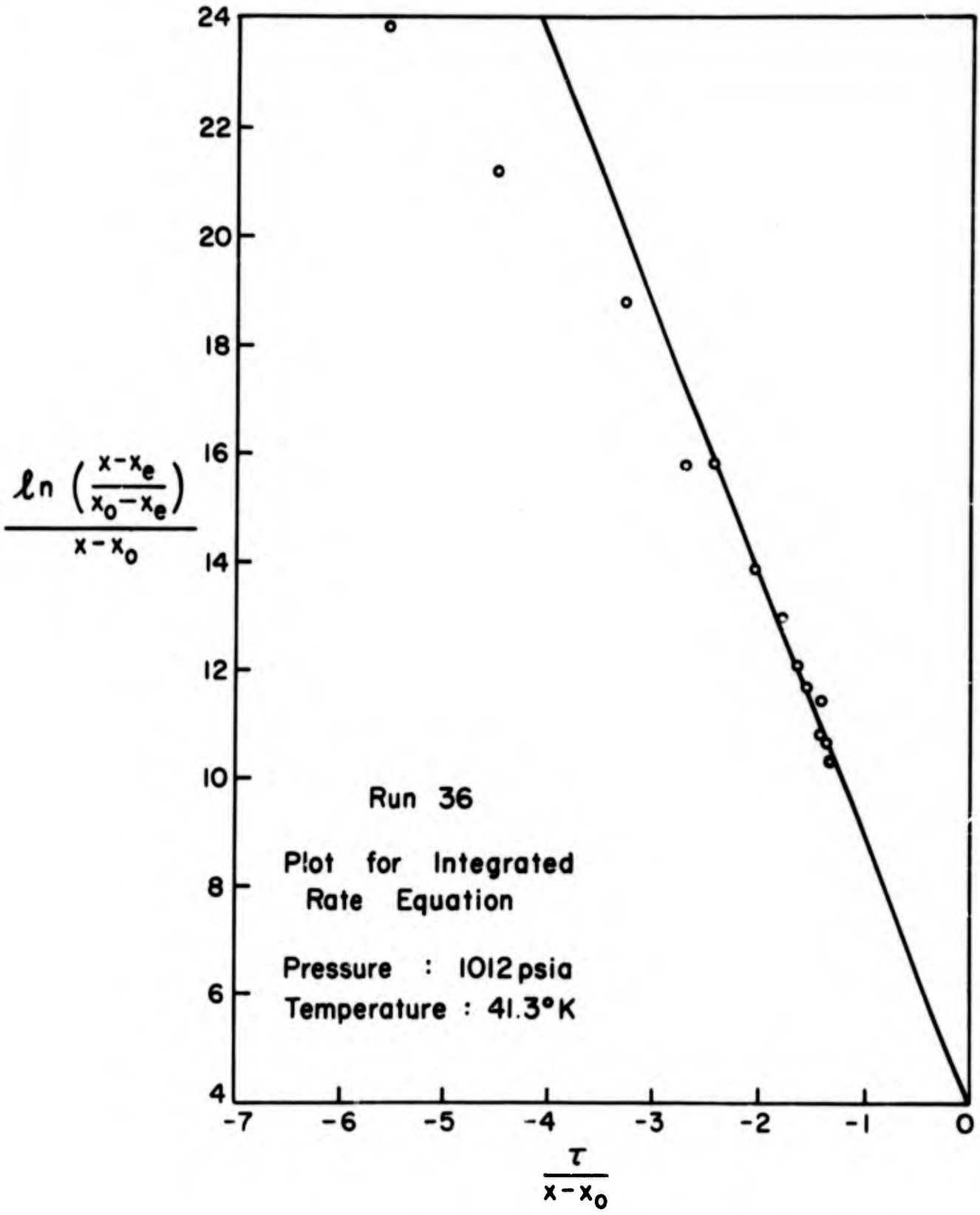
$\frac{\ln\left(\frac{x-x_e}{x_0-x_e}\right)}{x-x_0}$
24
22
20
18
16
14
12
10
8
6
4
-7
-6
-5
-4
-3
-2
-1
0
$\frac{\tau}{x-x_0}$
Run 36
Plot for Integrated Rate Equation
Pressure : 1012 psia
Temperature : 41.3°K

Figure II 54

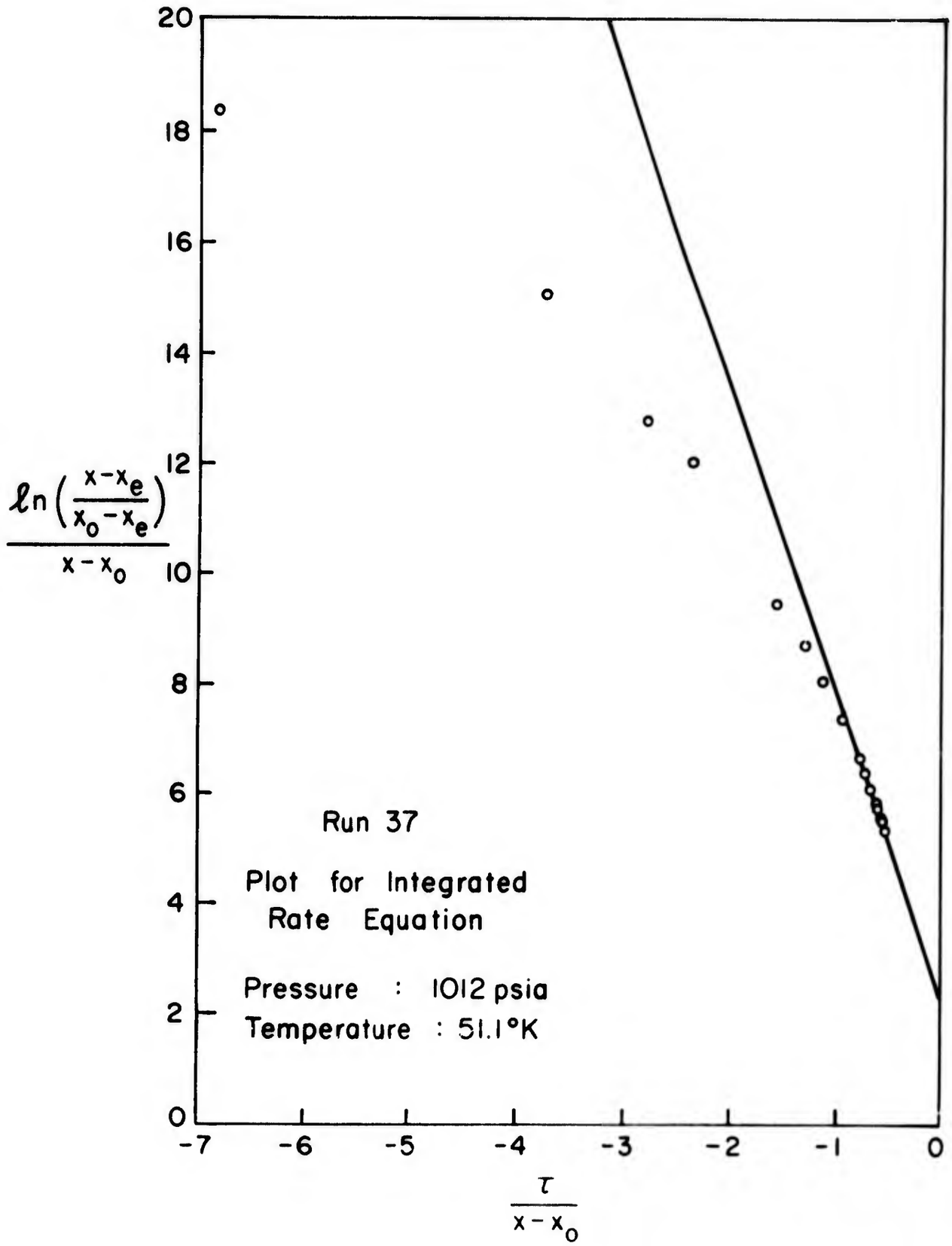
20
18
16
14
12
10
8
6
4
2
0
-7
-6
-5
-4
-3
-2
-1
0
$\frac{\ell n\left(\frac{x-x_e}{x_0-x_e}\right)}{x-x_0}$
$\frac{\tau}{x-x_0}$
Run 37
Plot for Integrated Rate Equation
Pressure : 1012 psia
Temperature : 51.1°K

Figure II 55

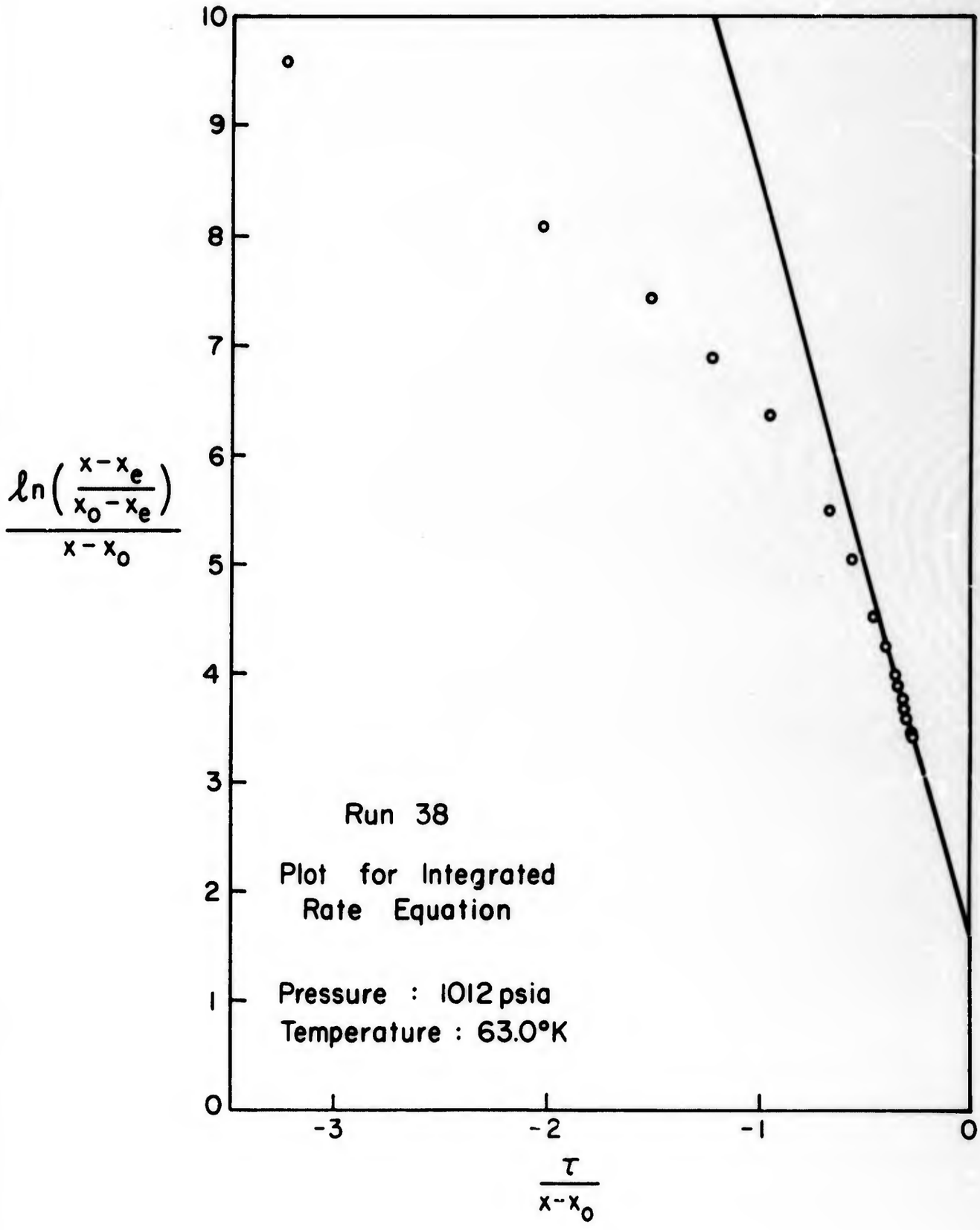
10
9
8
7
6
5
4
3
2
1
0
-3
-2
-1
0
$\ln\left(\frac{x-x_e}{x_0-x_e}\right)$
$x-x_0$
$\frac{\tau}{x-x_0}$
Run 38
Plot for Integrated
Rate Equation
Pressure : 1012 psia
Temperature : 63.0°K

Figure II 56

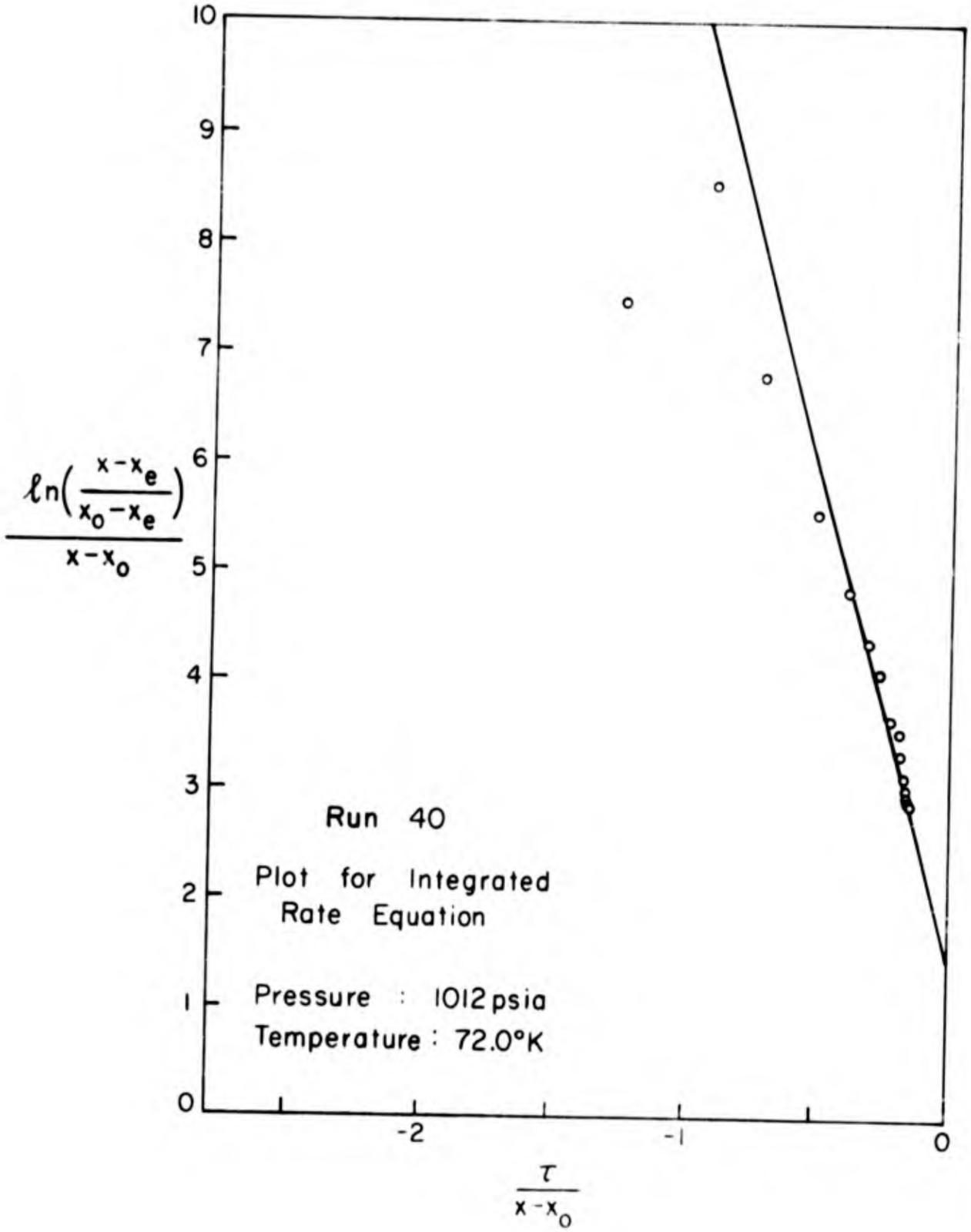
10
9
8
7
6
5
4
3
2
1
0
$\frac{\ell n\left(\frac{x-x_e}{x_0-x_e}\right)}{x-x_0}$
Run 40
Plot for Integrated
Rate Equation
Pressure : 1012 psia
Temperature : 72.0°K
-2
-1
0
$\frac{\tau}{x-x_0}$

Figure II 57

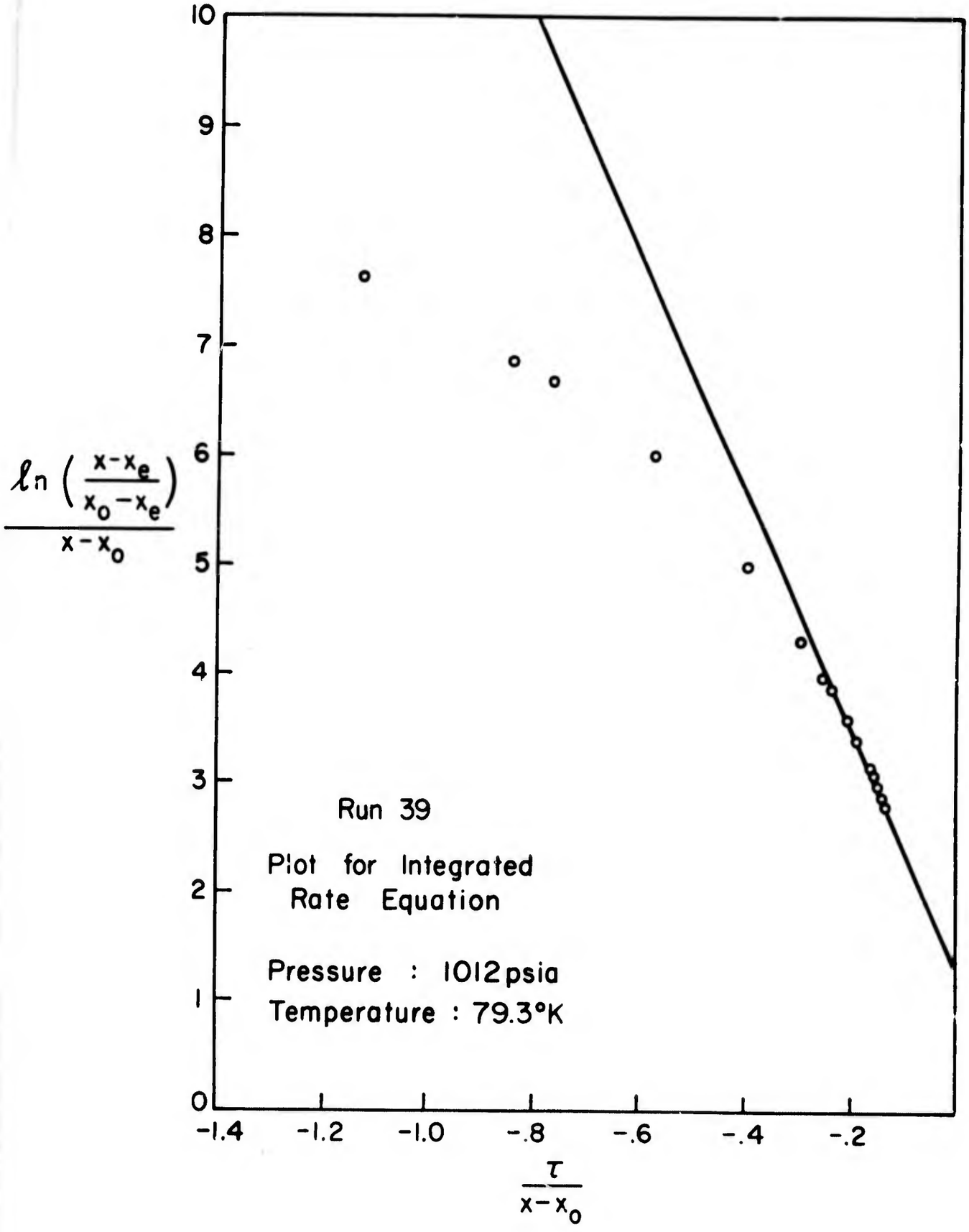
10
9
8
7
6
5
4
3
2
1
0
-1.4
-1.2
-1.0
-.8
-.6
-.4
-.2
$\frac{\ell n\left(\frac{x-x_e}{x_0-x_e}\right)}{x-x_0}$
$\frac{\tau}{x-x_0}$
Run 39
Plot for Integrated Rate Equation
Pressure : 1012 psia
Temperature : 79.3°K

Figure II 58

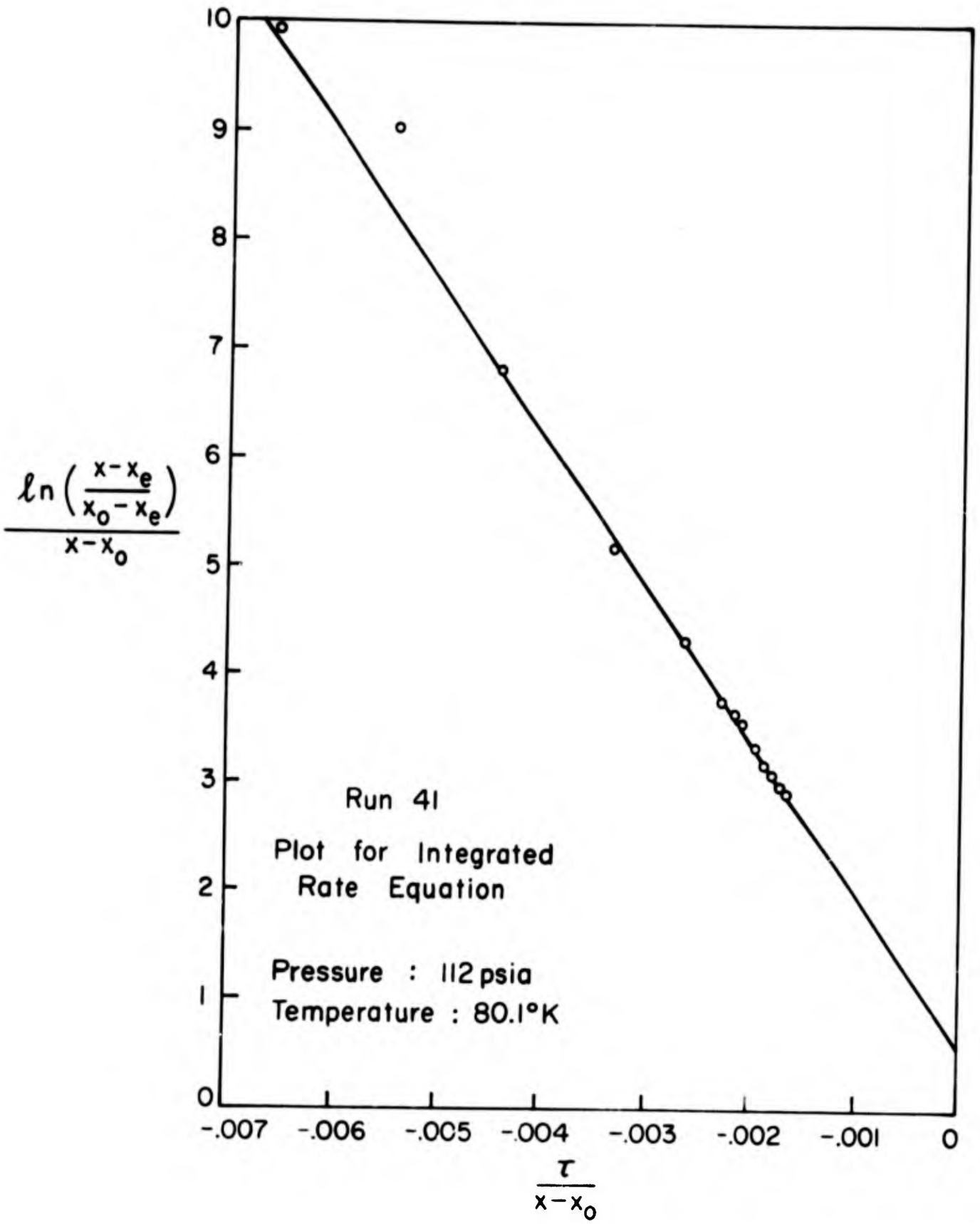
$\frac{\ell n\left(\frac{x-x_e}{x_o-x_e}\right)}{x-x_o}$
10
9
8
7
6
5
4
3
2
1
0
Run 41
Plot for Integrated Rate Equation
Pressure : 112 psia
Temperature : 80.1°K
-.007
-.006
-.005
-.004
-.003
-.002
-.001
0
$\frac{\tau}{x-x_o}$

Figure II 59

VI) Diffusion of product through the pore to the exterior surface of the catalyst pellet.

VII) Diffusion of product into the bulk stream.

One of these steps usually has a smaller rate than the rest; this step is called the "slow" or "rate-controlling" step.

The diffusion steps were found to exhibit little resistance to the overall rate of reaction. It was concluded that the surface phenomenon presented the significant resistance to the reaction rate. A derivation based on these facts will be presented later, which will show how the rate law given by Eq. (II-14) can be interpreted theoretically.

## A. External Diffusion

The significance of interparticle diffusion compared to the overall resistance was checked by calculating mass transfer coefficients and comparing them to pseudo simple first-order rate constants. If the mass transfer coefficient were several orders of magnitude greater than the rate constant, it would be safe to assume that diffusional resistance was not significant.

McCabe and Smith show a correlation for a mass transfer in a packed bed as a function of Schmidt and Reynolds numbers (18). A mass velocity corresponding to an STP space velocity of 1000 $min^{-1}$ was chosen as a typical velocity in that this was where deviation from first-order began to be seriously encountered.

The reaction conditions and mass transfer coefficients that were calculated are shown in Table II-III.

Table II-III

| Pressure (psia) | Temperature (°K) | $K_M$ ($lb_M$ / $ft^2$-sec) |
|---|---|---|
| 42 | 40 | $1.28 \times 10^{-3}$ |
| 1012 | 40 | $1.4 \times 10^{-3}$ |
| 42 | 80 | $8.16 \times 10^{-4}$ |

Table II-III shows that mass transfer is more likely to be significant at low pressure and high temperature. Thus, a pseudo first-order rate constant for Run 43(42 psia, 80°K) was calculated and compared to the mass transfer coefficient for these conditions.

Fig. II-10 shows the plot from which the rate constant was obtained. The value of the rate constant was 3.1 $min^{-1}$, while the mass transfer coefficient in the same units was about $10^5$ $min^{-1}$. From these figures it was concluded that external diffusion had very little effect upon the overall rate of reaction.

## B. Internal Diffusion

Wheeler has shown that pore diffusion can be accounted for by the use of the Thiele Modulus h and the effectiveness factor E (28). If the value of the Thiele modulus lies below 0.5, the reaction is kinetically controlled, and if it lies above 2.0, the reaction is purely diffusion controlled. The Thiele modulus is given by

$$h = L\sqrt{\frac{Sk_s}{D\chi}} \qquad \text{(II-22)}$$

where

L = radius of catalyst pellet, cm.

S = surface area of catalyst per unit volume reactor, $cm^2\ cm^{-3}$.

$k_s$ = first order rate constant per unit area surface per unit volume reactor cm $sec^{-1}$.

D = effective diffusivity of gas, $cm^2\ sec^{-1}$.

$\chi$ = tortuosity factor

The effectiveness factor is given by

$$E = \frac{1}{h}\tanh h \qquad \text{(II-23)}$$

Geddes had previously measured the area of the catalyst and found it to be about 387 $cm^2$ / $cm^3$ reactor (10). Using this figure, the values of h and E were found to be 0.49 and 0.93 respectively. This value of h indicated a kinetically controlled situation and the value of 0.93 for E meant that the surface was essentially all effective. Thus, it was concluded that pore diffusion was not a controlling factor in the reaction.

## C. Surface Reaction

Since the diffusion steps were shown not to be rate controlling, one or more of the surface steps must be the slow step. In order that the final form of the rate law and the interpretation of the temperature and pressure dependence of k and k' may be more meaningfully discussed, the theoretical development of the rate law will be presented.

## II. 5 Theory

The overall reaction is represented by Eq. (II-24). Since the reaction

$$p\text{-}H_2\ (g) \rightleftarrows o\text{-}H_2\ (g) \qquad \text{(II-24)}$$

takes place on a catalytic surface, it is envisioned to occur in a series of seven steps as was previously mentioned. These steps include diffusion, adsorption, and chemical reaction.

Calculations were presented which showed that diffusion effects are, to a large extent, negligible. Hence, the only steps that need be considered are the adsorption of reactant, chemical reaction on the surface, and desorption of product. Eqs. (II-25), (II-26) and (II-27) show these steps.

$$p\text{-}H_2\ (g) + S \underset{k_2}{\overset{k_1}{\rightleftarrows}} p\text{-}H_2 \cdot S \qquad \text{(II-25)}$$

$$p\text{-}H_2 \cdot S \underset{k_4}{\overset{k_3}{\rightleftarrows}} o\text{-}H_2 \cdot S \qquad \text{(II-26)}$$

$$o\text{-}H_2 \cdot S \underset{k_6}{\overset{k_5}{\rightleftarrows}} o\text{-}H_2\ (g) + S \qquad \text{(II-27)}$$

Eqs. (II-28), (II-29) and (II-30) show the corresponding rate equations for these steps.

$$r_2 = k_1 c_p (1 - \theta_o - \theta_p) - k_2 \theta_p \qquad \text{(II-28)}$$

$$r_3 = k_3 \theta_p - k_4 \theta_o \qquad \text{(II-29)}$$

$$r_4 = k_5 \theta_o - k_6 c_o (1 - \theta_o - \theta_p) \qquad \text{(II-30)}$$

Here

$c_p$ = Concentration of parahydrogen in gas phase.

$c_o$ = Concentration of orthohydrogen in gas phase.

$\theta_o$ = Fraction of catalyst surface covered by adsorbed ortho-hydrogen molecules.

$\theta_p$ = Fraction of surface covered by adsorbed parahydrogen molecules.

$k_1, k_2, k_3, k_4, k_5, k_6,$ = Rate constants for individual steps in directions shown.

The quantity $(1 - \theta_o - \theta_p)$ is therefore the fraction of surface not covered by adsorbed molecules, and $c_p$ and $c_o$ are the only variables which can be experimentally measured. Thus $\theta_o$ and $\theta_p$ must be eliminated from the rate equations. This may be done by assuming that one of the three steps is slower than the other two. The individual rates of the forward and reverse reactions of the two fast steps are assumed to be so large that they maintain essentially an equilibrium condition throughout the course of the reaction. Under these conditions, the overall rate of these two steps is so small compared to the forward and reverse reaction rates that it is approximately zero. This assumption is used to elimate $\theta_o$ and $\theta_p$ as variables.

A. If (II-25) is rate controlling, then $r_3 = r_4 \approx 0$, as explained above. Then

$$k_3\theta_p = k_4\theta_o \qquad \text{(II-31)}$$

$$k_5\theta_o = k_6 c_o (1 - \theta_p - \theta_o) \qquad \text{(II-32)}$$

Elimination of $\theta_o$ and $\theta_p$ from Eqs. (II-31), (II-32) and (II-28) yields

$$r_2 = \frac{k_1 c_p - \frac{k_2 k_4 k_6}{k_3 k_5} c_o}{1 + \frac{k_6}{k_5}\left(1 + \frac{k_4}{k_3}\right) c_o} \qquad \text{(II-33)}$$

Utilization of the facts that $c_o + c_p = c_H$, the total hydrogen concentration, and that at equilibrium, $r_2 = 0$, yields

$$k_1 c_{p_e} = \frac{k_2 k_4 k_6}{k_3 k_5} c_{o_e} \qquad \text{(II-34)}$$

Eq. (II-33) may then be put in the form

$$r_2 = r = \frac{\left[ k_1 + \frac{k_2 k_4 k_6}{k_3 k_5} \right] (c_p - c_{p_e})}{1 + \frac{k_6}{k_5}\left(1 + \frac{k_4}{k_3}\right) c_H} \Bigg/ \left[ 1 - \left[ \frac{\frac{k_6}{k_5}\left(1 + \frac{k_4}{k_3}\right)}{1 + \frac{k_6}{k_5}\left(1 + \frac{k_4}{k_3}\right) c_H} \right] c_p \right] \qquad \text{(II-35)}$$

or

$$r = \frac{k\,(c_p - c_{p_e})}{1 - k' c_p} \qquad \text{(II-36)}$$

where k and k' are equal to the bracketed combinations of the individual rate constants and the total hydrogen concentration.

B. If (II-26) is the rate controlling step, then $r_2 = r_4 \approx 0$ as above. Then,

$$k_1 c_p (1 - \theta_o - \theta_p) = k_2 \theta_p \qquad \text{(II-37)}$$

$$k_5 \theta_o = k_6 c_o (1 - \theta_o - \theta_p) \qquad \text{(II-38)}$$

By a procedure analogous to the treatment in part A, utilization of Eqs. (II-37), (II-38), (II-29), and the equivalent of (II-34), the rate expression is obtained.

$$r_3 = r = \frac{\left[ \left( \frac{k_3 k_1}{k_2} + \frac{k_4 k_6}{k_5} \right) \right] (c_p - c_{p_e})}{1 + \frac{k_6}{k_5} c_H} \Bigg/ \left[ 1 + \frac{\frac{k_1}{k_2} - \frac{k_6}{k_5}}{1 + \frac{k_6}{k_5} c_H} c_p \right] \qquad \text{(II-39)}$$

or

$$r = \frac{k(c_p - c_{p_e})}{1 \pm k'c_p} \qquad \text{(II-40)}$$

where again k and k' are given by the bracketed terms in Eq. (II-39). Whether k' takes the positive or negative sign depends on whether $k_1/k_2$ is greater than $k_6/k_5$ or not.

Since $k_1/k_2$ and $k_6/k_5$ can be recognized as the adsorption equilibrium constants for parahydrogen and orthohydrogen, respectively, this is tantamount to saying that k' is positive if parahydrogen is more strongly adsorbed than orthohydrogen, and vice-versa if k' is negative. If the two forms are adsorbed equally (which has not been assumed) then k' will be zero and the equation reduces to simple first order kinetics.

C. Similarly, if (II-27) is rate controlling, $r_2 = r_3 \neq 0$ and

$$k_1 c_p (1 - \theta_o - \theta_p) = k_2 \theta_p \qquad \text{(II-41)}$$

$$k_3 \theta_p = k_4 \theta_o \qquad \text{(II-42)}$$

Treatment analogous to that of parts A and B is applied to Eqs. (II-41), (II-42), (II-30), and the equivalent of (II-34) with the resulting rate expression

$$r_4 = r = \frac{\left[ k_6 + \frac{k_1 k_3 k_5}{k_2 k_4} \right] (c_p - c_{p_e})}{1 + \left[ \frac{k_1}{k_2} \left(1 + \frac{k_3}{k_4}\right) \right] c_p}$$

or

$$r = \frac{k(c_p - c_{p_e})}{1 + k'c_p} \qquad \text{(II-44)}$$

where k and k' are given by the bracketed terms in Eq. (II-43). Here k and k' are not functions of the total hydrogen concentration as they are in Eqs. (II-36) and (II-40).

It can be seen that Eq. (II-36), (II-40), and (II-44) are the same except for the sign of k'. Thus, as far as the rate law is concerned, (II-26) cannot be distinguished from (II-25) or (II-27) because of k'; but if k' is found to be positive, (II-25) may be eliminated, and if negative, (II-27) may be eliminated as the rate controlling step.

Eq. (II-44) was taken as the rate law. The sign of k' and the concentration dependence of k and k' were then experimentally determined, as was mentioned previously.

## II. 6 Interpretation of Results

It was found experimentally that k was a function of pressure and that k' was negative. Comparison of these results to Eq. (43) showed that desorption of orthohydrogen was not the rate controlling step and further, that if chemical reaction were rate controlling, the adsorption equilibrium constant for orthohydrogen was greater than the adsorption equilibrium constant for parahydrogen.

A closer look at the constant k' yielded a method by which the rate controlling step could be determined.

If adsorption of parahydrogen is controlling, the form of k' is (from Eq. (II-35)).

$$k' = \frac{a}{1 + ac_H} \qquad \text{(II-45)}$$

where a is a combination of the individual rate constants and $c_H$ is the hydrogen concentration (g moles/$cm^3$). On the other hand, if surface reaction is controlling, k' has the form (from Eq. (II-39)).

$$k' = \frac{b - d}{1 + dc_H} \qquad \text{(II-46)}$$

where b and d are combinations of the individual rate constants. Both (II-45) and (II-46) are of the same form. If (II-45) is multiplied by $(1 + ac_H)$ and divided by k'a, the result is

$$\frac{1}{k'} = c_H + \frac{1}{a} \qquad \text{(II-47)}$$

while if (II-46) is multiplied by $(1 + dc_H)$ and divided by k' (b - d), the result is

$$\frac{1}{k'} = \frac{d}{b - d} c_H + \frac{1}{b - d} \qquad \text{(II-48)}$$

Thus, $1/k'$ should be a linear function of $c_H$. Plots of this type were made, both for individual temperatures (see Figs. (II-60 - II-64) and for all concentrations (see Fig. II-28). As was previously pointed out Fig. II-28 shows that $1/k'$ is approximately proportional to $c_H$. However, it was noticed upon closer inspection of the plots for individual temperatures (Figs. II-60 - II-64) that the data indicated that the curves did not pass through the origin. Both Eq. (II-47) and (II-48) predict this phenomenon. Further, Eq. (II-47) predicts that if adsorption of parahydrogen were rate controlling, the slope of the curves should equal unity, while Eq. (II-48) predicts that if surface reaction controlled, the slope would not equal unity.

As shown by Figs. II-60 - II-64, the latter was found to be the case. Consequently, it was assumed that surface reaction is the controlling step in the reaction.

It can be seen by comparison of Eq. (II-46) to Eq. (II-39) that $b = k_6/k_5$ and $d = k_1/k_2$, the adsorption equilibrium constants for ortho- and parahydrogen, respectively. These could be determined from the slopes and intercepts of Figs. II-60, II-64.

Cunningham and Johnston, following a procedure outlined by Sandler (20) have defined a separation coefficients as (8)

$$s = \frac{\left(\frac{1 - x_s}{x_s}\right)}{\left(\frac{1 - x_g}{x_g}\right)} \qquad \text{(II-49)}$$

where

$x_g$ = mole fraction parahydrogen in gas phase.

$x_s$ = mole fraction parahydrogen adsorbed on surface.

They proceed to calculate s for the ortho → para reaction, assuming first order conversion on the surface to be rate controlling. Their other assumptions are the same that were made in the derivations of Eqs. (II-35), (II-39), and (II-43).

½ FRAMES

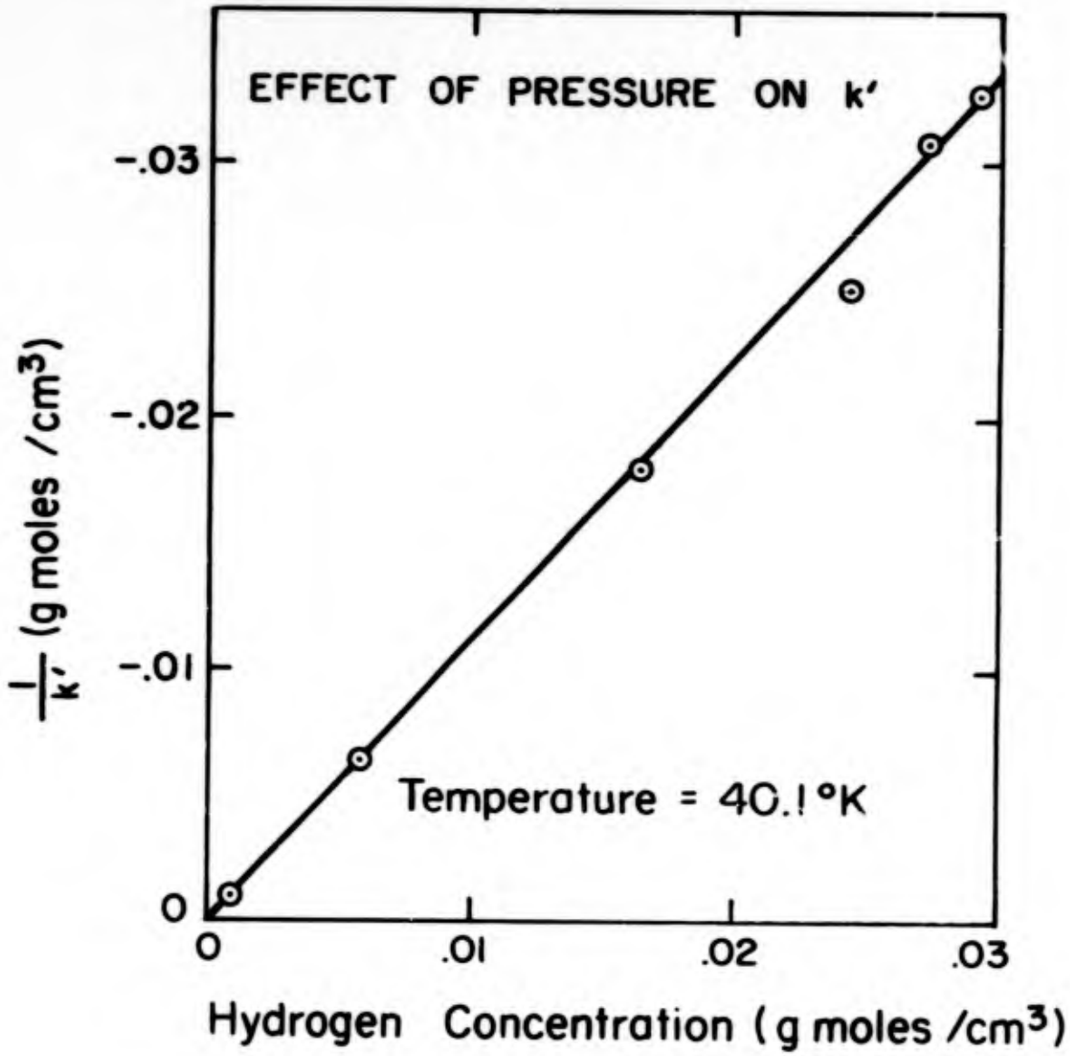


Figure II 60

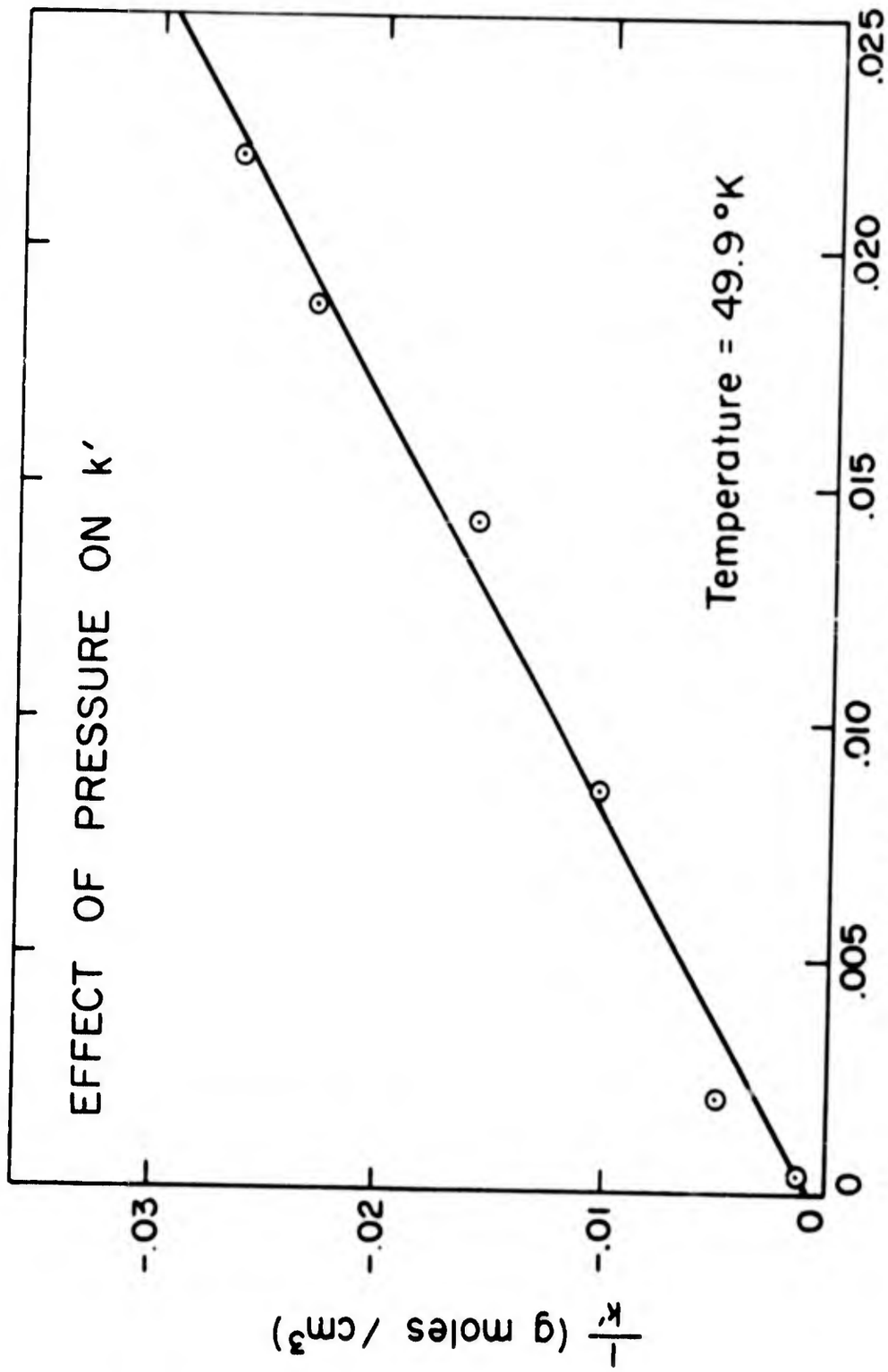
EFFECT OF PRESSURE ON k'
Temperature = 49.9 °K
-.03
-.02
-.01
0
0
.005
.010
.015
.020
.025
Hydrogen Concentration (g moles /cm³)
1/k' (g moles /cm³)

Figure II 61

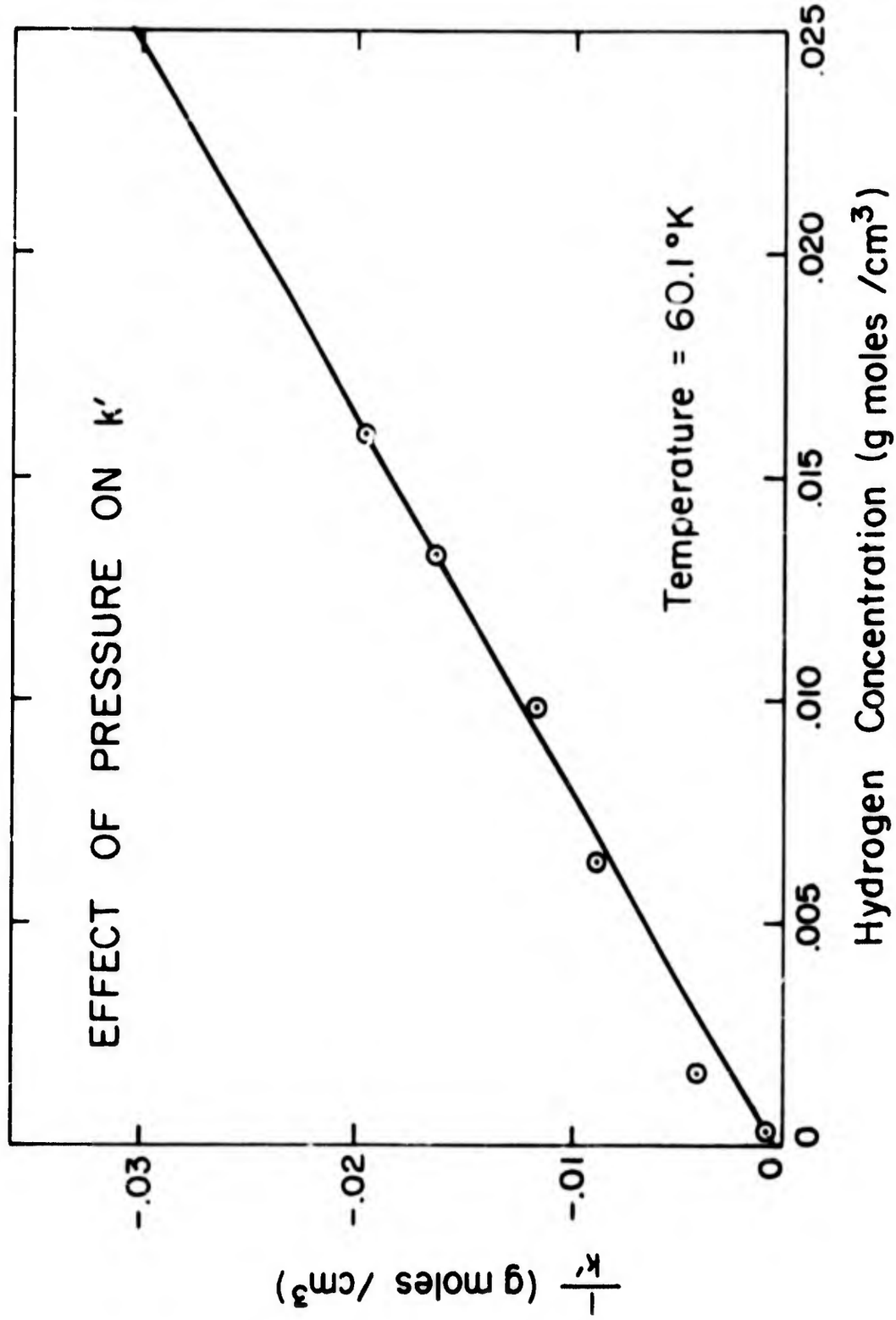
EFFECT OF PRESSURE ON k'
Temperature = 60.1 °K
$\frac{1}{k'}$ (g moles /cm³)
-.03
-.02
-.01
0
0
.005
.010
.015
.020
.025
Hydrogen Concentration (g moles /cm³)

Figure II 62

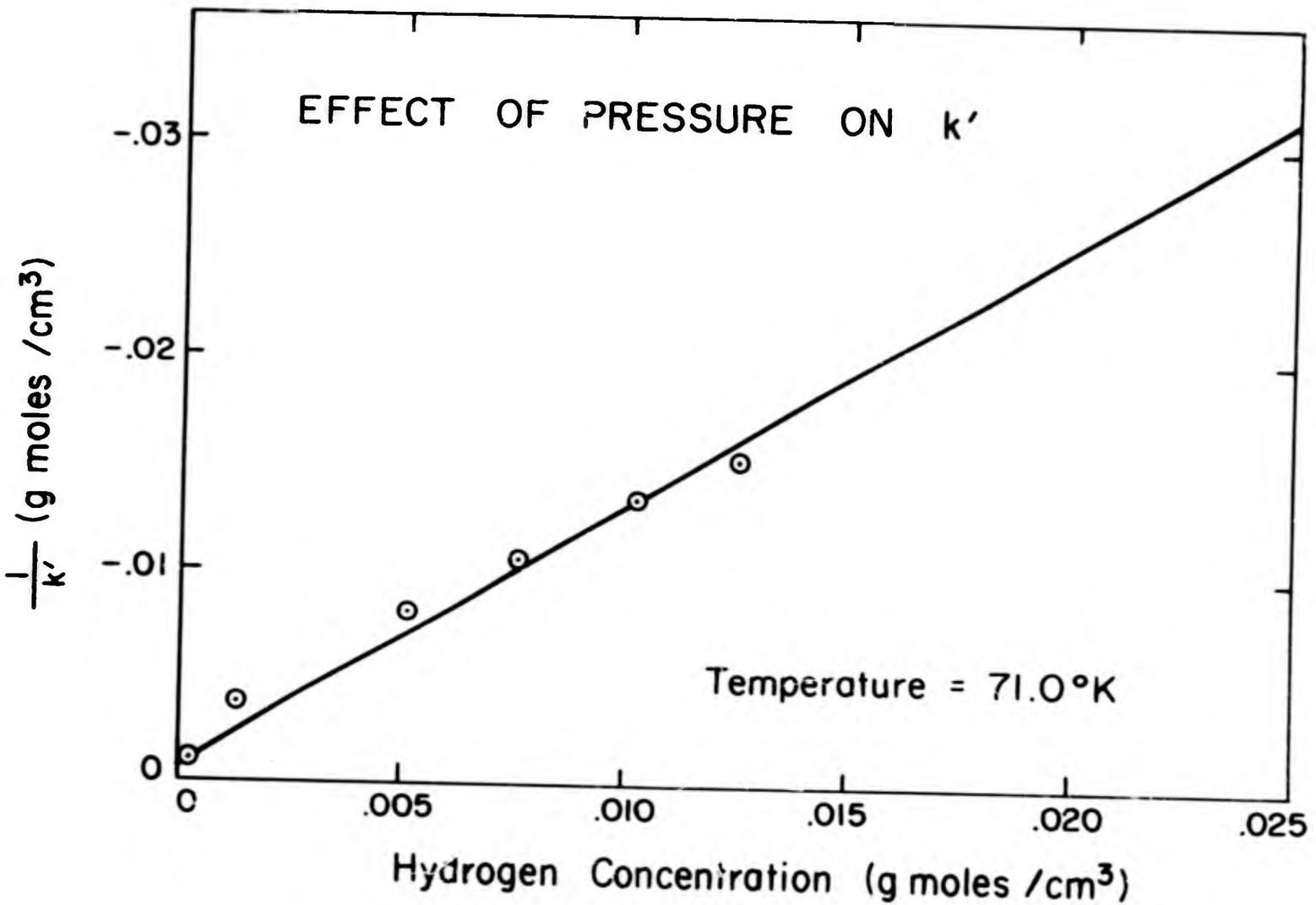
EFFECT OF PRESSURE ON k'
-.03
-.02
-.01
0
$\frac{1}{k'}$ (g moles /cm³)
Temperature = 71.0°K
0
.005
.010
.015
.020
.025
Hydrogen Concentration (g moles /cm³)

Figure II 63

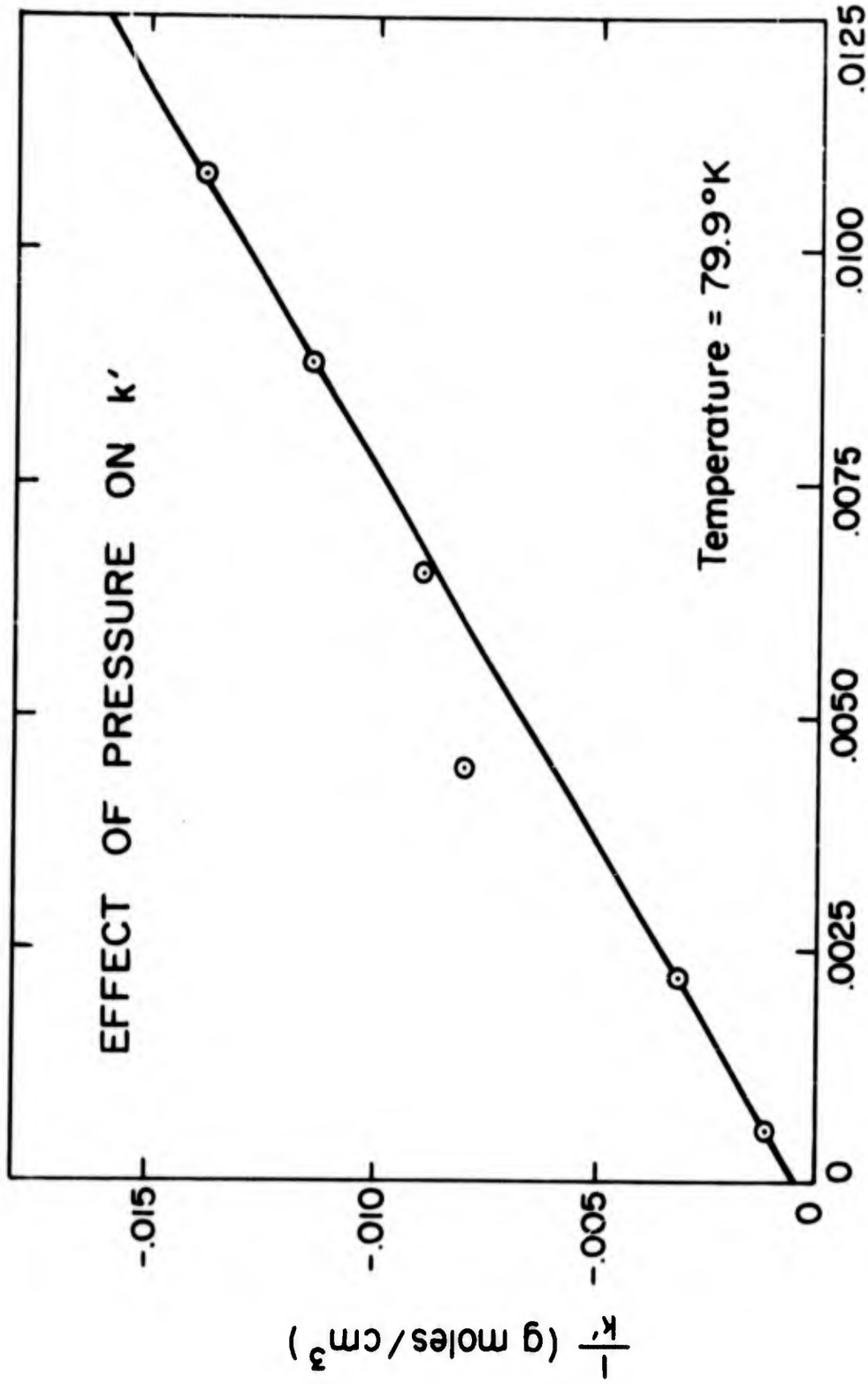
EFFECT OF PRESSURE ON k'
Temperature = 79.9°K
$\frac{1}{k'}$ (g moles/cm$^3$)
-.015
-.010
-.005
0
0
.0025
.0050
.0075
.0100
.0125
Hydrogen Concentration (g moles /cm$^3$)

Figure II 64

It can be seen that

$$(1 - x_g)c_H = c_o \tag{II-50}$$

$$x_g c_H = c_p \tag{II-51}$$

and

$$1 - x_s = \frac{\theta_o}{\theta_o + \theta_p} \tag{II-52}$$

$$x_s = \frac{\theta_p}{\theta_o + \theta_p} \tag{II-53}$$

Substitution of Eqs. (II-50), (II-51), (II-52), and (II-53) into Eq. (II-49) yields

$$s = \frac{\left(\frac{\theta_o}{\theta_p}\right)}{\left(\frac{c_o}{c_p}\right)} = \frac{\left(\frac{\theta_o}{c_o}\right)}{\left(\frac{\theta_p}{c_p}\right)} \tag{II-54}$$

Eqs. (II-32) and (II-41) show the equilibrium relationships for ortho- and para-hydrogen, respectively. If they are rewritten in the form

$$\frac{k_6}{k_5} = \frac{\theta_o}{c_o} \quad \frac{1}{(1 - \theta_o - \theta_p)} = b \tag{II-32a}$$

$$\frac{k_1}{k_2} = \frac{\theta_p}{c_p} \quad \frac{1}{(1 - \theta_o - \theta_p)} = d \tag{II-41a}$$

it can be seen that division of (II-32a) by (II-41a) yields

$$\frac{\left(\frac{\theta_o}{c_o}\right)}{\left(\frac{\theta_p}{c_p}\right)} = \frac{b}{d} = s \tag{II-55}$$

Thus, s is seen to be the ratio of the adsorption equilibrium constants of ortho- and parahydrogen.

Sandler obtained values of s which ranged from 1.1 at 77°K to 1.3 at 90°K (21). Cunningham, et. al., report values of s at 20°K of 12 to 22 (9). In another work Clark and co-workers present values of s of 1.22 to 1.86 at 77°K and 1.14 at 90°K (8).

Values of s were obtained from the present data in the following manner: Eq. (II-48) shows that $d/(b - d) = S'$ and $1/(b - d) = I'$, where S' and I' are the slope and Intercept, respectively, of the lines in Figs. II-60-II-64. If these relations are solved for b and d, the following are obtained.

$$b = \frac{S'}{I'} \qquad \text{(II-56)}$$

$$d = \frac{S' + 1}{I'} \qquad \text{(II-57)}$$

Therefore

$$s = \frac{b}{d} = \frac{S'}{S' + 1} \qquad \text{(II-58)}$$

Eqs.(II-56-57) and (II-58) show that although b and d are dependent on I', s is independent of I'. Hence, values of s obtained from Figs. II-60-II-64 should be more accurate than values of b and d, since I' will be subject to much greater chance for error than will S'.

Table II-IV presents the values of S', I', b, d, and s that were calculated from Figs. II-60-II-64. It is apparent that the trend in b and d is for them to decrease as temperature increases. The value of s also decreases with increasing temperature.

Sandler derived a relationship, based on the rotational partition functions of ortho- and parahydrogen, which predicts that s is an exponential function of 1/T, i.e.

$$s = 2/3 \exp\left(\frac{\epsilon_r}{2RT}\right) \qquad \text{(II-59)}$$

According to Sandler, $\epsilon_r$ is the energy difference between the rotational states in the gas phase, 338 cal/mole.

TABLE II-IV

CALCULATION OF SEPARATION FACTORS

| T(°K) | 40 | 50 | 60 | 70 | 80 |
|---|---|---|---|---|---|
| S' | -1.116 | -1.166 | -1.201 | -1.235 | -1.250 |
| I' | -0.00005 | -0.00032 | -0.00048 | -0.00056 | -0.00039 |
| b | 22,300 | 3650 | 2510 | 2210 | 3210 |
| d | 2320 | 519 | 419 | 420 | 641 |
| $s_{exp.}$ | 9.61 | 7.03 | 5.99 | 5.27 | 5.00 |
| $s_{th}$ | 5.55 | 3.67 | 2.75 | 2.21 | 1.93 |

Table II-IV lists the values of s that were calculated from Sandler's formula for comparison with the values of s that were calculated with the present data. It is apparent that the experimental values are approximately twice the theoretical values. However, the orders of magnitude are the same, and the experimental values compare with those previously reported.

The experimental correlation of the rate constant k was also predicted by the theoretical development. For the situation in which surface reaction controls, Eq. (II-39) shows that k is given by

$$k = \frac{k_3 \frac{k_1}{k_2} + k_4 \frac{k_6}{k_5}}{1 + \frac{k_6}{k_5} c_H} \qquad \text{(II-60)}$$

Since $k_1/k_2$ and $k_6/k_5$ are the adsorption equilibrium constants for para- and orthohydrogen, thermodynamics predicts that their temperature dependence will be of the form

$$K_i = A_i \exp(-\Delta H_i/RT) \qquad \text{(II-61)}$$

where

$K_i$ = Equilibrium constant.

$A_i$ = Constant

$\Delta H_i$ = Heat of reaction, in this case, heat of adsorption.

First, let it be assumed that $(k_6/k_5)c_H \gg 1$, which is justified by the values of d in Table II-IV. With this assumption

$$k = \frac{k_3 \frac{k_1}{k_2} + k_4 \frac{k_6}{k_5}}{\frac{k_6}{k_5} c_H} \qquad \text{(II-62)}$$

or

$$k = \frac{k_4}{c_H} \left(\frac{k_3}{k_4} \frac{d}{b} + 1\right) \qquad \text{(II-63)}$$

where d and b are as before, the equilibrium adsorption constants for para- and orthohydrogen. If $k_4$ is assumed to have an Arrhenius Law dependence, then

$$k = \frac{A_4}{c_H} e^{-E_4/RT} \left[\frac{k_3}{k_4} \frac{d}{b} + 1\right] \qquad \text{(II-64)}$$

If the term $(k_3/k_4) \cdot (d/b)$ is much less than unity, which, though not true for all temperatures, is assumed, it can be neglected, and Eq. (II-64) is reduced to the form

$$k = B[\exp(-E^{\neq}/RT)]/c_H \qquad \text{(II-65)}$$

The largest value of the term $(k_3/k_4)$ (d/b) was calculated to be 0.2 at 80°K. The values of d/b (= 1/s) that were used in the calculation were taken from Table IV and the assumption was made that $k_3/k_4$, which is the equilibrium constant for the surface reaction, was equal to the equilibrium constant for the gas phase reaction. A value of 0.2 is not negligible in comparison to unity, but its effects on the frequency factor could be masked by experimental error. Eq. (II-65) does correspond to the experimental dependence of k on pressure and temperature, since $c_H$ is proportional to the total pressure. More work should be done to clarify whether or not the term in question is significant or not.

A mechanism has been presented which leads to the form of the rate law which best correlated all the data. It was shown that the form of the rate constants that were predicted by the theoretical development were the same as the experimental correlation of the rate constants with temperature and pressure. It was also shown

that the separation factor introduced by Sandler could be obtained from the data, although it is believed that the development presented herein lays a more logical development for the existence of this factor.

The fact that previous investigators have obtained a first order reaction for the ortho → para reaction can be explained in the following manner: first, it was noted that most investigators were working in the temperature range 65-80°K. In this region the present investigators also found a fair (but not exact) correlation for first order. But first order didn't hold as temperature was decreased and pressure was increased, and few investigators operated in these latter regions.

It can be observed in Fig. II-29 - II-59 that the data for the integrated rate expression fit a straight line quite well at the lower values of the ln term i.e., at higher velocities. While there is in some cases quite a marked deviation of the data from the curve at higher values of the ln term, it should be noted that the points in these regions represent driving forces of less than two or three mole per cent i.e., $(x - x_e) \leq 0.02 - 0.03$. The uncertainty in the measurements is on the order of $x = 0.002$, which represents a 10% uncertainty in the regions under consideration. The natural logarithm of 0.002 is -6.22 and of .02 is 3.92, so this gives an idea of how a small error can influence the location of a point in this region on the plot. At higher values of the driving force $(x - x_e)$, errors of the magnitude given are not as significant. In the taking of the data, a relatively high ($\sim$0.41/min) flow rate through the analyzer was encountered. The stream flowing through the analyzer was metered by a rotameter, which could not be read precisely. Small and undetected variations in the flow at this point might have a significant effect upon the results of calculation at low flows. The scattering of points at low space velocities bears this out (Cf. Fig. II-4). However, the deviation is in the same direction. Diffusion effects are possible at the lower flow rates, as, in these regimes, the flow is nearly laminar, and thus the transport mechanism is molecular diffusion, as opposed to eddy diffusion at higher velocities. In general, designers would be interested in data at higher flow rates (corresponding to STP space velocities of around 800 $min^{-1}$ and up) and in all cases these flow rates are represented by the regions in which the data most nearly fit the curve. It should be noted that there is not necessarily greater deviation at higher pressures. The reason for apparently more deviation is that more data points were obtained at

the low flow rates at high pressures than were obtained at low pressures, i.e. the amounts of conversion of points which lie on the curve are roughly the same at high and low pressures.

The rate expression chosen correlated the data in general better than any other rate expression of the many that were tried. The rate expressions that were tried have already been listed. Individual cases, in some instance, were found to be well correlated by different rate expressions, but there was no other expression which correlated more than three or four runs well.

If the lines show in Figs. II-29 - II-59 had intercepted at the origin, then k' would have become zero and a simple first order expression would apply. The fact that this is not the case suggests that a more complex mechanism than simple first order reaction exists.

All of the above development assumes that the reaction takes place under isothermal conditions. The experimental conditions were such that this assumption wasn't strictly justified. The two resistance thermometers gave temperature differences of up to 9°K between the top and bottom of the reactor. Again, however, the temperatures measured were averages between the heater temperature and the incoming hydrogen temperatures, both of which were higher than the temperature of the bed. It is safe to assume that the temperatures in the bed itself were not as different as the thermometers indicated due to the construction of the reactor. The large block, which had a relatively high thermal diffusivity, tended to even out temperature gradients. However, it cannot be claimed that the reactor was truly isothermal. The extremes in temperature gradients were encountered at the lower flow rates, another fact which might account for the deviations of the curves in the low flow rate regions. The temperature gradients outside the reactor were only about one or two degrees at the most at high flow rates and again the gradient wouldn't be this extreme inside the reactor. It is felt that at the higher flow rates, roughly corresponding to the flow rates at which the given kinetic law applies, isothermal conditions were closely approximated.

It is felt that the rate expression chosen correlates the data sufficiently well for design purposes. More data could be obtained, particularly in the pressure region below 200 psi and covering the same temperature ranges that were covered here.

## II.7 Conclusions and Recommendations

It was concluded from the above studies that the reversible reaction

$$\text{parahydrogen} \rightleftarrows \text{orthohydrogen}$$

could be represented at medium to high flow rates, i.e., corresponding to STP space velocities of about 800 $min^{-1}$ and above, by the rate equation

$$r = \frac{kc_H(x - x_e)}{1 + k'c_H x}$$

where the rate constant k is described by Arrhenius' Law

$$k = A \exp(-E^{\neq}/RT) = A \exp(-159/T)$$

where A was given by

$$A = K\Pi^{-n} = 86{,}500\Pi^{-1.06}$$

and k' is inversely portional to the concentration

$$k' = K'/c_H = -0.85/c_H$$

It was further concluded that the data agreed with the mechanism that was postulated, and that the surface reaction is the rate controlling step. The forms of the rate constants that were obtained experimentally were predicted by the postulated mechanism. It was also shown that orthohydrogen is more strongly adsorbed than parahydrogen, as predicted by Sandler and others, and that the ratio of adsorption equilibrium constants was the same order of magnitude that they had predicted.

It is recommended that further data be obtained in the temperature ranges 40 - 80°K and covering the pressure range 20 - 180 psia.

It is also recommended that the following work be performed:

A. The reaction

$$\text{orthohydrogen} \rightleftarrows \text{parahydrogen}$$

should be studied using the same apparatus that was used in the present study and covering the same pressure and temperature regimes. This would enable determination of the reverse reaction equation so that the two could be compared. The mechanism of conversion should be the same in either direction so that study of the forward and reverse reaction should yield valuable information about the actual mechanism.

B. Hydrogen adsorption isotherms need to be obtained. These would help facilitate the prediction of the effects of adsorption on the overall reaction. Also, if possible, adsorption of para-hydrogen and orthohydrogen should be compared.

C. Other mechanisms should be studied and data treated by them.

It is felt that if experiments along the lines of (A) and (B) were performed, and combined with the present data, a good understanding of the fundamental mechanism could be obtained.

## NOTATION

$a$ = constant in Eq. (II-45) = $(k_6/k_5)(1 + k_4/k_3)$.

$A$ = frequency factor in Arrhenius' Law, $min^{-1}$.

$A_i$ = constant in Eq. (II-61).

$b$ = constant in Eq. (II-46) = $k_1/k_2$.

$B$ = constant in Eq. (II-65).

$c_p$ = parahydrogen concentration, g moles-$cm^{-3}$.

$c_H$ = hydrogen concentration, g moles-$cm^{-3}$.

$c_o$ = orthohydrogen concentration, g moles-$cm^{-3}$.

$d$ = differential operator.

$d$ = constant in Eq. (II-46) = $k_6/k_5$.

$D$ = effective diffusivity of hydrogen, $cm^2 sec^{-1}$.

$E$ = effectiveness factor.

$E^{\neq}$ = measured activation energy, cal-g $mole^{-1}$.

$E^{\circ}$ = theoretical activation energy, cal-g $mole^{-1}$.

$F$ = feed rate of total gas, l-$min^{-1}$.

$h$ = Thiele modulus.

$\Delta H_i$ = heat of adsorption, Eq. (II-61) cal-g $mole^{-1}$.

$\Delta H_r$ = heat of reaction, cal-g $mole^{-1}$.

$I'$ = plotted intercept, Eqs. (II-56), (II-57), (II-58).

$k_1, k_2, k_3, k_4$
$k_5, k_6$ = rate constants in Eqs. (II-25), (II-26), (II-27).

$k_r$ = rate constant for $n^{th}$ order reactions, $min^{-1}$.

$k$ = rate constant, $min^{-1}$

$k'$ = rate constant, $cm^3$-g $mole^{-1}$.

$k_s$ = first order rate constant per unit area surface per unit volume, cm $sec^{-1}$.

K = constant for pressure dependence of frequency factor.

K' = proportionality constant for concentration dependence of k'.

$K_i$ = adsorption equilibrium constant, Eq. (II-61).

$K_m$ = mass transfer coefficient in Table II-III, $lb_M$-$ft^{-2}$-$sec^{-1}$.

L = radius of catalyst pellet, cm.

n = exponent in pressure dependence of frequency factor.

n = exponent in empirical reaction order in Eq. (II-15).

r = rate of production of orthohydrogen per unit volume of reactor, g mole-$min^{-1}$-$cm^{-3}$.

$r_2, r_3, r_4$ = rate of reaction of individual reactions, Eqs. (II-28), (II-29) (II-30).

R = gas constant, 1.99 cal-g $mole^{-1}$-$°K^{-1}$.

s = separation factor.

S = active site, Eqs. (II-25), (II-26), (II-27).

S' = slope of lines, Eq. (II-56), (II-57), (II-58).

S = surface area of catalyst per unit volume of reactor, $cm^2$ - $cm^{-3}$.

T = temperature of run, °K.

$V_r$ = volume of reactor, $cm^3$.

$V_{cat}$ = volume of catalyst bed, $cm^3$.

x = mole fraction parahydrogen in stream leaving reactor.

$x_e$ = equilibrium mole fraction parahydrogen.

$x_g$ = mole fraction parahydrogen in gas phase, Eq. (II-49).

$x_o$ = mole fraction parahydrogen in feed stream.

$x_s$ = mole fraction parahydrogen on surface, Eq. (II-49).

Greek

$\epsilon_r$ = heat of conversion in gas phase, Eq. (59), cal-g mole$^{-1}$.

$\theta_o$ = fraction of surface covered by orthohydrogen.

$\theta_p$ = fraction of surface covered by parahydrogen.

$\Pi$ = total operating pressure, psia.

$\tau$ = space time, min.

$\chi$ = tortuosity factor, Eq. (II-22).

REFERENCES


1. Arrhenius, S., Z. Physik. Chem., Vol. 4, p. 228 (1889).
2. Blake, J. H., personal communication.
3. Bonhoeffer, K. F., and P. Harteck., Z. physik. Chem., B. 5, (1929).
4. Buyanov, R. A., Kinetika i Kataliz, Vol. 1, No. 2, p. 306 (1960).
5. _____, Kinetika i Kataliz, Vol. 1, No. 4, p. 617 (1960).
6. Chapin, D. S., and H. L. Johnston, J. Am. Chem. Soc., Vol. 79, p. 2406 (1957).
7. Chelton, D. B., Safety in the Use of Liquid Hydrogen, NBS Report 7253 (1962).
8. Cunningham, C. M., and H. L. Johnston, J. Am. Chem. Soc., Vol. 80, p. 2377 (1958).
9. Clark, R. G., J. F. Kucirka, A. Jambhakar, and G. E. Schmanch, Investigation of the Para-Ortho Shift of Hydrogen, ASD-TDR Report 62-833, Part II, Wright-Patterson AFB, Ohio, p. 30 (1963).
10. Farkas, A., Orthohydrogen, Parahydrogen, and Heavy Hydrogen, Cambridge Press, p. 13 (1935).
11. Geddes, D. D., M. S. Thesis, University of Colorado (1963)
12. Harrison, L. G., and C. A. McDowell, Proc. Roy. Soc., (London), A220, p. 77 (1953).
13. Hougen, O. A., and K. M. Watson, Ind. Eng. Chem., Vol. 35, p. 529 (1943).
14. Hutchinson, H. L., M.S. Thesis, University of Colorado, 1964.
15. Johnson, V. J., ed., Properties of Materials at Low Temperatures, Phase 1, NBS- Wright Air Development Center, Sec. 5.002 (1959).
16. Keeler, R. N., D. H. Weitzel, J. H. Blake, and M. Konecnik, Adv. Cryo. Eng. Vol. 5, New York, Plenum Press Inc., p. 511 (1960).
17. Levenspiel, O., Chemical Reaction Engineering, New York, John Wiley and Sons, p. 108 (1963).
18. _____, ibid., p. 435.
19. McCabe, W. L., and J. C. Smith, Unit Operations in Chemical Engineering, New York, McGraw-Hill Book Co., Ch. 10 (1956).
20. Purcell, J. R., and R. N. Keeler, Rev. Sci. Inst., Vol. 31, No. 3, p. 304 (1960).
21. Sandler, Y. L., J. Chem. Phys. Vol. 58, p. 58 (1954).

22. Schmauch, G. E., and A. H. Singleton, "Technical Aspects of Ortho-Parahydrogen Conversion," paper presented at ACS-Petroleum Div. Meeting, (Sept., 1963).

23. Shaffer, A., and J. Rousseau, Thermodynamic Properties of 20.4°K, - Equilibrium Hydrogen, ASD Tech. Report 61-360, Wright-Patterson AFB, Ohio (1961).

24. Wakao, N., P. W. Selwood, and J. M. Smith, A.I.Ch.E. Journal, Vol. 8, No. 4, p. 478 (1962).

25. Wakao, N., J. M. Smith, and P. W. Selwood, J. Catalysis, Vol. 1, No. 1, p. 62 (1962).

26. Weitzel D. H., J. H. Blake, and M. Konecnik, Adv. Cryo. Eng., Vol. 4, New York, Plenum Press Inc., p. 286 (1960).

27. Weitzel, D. H., J. W. Draper, O. E. Park, K. D. Timmerhaus and C. C. Van Valin, Adv. Cryo. Eng., Vol. 2, New York, Plenum Press. Inc., p. 12 (1957).

28. Weitzel, D. H., C. C. Van Valin, and J. W. Draper, Adv. Cryo Eng. Vol. 3, New York, Plenum Press, Inc., p. 73 (1960).

29. Wheeler, A., Advances in Catalysis, Vol. III, New York Academic Press Inc., p. 250 (1951).

30. Wigner, E., Z. Physik. Chem., B 23, p. 28 (1933).

# SECTION III

# EFFECTS OF DIFFUSION RATES AND CATALYST SURFACE AREA ON CATALYST ACTIVITY

## III. 1 Introduction

This section reports the results of an investigation into the effects of diffusion rates and surface area on the activity of the ferric oxide gel catalyst for the ortho-parahydrogen conversion. This investigation was carried out by obtaining the physical structures of several catalysts of similar composition but widely differing activities, and analyzing the relationship between physical structure and activity by methods developed over the last 25 years by investigators in this field. By the physical structure is meant the surface area, the porosity, and the pore size distribution of the catalyst.

Most solid catalysts, including the ones used in this study, consist of pellets, grains, or granules, pierced by myriad small pores. The diffusion of the reactants through these pores in many cases reduces or entirely controls the rate of reaction. The first effort at predicting the effect of diffusion within the catalyst particle upon the catalyst activity was made by Damköhler (9). The first quantitative treatment of the effect of simultaneous diffusion and reaction in catalyst pores was carried out independently by Thiele (37) in the United States and Zeldowitsch (53) in the USSR. They derived equations for predicting the relative importance of diffusion rates and reaction rates when the reaction took place on the interior surface of a porous catalyst.

Thiele also introduced the concept of the "effectiveness factor," which indicates the extent to which the activity of the catalyst is lowered by intraparticle diffusion. For example, an effectiveness factor of 0.7 indicates that the catalyst is only 70% as active as it would be if intraparticle diffusion did not hinder the catalyst activity, and the interior surface of the catalyst were exposed to the same concentration of reactants as is the exterior surface of the catalyst pellet.

Thiele's work was extended by Wheeler (47) in a classic review of the state of the art through 1951. This review gave a thorough treatment of isothermal reaction rates in catalyst pores. Progress since that time has largely been in the field of non-isothermal reactions and complex reactions. These advances are covered through early 1963 in a comprehensive and critical review by Satterfield and Sherwood (33).

## III.2 Theory

### III.2.A Effects of Diffusion Rates on Catalyst Activity

In the various analyses of the effect of diffusion rates upon catalyst activity, three models of the shape of a catalyst pellet have been used in order to make the mathematics tractable. The three models are the slab of a given width, neglecting end effects; a cylinder, again neglecting end effects; and a sphere. The mathematical analyses used in the investigation reported here considered only the sphere and slab, since the solutions for the equations resulting from the cylindrical model resulted in values which lay between the values obtained from the solutions of the slab and spherical models. The sphere and slab thus represent the two extremes which have been analyzed.

In all of the models considered, the principal parameter which results from the equations is a dimensionless number which represents the square root of the ratio:

$$\frac{\text{reaction rate in which diffusion effects can be ignored}}{\text{reaction rate in which surface effects can be ignored}}$$

This dimensionless number has been called the "Thiele Modulus" by later workers in the field in recognition of the importance of Thiele's work. When a first order reaction is occurring, the values of the Thiele Modulus for the slab model and the spherical model of a catalyst pellet are given by the equations:

Slab Model:

$$h_{sl} = L\sqrt{\frac{k_s S}{D_e}} \qquad \text{(III-1)}$$

Sphere model:

$$h_{sp} = \frac{R_p}{3}\sqrt{\frac{k_s S}{D_e}} \qquad \text{(III-2)}$$

In these equations $h_{sl}$ and $h_{sp}$ are the Thiele Moduli for the slab and sphere, respectively, L is half the width of the slab, $R_p$ is the radius of the sphere, $k_s$ is the first order surface reaction rate constant, S is the specific surface of the catalyst, and $D_e$ is the effective diffusivity of the reactants within the catalyst pellet.

The physical significance of the Thiele Modulus, and the derivations of the relationships presented above are discussed in Appendix III-A.

Thiele showed that for first order reactions the effectiveness factors for the two models of catalyst granules were related to the Thiele Modulus by the equations:

$$E_{sl} = \frac{1}{h_{sl}} \tanh h_{sl} \qquad \text{(III-3)}$$

$$E_{sp} = \frac{1}{h_{sp}} \left[ \frac{1}{\tanh 3h_{sp}} - \frac{1}{3h_{sp}} \right] \qquad \text{(III-4)}$$

in which $E_{sl}$ and $E_{sp}$ are the effectiveness factors for the slab model and the sphere model, respectively.

In his review, Wheeler (48) showed that the Thiele Modulus, and as a result the effectiveness factor, could be related to the overall catalyst activity, the diffusivity of the reactants within the catalyst particle, and the physical structure of both the catalyst particle and the catalyst bed. As a result, if the diffusivity of the reactants within the catalyst particle were known, and the physical structure of the catalyst had been determined, the Thiele Modulus and the effectiveness factor could be obtained from one activity measurement. The equations resulting from this method of approach were:

Slab model:

$$h_{sl} \tanh h_{sl} = \left[ \ln \frac{(c_{pe} - c_{pb})_1}{(c_{pe} - c_{pb})_2} \right] (L^2) \left(\frac{F}{V_r}\right) \left(\frac{1}{\gamma D_e}\right) \qquad \text{(III-5)}$$

Sphere model:

$$\frac{3h_{sp}}{\tanh 3h_{sp}} = \left[ \ln \frac{(c_{pe} - c_{pb})_1}{(c_{pe} - c_{pb})_2} \right] \left(\frac{R_p^2}{3}\right) \left(\frac{F}{V_r}\right) \left(\frac{1}{\gamma D_e}\right) + 1 \qquad \text{(III-6)}$$

In these equations, $c_{pe}$ is the equilibrium concentration of parahydrogen at the temperature of the reaction, $c_{pb}$ is the concentration of parahydrogen in the bulk gas phase, F is the feed rate to the catalyst chamber at the temperature and pressure of the reaction, $V_r$ is the total volume of the reaction zone, and $\gamma$ is the fraction of the chamber that is occupied by the catalyst pellets. The subscripts 1 and 2 refer to the entrance and exit of the reaction zone respectively.

It may be noted that Equation (III-5) differs from that presented by Wheeler (49). This is caused by differences in assumptions concerning the nature of

the catalyst pellet. It is believed that Equation (III-5) is more general. The derivations of equations (III-5) and (III-6) are presented in Appendix III-B.

From these equations, the Thiele Modulus, and as a result the effectiveness factor, can be estimated if the effective diffusivity within a catalyst is known, together with the pertinent physical properties. The exact result will depend on which particular model of a catalyst pellet is chosen as the more reasonable for a particular situation. Conversely, if the effectiveness factor and all the physical parameters except one is known, then the value of the remaining parameter can be estimated from the relationships presented above. In one part of this investigation, the effectiveness factor was known, and accurate values or estimates were obtainable for all the other parameters in the above equations except the effective diffusivity. The effective diffusivity was determined from these equations.

III. 2.B Diffusion Within Porous Solids

The diffusion of the reactants and products within a porous catalyst is usually assumed to obey Fick's Law of Diffusion:

$$\frac{N_A}{A} = - D_A \nabla c_A \qquad \text{(III-7)}$$

in which $N_A/A$ is the number of moles of substance A crossing a unit cross section of area per unit time, $\nabla c_A$ is the gradient of the concentration of substance A, and $D_A$ is the constant of proportionality for the diffusion of substance A under these particular conditions. The constant of proportionality is called the diffusivity.

Diffusion within porous catalysts can take place either within the gas phase or along the internal surface of the catalyst. If the diffusion takes place within the gas phase, the effective diffusivity has been shown to follow the relationship:

$$D_e = D_{calc} \epsilon\chi \qquad \text{(III-8)}$$

in which $D_{calc}$ is the diffusivity which would be calculated for a substance diffusing in a direction normal to the external surface of the catalyst across a cross sectional area equal to a cross sectional area of the catalyst, $\epsilon$ is the porosity of the catalyst, and $\chi$ is the tortuosity factor.

The value of $D_{calc}$ can be obtained from the theoretical relationships developed for the various cases. If the collisions of the molecules one with another are insignificant in number when compared with the collisions of the molecules with the surface of the catalyst, then Knudsen flow is said to be taking place, and the relationship used in this case was developed by Knudsen (25). If the collisions of the molecules with the wall are insignificant when compared with the collisions with other molecules, then ordinary diffusion is occurring, and equations for this are presented in several places (e.g., 32). For the intermediate case when both types of collisions are significant, equations have also been developed (35).

The tortuosity factor is an empirical factor which accounts for the fact that catalyst pores are not smooth, circular pores, oriented in the direction normal to the surface of the catalyst, as simple diffusion theory would require. Rather, the pores are of widely varying cross section, randomly oriented, and interconnected.

Measurements of diffusion within porous solids have been made by many investigators (e.g., 1,2,3,13,20,21,22,23,30,39,44,45), and tortuosity factors may be obtained from these measurements. The tortuosity factors obtained have varied over a wide range, but values greater than 1.0 have been exhibited thus far only by compressed powders or gels (2,22,45), which usually have a bidisperse pore size distribution,i.e., a distribution in which the pore sizes are concentrated within two size ranges--a low range caused by the porous nature of the gel itself, and a high range resulting from the interstices between the compressed gel particles. Tortuosity factors above 0.2 have been found only in compressed powders and gels or in substances with porosity above 0.5 (39,45). For porous solids with a distribution of pore sizes over a narrow range, and porosity below 0.5, the tortuosity factor appears to vary between 0.1 and 0.2 when diffusion takes place within the gas phase (13,20,21,23).

Several attempts have been made to predict the tortuosity factor. From an idealized model of a catalyst pellet, Wheeler predicted that the tortuosity factor should approximate 0.5 (51). Weisz and Schwartz (45) predict that the tortuosity factor should follow the relationship:

$$\chi = \sqrt{\frac{3}{2}}\,\epsilon \qquad \text{(III-9)}$$

for Knudsen flow. They present data obtained from the diffusion of gases through silica and alumina catalyst pellets to support this prediction. Geddes (19) states that one of the reasons that the factors vary so widely is that rate of Knudsen flow is dependent upon the cube of the radius, and the standard method of obtaining the average radius--by dividing twice the pore volume per gram by the surface area per gram--gives the average of the radius squared over the average radius. He suggests that the radius used in evaluating the Knudsen diffusivity be evaluated from the pore size distribution using the average of the radius cubed divided by the average of the radius squared, $r^3/r^2$. He implies that the tortuosity factor found for substances with a narrow pore size distribution can then be used. The most consistent tortuosity factor is that obtained from measurements of diffusion through Vycor glass, which has a very narrow distribution of pore sizes. The average value of the tortuosity factor from the various measurements made through Vycor glass (1,20,21) is 0.17.

It has also been shown that it is possible for diffusion to take place along the interior surface of a porous solid, in addition to occurring in the gas phase. The work of Gilliland, Baddour, and Russell (21) indicates that this type of diffusion does not follow Fick's Law, and also does not occur to any large extent without considerable adsorption. It would thus be expected to be relatively unimportant when the reaction under investigation is carried out at temperatures well above the boiling point of the reactants and products.

III. 2.C The Surface Area of Catalysts

The surface area of porous substances is usually measured by the method developed by Brunauer, Emmett, and Teller (5), and is referred to as the BET method. The usual BET equation was derived for adsorption on flat surfaces, and does not represent the situation when small pores are present.

Another equation was derived for the case when the substance whose surface area is being measured has capillaries too narrow for the application of the flat surface equation. This equation (5) involves the use of a parameter which represents the number of molecular layers that can be formed on each wall of the narrow capillary without the layer meeting one from the other side. The application of this more general equation, with any assumed value for the number of layers that can be formed on a capillary wall, presupposes that there

are capillaries of only one radius present in the pore solid. Since the capillaries in most porous solids cover a range of at least 50 Angstrom units, and often a far wider range, this is obviously not true. But application of the flat surface equation to a porous solid with pores of only 4 Angstrom units radius results in a surface area that is within 18% of the area measured by the more exact equation. Thus, it would seem that the equation for a flat surface would be suitable for porous solids with very few pores below a radius of 4 Angstrom units.

The BET equations, both the equation for a flat surface and for adsorption on the walls of narrow capillaries, assume that the entire surface is available to the adsorbent. In a capillary with a radius that is less than the diameter of an adsorbent molecule, however, this area would not be completely reported because the adsorption of one molecule on the wallof the capillary would prevent the adsorption of a molecule on the opposite wall of the capillary. This would cause the apparent surface area to be somewhat less than the actual surface area.

Other methods have been developed for obtaining the surface area of porous substances, though none of these can be carried out with the ease of the BET method. Two of these--the heat of wetting method and the use of low angle x-ray scattering techniques--have been used to check the surface areas of porous substances obtained by the BET method. In the cases of porous substances that do not contain many fine pores the surface areas obtained by both of these methods are almost identical with the surface areas obtained by the BET method (6,15). Conversely, when measuring the surface areas of porous solids which contain many fine pores, it was found that both the heat of wetting method and the use of low angle x-ray scattering techniques gave surface areas that were considerably higher than the surface areas obtained by the BET method (6,12,15,16,18,28).

One example of these comparisons is the study by Elkin, Shull, and Roess (16), in which they compared the area obtained by the use of low angle x-ray scattering techniques to the surface area obtained by BET method for several silica gels. In every case, they found the surface area obtained by low angle x-ray techniques greater than that obtained by the BET method. The differences ranged from 14% to 50%. It was impossible to say which method was the more reliable, but it is worthwhile to note that these results would be what might be expected if these gels possessed many pores with radii below 4 Angstrom units.

Ordinarily, the surface area of pores with radii below 4 Angstrom units would not be of great interest in studies of catalytic kinetics, because the diffusion of gases within these pores is too slow for the amount of reaction taking place to be significant when compared with the amount of reaction taking place within the larger pores. However, if surface diffusion were more than a minor factor in the transport of reactants and products, than these pores might assume significance in the amount of reaction taking place. The possible conclusion from these speculations is that under normal circumstances, the surface area obtained by the BET method would be expected to be the area which is of major importance during a catalytic reaction. If surface diffusion is present to a significant extent, and the catalyst possesses many fine pores, than the BET area might not represent the total area available to the reactants.

## III. 3 Experimental Apparatus and Procedures

Two types of experimental measurements were taken in this investigation--nitrogen adsorption isotherms and evaluations of catalyst activity. The apparatus used to find the nitrogen adsorption isotherms was developed by Loebenstein and Deitz (27). A diagram of the apparatus is shown in Figure III-1, and a photograph in Figure III-2.

The adsorption tube, T, was a glass tube with an inside diameter of 12 mm and was 30 cm long. The tube had a ground glass joint at the top and tapered into a capillary tube at the bottom. The inner member of the tube was shaped like a test tube and reached a depth of 3 or 4 cm from the bottom of the outer tube. The annular space between the two tubes and also the space at the bottom of the inside tube was kept as small as possible. The sample was placed at the bottom of the outer tube and was kept in place by glass wool.

Gas was admitted into the adsorption tube through capillary tubes which were made as long as possible for heat transfer purposes.

The capillary tubing terminated in a ball and socket joint. The other half of each of these joints was also capillary tubing which led to the top of the two equal volume burets, P and S.

These two burets had a volume of approximately 200 ml. The volume of buret P was bounded by stopcocks E and I at the top and by a mark (A) etched at the bottom of the buret. Buret S was bounded by marks (B) and (C) etched at the top and bottom of the buret. The two burets were then connected to the

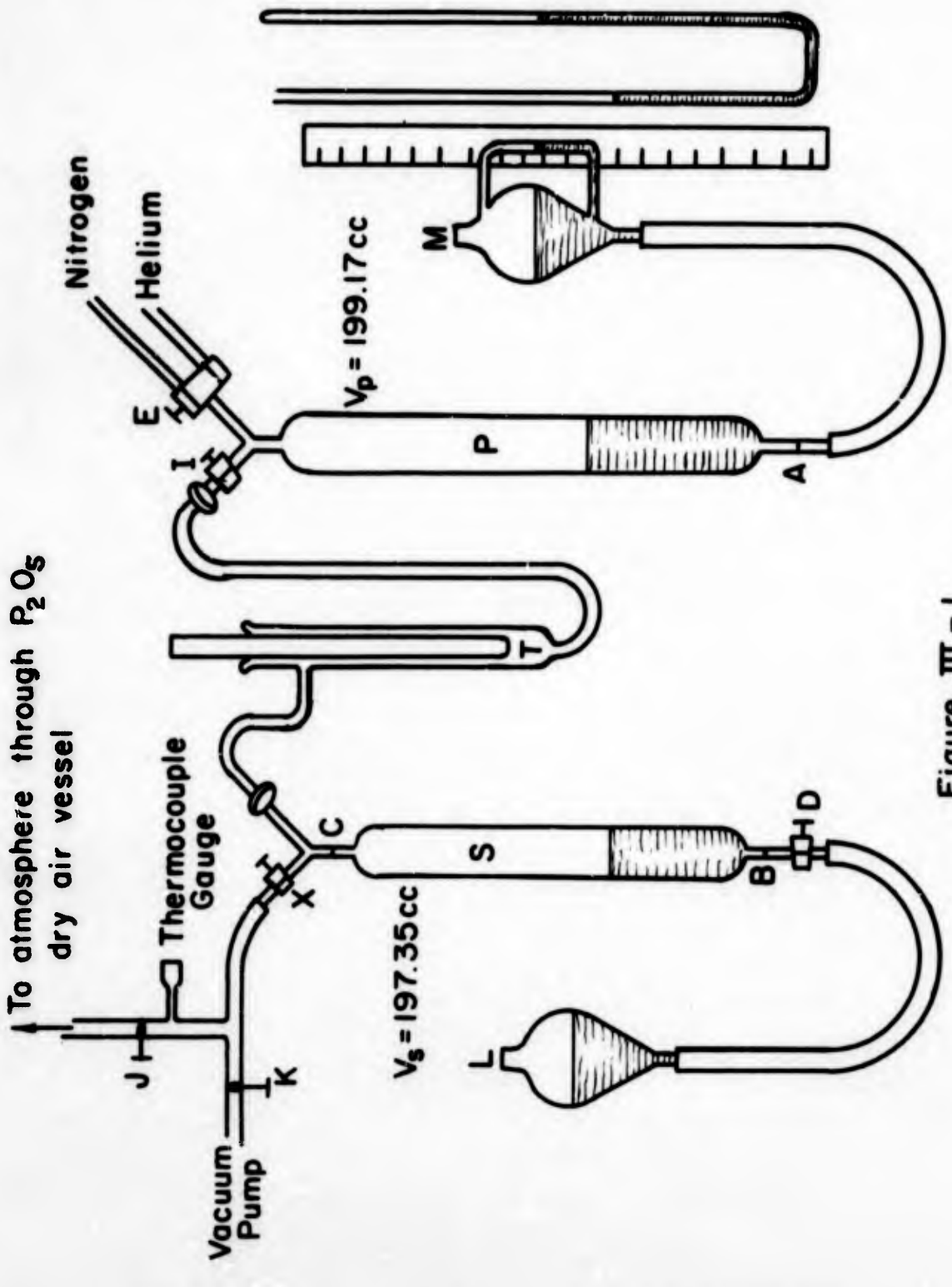


Figure III - 1

GAS ADSORPTION APPARATUS

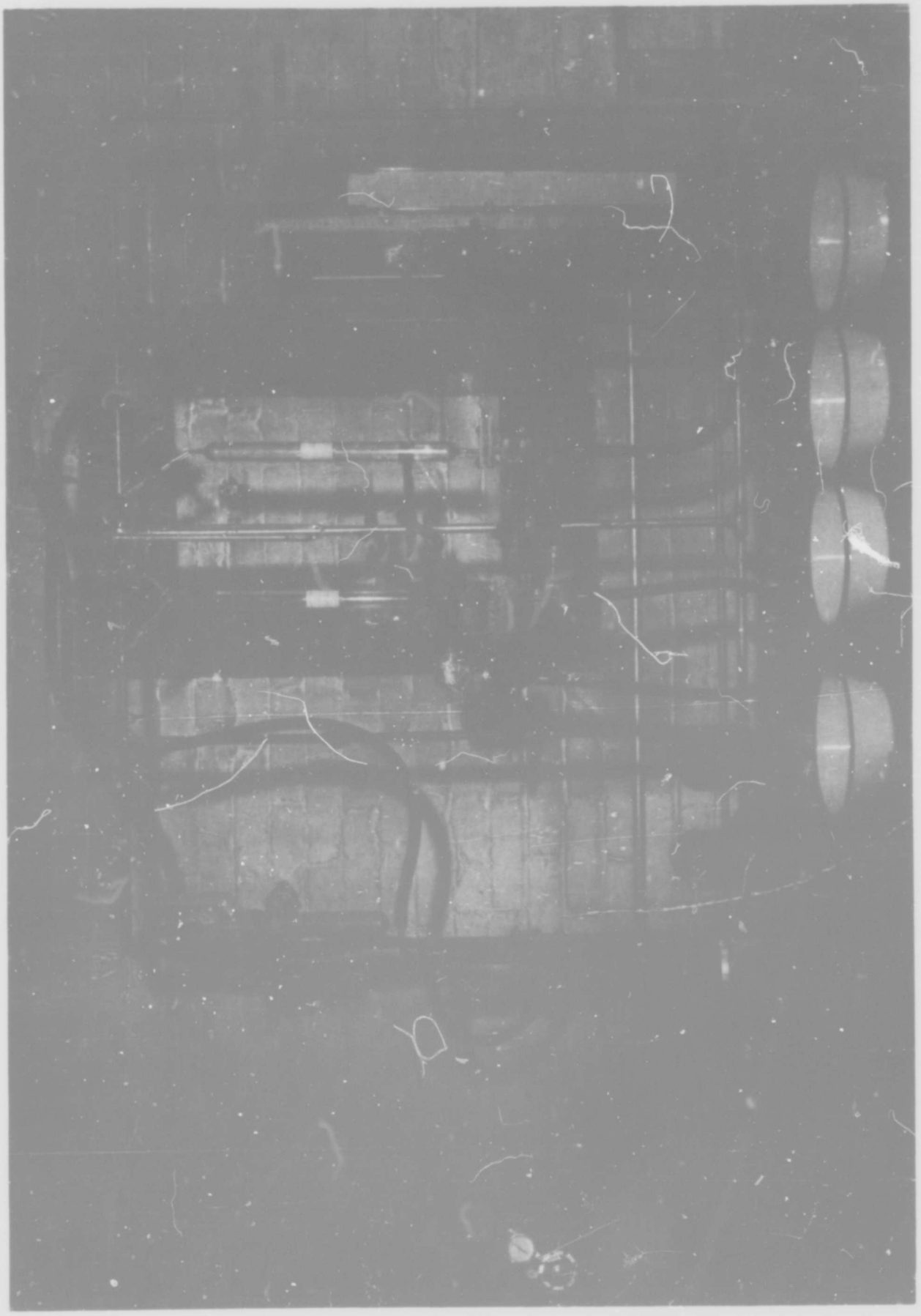

Figure III-2 GAS ADSORPTION APPARATUS

mercury leveling bulbs L and M by means of long rubber tubing. A stopcock D was placed below the mark (B) on buret S to serve as a cutoff to hold the mercury level constant while readings were being taken. Mercury leveling bulb M had a sidearm of 10 mm glass tubing to facilitate pressure readings on the scale. Pressure readings were made when the mercury in buret P was at A, and the mercury in buret S was either at B or C.

Nitrogen and helium were admitted through the stopcock E. Buret P was isolated from the adsorption tube. The entire system was isolated from the atmosphere by stopcock X.

A 20 liter dry air surge tank was also provided which was used so the catalyst was exposed to a uniform and relatively dry air supply. The surge tank was connected to the adsorption tube by valve J. Valve K connected the adsorption tube to a Duo-Seal vacuum pump.

The thermocouple gauge was connected to the system by valve J, and was used to give pressure readings during activation.

The catalyst activity was evaluated by converting a mixture of hydrogen gas containing 75% orthohydrogen and 25% parahydrogen to a mixture containing 48% parahydrogen, and measuring the volume of gas which passed through the reactor during the conversion. The reaction was carried out at a pressure of 10 psig, or 22.2 psia, and 76°K (-197.2°C). The apparatus used for these measurements consisted of three sections--a hydrogen purification section, the reactor and the analysis section. A schematic diagram of the apparatus is presented in Figure III-3. A photograph is shown in Figure III-4.

The hydrogen used in these studies was purchased from the National Bureau of Standards, who obtained it by vaporizing liquid hydrogen. In order to remove any impurities that might be present the hydrogen was passed through a bed of silica gel immersed in a bath of liquid nitrogen. To insure that the hydrogen entering the converter was "normal" hydrogen, or hydrogen containing 75% orthohydrogen, following the passage through the bed of silica gel at 76°K, the hydrogen was passed through a "normalizer" containing a nickel catalyst at a very high temperature--above 500°C.

After passing through the normalizer, the hydrogen was cooled to 76°K in a precooler, then admitted to the catalyst chamber. After the reaction, the hydrogen was split into two flows--one which went directly to a wet test meter while the other passed through the analyzer.

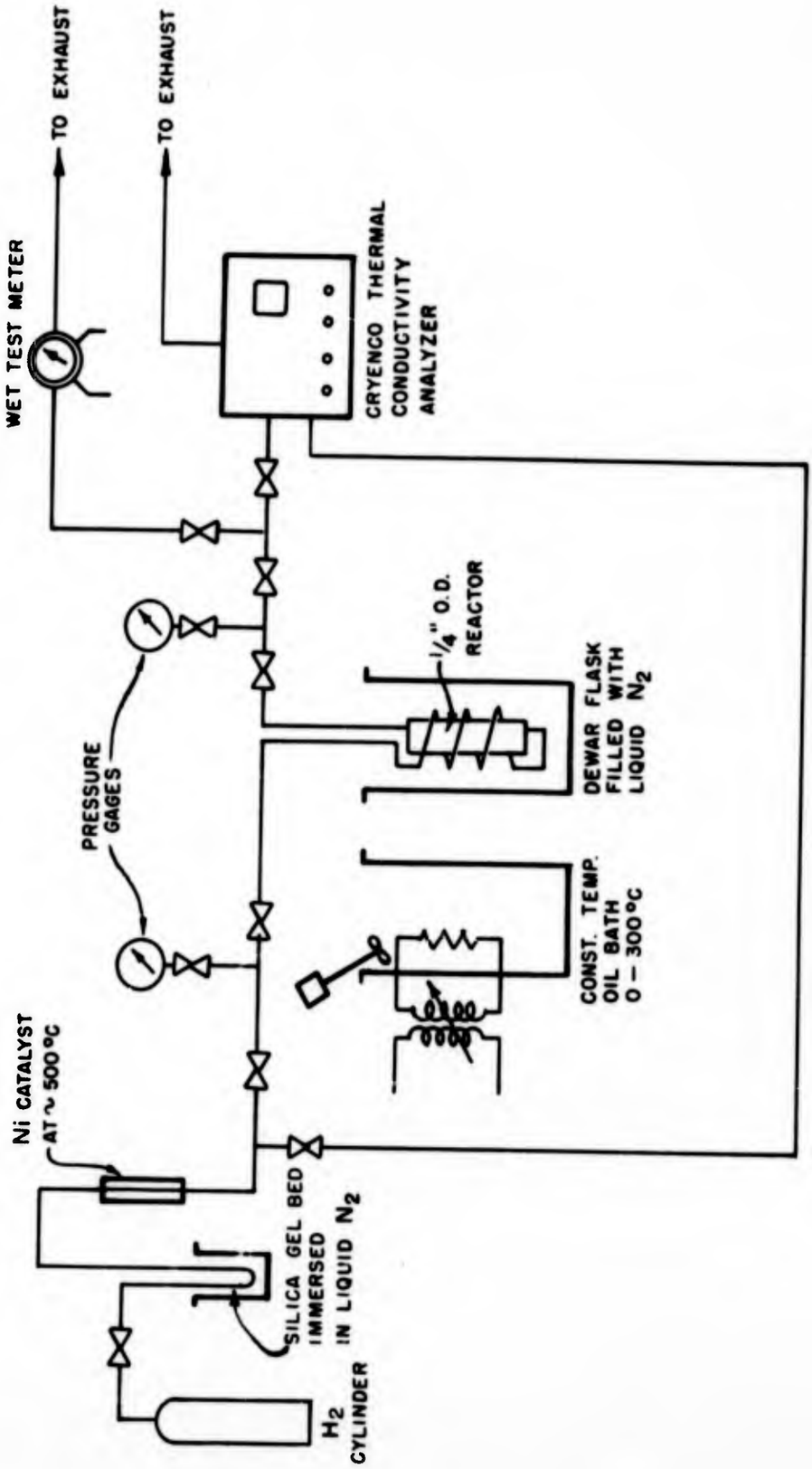


Figure III - 3

ACTIVITY TESTING APPARATUS

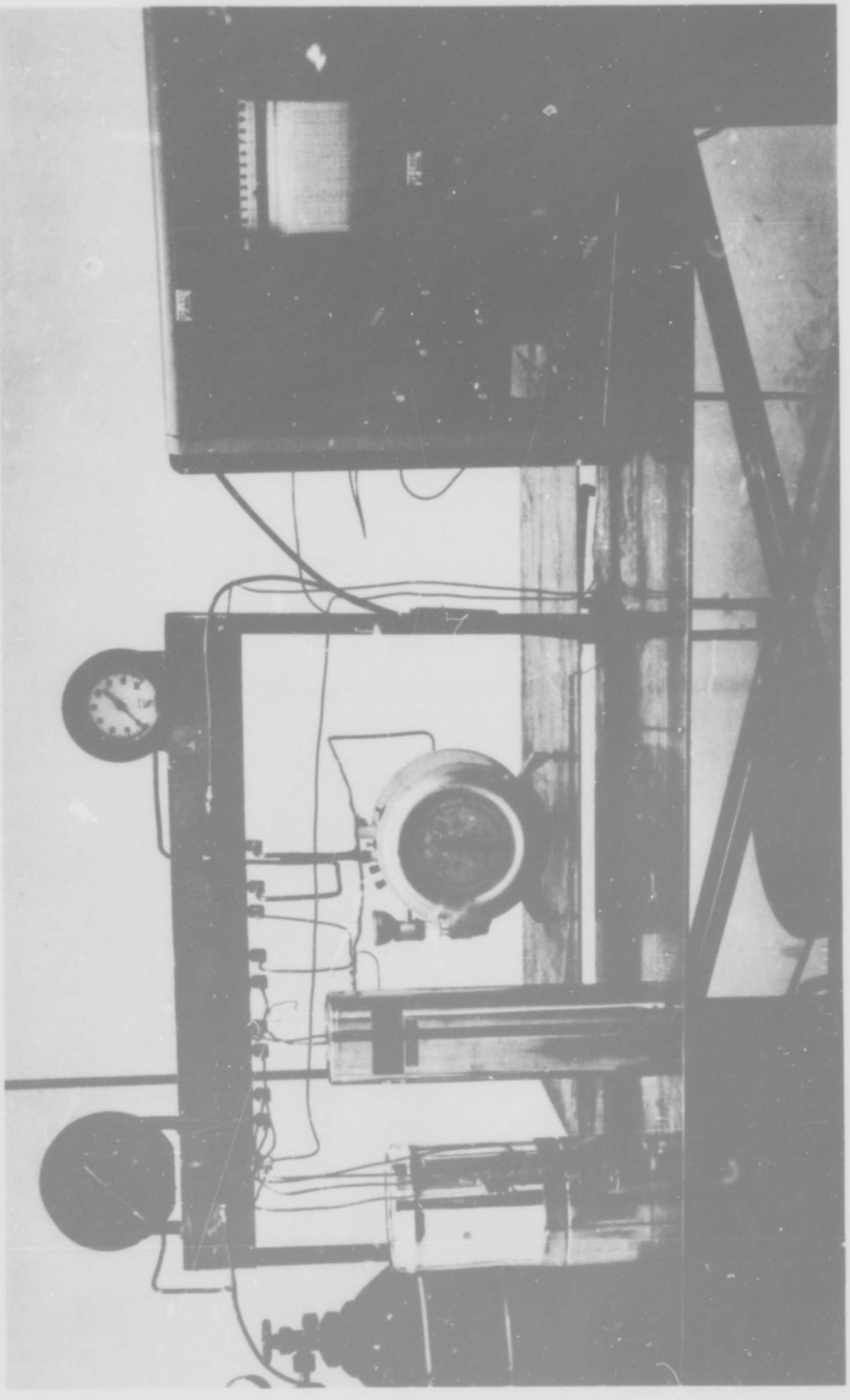

Figure III-4 ACTIVITY TESTING APPARATUS

The ortho-para content of the gas mixture was determined by thermal conductivity. The analytical instrument for determining the per cent of ortho and para hydrogen was purchased from the Cryotronics Division of Cryogenic Engineering Company, and was identical in design to the instrument reported by Purcell, Draper and Weitzel (31).

## III.4 Results

Ten ferric oxide gel catalysts, covering a threefold range in activity, were studied in an effort to determine the effects of surface area and diffusion rates on catalyst activity. These different catalysts are listed in Table III-I with their activities and a brief comment on the method of manufacture of the different catalysts. For the purpose of this study, the catalyst activity is defined as the volume of hydrogen (measured at standard temperature and pressure) per minute per unit volume of catalyst required at 76°K to convert a mixture containing 75% orthohydrogen and 25% parahydrogen to a mixture containing 48% parahydrogen. The methods of manufacture of the catalysts are presented in more detail in Section V of this report.

The physical characteristics of the different catalysts, such as surface area, pore volume, porosity, different averages of the pore radii, and bulk density are presented in Table III-II.

It will be shown that both interparticle diffusion and temperature gradients had negligible effects on the activity measurements. It will then be shown that the effectiveness factor for the catalyst which should have had the lowest effectiveness factor was high enough so that diffusion apparently did not play a significant role in limiting the reaction rate. This meant that diffusion rates were unexpectedly high. Under these conditions, it would be predicted that the activity might be directly proportional to the surface area of the catalysts. Some possible reasons will be offered to explain the high diffusion rates and the fact that the activity was not directly proportional to the surface area.

Table III-III shows the precision which was obtained in the adsorption measurements. A high degree of precision was obtained in measuring the pore volume, but the surface area measurements could only be reproduced to ± 5%. The variation in the surface area measurements could have been the result of inaccuracies in plotting the BET equation. In an attempt to reduce the errors in determining the surface area from the BET equation, a least square fit of data was used, but this did not significantly improve the precision of the calculations.

ACTIVI[illegible]

| Catalyst | [illegible] | Method of Preparation** |
|---|---|---|
| 22 | [illegible] | [illegible] added to obtain pH of [illegible] |
| 11 | [illegible] | [illegible] |
| 17B | [illegible] | [illegible] used contained 0.25% $FeCl_2$ |
| 19B | [illegible] | [illegible] precipitated in magnetic [illegible] of 4000 gauss |
| 16A | 1080 | [illegible] contained 0.25% $CoCl_2$ |
| 00 | 1110 | Obt[illegible] National Bureau of [illegible] standard prep[illegible] parat[illegible] |
| 21A | 1330 | Reagent g[illegible] |
| 13 | 1420 | precipitated [illegible] permanent mag[illegible] |
| 339-6 | 1510 | Cryenco catalyst--[illegible] preparation |
| 12 | 1585 | precipitated in field o[illegible] permanent magnet |

*Volume of hydrogen (measured at standard temperature and pressure) per minute per unit volume of catalyst required at 76°K to convert a mixture containing 75% orthohydrogen and 25% parahydrogen to a mixture containing 48% parahydrogen.

**Cf. Section V of this report

TABLE III-II

PHYSICAL CHARACTERISTICS OF CATALYSTS

| CATALYST | ACTIVITY* | SURFACE AREA | SPECIFIC SURFACE* | PORE VOLUME | POROSITY** | $\bar{r}$ | $\frac{\overline{r^3}}{\overline{r^2}}$ |
|---|---|---|---|---|---|---|---|
| | $min^{-1}$ | $m^2/gm$ | $m^2/cc$ | cc/gm | cc/cc | Å | Å |
| 11 | 507 | 120 | 231 | .118 | 0.21 | 18.3 | 21.4 |
| 23 | 512 | 109 | 210 | .110 | 0.23 | 21.6 | 30.5 |
| 19B | 824 | 167 | 321 | .161 | 0.30 | 18.7 | 23.1 |
| 17B | 856 | 198 | 381 | .156 | 0.31 | 16.2 | 20.5 |
| 16A | 1010 | 190 | 365 | .135 | 0.26 | 14.2 | 18.7 |
| 00 | 1110 | 190 | 365 | .158 | 0.30 | 16.6 | 20.8 |
| 13 | 1400 | 200 | 385 | .185 | 0.39 | 20.3 | 28.6 |
| 21A | 1450 | 172 | 331 | .203 | 0.36 | 21.5 | 29.7 |
| 339-6 | 1510 | 234 | 450 | .204 | 0.39 | 17.4 | 28.3 |
| 12 | 1650 | 215 | 413 | .201 | 0.39 | 18.7 | 24.3 |

*Based on an average bulk density of 1.25 gm/cc.

**Based on an assumed void fraction of 0.35.

TABLE III-III

ACCURACY OF RESULTS

| CATALYST | SURFACE AREA $m^2/gm$ | PORE VOLUME $ccN_2(STP)/gm$ |
|---|---|---|
| 12 | 216 | 129 |
| | 195 | 130 |
| 00 | 191 | 102 |
| | 170 | 99 |

III. 4.A Interparticle Diffusion

In a packed bed tubular reactor, diffusion in the gas phase exterior to the catalyst particle can affect the apparent reaction rate in two different ways. The diffusion through the boundary layer surrounding the catalyst particles may be slow enough so that the overall reaction rate is decreased. Also, concentration gradients in the axial direction may be steep enough or the diffusivity of the gases may be high enough so that the equations assuming plug flow through the catalyst bed are not entirely valid. Each of these possibilities will be treated in turn.

The approach to diffusion through the boundary layer surrounding the catalyst particles is the same as that used by Wakao, Selwood, and Smith (41). It is shown in Section IV of this report - the section treating interparticle diffusion - that, for a first order reaction, the apparent overall reaction rate constant per unit volume of catalyst pellet is related to the mass transfer coefficient per unit volume of catalyst pellet and to the reaction rate constant for the catalyst particle by the equation:

$$\frac{1}{K_{ov}} = \frac{1}{k_f} + \frac{1}{k_p} \qquad \text{(III-10)}$$

The mass transfer coefficient per unit volume of catalyst pellet may be obtained from the effective mass transfer coefficient per unit external area of catalyst from the equation:

$$k_F = 3k_f/R_p \qquad \text{(III-11)}$$

in which $R_p$ is the effective radius of the catalyst pellet. The mass transfer coefficient $k_f$ may be predicted from the available correlations for mass transfer in packed beds. Several of these are available (4,7,11,40,52), and all were found to give results of the same order of magnitude in the region for which interest lay in this study.

Some area coefficients of mass transfer for catalyst 00 were obtained from some of these different correlations, and from these the volume coefficients of mass transfer were calculated. These values were then compared with the overall reaction rate constant obtained from the experimental measurements. The results for catalyst 00 are presented in Table III-IV.

TABLE III-IV

COMPARISON OF MASS TRANSFER COEFFICIENTS
WITH OVERALL REACTION RATE CONSTANTS

CATALYST: 00
ACTIVITY: 1110 $min.^{-1}$

| | Ref. (4) | (7) | (11) | (40) | (52) |
|---|---|---|---|---|---|
| Coefficient of mass transfer per unit external area, $k_f$, cm/sec. | 23.8 | 17.2 | 16.1 | 18.7 | 32.7 |
| Coefficient of mass transfer per unit volume of catalyst $k_F$, $sec^{-1}$ | 3400 | 2460 | 2300 | 2670 | 4670 |
| Overall reaction rate constant $K_{ov}$, $sec^{-1}$ | | | 10.7 | | |

It may be seen from the above table that the various coefficients of mass transfer per unit volume of catalyst perdicted by the different investigators all have the same order of magnitude. It is apparent, moreover, that even the lowest value of $k_F$ obtained from the existing correlations predicts a negligible difference between the apparent overall reaction rate constant $K_{ov}$ and the rate constant for the catalyst particle, $k_p$. The lowest value of $k_F$ would predict a value of $k_p$ of

$$(1/k_p) = (1/10.7) - (1/2300)$$

$$k_p = 10.7$$

Thus the difference between $K_{ov}$ and $k_p$ in this case is less than 1%. It was concluded that the effect of diffusion through the boundary layer surrounding the catalyst was negligible in this investigation.

It is recognized that this reaction is not true first order reaction (cf. Sections II and IV of this report) and thus possesses no true first order reaction rate constant valid over all ranges of concentrations of the reactants. It is shown in Section IV of this report however, that the comparison of the apparent first order reaction rate constant at a given conversion with the mass transfer coefficient per unit volume of catalyst which occurs at this conversion can be used to determine the relative effect of interparticle diffusion.

When the diffusion of the reactants or products in the axial direction is high enough so that there is no longer essentially plug flow in the reactor, it is said that the reaction rate is affected by the longitudinal diffusion. The problem of handling this phenomenon mathematically has been attacked by many workers in the field, notable Damköhler (10), Wehner and Wilhelm (42), and Noller, Andreu, and Schwab (29). The method followed here is developed in greater detail in Section IV of this report. It is shown there that, for a reversible, first order reaction, that if the effect of longitudinal diffusion is assumed to be small, then the ratio of the concentration of the product at the exit of the reaction zone to what it would be if true plug flow were present may be obtained from the equation:

$$\frac{(c_{pe} - c_{pb})_2}{(c_{pe} - c_{pb})_{2\text{-plug flow}}} = 1 + (K_{RV}\tau)^2 \left(\frac{D}{uL}\right) \qquad \text{(III-12)}$$

In the above equation $c_{pb}$ is the concentration of parahydrogen in the bulk phase of the gas, $c_{pe}$ is the equilibrium concentration of parahydrogen at the reaction temperature, the quantity $(c_{pe} - c_{pb})_{2\text{-plug flow}}$ is the difference that would exist in these concentrations if true plug flow existed in the reactor, $K_{RV}$ is the overall reaction rate constant based on reactor volume, $\tau$ is the residence time of the reactant in the reactor, frequently called the space time, D is the effective diffusivity of the materials under the flow conditions existing in the reactor, u is the superficial velocity of the gases in the reactor, and L is the length of the reaction zone.

The parameter D/uL is the reciprocal of the axial Peclet Number for mass transfer. There are available correlations in the literature from which the value of this parameter may be estimated, such as those given by Levenspiel (26). These predict a value for the axial Peclet Number for catalyst 00 of approximately 1.2 under the conditions at which the activity test was carried out. The value of $K_{RV}\tau$ may be obtained from the equation:

$$K_{RV}\tau = \ln \frac{(c_{pe} - c_{pb})_1 \text{ plug flow}}{(c_{pe} - c_{pb})_2 \text{ plug flow}} \qquad \text{(III-12)}$$

As a first approximation in calculating the value of $K_{RV}\tau$, the values $(c_{pe} - c_{pb})$ plug flow may be approximated by the values of $(c_{pe} - c_{pb})$. If the results indicate that the effect of longitudinal diffusion is negligible, then the two values are approximately the same, and the approximation is justified. Using this approximation, for the activity tests carried out in this study, $K_{RV}\tau$ is equal to 2.05.

This value means that longitudinal diffusion affects the value of the concentration of the product in the exiting gas stream approximately 2% in this case. This in turn affects the value of the overall first order rate constant by less than 1%. It was concluded from these calculations that the effect of longitudinal diffusion was negligible.

A more complete discussion of interparticle diffusion may be found in Section IV of this report.

## III. 4.B Isothermality of Catalyst

The work of Thiele (37), as expanded and developed by Wheeler (47), concerned catalytic reactions that had negligible temperature gradients within the catalyst pellets. Further, the equations developed concerning the reactions within a packed tubular reactor assume that the reaction rate constant does not change through the reactor, i.e., that temperature gradients within the catalyst bed are also negligible.

Reactions within nonisothermal catalyst pellets, i.e., reactions that have rates that are affected to a significant degree by the temperature gradients within the catalyst pellets, have been studied within recent years by several workers, notably Carberry (8), Tinkler and Metzner (38), and Weisz and Hicks (43). These investigators show that the effect of nonisothermal reactions within catalyst pellets is dependent primarily upon the heat of the chemical reaction, the energy of activation of the reaction, the effective diffusivity of the reactants and products within the catalyst pellet, the concentration of the reacting substance at the pellet surface, and the absolute temperature at which the reaction is taking place. Weisz and Hicks have plotted the effect of temperature gradients within porous catalysts by showing for a first order irreversible reaction, how Thiele's effectiveness factor is affected by the behavior of the dimensionless parameters

$$\gamma = E^{\neq}/RT \qquad \text{(III-14)}$$

and

$$\beta = \frac{c_s(-\Delta H_r)D_e}{\lambda T_s} \qquad \text{(III-15)}$$

In these equations, $E^{\neq}$ is the activation energy of the catalyzed chemical reaction, R is the universal gas constant, T is the absolute temperature at which the reaction is taking place, $c_s$ is the concentration of the reactant at the surface, $\Delta H_r$ is the heat of the chemical reaction, $D_e$ is the effective diffusivity of the reactants within the catalyst pellet, $\lambda$ is the thermal conductivity of the catalyst particle, and $T_s$ is the temperature of the surface of the catalyst. For the ortho-para hydrogen reaction, the heat of chemical reaction at 75.7°K is 331 cal./mole (17). It is shown in Section II of this report that the activation energy is approximately 317 cal./mole. The thermal conductivity of the iron oxide

catalyst has not been measured, but Sehr (36) has measured the thermal conductivity of several porous catalysts, and the thermal conductivity averages approximately 0.7 cal./(sec)(cm)(°C). The variation in this value among many different catalysts is small enough so that this may be regarded as a reasonably dependable value for the thermal conductivity of a porous catalyst plus or minus approximately twenty per cent. For a first order reversible reaction, the quantity $(c_{pe} - c_{ps})$ should be substituted for $c_s$ in the evaluation of the parameter $\beta$. The largest value of $(c_{pe} - c_{ps})$ enountered in the catalyst bed is at the entrance to the reactor, where it has a value of $6.41 \times 10^{-5}$ gm-moles/cc. For catalyst 00, using a tortuosity factor of 1.0 the effective diffusivity is calculated to be $1.24 \times 10^{-2}$ $cm^2$/sec. Using these values, the values of the dimensionless parameters $\lambda$ and $\beta$ are calculated to be:

$$\gamma = 1.5$$

$$\beta = 0.0057$$

Weisz and Hicks show in several plots the effect of these dimensionless parameters upon the effectiveness factor and the effect of these dimensionless parameters grows greater as the values of the parameters increase. However, the smallest value of $\gamma$ they show is 10, and the smallest value of $\beta$ they show the effect of is 0.2. Interpolation of the effect of these paramaters to give the effect of values of $\gamma = 1.5$ and $\beta = 0.006$ shows that the effect of temperature gradients within the catalyst pellets for the ortho-para hydrogen reaction at 75.7°K and 22.2 psia is entirely negligible.

That the temperature gradients within the catalyst bed in this study were negligible was shown by the work of Weitzel, Blake and Konecnik (46). In their study, they showed that a one-fourth inch o.d. copper catalyst chamber containing three cubic centimeters of the hydrous ferric oxide catalyst operated at essentially isothermal conditions throughout the range of conversions that they studied. Since the catalyst chamber used in the investigation presented in this section of the report only used two cubic centimeters of catalyst, and the range of conversion was well within the range covered by Weitzel and co-workers, it was concluded that essentially isothermal conditions existed throughout the catalyst bed for the study reported here.

## III. 4.C. Experimental Effectiveness Factor

The effectiveness factor indicates the extent of the effect of intraparticle diffusion. The effectiveness factor can be obtained in two different ways. It can be estimated from the relationships presented in Equations (III-3) or (III-4) or it may be obtained experimentally by continually decreasing the catalyst pellet size until diffusion within the particle is no longer an important factor in the overall rate of the reaction.

The latter approach was adopted in this investigation. It was apparent that intraparticle diffusion did inhibit the rate of reaction somewhat, because the overall rate of reaction per unit weight of catalyst increased as the particle size was reduced. The particle size was therefore reduced from the usual 30-50 weak size until the rate no longer increased, and the effectiveness factor in this case was taken to be 1. Then the ratio of the activities per unit weight gave the catalyst effectiveness factor for the 30-50 mesh catalyst. The results are presented in Table III-V.

TABLE III-V

Effectiveness Factor of Catalyst 00

| Average Particle Size, microns | Mesh Size | Catalyst Activity, cc $H_2$/(min) (gm catalyst) |
|---|---|---|
| 420 | 30-50 | 890 |
| 163 | 80-100 | 968 |
| 120 | 100-150 | 932 |

These figures indicate that the effectiveness factor of catalyst 00 is in the neighborhood of 0.94. In a similar investigation carried out at a pressure five times as great, Keeler, Weitzel, Blake and Konecnik (24) report an effectiveness factor of approximately 0.85 for a catalyst particle of the same size. Since different samples of the ferric oxide catalyst can show widely varying activities, it would not be expected that very close agreement would be obtained for effectiveness factors obtained on different batches of this catalyst manufactured several years apart and activated by different procedures. For this reason the difference between the two values of 0.85 and 0.94 is considered to be slight. It is concluded that the effectiveness factor of 0.94 is a reasonable value.

If the diffusion within the catalyst pellet occurs in the gas phase, catalyst 00 should have the lowest effectiveness factor for the catalysts studied in this investigation and listed in Table III-I. This is true because catalyst 00 has the lowest average pore radius, and as a result should have the lowest gas phase diffusivity. Using this, together with the surface areas and porosities reported in Table III-II, the predicted Thiele modulus for catalyst 00 is the highest of the catalysts investigated, which results in the predicted effectiveness factor for catalyst 00 being the lowest.

An effectiveness factor of 0.94 means that only six per cent of the possible activity of the catalyst is lost because of diffusion effects. This is very slight, and means that any efforts at increasing the effective diffusion rates, as, for instance, by altering the physical structure of the catalyst, would be largely ineffective.

III. 4.D Effective Diffusivity

The discussion of the theory pertaining to the effect of diffusion on the reaction rate mentions that the effective diffusivity may be computed from the effectiveness factor for a given catalyst if the void fraction in the catalyst bed and the catalyst porosity is known. The porosity of catalyst 00 was 0.34, and the void fraction of the bed was assumed to be 0.35, which is a typical void fraction under the circumstances (14). Using these values, for catalyst 00 the effective diffusivities calculated were:

Effective diffusivities of $H_2$ within catalyst 00, $cm^2/sec.$

| | |
|---|---|
| Slab model: | $3.9 \times 10^{-3}$ |
| Sphere model: | $5.0 \times 10^{-3}$ |

These values of the effective diffusivity can be compared with those that would be predicted by the different methods assuming Knudsen flow. That Knudsen flow should be occuring within the pores of catalyst 00 is demonstrated by the fact that the mean free path of the hydrogen molecule at 75.7°K is approximately 170 Angstrom units, and the average radius of catalyst 00 is approximately 21 Angstrom units. Since the mean free path of the molecule is much larger than the average pore radius, Knudsen diffusion should predominate in the gas phase within the catalyst pellet.

The two methods of predicting the effective diffusivity that are applicable to catalysts with a narrow pore-size distribution are those mentioned in the discussion of the theory--those of Weisz and Schwartz (45) and of Geddes (19). The values predicted by these two methods are:

Predicted Effective diffusivities of $H_2$ within catalyst 00, $m^2/sec.$

| | |
|---|---|
| Weisz and Schwartz: | $9.9 \times 10^{-4}$ |
| Geddes: | $7.1 \times 10^{-4}$ |

It can be seen from these values that the experimental values of the diffusivity are an order of magnitude greater than are predicted using the available correlations for transport in porous substances, if it is assumed that Knudsen diffusion is the principal mode of transport of the reactants and products. This order of magnitude difference is well outside the bounds of experimental error.

It apparently can only be concluded from this study that Knudsen diffusion is not the principal mode of transport of the reactants and products in this reaction over the ferric oxide catalyst. The only other possibility which is apparent at the present writing is considered to be transport of the hydrogen along the surface of the catalyst. This is suggested even though it is recognized that normally in reactions carried out well above the boiling point of the reactants, surface diffusion is an unimportant mode of transport of the reactants (34,51). This study was carried out at 75.7°K, which is over twice the critical temperature of hydrogen, which is 33°K. Because of this it would have been predicted that surface transport would have little effect on the overall transport rate within the catalyst pellet. However, since it is apparent that diffusion within the gas phase cannot account for the transport observed within the catalyst pellet, and also that large increases in transport have been caused by surface migration, it is suggested that surface diffusion of the hydrogen is the major mode of transport of hydrogen within the ferric oxide catalyst. This phenomenon needs further investigation.

III. 4.E Use of the First-Order Reaction

Throughout the analysis presented above in which the effective diffusivities of hydrogen within the catalyst pellet were derived, it was assumed that the reaction was kinetically a first-order reaction. It is recognized that the first order rate equation:

$$\frac{1}{V_r}\frac{dn_o}{dt} = k_{fo}(c_{pe} - c_p) \qquad \text{(III-16)}$$

is not the most accurate representation of the dependence of the reaction rate upon concentration

In the second section of this report, it is shown that for the change of para hydrogen to ortho hydrogen, the rate of reaction follows the relationship:

$$\frac{1}{V_r}\frac{dn_p}{dt} = \frac{k(c_p - c_{pe})}{1 + k'c_p} = \frac{kc_H(x - x_e)}{1 + k'c_H x} \qquad \text{(III-17)}$$

Since this is proposed to represent the true mechanism of the reaction, then the reverse reaction--the change of ortho to para hydrogen-- should be represented by the relationship:

$$\frac{1}{V_r}\frac{dn_o}{dt} = \frac{k(c_{pe} - c_p)}{1 + k'c_p} = \frac{kc_H(x_e - x)}{1 + k'c_H x} \qquad \text{(III-18)}$$

In the first section of this report, the value of $k'c_H$ is shown to possess an average value of approximately -0.85. Under the conditions at which this investigation was carried out, the value of x varied from 0.250 to 0.514. From these values, it is a simple calculation to show that the value of the denominator varies from approximately 0.80 to 0.56. Since the denominator varies over a range which is this limited, the approximation may be made:

$$k_{fo} = k/(1 + k'c_H x) \qquad \text{(III-19)}$$

and this approximation is valid within 35%.

It is generally desired to use approximations which are more accurate than this. Unfortunately, use of Equation (III-18), the more accurate relationship, introduces nonlinear terms into the equations relating the effect of diffusion on the reaction rate within porous catalysts. No general solution has yet been reported for the resulting equations, and thus relationships such as Equations (III-5) and (III-6), which were developed for the first-order case, have not been developed for the modified first-order relationship presented in Equation (III-18). For this reason, the simple first-order approximation was used.

It should be noted that the use of the first-order relationship in no way vitiates the conclusion that most probably the principal mechanism of diffusion within the catalyst pellets is surface migration. The experimentally determined diffusivities, assuming a first-order reaction, were an order of magnitude greater than those predicted by the available correlations. The possible thirty-five per cent variation of the first-order reaction rate constant over the course of the experiment could not cause this large a difference in the predicted and observed diffusivities.

III. 4.F. Effect of Surface Area on Catalyst Activity

The surface areas obtained from BET measurements are presented in Table III-II. In Figure III-5 the activity is plotted as a function of this surface area. It is readily apparent from both the figure and the table that the catalyst activity is not directly proportional to the BET surface area of the catalyst. However, it is generally true that the higher the surface area of the catalyst, the higher the activity that the catalyst possesses.

It was pointed out in the discussion of the theory relating to catalyst surface area that in materials with fine pores, the BET surface area may not be an accurate representation of the true area of the substance. It is also true that the area represented by these fine pores may be more than normally available to the reactants, since the principal mode of transport within the catalyst pellet appears to be surface diffusion.

The amount of surface diffusion that takes place is proportional to the surface (21), and in fine pores the ratio of surface to cross-sectional area is higher than in larger pores.

There are probably many very small pores in the catalysts studied in this part of the investigation. Figures III-6 to III-15 present the pore-size distributions of these over the range of pore radii from 100 Angstrom units down to 7 Angstrom units. With the present state of the art of measuring pore-size distributions, it is extremely difficult to obtain any meaningful results below a pore radius of 7 Angstroms. These pore-size distributions are plotted in the form of the distribution function L(r) as a function of r, where L(r)dr is the total length of all the pores between (r) and (r + dr).

In all of the catalysts studied, the distribution function had not decreased to zero at the 7 Angstrom point, indicating that there were still many pores with radii below 7 Angstrom units. In six of the ten catalysts, the distribution function was still increasing at the 7 Angstrom point. It seems reasonable to

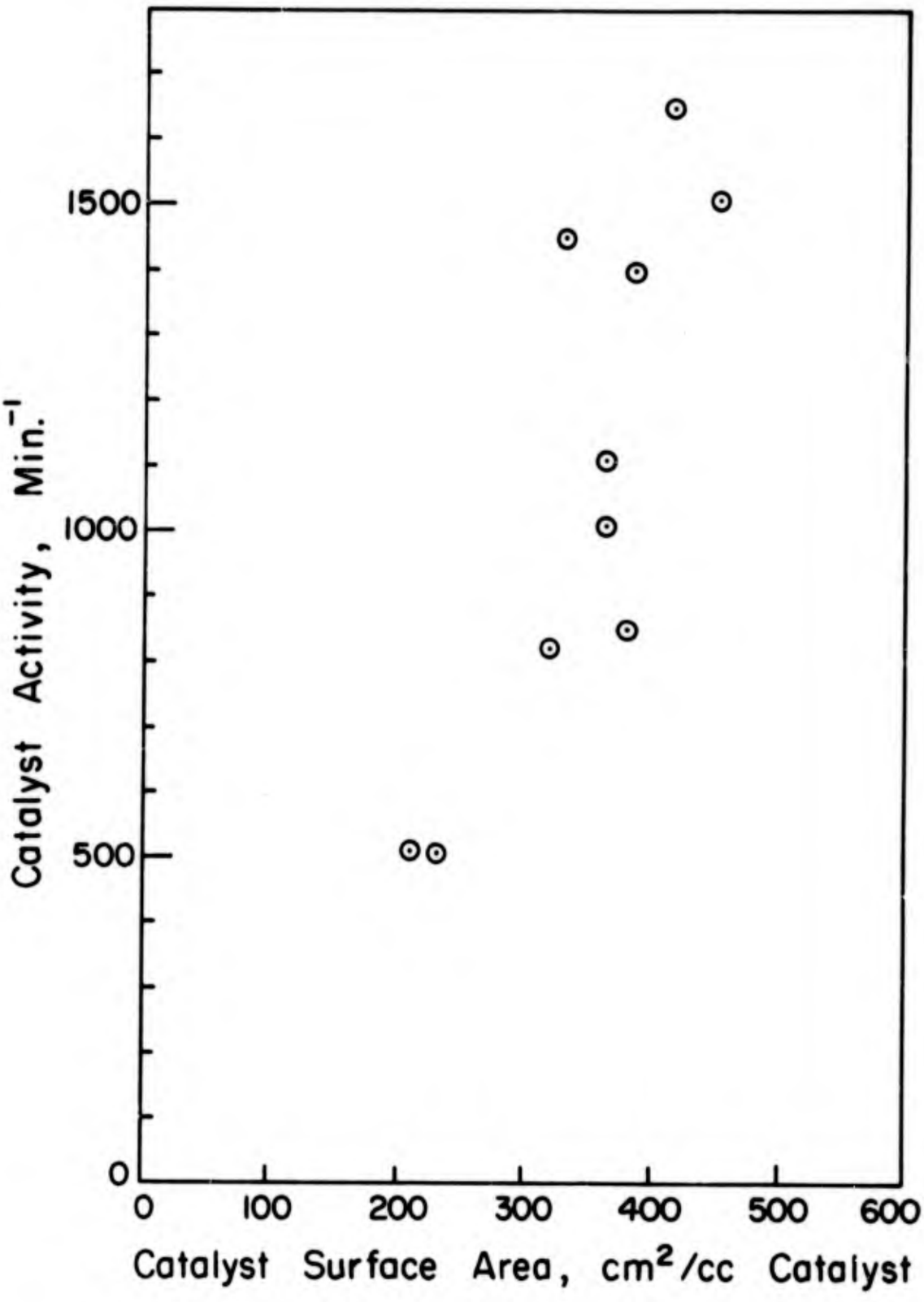


Figure III-5

Effect of Catalyst Surface Area on Catalyst Activity

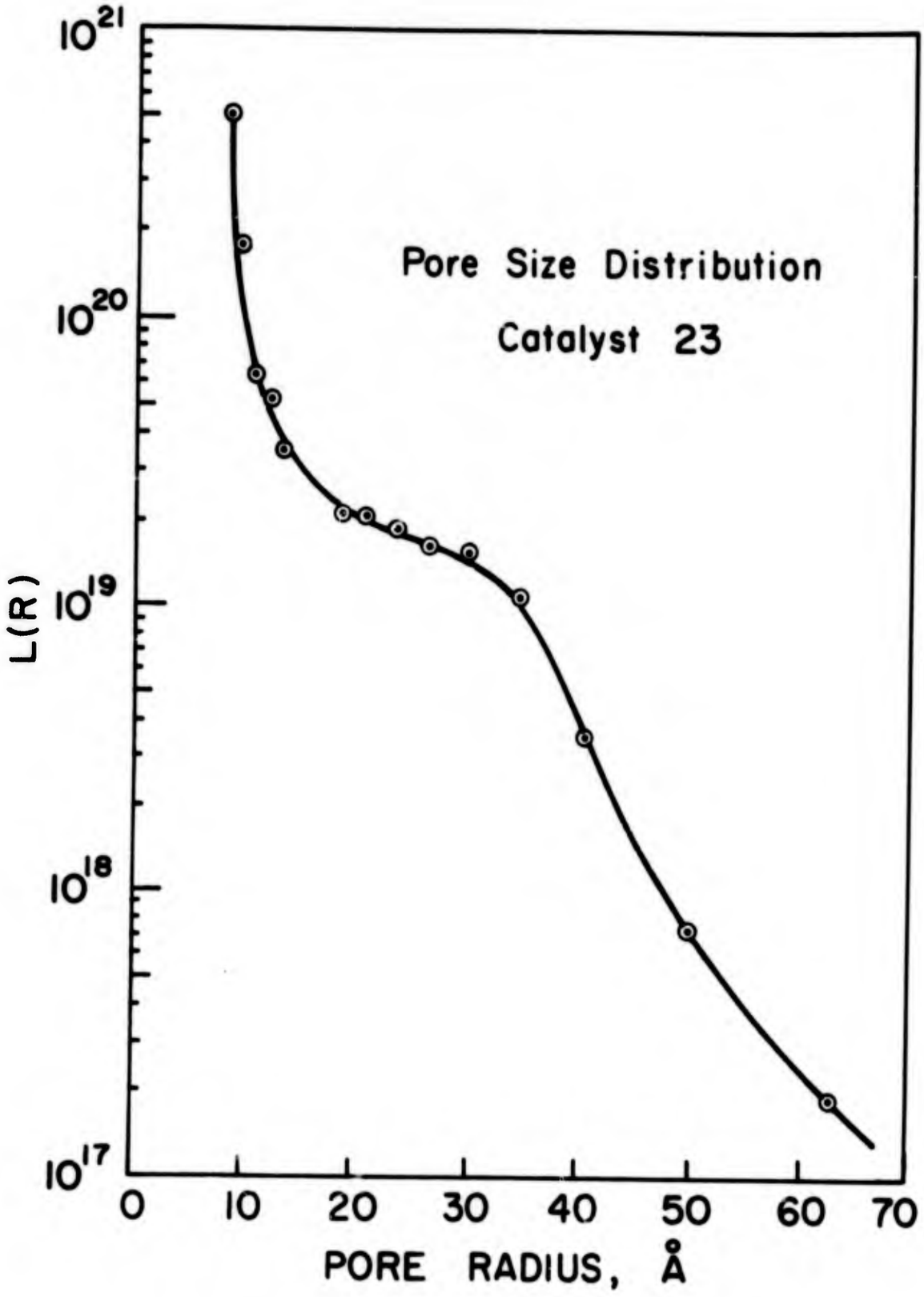
Pore Size Distribution
Catalyst 23
L(R)
$10^{21}$
$10^{20}$
$10^{19}$
$10^{18}$
$10^{17}$
0
10
20
30
40
50
60
70
PORE RADIUS, Å

Figure III - 6

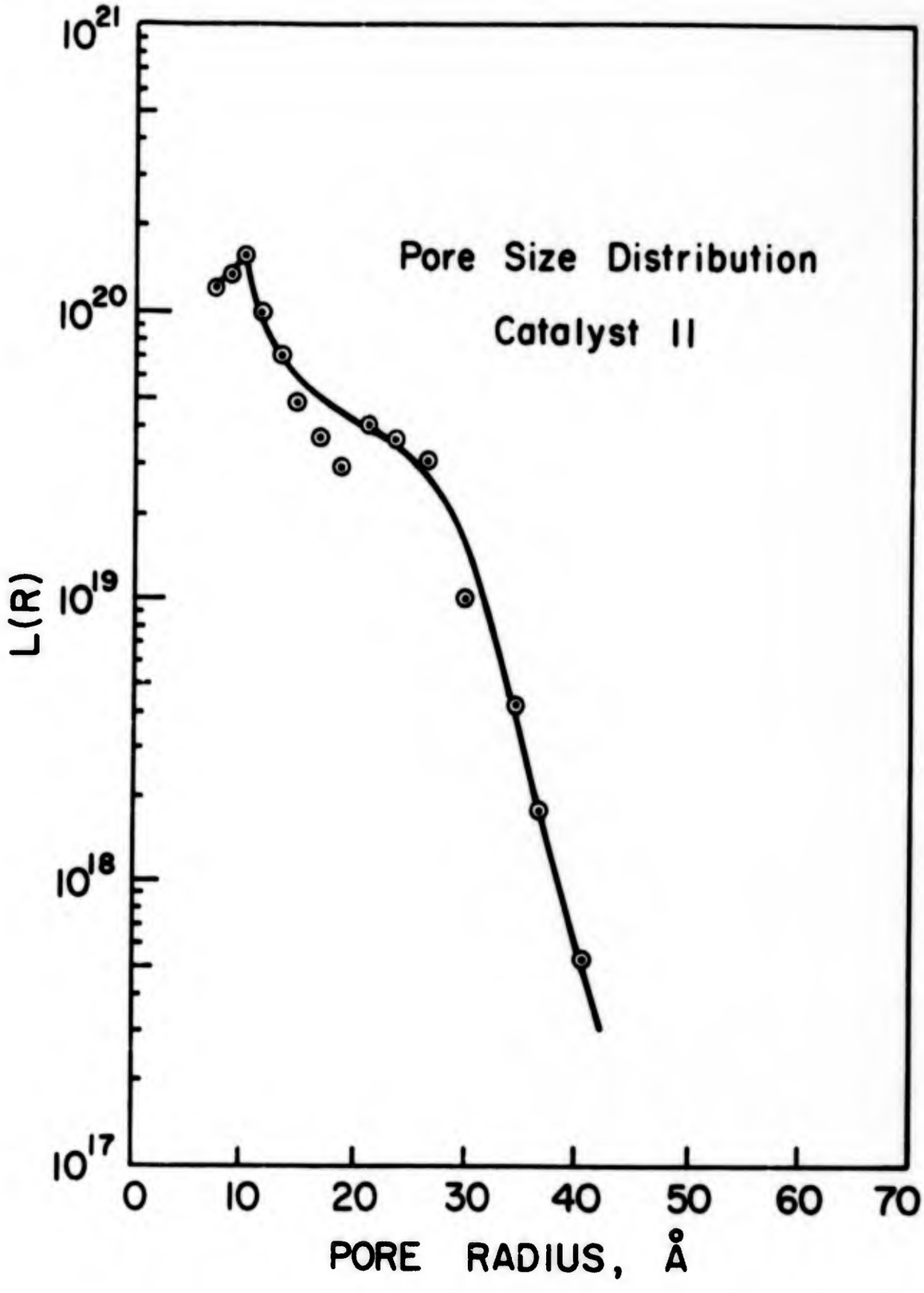
Pore Size Distribution
Catalyst II
L(R)
$10^{21}$
$10^{20}$
$10^{19}$
$10^{18}$
$10^{17}$
0
10
20
30
40
50
60
70
PORE RADIUS, Å

Figure III-7

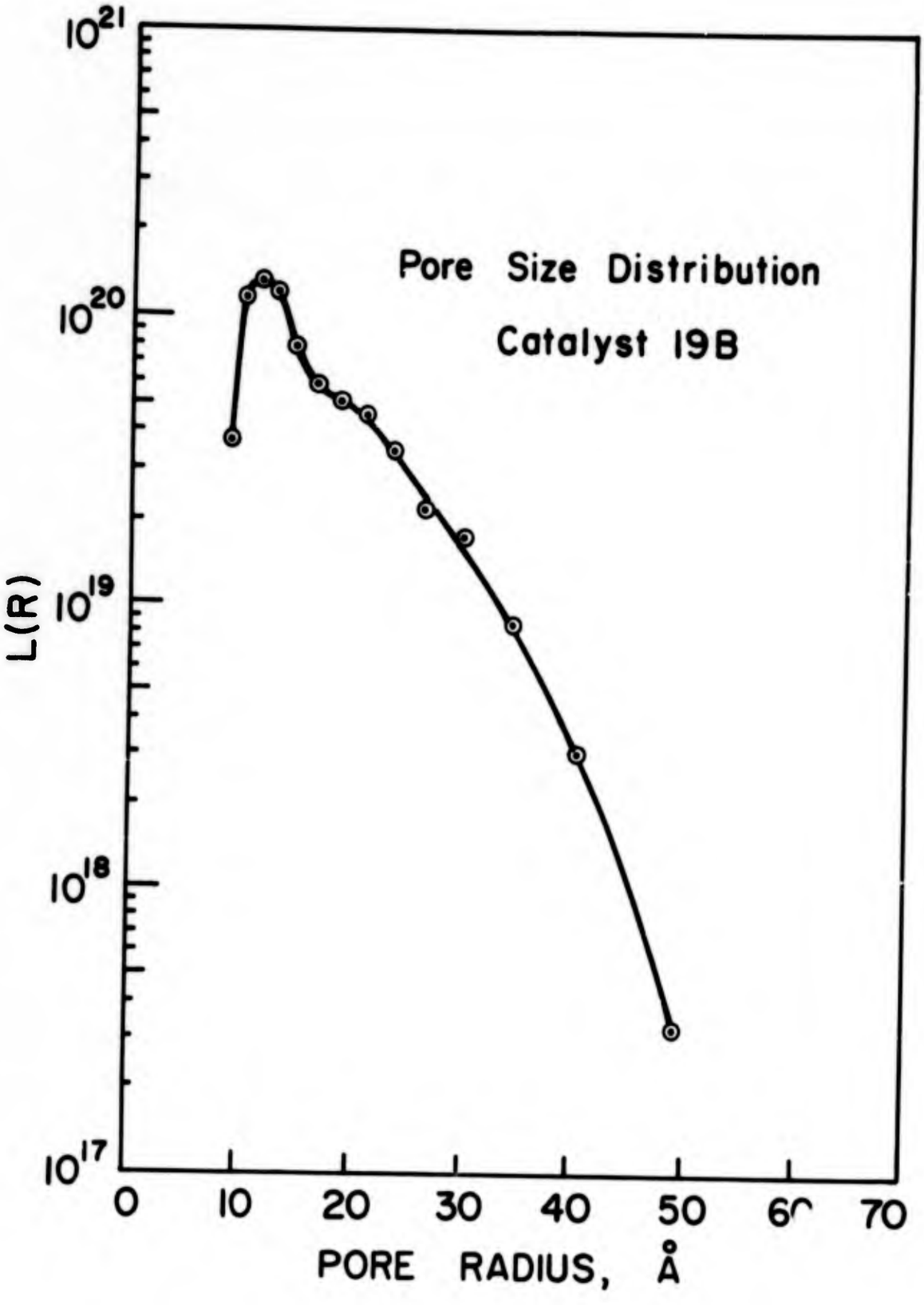
Pore Size Distribution
Catalyst 19B
L(R)
$10^{21}$
$10^{20}$
$10^{19}$
$10^{18}$
$10^{17}$
0
10
20
30
40
50
60
70
PORE RADIUS, Å

Figure III - 8

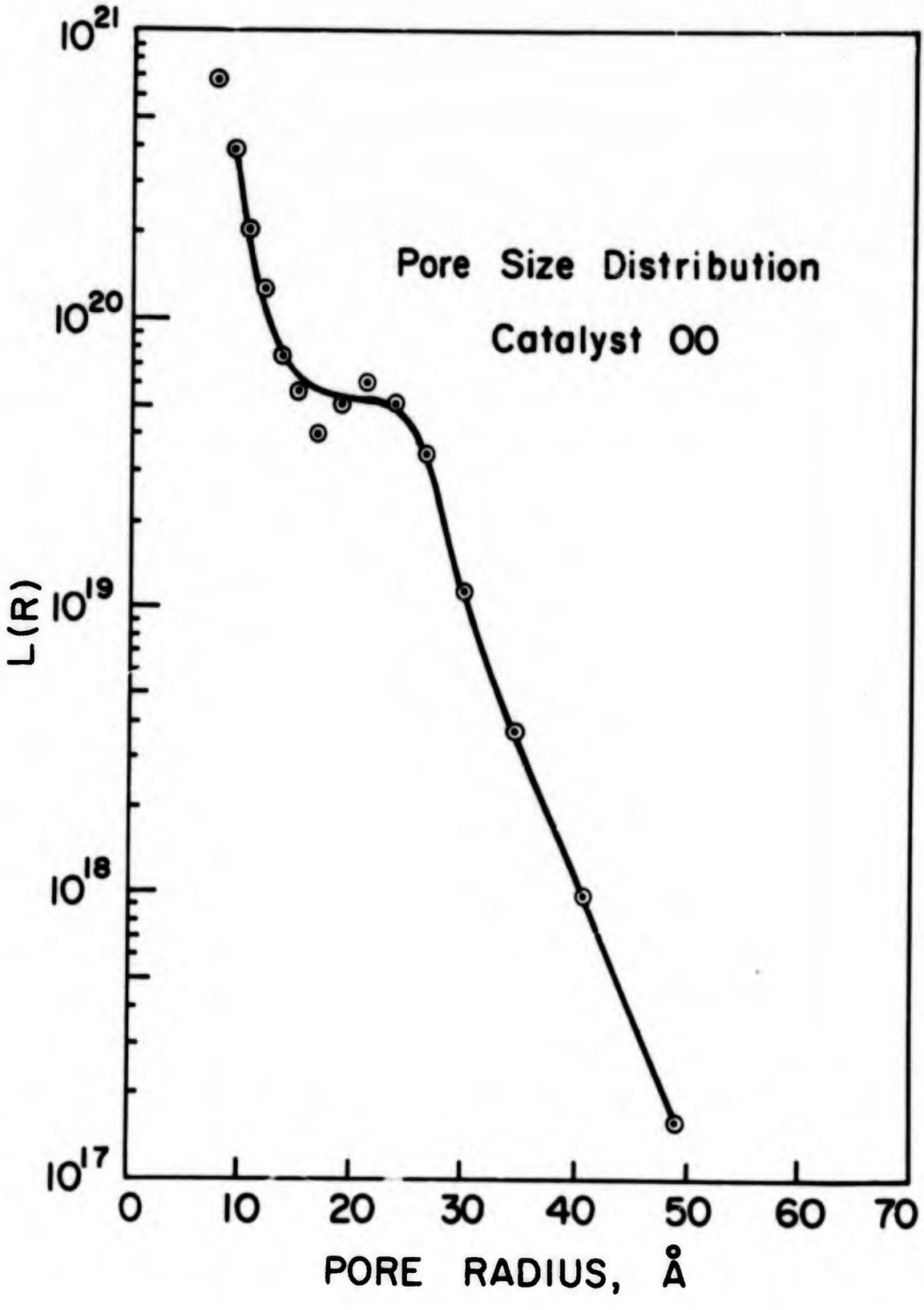
Pore Size Distribution
Catalyst 00
L(R)
$10^{21}$
$10^{20}$
$10^{19}$
$10^{18}$
$10^{17}$
0
10
20
30
40
50
60
70
PORE RADIUS, Å

Figure III - 9

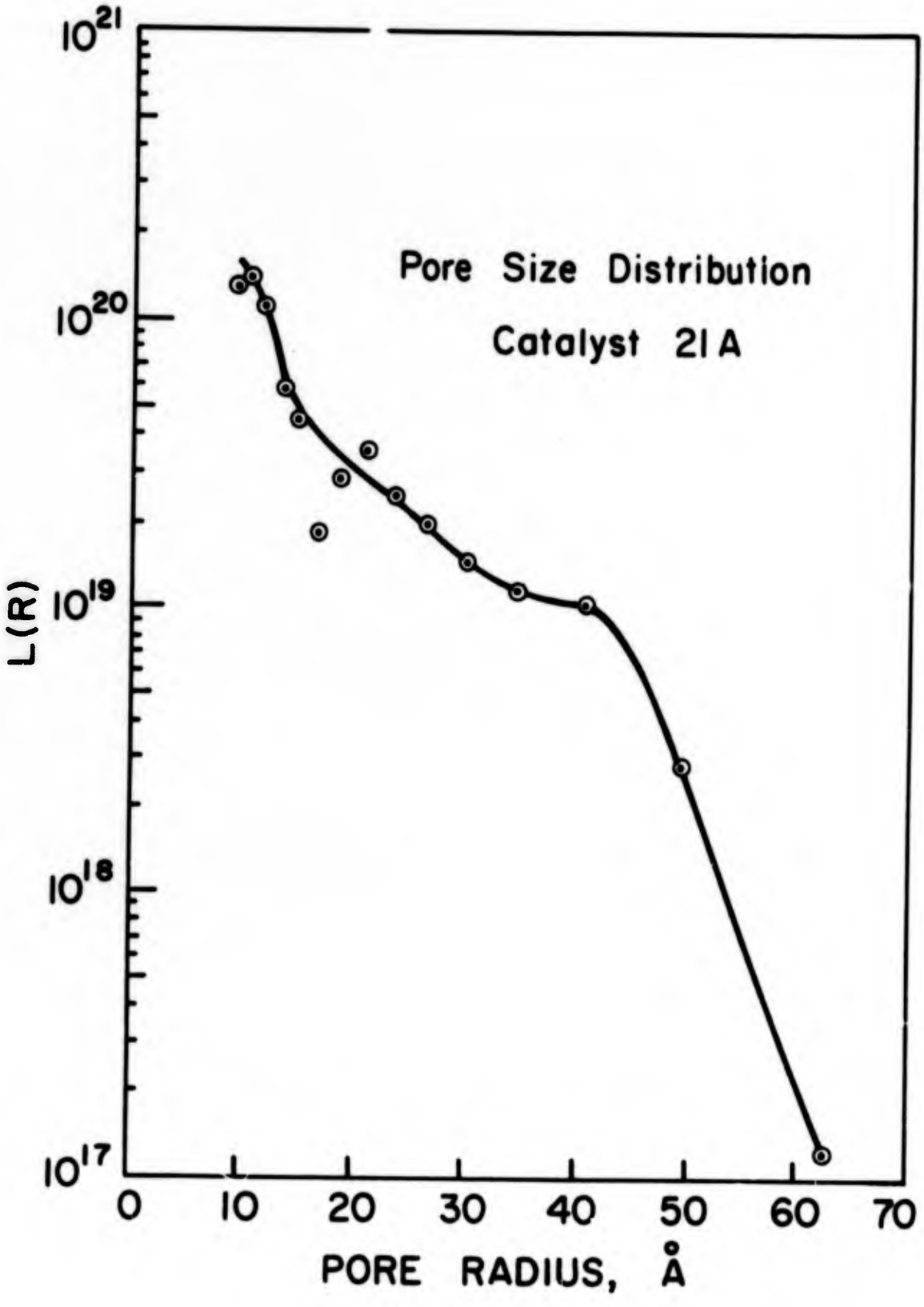


Figure III - 10

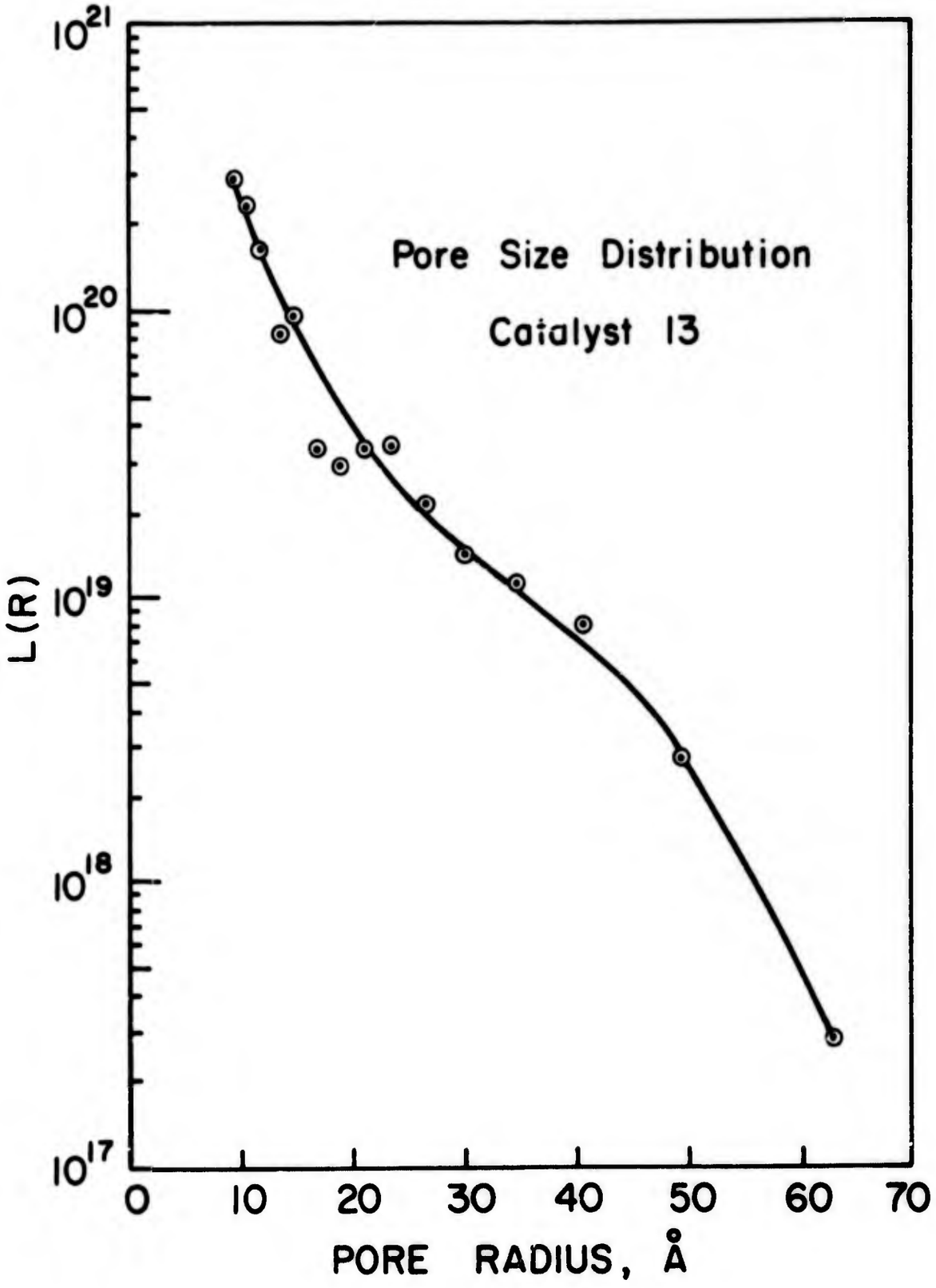


Figure III - 11

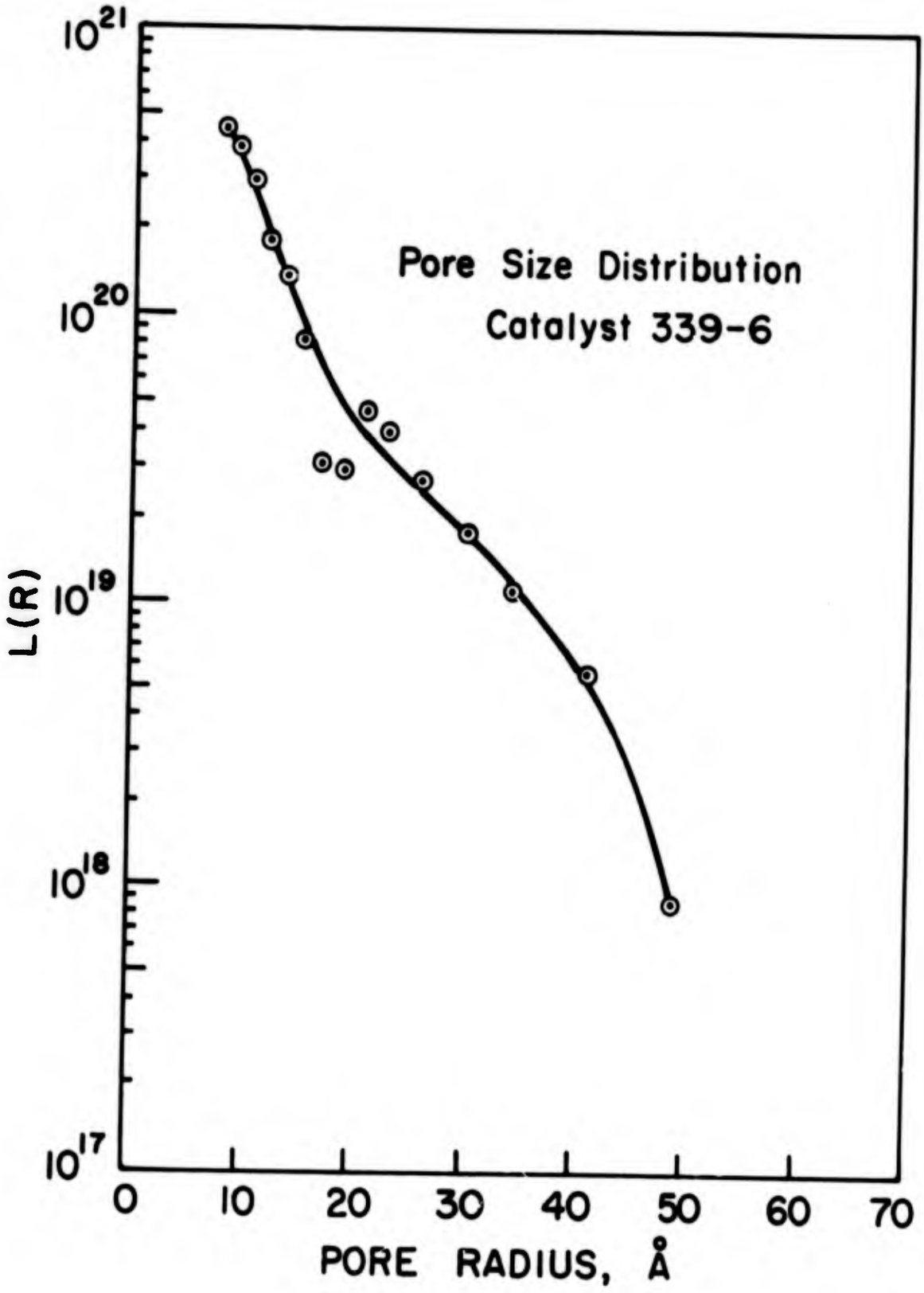


Figure III-12

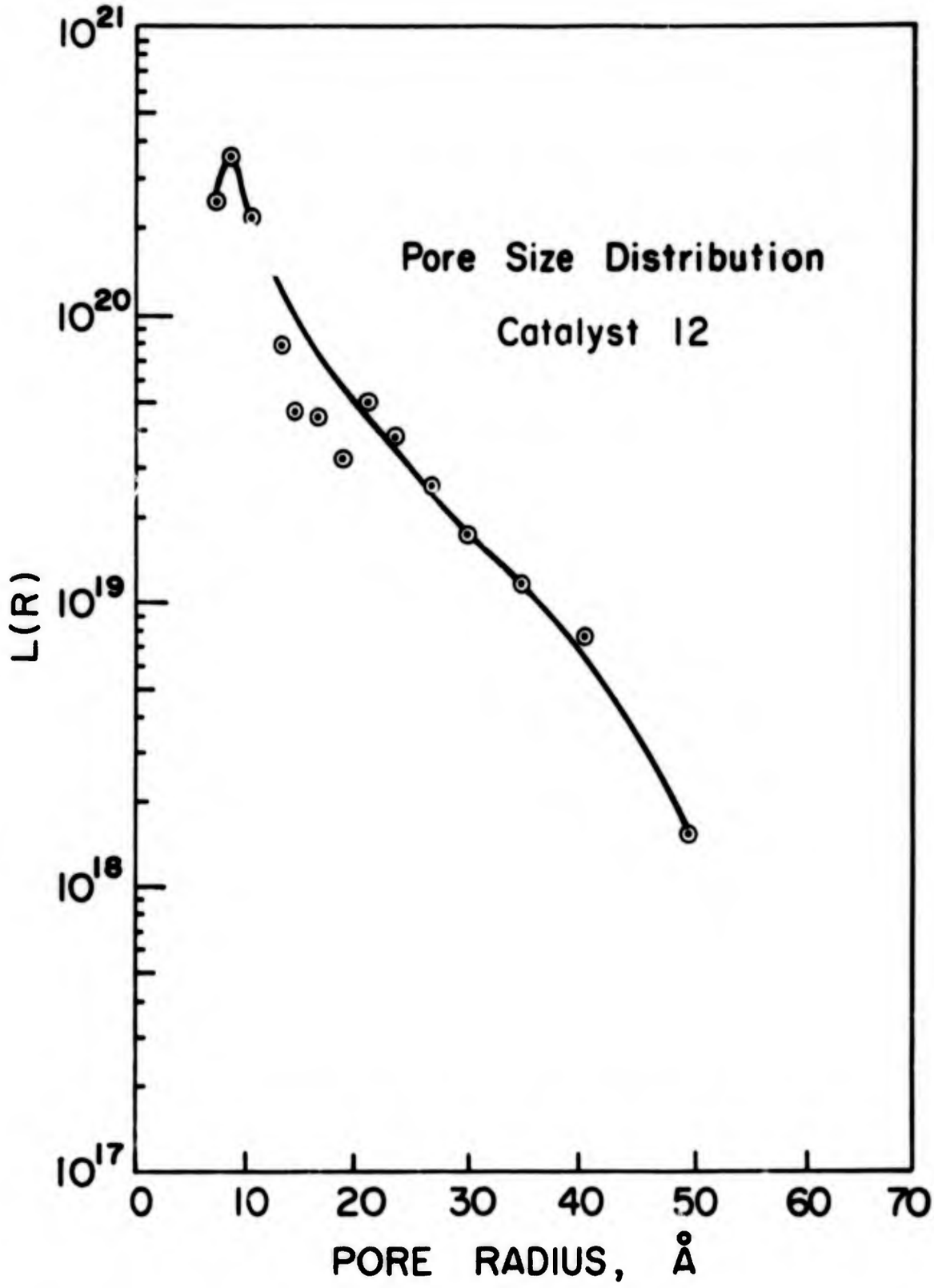


Figure III-13

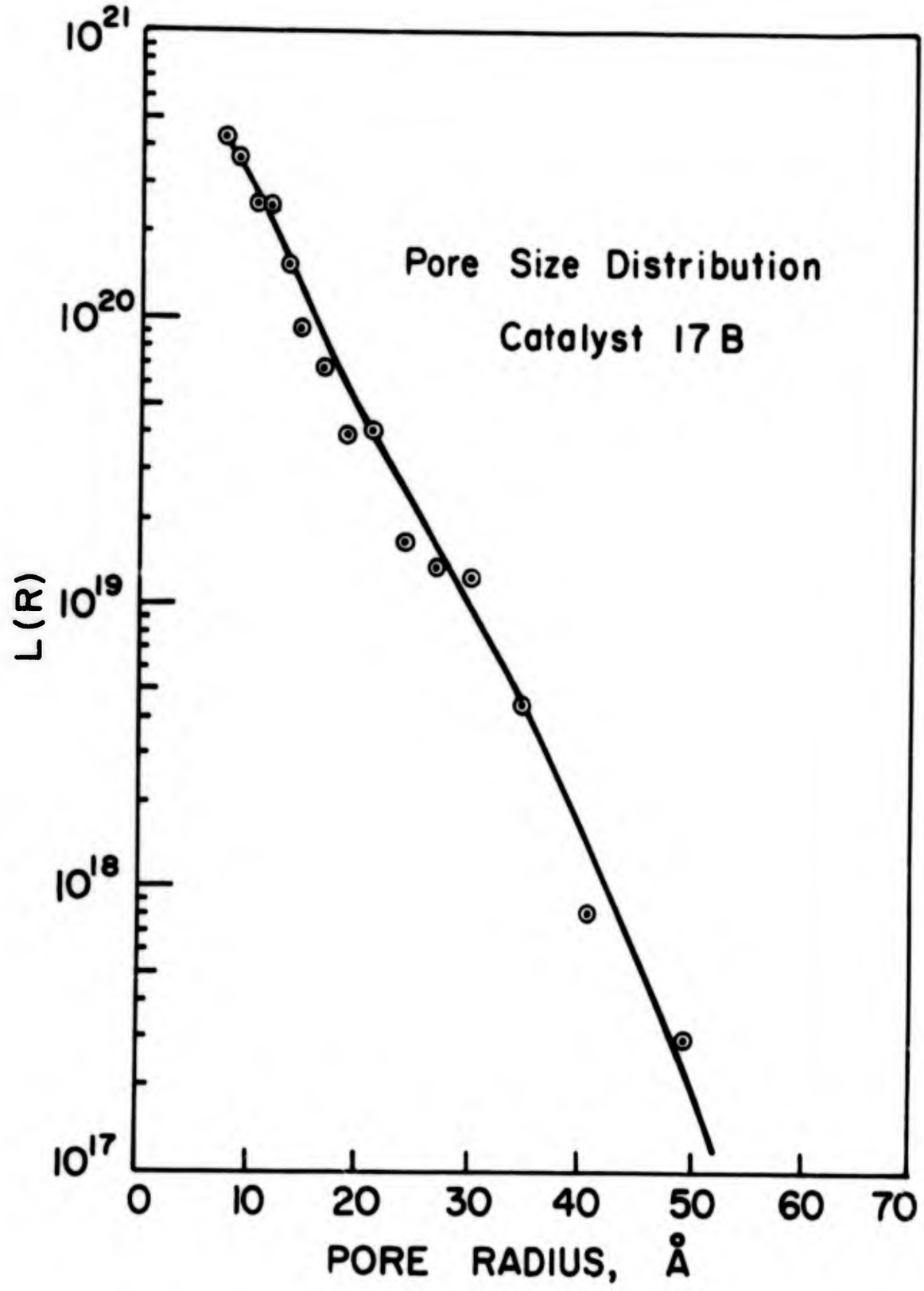


Figure III - 14

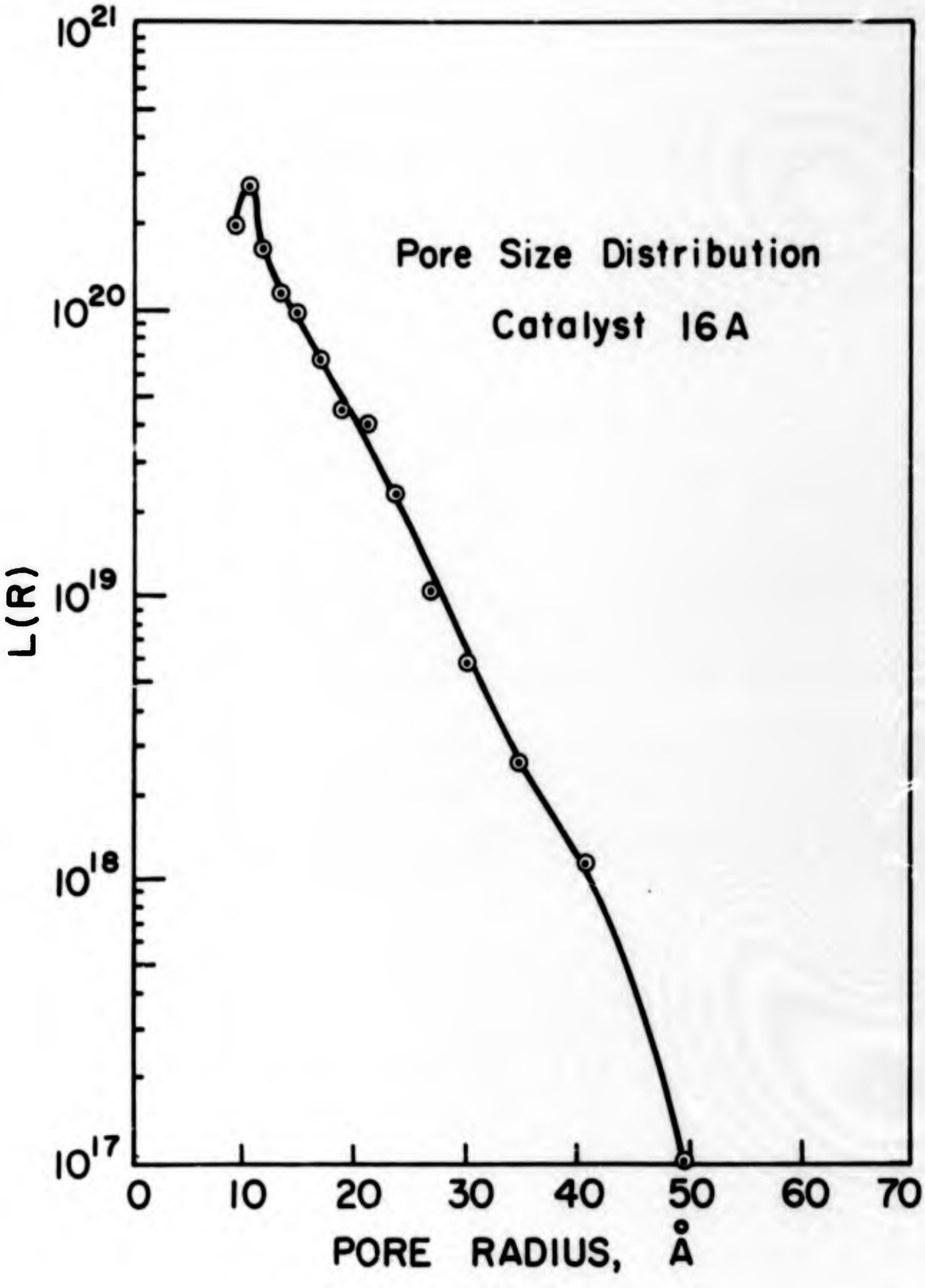


Figure III - 15

conclude from these data that there are still many pores of smaller radii that were not measured in this pore-size distribution.

It has been shown that in cases of substances with very fine pores that the surface area measured by the BET method may not be a true indication of the total amount of surface, and that the surface in fine pores may be available in this reaction because the principal mode of transport in surface diffusion. Because of this, there is no reason to expect that even if all the catalysts had the same activity per unit surface area, that the activity would be directly proportional to the BET surface area. Since the total area available to the reactants probably increases with the BET surface area, it might be expected that as the BET surface area increases, the activity would increase, and this has been shown to be true. Other than this, no conclusions are presently possible concerning the relationships between surface area and activity for these catalysts.

It might also be noted that the catalyst activity increases with the porosity of the catalyst. There is no present explanation of this effect, other than the observation that normally the higher surface area catalysts are also more porous.

## III.5 Conclusions

1. Intraparticle diffusion apparently has only a small inhibiting effect upon the ortho-para hydrogen shift reaction using ferric oxide gel catalysts in the activity range studied in this investigation. Attempts to improve catalyst activity by increasing diffusion rates would probably have slight effect.

2. The diffusion rates measured were an order of magnitude greater than are predicted using available correlations for diffusion in the gas phase. It is concluded that surface migration is probably the principal mode of transport of the reactants and products in this reaction using the ferric oxide gel catalyst.

3. The higher surface area catalysts generally have higher activities. Since the surface area measured by the BET method is not an accurate indication of the total surface area of substances with many fine pores, as is the ferric oxide gel catalyst, it should not be expected that the activity should be directly proportional to the BET surface area. Experimentally, the catalyst activity is not directly proportional to the BET surface area.

III. 6 Recommendations for Further Work

1. It is recommended that the surface diffusion of hydrogen be studied in order to clarify the mechanism of transport of the reactants and products in this reaction. This would be of advantage in the development of more powerful catalysts for this reaction.

2. It is recommended that other methods of the determination of surface area--such as the heat of wetting method and low-angle x-ray scattering--be investigated in order to determine if the total surface area available to the hydrogen molecule is the principal variable in the activity of the ferric oxide gel catalyst. From information of this type can be obtained rate constants per unit surface, which could be used to determine the maximum potentiality of any particular type of catalyst.

## NOTATION

$A$ = Cross-sectional area across which material is diffusing, sq cm

$c_A$ = Concentration of substance A, gm-moles/cc

$c_H$ = Total concentration of hydrogen in gas, gm-moles/cc

$c_p$ = Concentration of para hydrogen in gas, gm-moles/cc

$c_{pb}$ = Concentration of para hydrogen in the bulk phase of the gas exterior to the catalyst pellet, gm-moles/cc

$c_{pe}$ = Equilibrium concentration of para hydrogen at the temperature of the reaction, gm-moles/cc

$c_{ps}$ = Concentration of para hydrogen at exterior surface of catalyst pellet, gm-moles/cc

$c_s$ = Concentration of reactant at exterior surface of catalyst pellet gm-moles/cc

$D$ = Effective longitudinal diffusivity of para hydrogen in bulk gas stream, sq cm/sec

$D_A$ = Diffusivity of substance A, sq cm/sec

$D_{calc}$ = Calculated diffusivity for straight circular pores of the same radius as the average catalyst pore radius, sq cm/sec

$D_e$ = Effective diffusivity of para hydrogen within catalyst pellet, sq cm/sec

$E^{\neq}$ = Energy of activation of reaction, cal/gm-mole

$E_{sl}$ = Effectiveness factor assuming that catalyst pellet may be approximated by a slab, dimensionless

$E_{sp}$ = Effectiveness factor assuming that catalyst pellet may be approximated by a sphere, dimensionless

$F$ = Feed rate at reaction conditions, cc/sec

$h_{sl}$ = Thiele modulus assuming that catalyst pellet may be approximated by a slab, dimensionless

$h_{sp}$ = Thiele modulus assuming that catalyst pellet may be approximated by a sphere, dimensionless

$\Delta H_r$ = Heat of reaction, cal/gm-mole

$k$ = Reaction rate constant in ortho-para hydrogen shift rate equation, $sec^{-1}$

$k'$ = Reaction rate constant in ortho-para hydrogen shift rate equation, cc/gm-mole

$k_f$ = Mass transfer coefficient based on catalyst external surface area, cm/sec

$k_{fo}$ = First-order reaction rate constant, $sec^{-1}$

$k_F$ = Mass transfer coefficient based on catalyst volume, $sec^{-1}$

$k_p$ = First-order reaction rate constant based on catalyst volume, $sec^{-1}$

$k_s$ = First-order surface reaction rate constant, cm/sec

$K_{ov}$ = Overall first-order reaction rate constant based on catalyst volume, $sec^{-1}$

$K_{RV}$ = Overall first-order reaction rate constant based on reactor volume, $sec^{-1}$

$n_o$ = Number of moles of ortho hydrogen

$n_p$ = Number of moles of para hydrogen

L = Half the width of the slab which approximates the catalyst pellet, cm

$N_A$ = Number of moles of substance A diffusing across an area, moles/sec

r = Radius of catalyst pore, cm

R = The universal gas constant, cal/(°K)(gm-mole)

$R_p$ = Radius of sphere which approximates the catalyst pellet, cm

S = Surface area of catalyst, sq cm/cc

T = Absolute temperature of reaction, °K

$T_s$ = Temperature at surface of catalyst pellet, °K

u = Superficial gas velocity in catalyst chamber, cm/sec

$V_r$ = Reactor volume, cc

x = Mole reaction of para hydrogen in gas phase, dimensionless

$x_e$ = Equilibrium mole fraction of para hydrogen at temperature of reaction dimensionless

$\beta$ = Dimensionless parameter in correlating effects of temperature gradients within catalyst pellets

$\gamma$ = Fraction of catalyst chamber occupied by catalyst--is equal to (1 - void fraction)

$\epsilon$ = Catalyst porosity, cc pores/cc catalyst

$\eta$ = Dimensionless parameter used in correlating effects of temperature gradients within catalyst pellets

$\lambda$ = Thermal conductivity of catalyst pellet, cal/(sec)(cm)(°K)

$\tau$ = Residence time of reactants in catalyst chamber, or space time, sec

$\chi$ = Tortuosity factor, dimensionless

SUBSCRIPTS

1 = Measured at entrance to reaction zone

2 = Measured at exit from reaction zone

## REFERENCES


1. Barrer, R. M., and J. A. Barrie, Proc. Roy. Soc. A213, 250 (1952).
2. Barrer, R. M., and T. Gabor, Proc. Roy. Soc. A251, 353 (1959).
3. Bokhoven, C., and W. van Raayen, J. Phys. Chem. 58, 471 (1954).
4. Bradshaw, R. D., and C. O. Bennet, A.I.Ch.E. Journal 7, 48 (1961).
5. Brunauer, S., P. H. Emmett, and E. Teller, J. Am. Chem. Soc. 60, 309 (1938).
6. Brusset, H., B. LeRat, and M. Makki, Ann. Chim. (Paris) 9, (Sev. 12), 477-506 (1954).
7. Carberry, J. J., A.I.Ch.E. Journal 6, 460 (1960).
8. Carberry, J. J., A.I.Ch.E. Journal 7, 350 (1961).
9. Damköhler, G., in "Der Chemie-Ingenieur," Band III, A. Eucken and M. Jakob, ed., Akademische Verlagsgesellschaft, 1937, pp. 430-436.
10. ibid., pp. 381-402
11. DeAcetis, J., and G. Thodos, Ind. Eng. Chem. 52, 1003 (1960).
12. Debye, P., H. R. Anderson, Jr., and H. Brumberger, J. Appl. Phys. 28, 679 (1957).
13. Deisler, P. F., and R. H. Wilhelm, Ind. Eng. Chem. 45, 1219 (1953).
14. Drew, T. B., H. H. Dunkle and R. P. Genereaux, in "Chemical Engineer's Handbook," 3rd ed., J. H. Perry, ed., McGraw-Hill, 1950, p. 394.
15. Durif, Simone, J. chim. phys. 54, 633 (1957).
16. Elkin, P. B., C. G. Schull and L. C. Roess, Ind. Eng. Chem. 37, 327 (1945).
17. Farkas, A., "Orthohydrogen, Parahydrogen and Heavy Hydrogen," Cambridge, 1935, p. 17.
18. Ganguli, N. C., P. N. Mukherjee, and A. Lahiri, Fuel 40, 525 (1961).
19. Geddes, D. D., M. S. Thesis, University of Colorado, 1964.
20. Gilliland, E. R., R. F. Baddour, and H. H. Engel, A.I.Ch.E. Journal 8, 530 (1962).
21. Gilliland, E. R., R. F. Baddour, and J. L. Russell, A.I.Ch.E. Journal 4, 90 (1958).
22. Henry, J. P., B. Chennakesavan, and J. M. Smith, A.I.Ch.E. Journal 7, 19 (1961).
23. Hoogschagen, J., Ind. Eng. Chem. 47, 906 (1955).
24. Keeler, R. N., D. H. Weitzel, J. H. Blake and M. Konecnik, in "Advances in Cryogenic Engineering," Vol. 5, K. D. Timmerhaus, ed., Plenum Press, 1960, pp. 511-517
25. Knudsen, M., Ann. Physik 28, 75 (1909); 35, 389 (1911).

26. Levenspiel, O., "Chemical Reaction Engineering," Wiley, 1962, pp. 275-6.

27. Loebenstein, W. V., and V. R. Dietz, J. Research of the N.B.S. 46, 51 (1951).

28. Malherbe, P. LeR., Fuel 30, 97 (1951).

29. Noller, H., P. Andreu and G. M. Schwab, Z. physik. Chem. (Frankfurt) 36, 187.

30. Piret, E. L., R. A. Ebel, C. T. Kiang, and W. P. Armstrong, Chem. Eng. Prog. 47, 405, 628 (1951).

31. Purcell, J. R., J. W. Draper and D. H. Weitzel, in "Advances in Cryogenic Engineering," Vol. 3, K. D. Timmerhaus, ed., Plenum Press, 1960, pp. 191-195.

32. Reid, R. C., and T. K. Sherwood, "The Properties of Gases and Liquids," McGraw-Hill, 1958, pp. 266-381.

33. Satterfield, C. N., and T. K. Sherwood, "The Role of Diffusion in Catalysis," Addison-Wesley, 1963.

34. ibid., pp. 19-20.

35. Scott, D. S., and F. A. L. Dullien, A.I.Ch.E. Journal 8, 113 (1962).

36. Sehr, R. A., Chem. Eng. Sci. 9, 145 (1958).

37. Thiele, E. W., Ind. Eng. Chem. 31, 916 (1939).

38. Tinkler, J. D., and A. B. Metzner, Ind. Eng. Chem. 53, 663 (1961).

39. Villet, R. H., and R. H. Wilhelm, Ind. Eng. Chem. 53, 837 (1961).

40. Wakao, N., T. Oshima and Sakae Yagi, Chem. Eng. (Japan) 22, 780 (1958) (quoted in reference (41)).

41. Wakao, N., P. W. Selwood, and J. M. Smith, A.I.Ch.E. Journal 8, 478 (1962).

42. Wehner, J. G., and R. H. Wilhelm, Chem. Eng. Sci. 6, 89 (1956).

43. Weisz, P. B., and J. S. Hicks, Chem. Eng. Sci. 17, 265 (1962).

44. Weisz, P. B., and C. D. Prater, in "Advances in Catalysis," Vol. VI, W. G. Frankenburg, V. I. Komarewsky and E. K. Rideal, ed., Academic Press, 1954, pp. 143-196.

45. Weisz, P. B., and A. B. Schwartz, J. of Catalysis 1, 399 (1962).

46. Weitzel, D. H., J. H. Blake, and M. Konecnik, in "Advances in Cryogenic Engineering," Vol. 4 , K. D. Timmerhaus, ed., Plenum Press, 1960, pp. 286-295.

47. Wheeler, A., in "Advances in Catalysis," Vol. III, W. G. Frankenburg, V. I. Komarewsky, and E. K. Rideal, ed., Academic Press, 1951, pp. 249-327.

48. ibid., p. 299-301.

49. ibid., p. 299, Equation (69).

50. ibid., pp. 256-260.

51. ibid., p. 274.

52. Yeh, G. C., J. Chem. Eng. Data 6, 526 (1961).

53. Zeldowitsch, J. B., Acta Physicochim. U.R.S.S. 10, 583 (1939).

## APPENDIX III-A

## THE PHYSICAL MEANING OF THE THIELE MODULUS

It is customary to speak of a "pure surface-kinetics-controlled reaction" as one in which the factors which affect diffusion rates may be ignored, because in this type of reaction the overall rate is influenced only by factors which affect the rate of the surface reaction. By the "surface reaction" is meant the adsorption of reactants from the gas phase onto the catalyst surface, the actual change from the reactants to the products on the catalyst surface, and the desorption of the products from the surface to the gas phase. A "pure surface-kinetics-controlled reaction" can occur when the surface reaction is far slower than the possible diffusion rates. The rate of a surface reaction is dependent upon the surface reaction rate constant, the amount of surface per unit volume of the catalyst pellet, the volume of the catalyst pellet involved, and the concentration of reactant molecules immediately above the surface where the reaction is taking place. In the case of a "pure surface-kinetics-controlled reaction," the concentration of reactant molecules throughout the catalyst pellet is everywhere almost identical with the concentration of reactant molecules at the exterior surface of the catalyst. Under this condition, the overall rate of reaction will be changed essentially only by factors which affect the rate of surface reaction.

It is customary to speak of a "pure diffusion-controlled reaction" as one in which the factors which affect the rate of the surface reaction may be ignored, because in this type of reaction the overall rate is influenced only by the factors which affect the rate of diffusion. However, when the possible rate of reaction is far faster than the possible rates of diffusion, the diffusion rate of the reactant molecules to the reaction sites determines the overall rate of reaction.

The rate of diffusion of reactant molecules within a porous catalyst pellet depends upon the area across which the molecules are diffusing, the concentration gradient of those molecules within the pellet, and the diffusivity of the molecules.

The reaction sites are spread throughout the catalyst pellet, and the rate of surface reaction will affect the concentration gradient of reactant molecules within the pellet. This in turn will affect the rate of diffusion. The kinetics of the surface reaction, therefore, are significant when the possible diffusion

rate is far slower than the possible reaction rate, and the "pure diffusion-controlled reaction," in which the factors affecting the surface kinetics may be ignored, does not physically occur in reactions taking place on the interior surface of porous catalysts.

The only situation in which a "pure diffusion-controlled reaction" might be pictured is one in which the entire reaction occurred at the end of the pore (or at another single point in the pore). In this case, under diffusion-controlled conditions, essentially no reactant would be present at that point or, if the reaction were a reversible reaction, essential equilibrium would exist at that point. Since the reaction took place at only one point, the concentration gradient within the pellet would be unaffected by factors which affect the rate of the surface reaction, and these factors could be ignored under diffusion controlled conditions.

The Thiele modulus is the square root of the ratio of the rate of the "pure surface-kinetics-controlled reaction" to the rate of the "pure diffusion-controlled reaction," if it is considered that the diffusion-controlled reaction takes place at the end of the pore. As an example, for the first order reversible reaction of ortho hydrogen to para hydrogen in a slab of width 2L:

$$h_{sl} = \sqrt{\frac{k_s SAL\,(c_{ps} - c_{pe})}{D_e A\,\frac{(c_{pb} - c_{pe})}{L}}} = L\sqrt{\frac{k_s S}{D_e}} \qquad \text{(III-A-1)}$$

The meaning of the symbols in this equation is the same as that used in the main part of this section of the report

For a sphere, the number of pores decreases as the distance from the center of the sphere decreases. Thus, even though the value of the modulus for each individual pore is the same as that given above for the slab:

$$h_p = b\sqrt{\frac{k_s S}{D_e}} \qquad \text{(III-A-2)}$$

the average Thiele modulus for the entire sphere would be expressed by the relationship:

$$h_{sp} = \frac{\sum^{n_p} b\sqrt{\frac{k_s S}{D_e}}}{n_p} \qquad \text{(III-A-3)}$$

If it is assumed that the number of pores is a continuous function of the radius, following the relationship:

$$n_p(r) = 4\pi r^2 \alpha \qquad \text{(III-A-4)}$$

then Equation (III-A-3) may be expressed as:

$$h_{av} = \frac{\int_0^{R_p} (R_p - r)\sqrt{\frac{k_s S}{D_e}}\,(8\pi r\alpha)\,dr}{4\pi R_p^2 \alpha} \qquad \text{(III-A-5)}$$

with the resulting average Thiele modulus for the sphere:

$$h_{av} = \frac{R_p}{3}\sqrt{\frac{k_s S}{D_e}} \qquad \text{(III-A-6)}$$

This is the same result that is given by Wheeler (1).

## NOTATION

$A$ = Cross-sectional area across which the hydrogen is diffusing, sq cm.

$b$ = Length of an individual pore within the catalyst, cm.

$c_{pe}$ = Equilibrium concentration of para hydrogen at the temperature of reaction, gm-moles/cc.

$c_{ps}$ = Concentration of para hydrogen at the surface of the catalyst particle gm-moles/cc.

$D_e$ = Effective diffusivity of hydrogen within the catalyst particle, sq cm/sec.

$h_p$ = Thiele modulus for a single pore, dimensionless.

$h_{sl}$ = Thiele modulus for a slab, dimensionless.

$k_s$ = First-order surface reaction rate constant, cm/sec.

$L$ = Half the width of the slab, or the distance from the exterior surface to the center of the slab, cm.

$n_p$ = Total number of pores within the catalyst particle.

$n_p(r)$ = Number of pores intersecting the cross-sectional area of the spherical catalyst particle at a distance r from the center.

$r$ = Distance from the center of a catalyst particle, cm.

$R_p$ = Radius of a spherical catalyst particle, cm.

$\alpha$ = Number of pores intersecting the cross-sectional area of the spherical catalyst particle per unit cross-sectional area, pores/sq cm.

## REFERENCE

1. Wheeler, A., in "Advances in Catalysis," Vol. III, W. G. Frankenburg, V. I. Komarewsky, and E. K. Rideal, ed., Academic Press, 1951, p. 298.

## APPENDIX III-B

## DERIVATION OF EQUATIONS RELATING RATE OF REACTION, PHYSICAL PARAMETERS, AND THIELE MODULUS

A. For a Slab:

It is assumed that a catalyst pellet may be represented by a thin slab of infinite length in both directions, but of thickness 2L. A material balance over a slice of this slab $\delta z$ gives:

$$-D_e A \frac{dc_p}{dz} + A\delta z \, Sk_s(c_{pe} - c_p) = -D_e A \frac{d}{dz}\left(c_p + \frac{dc_p}{dz}\delta z\right) \qquad \text{(III-B-1)}$$

Cancelling and collecting terms gives the second-order linear ordinary differential equation:

$$\frac{d^2 c_p}{dz^2} + \frac{k_s S}{D_e}(c_{pe} - c_p) = 0 \qquad \text{(III-B-2)}$$

The boundary conditions are:

$$\text{at } z = 0: \qquad c_p = c_{po} \qquad \text{(III-B-3)}$$

$$z = L: \qquad \frac{dc_p}{dz} = 0 \qquad \text{(III-B-4)}$$

The method of solution for this equation may be found in many locations (e.g.,5) The solution may be expressed in the following form:

If we let

$$h_{sl} = L\sqrt{\frac{k_s S}{D_e}} \qquad \text{(III-B-5)}$$

then

$$\frac{c_{pe} - c_p}{c_{pe} - c_{po}} = \frac{\cosh\left[h_{sl}\left(1 - \frac{z}{L}\right)\right]}{\cosh\left(h_{sl}\right)} \qquad \text{(III-B-6)}$$

This is very similar to the result obtained by Wheeler ( 3 ) for a simple first-order reaction. The rate of reaction occurring within one slab is:

$$(\text{reaction rate/slab}) = AD_e \left.\frac{dc_p}{dz}\right|_{z=0} \qquad \text{(III-B-7)}$$

If equation (III-B-6) is differentiated with respect to z, the result evaluated at z = 0, there is obtained:

$$(\text{reaction rate/slab}) = (c_{pe} - c_{po})\,(D_e A)\left(\frac{h_{sl}}{L}\right)\left[\tanh\,(h_{sl})\right] \qquad \text{(III-B-8)}$$

Since the volume of one slab is equal to (2AL), and the average volume of the reactor occupied by a slab is equal to (2AL/$\gamma$), it follows that:

$$(\text{reaction rate/reactor volume}) = (c_{pe} - c_{po})\,\frac{D_e\gamma}{2L^2}\left[h_{sl}\tanh\,(h_{sl})\right] \qquad \text{(III-B-9)}$$

In order to allow for end effects, it is assumed that the ends are equal in area to the sides, i.e., that the rate of reaction is twice what is expressed by equation (III-B-9):

$$(\text{reaction rate/reactor volume}) = (c_{pe} - c_{po})\,\frac{D_e\gamma}{L^2}\left[h_{sl}\tanh\,(h_{sl})\right] \qquad \text{(III-B-10)}$$

Under conditions of plug flow in the reactor:

$$F dc_{po} = (c_{pe} - c_{pc})\,\frac{D_e\gamma}{L^2}\left[h_{sl}\tanh\,(h_{sl})\right] dV_r \qquad \text{(III-B-11)}$$

Integration gives

$$\ln\frac{(c_{pe} - c_{po})_1}{(c_{pe} - c_{po})_2} = \left[h_{sl}\tanh\,(h_{sl})\right]\left(\frac{V_r}{F}\right)\left(\frac{D_e\gamma}{L^2}\right) \qquad \text{(III-B-12)}$$

or, rearranging:

$$h_{sl}\tanh\,(h_{sl}) = \left[\ln\frac{(c_{pe} - c_{po})_1}{(c_{pe} - c_{po})_2}\right]\left(\frac{F}{V_r}\right)(L^2)\left(\frac{1}{D_e\gamma}\right) \qquad \text{(III-B-13)}$$

which is identical with Equation (III-5).

B. For a Sphere:

It is assumed that a catalyst pellet may be represented by a sphere of radius $R_p$. A material balance over a shell $\delta r$ gives:

$$-D_e A \frac{dc_p}{dr} + 4\pi r^2 \delta r S k_s (c_{pe} - c_p) = - D_e (A + \frac{dA}{dr} \delta r) \frac{d}{dr} (c_p + \frac{dc_p}{dr} \delta r) \quad \text{(III-B-14)}$$

Cancelling and collecting terms results in the second-order linear ordinary differential equation:

$$\frac{d^2 c_p}{dr^2} + \frac{2}{r} \frac{dc_p}{dr} + \frac{k_s S}{D_e} (c_{pe} - c_p) = 0 \quad \text{(III-B-15)}$$

The boundary conditions are:

$$\text{at } r = R_p: \qquad c_p = c_{po} \quad \text{(III-B-16)}$$

$$r = 0 \qquad \frac{dc_p}{dr} = 0 \quad \text{(III-B-17)}$$

This type of equation is quite common and the method of solution may be found easily (e.g.1). The solution may be expressed in the following form:

$$\text{If we let} \qquad h_{sp} = \frac{R_p}{3} \sqrt{\frac{k_s S}{D_e}} \quad \text{(III-B-18)}$$

then

$$\frac{c_{pe} - c_p}{c_{pe} - c_{po}} = \frac{R_p}{r} \frac{\sinh (\frac{3r}{R_p} h_{sp})}{\sinh (3h_{sp})} \quad \text{(III-B-19)}$$

This is almost identical with the result obtained by Thiele (2) for a first-order, irreversible reaction. The rate of reaction occurring within one sphere is:

$$\text{(reaction rate/sphere)} = 4\pi R_p^2 D_e \frac{dc_p}{dr} \Big|_{r = R_p} \quad \text{(III-B-20)}$$

Differentiating equation (III-B-19) with respect to r, then evaluating the result at $r = R_p$, followed by substitution into equation (III-B-20), yields:

$$(\text{reaction rate/sphere}) = (c_{pe} - c_{po})\ (4\pi R_p^2\ D_e) \left[ \frac{3h_{sp}}{R_p \tanh\ (3h_{sp})} - \frac{1}{R_p} \right] \qquad \text{(III-B-21)}$$

The volume of one sphere is equal to $(4\pi R_p^3/3)$, and the average volume of the reactor occupied by one sphere is equal to $(4\pi R_p^3/3\gamma)$. It follows that:

$$(\text{reaction rate/reactor volume}) = (c_{pe} - c_{po})\ \left(\frac{3\gamma D_e}{R_p^2}\right) \left[ \frac{3h_{sp}}{\tanh\ (3h_{sp})} - 1 \right] \qquad \text{(III-B-22)}$$

Under conditions of plug flow in the reactor:

$$F dc_{po} = (c_{pe} - c_{po})\ \left(\frac{3\gamma D_e}{R_p^2}\right) \left[ \frac{3h_{sp}}{\tanh\ (3h_{sp})} - 1 \right] dV_r \qquad \text{(III-B-23)}$$

Integration gives:

$$\ln \frac{(c_{pe} - c_{po})_1}{(c_{pe} - c_{po})_2} = \left( \frac{3\gamma D_e}{R_p^2} \right) \left(\frac{V_r}{F}\right) \left[ \frac{3h_{sp}}{\tanh\ (3h_{sp})} - 1 \right] \qquad \text{(III-B-24)}$$

or, rearranging:

$$\frac{3h_{sp}}{\tanh\ (3h_{sp})} = \left\{ \left[ \ln \frac{(c_{pe} - c_{po})_1}{(c_{pe} - c_{po})_2} \right] \left(\frac{R_p^2}{3}\right) \left(\frac{F}{V_r}\right) \left( \frac{1}{\gamma D_e} \right) \right\} + 1 \qquad \text{(III-B-25)}$$

Equation (III-B-25) is identical with (III-6).

## NOTATIONS

$A$ = Cross-sectional area across which material is diffusing, sq cm.

$c_p$ = Concentration of para hydrogen in gas, gm-moles/cc.

$c_{pe}$ = Equilibrium concentration of para hydrogen in gas at the temperature of the reaction, gm-moles/cc.

$c_{po}$ = Concentration of para hydrogen in gas at exterior surface of catalyst, gm-moles/cc

$D_e$ = Effective diffusivity of para hydrogen within catalyst pellet, sq cm/sec.

$F$ = Feed rate at reaction conditions, cc/sec.

$h_{sl}$ = Thiele modulus assuming that catalyst pellet may be approximated by a slab, dimensionless.

$h_{sp}$ = Thiele modulus assuming that catalyst pellet may be approximated by a sphere, dimensionless.

$k_s$ = First order surface reaction rate constant, cm/sec.

$L$ = Distance from the center of the spherical catalyst pellet, cm.

$R_p$ = Radius of spherical catalyst pellet, cm.

$S$ = Surface area of catalyst, sq cm/cc.

$V_r$ = Reactor volume, cc.

$\gamma$ = Fraction of catalyst chamber occupied by catalyst--equal to (1 - void fraction).

## SUBSCRIPTS

1 = Measured at entrance to reaction zone.

2 = Measured at exit from reaction zone.

## REFERENCES

1. Carslaw, H. S., and J. C. Jaeger, "Conduction of Heat in Solids," 2nd ed., Oxford, 1959, pp. 230-254. On p. 230 it is pointed out that equations of this type are best handled by a change of variable $u = c_p r$.

2. Thiele, E. W., Ind. Eng. Chem. 31, 916 (1939).

3. Wheeler, A., in "Advances in Catalysis," Vol. III, W. G. Frankenburg, V. I. Komarewsky, and E. K. Rideal, ed., Academic Press, 1951, p. 283.

4. ibid., pp. 299-301.

5. Wylie, C. R., Jr., "Advanced Engineering Mathematics," 1st ed., McGraw-Hill, 1951, pp. 24-58.

# SECTION IV

# EFFECTS OF INTERPARTICLE DIFFUSION ON THE KINETICS OF THE ORTHO-PARA HYDROGEN SHIFT OVER THE FERRIC OXIDE GEL CATALYST

## IV.1 Introduction

This section of the report presents the results of an investigation into the effects of diffusion within the gas phase exterior to the catalyst pellets. The reaction studied was the change of orthohydrogen to parahydrogen. It is shown that there are two types of diffusion that may affect the reaction in the region outside the catalyst pellet. After a brief review of the theory of these two types, a description of the experimental program is given. Following this is a comparison of the results of this program with the results that are predicted by the theory.

Diffusion is the process by which there is a net transfer of molecules of a substance through a concentration gradient of that substance. When considering the rate of a catalytic reaction which takes place on the surface of porous catalyst pellets, diffusion in the gas phase, exterior to the pellet, may affect the overall reaction rate in two different ways. The first of these is that diffusion through the boundary layer which surrounds the catalyst pellet may decrease the rate of reaction. The second is that diffusion in the axial direction of the reactor, or longitudinal diffusion, may be significant when compared to the overall flow rate, and so the assumption of plug flow in the reactor may not be valid.

There are many mechanisms by which diffusion can take place, but all of them require a random motion on either a micro or a macro scale. Diffusion can be caused by the motion of the individual molecules as they travel on their random paths. This is known as molecular, or ordinary, diffusion. Diffusion can also take place from the collision of the molecules with the wall of a capillary and the subsequent evaporation of the colliding molecule in a random direction. This is known as Knudsen diffusion. Diffusion can also be caused by the turbulent motion of a fluid, for the random swirling of the turbulent eddies can cause the transport of mass through a concentration gradient. This is known as turbulent diffusion.

All three of the mechanisms mentioned above are important in the study of heterogeneous catalysis. Any or all of these mechanisms may be significant in any given catalytic reaction. In this part of the study only the first and third mechanisms are of interest, since Knudsen diffusion, when it occurs in a catalytic reaction, normally occurs only in the interior of a catalyst particle. The effects of diffusion within the catalyst particles were considered in Section III of this report.

Diffusion through the boundary layer of gas surrounding a catalyst particle is primarily by the mechanism of molecular diffusion. However, the character of the boundary layer is controlled by the fluid mechanics of the situation, and so is dependent upon the Reynolds number of the fluid passing through the reactor zone. The lower the Reynolds number, the thicker is the boundary layer, and the lower is the diffusion rate. The lower the diffusion rate, the more this rate is likely to be a significant factor in the overall reaction rate.

Longitudinal diffusion has a significant effect on the reaction rate when the rate of diffusion of molecules is significant when compared with the rate of flow of the fluid within the reactor. In packed beds, this ratio is dependent upon the Reynolds number of the fluid in the bed, being higher at low Reynolds numbers. As the Reynolds number of the fluid passing through the packed bed decreases, therefore, both types of diffusion assume greater significance. It is thus at the lowest value of the Reynolds number investigated that the greatest effect of diffusion would be expected.

## IV.2 Theory

Whenever a fluid passes over a surface, whether it be a flat plate, inside of a tube, or a catalyst pellet, there is formed what is known as a boundary layer. Within this boundary layer the direction of velocity is primarily parallel to the surface. The velocity within the boundary layer varies from zero at the surface to the value of the main stream velocity at the edge of the layer.

The rate of mass transport through this boundary layer is frequently reported in terms of a mass-transfer coefficient, $k_f$, defined by the equation

$$N/A = k_f(c_b - c_s) \qquad \text{(IV-1)}$$

In this equation N is the number of moles of a substance passing through the boundary layer per unit time, A is the area, $c_b$ is the concentration of that substance in the bulk gas phase exterior to the catalyst pellet, $c_s$ is the gas phase concentration of the substance at the exterior surface of the catalyst pellet, and $k_f$ is the mass transfer coefficient. Typical units for these quantities may be found in the table of notation at the end of this section.

Theoretical considerations dictate that the mass transfer coefficient multiplied by a representative dimension of the flow passage divided by the molecular diffusivity of the substance being transferred across the boundary layer should be a function of the square root of the Reynolds number and the cube root of the Schmidt number. The dimensionless parameter formed by multiplying the mass transfer coefficient by the representative dimension of the flow passage divided by the molecular diffusivity of the substance under consideration is known as the Sherwood number. When considering mass transfer in packed beds, the characteristic dimension of the flow passage is commonly taken to be the diameter or equivalent diameter of the pellets which comprise the bed. These theoretical considerations are described and developed in many locations (e.g., 2).

There have been many correlations of the data on mass transfer to pellets in fixed beds. Five of the most recent correlations are those of Bradshaw and Bennett (1), Carberry (2), DeAcetis and Thodos (5), Wakao and Yagi (9) and Yeh (10). In the range of low Reynolds numbers, they express their correlations by the following equations:

Bradshaw and Bennett:
$$N_{Sh} = 2.0 + 1.97(N_{Re})^{\frac{1}{2}}(N_{Sc})^{1/3} \qquad \text{(IV-2)}$$

Carberry:
$$N_{Sh} = (1.15(1/\varepsilon)(N_{Re})^{\frac{1}{2}}(N_{Sc})^{1/3} \qquad \text{(IV-3)}$$

DeAcetis and Thodos:
$$N_{Sh} = (0.725)\left\{N_{Re}/[(N_{Re})^{0.41}-1.5]\right\}(N_{Sc})^{1/3} \qquad \text{(IV-4)}$$

Wakao and Yagi:
$$N_{Sh} = 2.0 + 1.45(N_{Re})^{\frac{1}{2}}(N_{Sc})^{1/3} \qquad \text{(IV-5)}$$

Yeh:
$$N_{Sh} = (1.91 \times 10^{0.04N_{Re}})(N_{Sc})^{1/3} \qquad \text{(IV-6)}$$

Thus, if the Reynolds number and the Schmidt number are known, the Sherwood number can be estimated from any of the above correlations and from this the approximate mass transfer coefficient can be calculated.

If the change of orthohydrogen to parahydrogen is regarded as a first-order reversible reaction, then the rate may be expressed by the relationship.

$$r = k_p(c_{pe} - c_{ps}) \qquad \text{(IV-7)}$$

In this equation, r is the rate of production of parahydrogen, $c_{pe}$ is the equilibrium gas phase concentration of parahydrogen at the temperature of the reaction, $c_{ps}$ is the gas phase concentration of parahydrogen at the exterior surface of the catalyst pellet, and $k_p$ is the first-order reaction rate constant based on the volume of the catalyst pellet.

Since the rate of production of parahydrogen is equal to the rate of parahydrogen diffusing through the boundary layer to the bulk stream, the following equality is valid:

$$k_p (c_{pe} - c_{ps}) = k_F(c_{pb} - c_{ps}) \qquad \text{(IV-8)}$$

in which $k_F$ is the mass transfer coefficient based upon the volume of a catalyst pellet, and is related to the mass transfer coefficient based upon the exterior surface of the pellet by the relationship:

$$k_F = 3k_f/R_p \qquad \text{(IV-9)}$$

Eliminating $c_{ps}$ from Equations (IV-7) and (IV-8), there is obtained:

$$r = \frac{k_F k_p}{k_F + k_p} (c_{pe} - c_{pb}) \qquad \text{(IV-10)}$$

Thus the overall reaction rate maintains first-order kinetics in the presence of diffusion through the boundary layer if we define an overall reaction rate constant $K_{ov}$:

$$K_{ov} = \frac{k_F k_p}{k_F + k_p} \qquad \text{(IV-11)}$$

or:

$$\frac{1}{K_{ov}} = \frac{1}{k_F} + \frac{1}{k_p} \qquad \text{(IV-12)}$$

From the relationships presented above, it is possible to predict the effect of flow rate on the first order reaction rate constant, by calculating the mass transfer coefficients from one of the Equations (IV-2) through (IV-6) and Equation (IV-9), and then using Equation (IV-11) or (IV-12) to calculate the overall reaction rate constant for a particular flow rate.

The relationships presented in Equations (IV-8) through (IV-12) depend upon the change of orthohydrogen to parahydrogen following a first-order rate law. This is not true, as was demonstrated in Section II. It was shown in Section III, however, that within a variation of ± 35%, the ortho-para hydrogen shift may be regarded as a first-order reaction. This simplification is useful for determining if either diffusion or surface reaction is controlling. For cases when both rates are significant, then the more complicated rate expression would have to be used in deriving an expression analogous to Equations (IV-11) and (IV-12).

The first-order rate constant for any particular conversion at a given flow rate may be found from the integrated form of the first-order rate expression for a reversible reaction in a flow reactor:

$$\ln \frac{(x_e - x_1)}{(x_e - x_2)} = K_{RV}\tau \qquad \text{(IV-13)}$$

and then $K_{ov}$ may be calculated from the relationship:

$$K_{ov} = K_{RV}/\gamma \qquad \text{(IV-14)}$$

In the above two equations, x is the mole fraction of parahydrogen in the gas stream, $x_e$ is the equilibrium mole fraction of parahydrogen in the gas phase at the temperature of the reaction, $\tau$ is the residence time or space time of the reactant over the catalyst at the reaction conditions, $K_{RV}$ is the overall first-order reaction rate constant based on the reactor volume, and $\gamma$ is the fraction of the reactor occupied by the catalyst. The subscripts 1 and 2 are used to denote the entrance and the exit of the reactor, respectively.

The value of $K_{ov}$ may be found from experimental data at any particular flow rate, and this value may then be compared with the value of $k_F$ calculated from the mass transfer relationships presented above. Using either Equation (IV-11) or (IV-12), it may be shown whether either the surface reaction or external

diffusion should be the controlling factor. If both $k_p$ and $k_F$ are shown to be the same order of magnitude, then more complicated expressions would have to be developed to account for this.

Longitudinal diffusion affects the analysis of the results of an investigation by affecting one of the assumptions on which this analysis is based. The method of attack on data from packed bed reactors is based on the assumption that "piston" or "plug" flow exists in the reactor, i.e., all the fluid moves through the reactor at the same velocity, for there are no radial velocity gradients, and there is no axial mixing of the fluid in the direction of flow. This is frequently a good assumption for packed bed reactors.

Longitudinal diffusion tends to mix the elements of fluid along the direction of flow. The effect of longitudinal diffusion is a function of the ratio between the linear velocity of the fluid through the reactor and the possible velocity of the fluid by means of diffusion. This ratio is a dimensionless number known as the axial Peclet number, and is expressed by the relationship:

$$N_{Pe} = uL/D \qquad \text{(IV-15)}$$

in which D is the effective diffusivity of the substance within the bulk stream in the reaction zone, u is the linear velocity of the gas in an open tube of the same cross-sectional area as the reactor, and L is the length of the reaction zone. When the flow is characterized by high values of the Peclet number, then axial diffusion is negligible, and the assumption of plug flow is essentially valid. When the flow is characterized by low values of the Peclet number, then axial diffusion must be considered.

The problem of the effect of longitudinal diffusion on chemical reaction rates has been considered by many investigators in this field. Damköhler (4) was one of the earliest, and his method was essentially what is being used at the present time. Many solutions covering different situations have been presented, and the solution used in this investigation was that presented by Levenspiel (6). The equation, for the first-order reversible change of ortho-hydrogen to parahydrogen, is:

$$\frac{(c_{pe} - c_{pb2})}{(c_{pe} - c_{pb2})_{pf}} = 1 + (K_{RV^T})^2 \left(\frac{D}{uL}\right) \qquad \text{(IV-16)}$$

In the above equation, the subscript pf refers to conditions that would exist if plug flow existed in the reactor.

In addition to Equation (IV-16) being valid only for a first-order reversible reaction, the following assumptions are necessary:

(1) Deviations from plug flow are small.

(2) That the diffusion in the spaces both before and following the reaction zone is negligible, making it a "closed reactor".

## IV.3 Experimental Apparatus and Procedure

Following the suggestion of Corrigan (3), an apparatus was designed so that the same amount of catalyst could be used in tubes of the same diameter, but with different bed lengths. An apparatus of this type could then have the fluid passed over the catalyst with the same space time but with different linear velocities. If the lower linear velocity gave a lower conversion, then interparticle diffusion was inhibiting the reaction rate. If the two reactors gave the same conversion, then interparticle diffusion was negligible. Unfortunately, the reproducibility of catalyst activity was not sufficiently accurate so that this scheme could be carried out, and the possible effects of diffusion had to be determined experimentally from the behavior of the reaction kinetics.

These reactors were installed in the same apparatus described in detail in Section III, which was used for activity tests. The same operating procedure was used for these tests as was used in the activity tests described in that section of this report. The catalyst used in this study was Catalyst 00, and the description of the properties of this catalyst are presented in detail in Section III. The size of the catalyst particles was 30-50 mesh, and the mean equivalent diameter was assumed to be 0.042 cm.

In all of the tests of this catalyst, the same activation procedure was used. The catalyst, under a flowing stream of hydrogen, was activated overnight at 150°C. in a air heater.

## IV.4 Experimental Program

The following series of runs was set up: for each reactor, a series of runs was made covering the range from very low flow rates to flow rates high enough

so that temperature effects were definitely noticeable, and the catalyst chamber was obviously not isothermal because of the energy being evolved by the reaction.

A total of eight series of runs were considered valid. These series are listed in Table IV-1. The data obtained from these series of runs are presented in Appendix IV-A.

TABLE IV-1

REACTOR SIZE AND CATALYST WEIGHT USED IN DIFFUSION EXPERIMENTS

| Series | Reactor o.d. | Gms. catalyst |
|---|---|---|
| B | 1/4" | 8.0 |
| C | 1/4" | 2.0 |
| F | 7/32" | 6.0 |
| G | 7/32" | 1.5 |
| H | 3/16" | 1.0 |
| J | 3/16" | 4.0 |
| K | 3/16" | 4.0 |
| L | 3/16" | 2.0 |

IV.5 Kinetics of Reaction

In Section II of this report, it was shown that the change of parahydrogen to orthohydrogen followed the equation:

$$-r = \frac{k(c_p - c_{pe})}{1 + k'c_p} \qquad \text{(IV-16)}$$

In this equation, identical with Equation (II-18), the quantity (-r) is the rate of consumption of parahydrogen, k and k' are rate constants, $c_p$ is the concentration of parahydrogen, and $c_{pe}$ is the equilibrium concentration of parahydrogen in the gas phase at the temperature of the reaction.

The change of orthohydrogen to parahydrogen is the reverse reaction of that analyzed in Section II. If the rate equation presented above truly represents the mechanism of the reaction, then by the principle of microreversibility (7) the negative of this expression should represent the rate of change of orthohydrogen to parahydrogen. If the rate r is defined as the production of parahydrogen, then the negative of Equation (IV-16) can be expressed as

$$r = \frac{k(c_{pe} - c_p)}{1 + k'c_p} \qquad \text{(IV-17)}$$

The integrated form of this equation is identical to Equation (II-19):

$$\frac{\ln \dfrac{(x_e - x_2)}{(x_e - x_1)}}{x_2 - x_1} = -\left[\frac{k}{1 + k'c_H x_e}\right]\left[\frac{\tau}{x_2 - x_1}\right] - \left[\frac{k'c_H}{1 + k'c_H x_e}\right] \qquad \text{(IV-18)}$$

If Equation (IV-17) represents the mechanism of this reaction, then a plot of $\left\{\ln\left[(x_e - x_2)/(x_e - x_1)\right]\right\}/(x_2 - x_1)$ as a function of $\tau/(x_2 - x_1)$ should yield a straight line. Figures IV-1 through IV-8 present the data from the different series of runs plotted in this fashion. It can be seen that, in all cases, at low flow rates, a straight line gives an excellent fit to the data. Only in some runs, at high flow rates, does the data veer away from the straight line. The runs in which this deviation from the straight line behavior was noted are also the runs in which a large amount of catalyst was used, necessitating large absolute flow rates of gas to achieve a desired conversion. Since these large flow rates

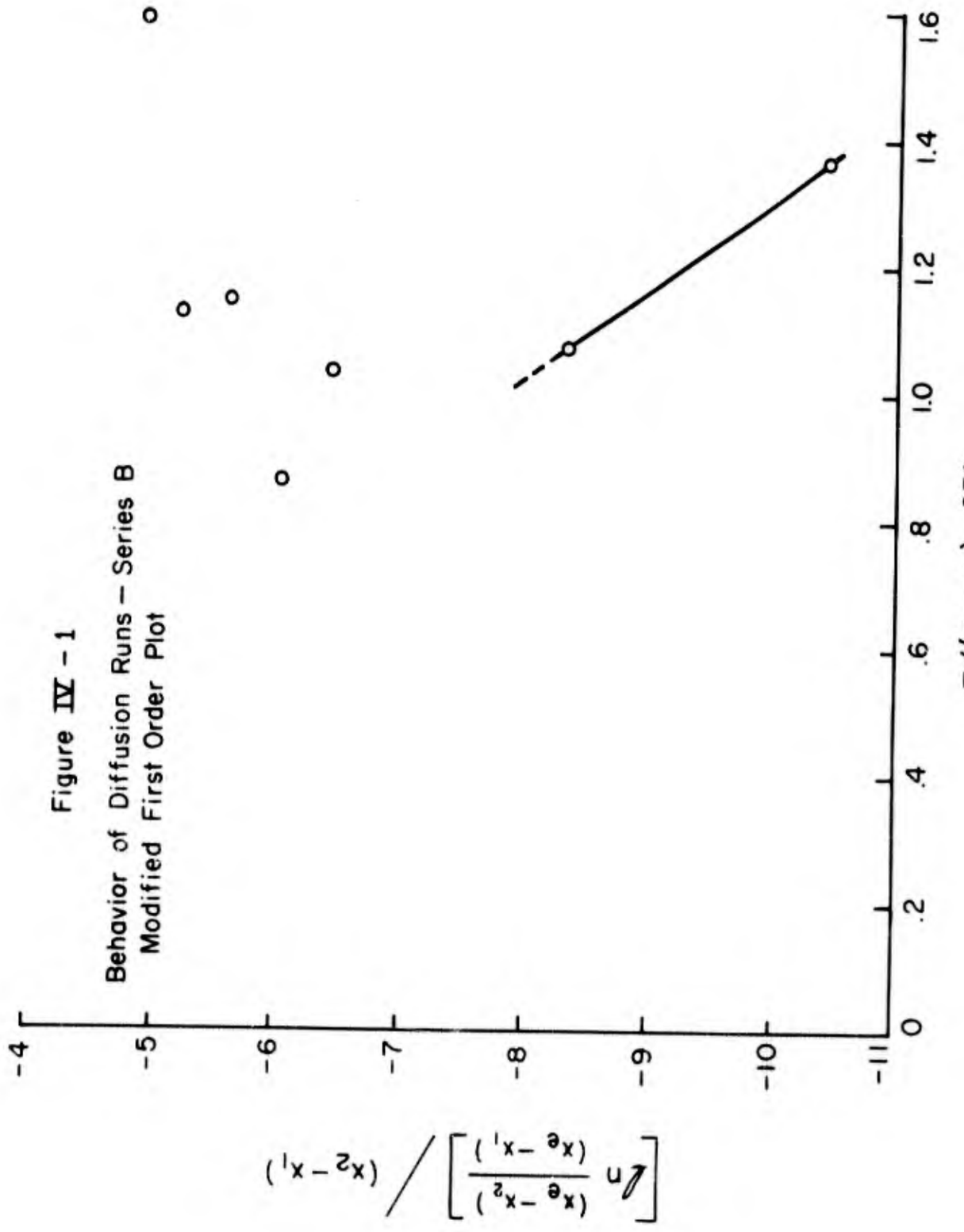


Figure IV - 1

Behavior of Diffusion Runs – Series B
Modified First Order Plot

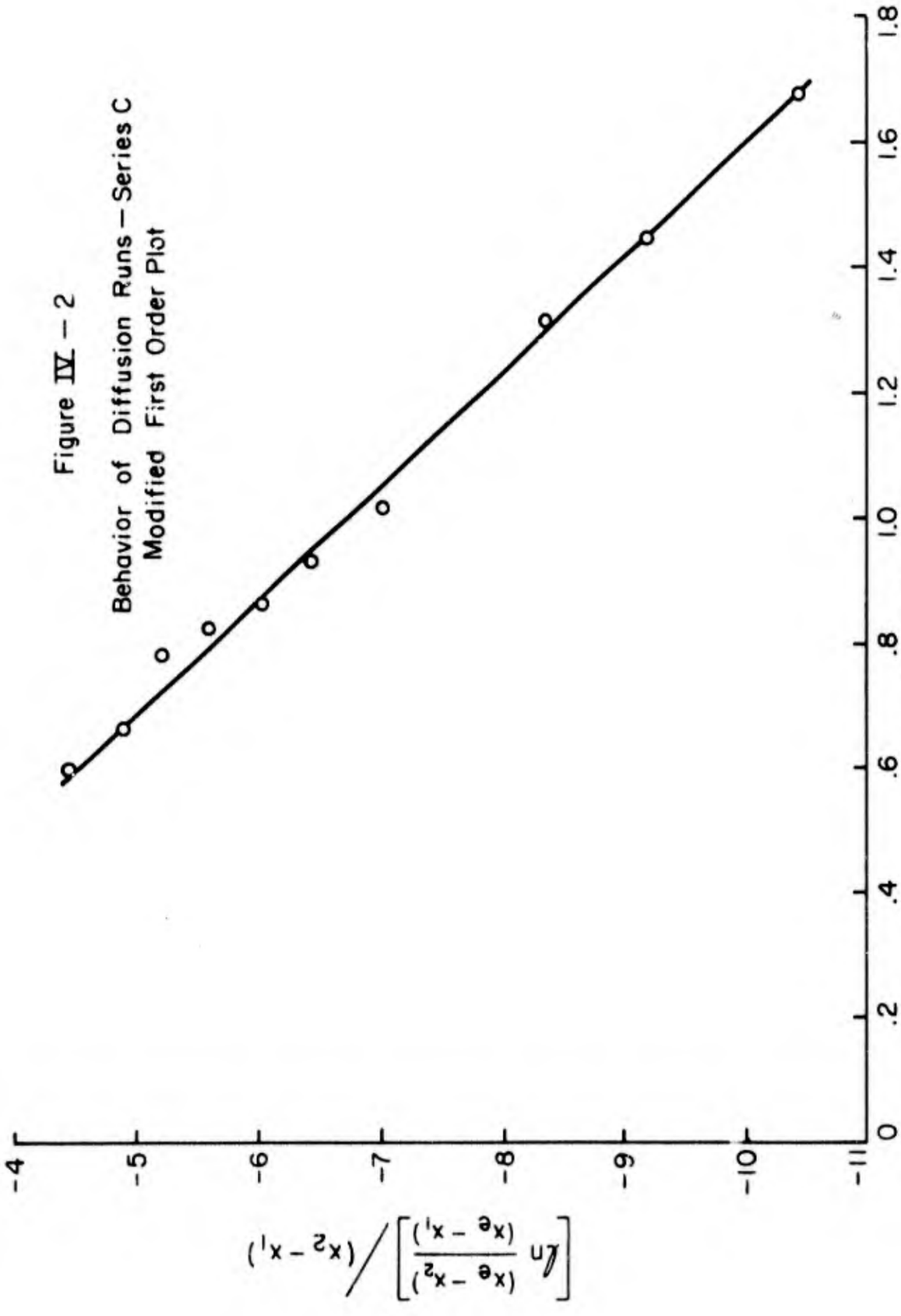


Figure IV – 2

Behavior of Diffusion Runs – Series C
Modified First Order Plot

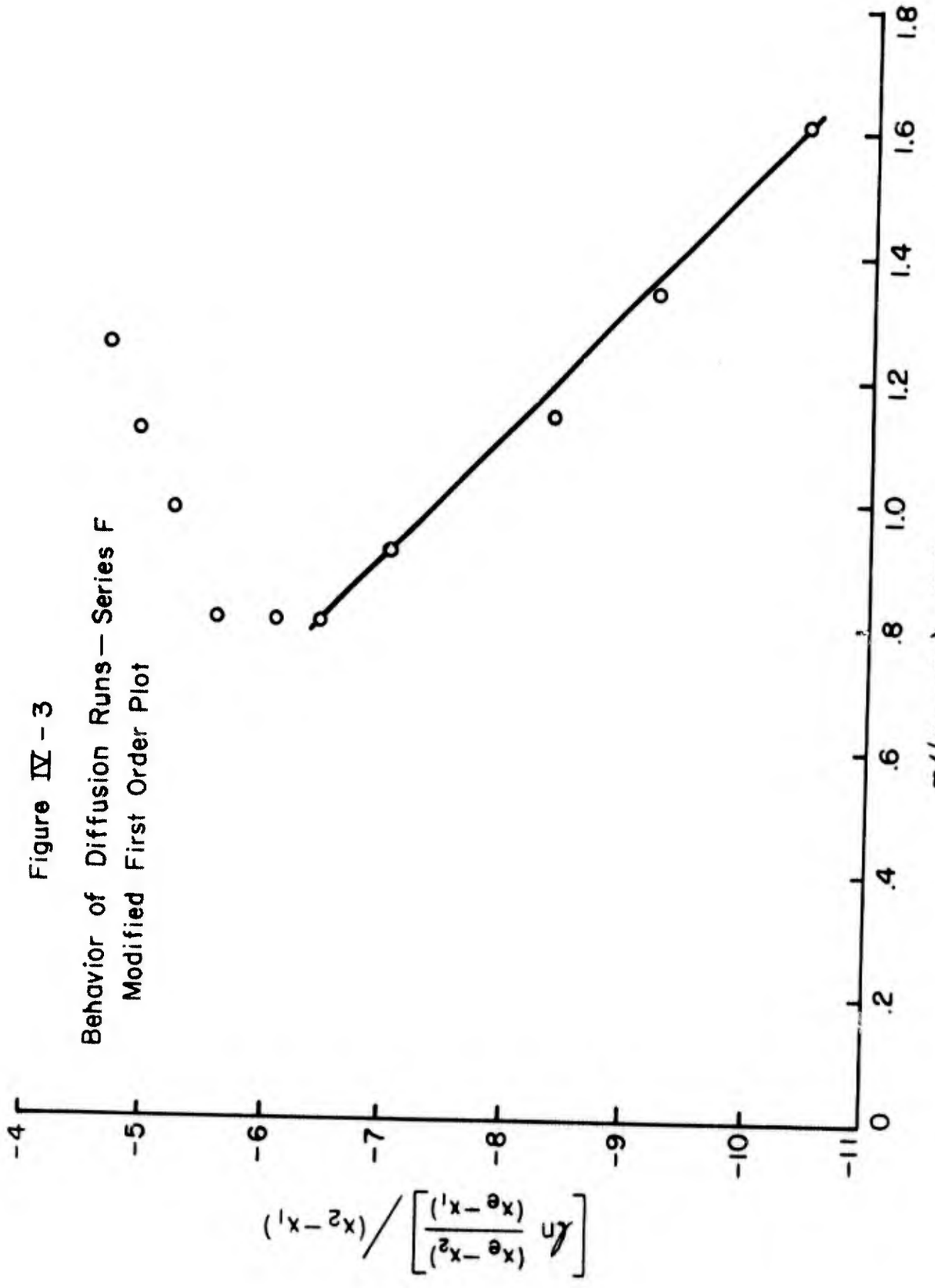


Figure IV - 3

Behavior of Diffusion Runs — Series F
Modified First Order Plot

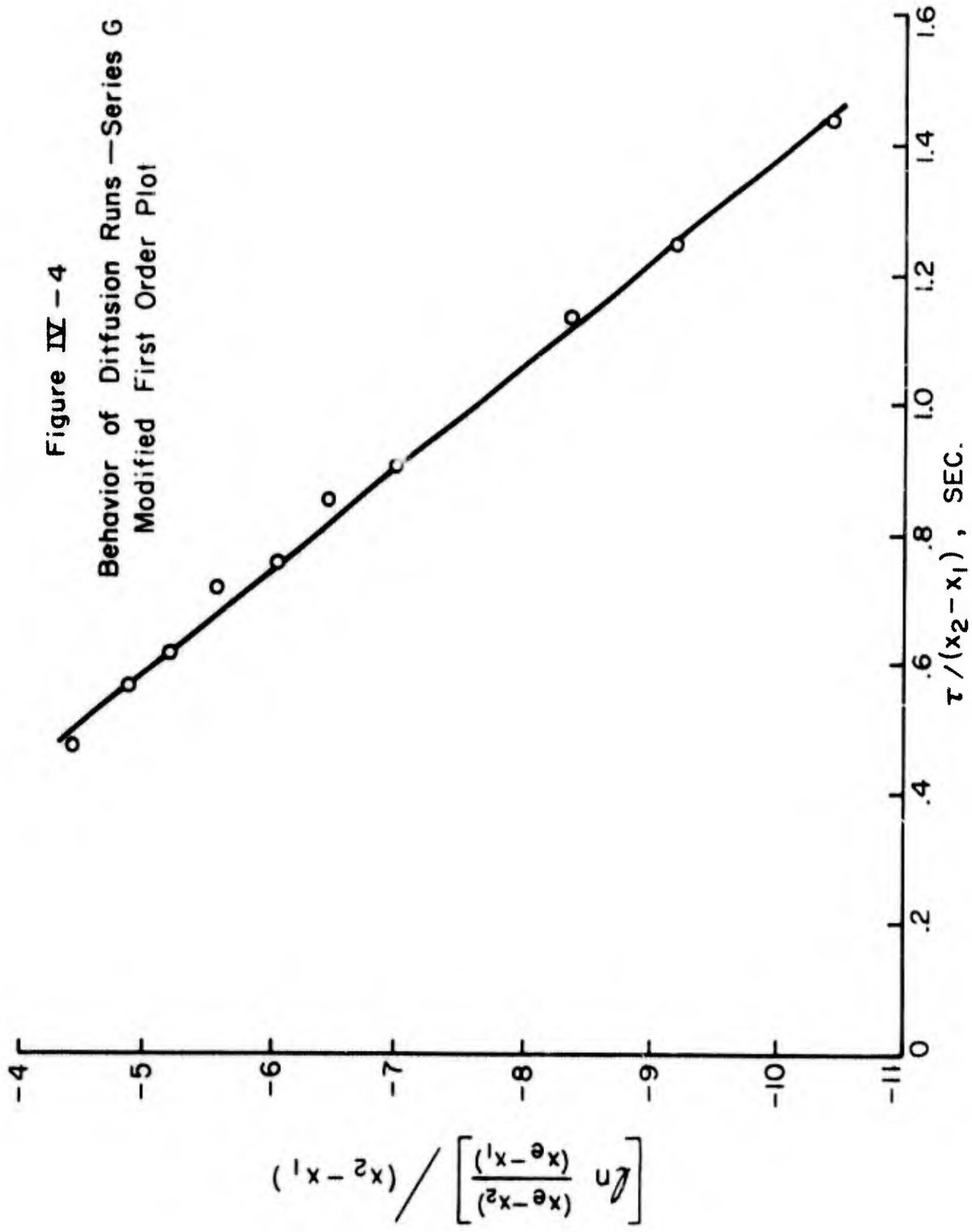
Behavior of Diffusion Runs —Series G
Modified First Order Plot
$\left[\ln \frac{(x_e - x_2)}{(x_e - x_1)}\right] / (x_2 - x_1)$
$\tau / (x_2 - x_1)$, SEC.
-4
-5
-6
-7
-8
-9
-10
-11
0
.2
.4
.6
.8
1.0
1.2
1.4
1.6

Figure IV - 4

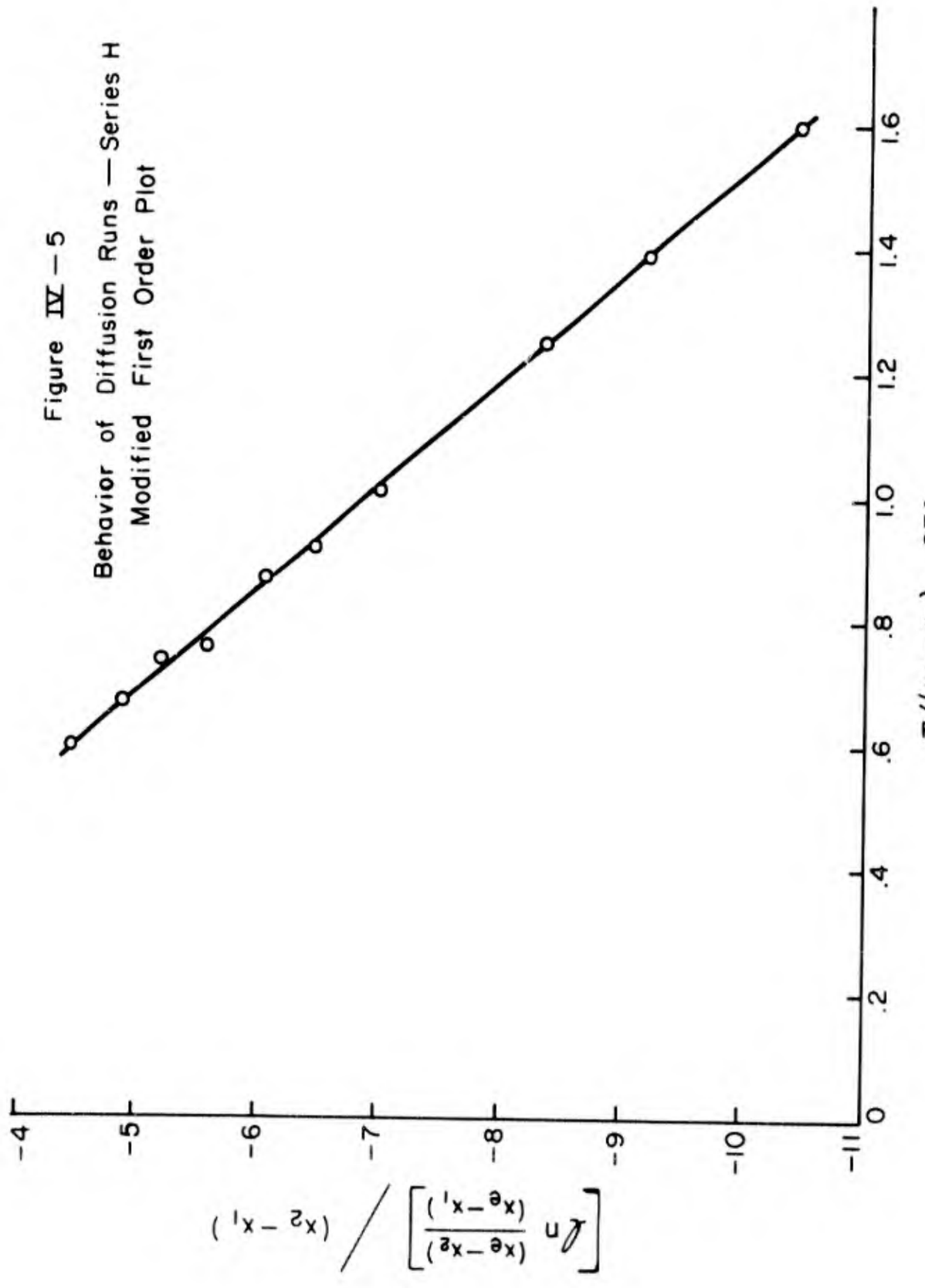


Figure IV-5
Behavior of Diffusion Runs — Series H
Modified First Order Plot

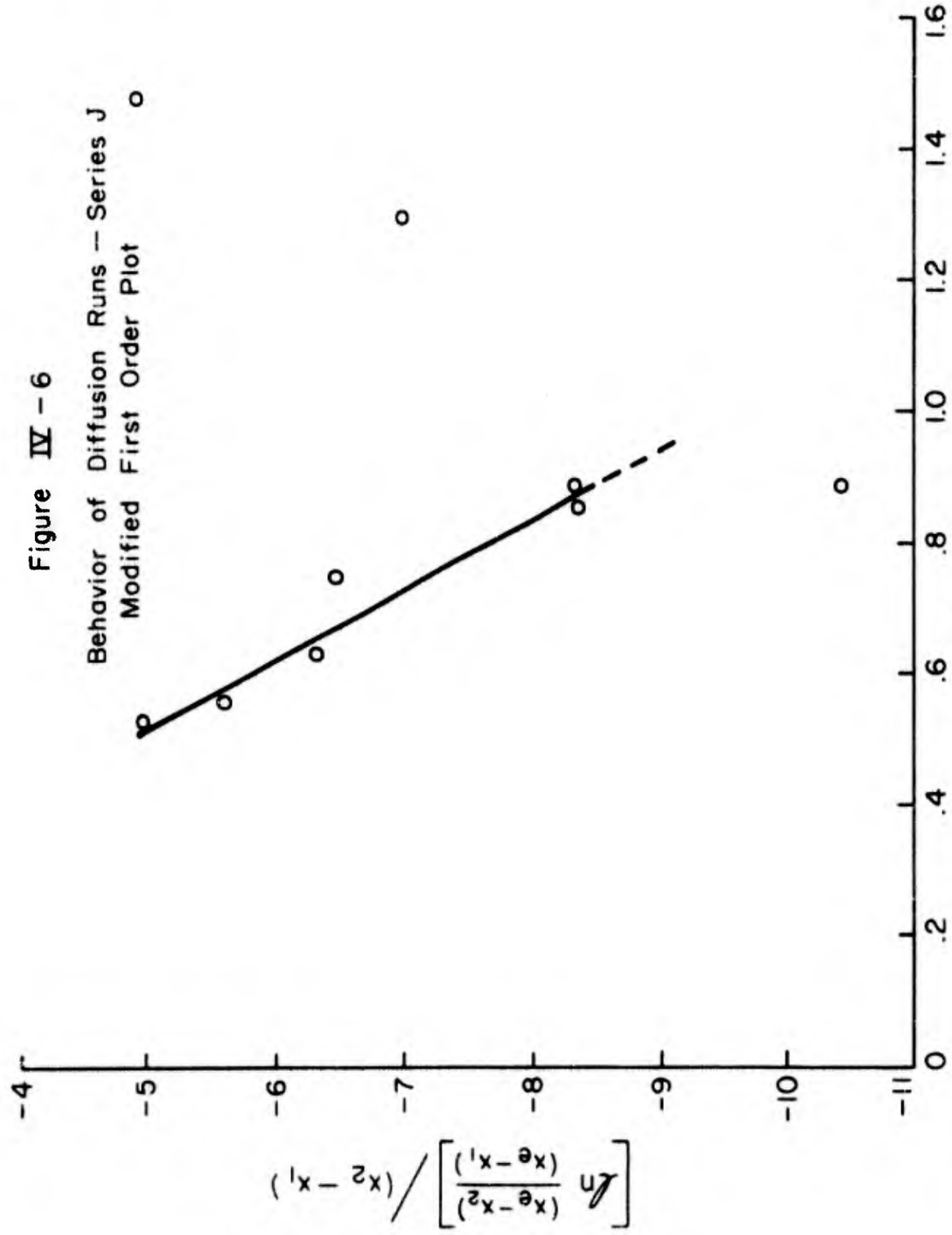
Behavior of Diffusion Runs — Series J
Modified First Order Plot
$\ln \left[\frac{(x_e - x_2)}{(x_e - x_1)}\right] / (x_2 - x_1)$
$\tau / (x_2 - x_1)$, SEC.
-4
-5
-6
-7
-8
-9
-10
-11
0
.2
.4
.6
.8
1.0
1.2
1.4
1.6

Figure IV-6

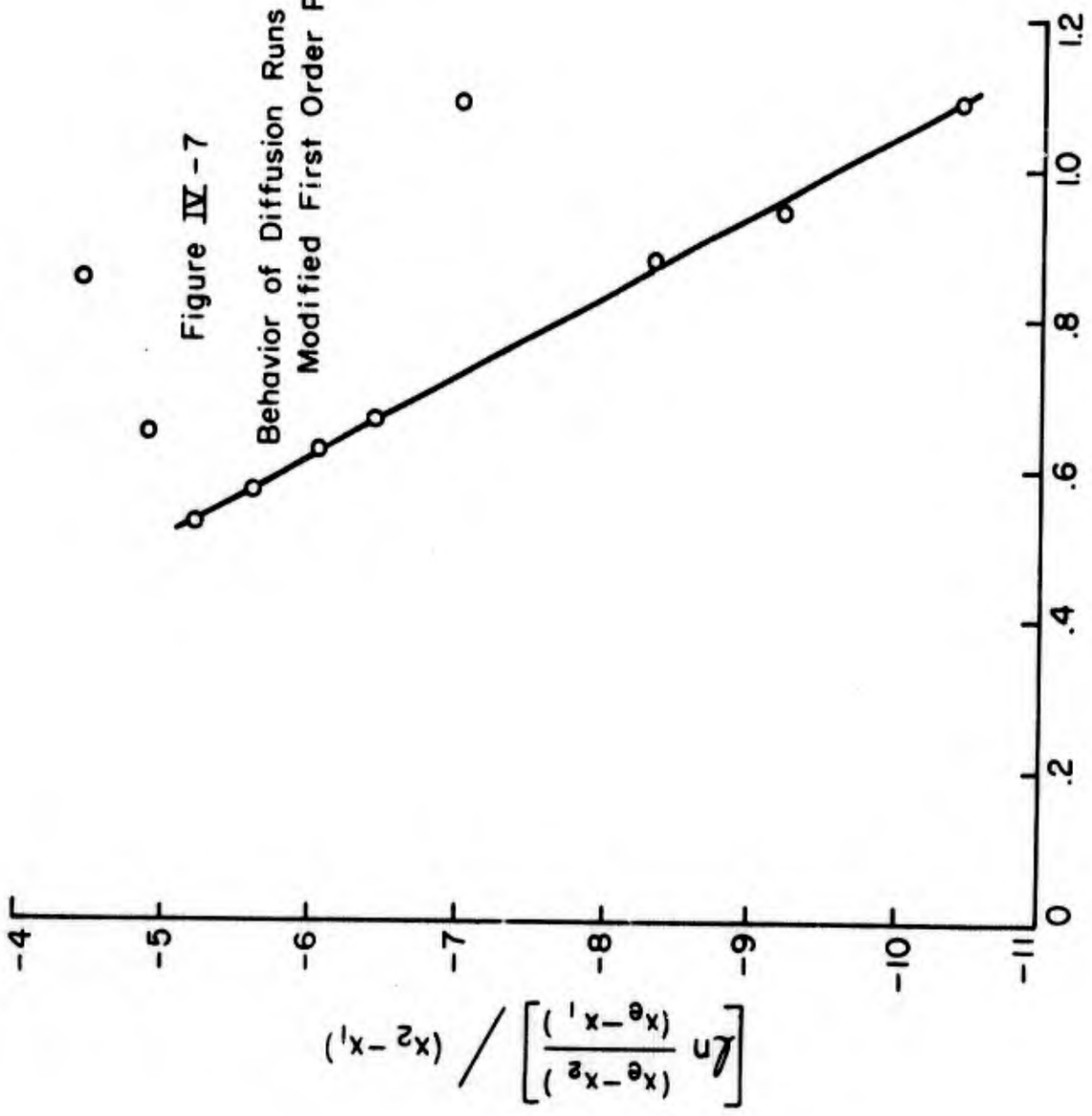
Behavior of Diffusion Runs — Series K
Modified First Order Plot
$\ln \left[\frac{(x_e - x_2)}{(x_e - x_1)}\right] / (x_2 - x_1)$
$\tau / (x_2 - x_1)$, SEC.
-4
-5
-6
-7
-8
-9
-10
-11
0
.2
.4
.6
.8
1.0
1.2

Figure IV-7

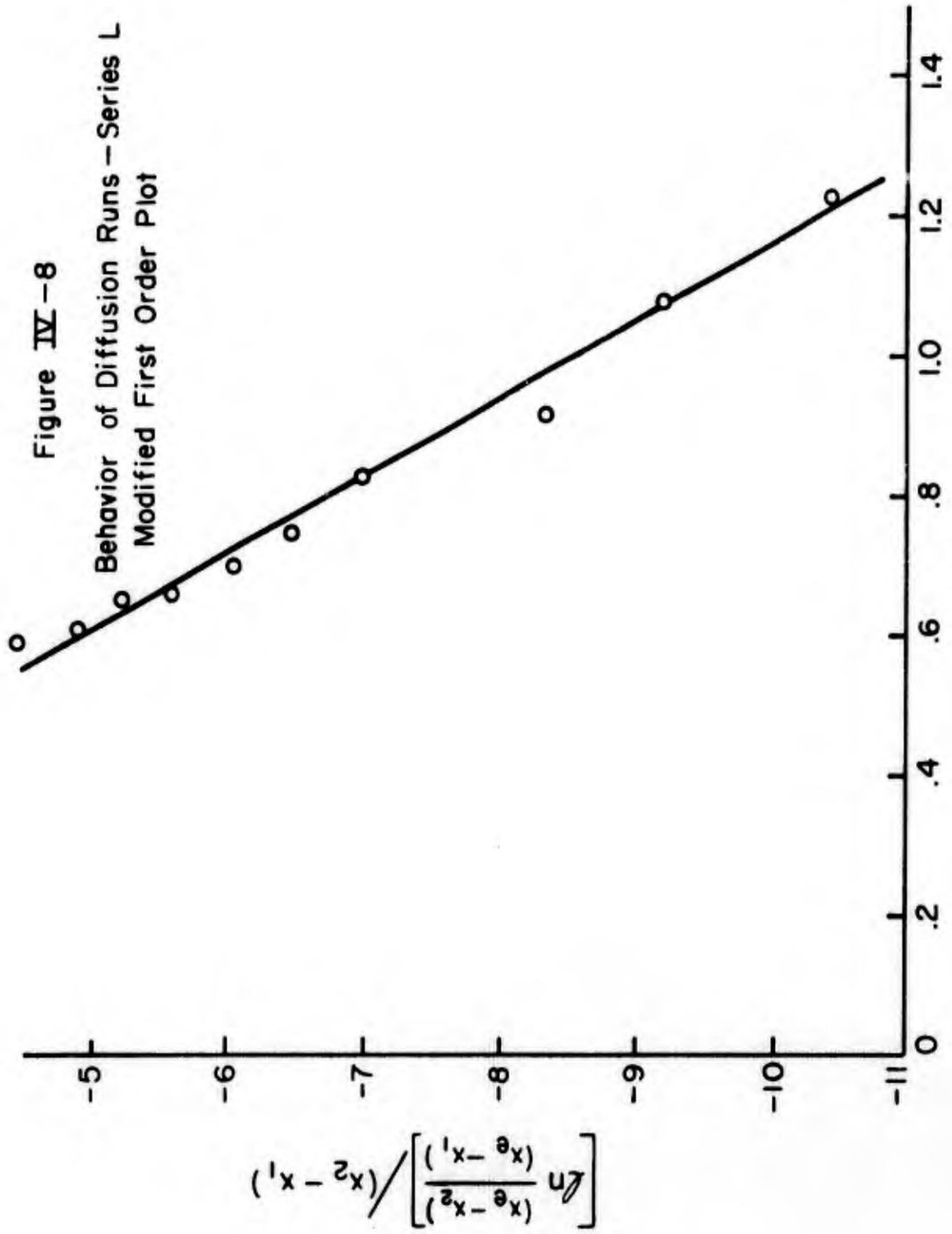
Figure IV-8
Behavior of Diffusion Runs – Series L
Modified First Order Plot
$\ln \left[\frac{(x_e - x_2)}{(x_e - x_1)}\right] / (x_2 - x_1)$
$\tau / x_2 - x_1)$, SEC.
-5
-6
-7
-8
-9
-10
-11
0
.2
.4
.6
.8
1.0
1.2
1.4

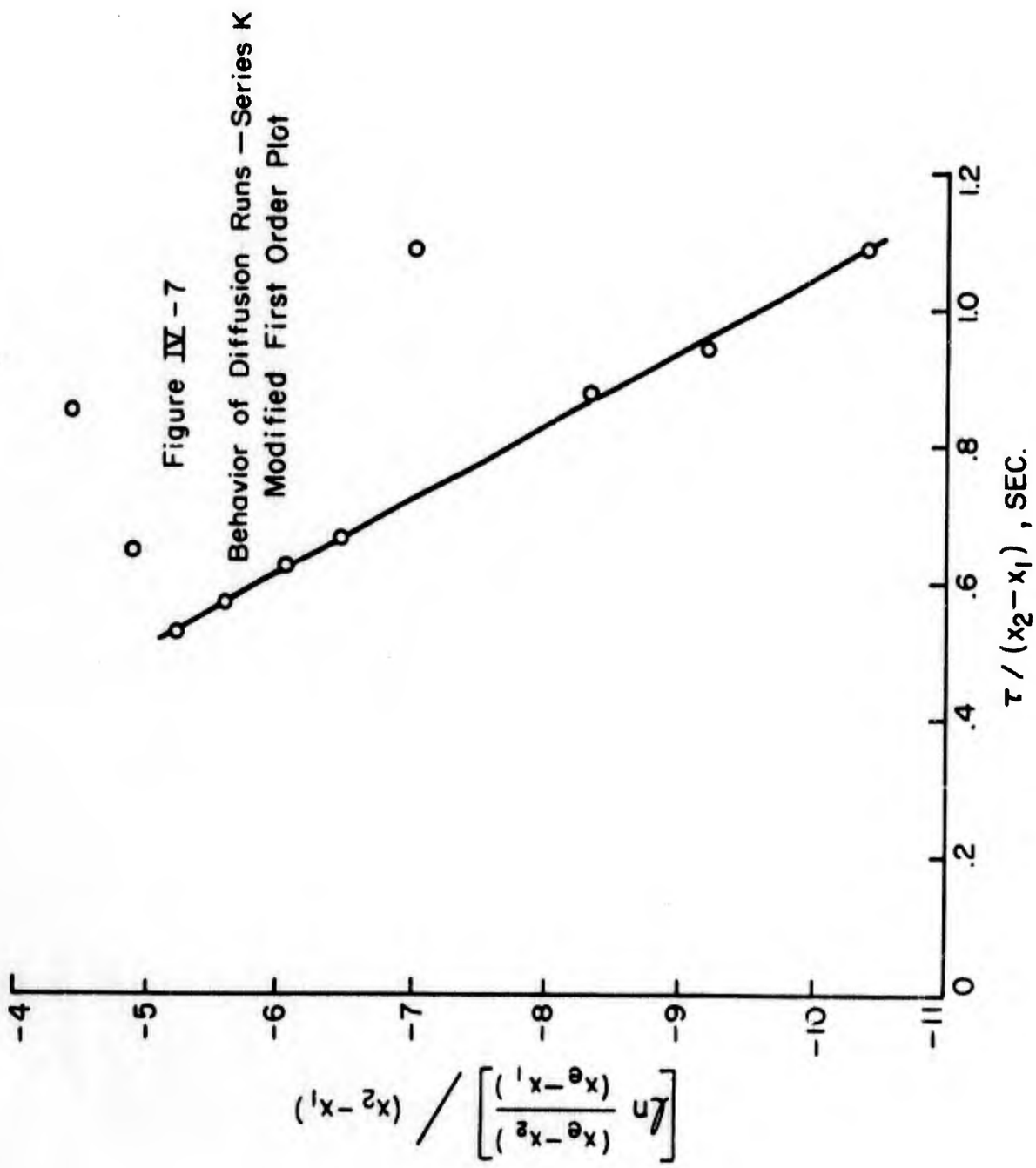
Behavior of Diffusion Runs — Series K
Modified First Order Plot
$\ln \frac{(x_e - x_2)}{(x_e - x_1)} \Big/ (x_2 - x_1)$
$\tau / (x_2 - x_1)$, SEC.
-4
-5
-6
-7
-8
-9
-10
-11
0
.2
.4
.6
.8
1.0
1.2

Figure IV-7

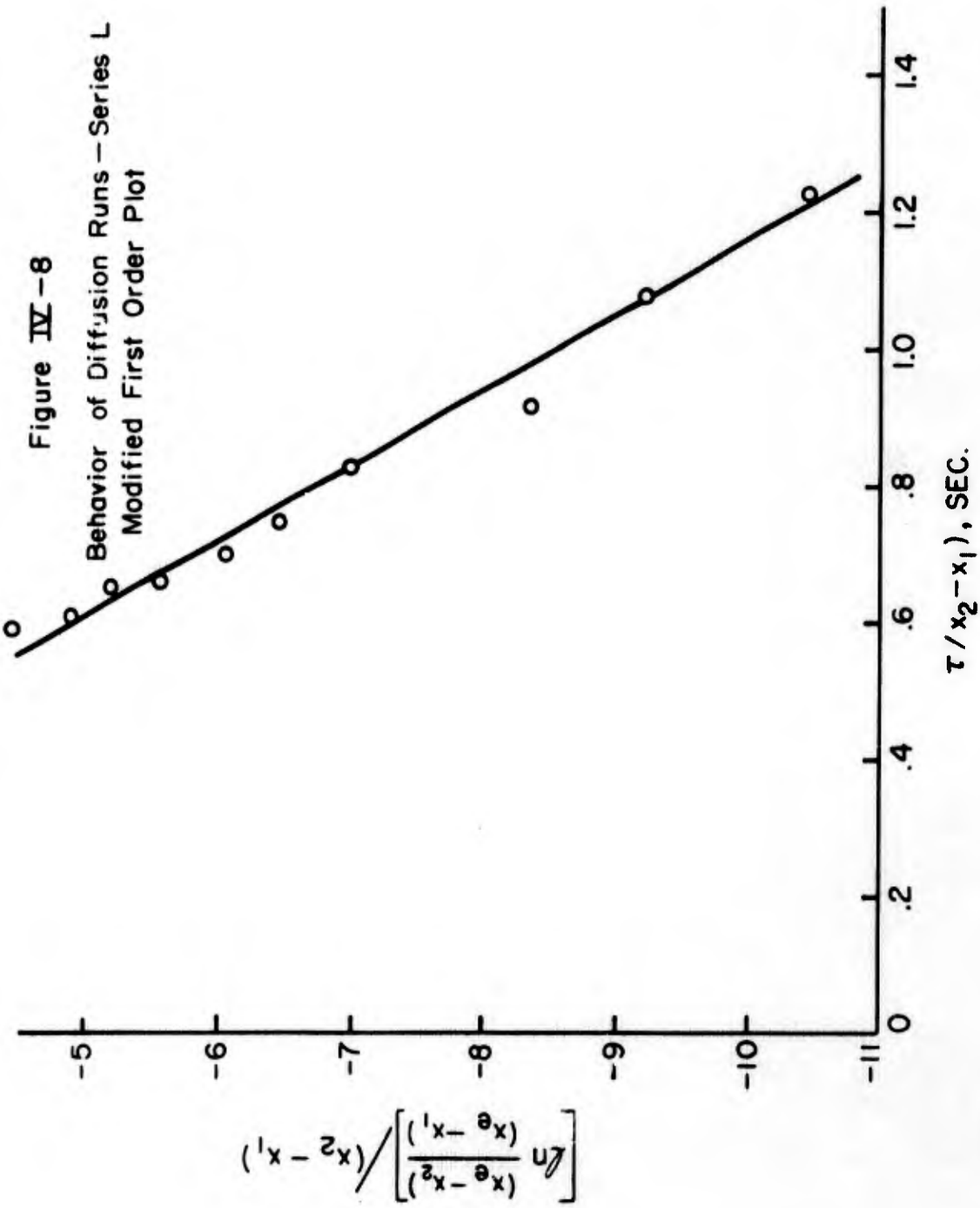


Figure IV-8
Behavior of Diffusion Runs—Series L
Modified First Order Plot

of gas result in an appreciable amount of energy being evolved in the form of heat, it is felt that the deviation from the straight line behavior exhibited in Series B, F and K can be explained by temperature effects, i.e., a temperature rise in the reactor resulted in a decrease in the observed reaction rate, and is indicated by a deviation in the observed from the predicted reaction rate. In the other five series of runs, a straight line is a satisfactory correlation of the data plotted in this fashion.

Thus, it is concluded that the mechanism presented in Section II as a justification for the given rate expression is probably the correct mechanism by which the catalytically promoted reaction takes place. This does not postulate any fundamental mechanism for the surface reaction, of course; it merely assumes it to be first order with respect to the concentration of hydrogen adsorbed on the surface of the catalyst.

It has been stated in many locations (Section II of this report may be consulted for the particular references) that the catalytically promoted change of orthohydrogen to parahydrogen may be represented by a first-order equation. That this is not so may be observed by the fact that extrapolations of the lines presented in Figures IV-1 through IV-8 do not pass through zero, as they would if a first-order rate expression adequately correlated the data presented in this fashion. In the usual method of correlating kinetic data by a first-order rate expression the term $\ln [(x_e - x_1)/(x_e - x_2)]$ is plotted as a function of the space time $\tau$. If the data can be adequately correlated by a straight line passing through the origin, then the reaction follows the first-order relationship within the range of the data studied.

The data is plotted in this form for Series H in Figure IV-9. There is a noticeable curve in the data, and a straight line cannot be drawn so as to represent the trend of the data accurately. Thus the data from Series H are not as well correlated by the first order assumption as they are by the modified first order relationship depicted in Figure IV-5.

## IV.6 Prediction of Mass-Transfer Relationships

The mass transfer relationships dealing with the theory predict a negligible effect of both axial diffusion and diffusion through the boundary layer surrounding the catalyst pellet. Since both types of diffusion assume greater importance as

1/5 FRAMES

Figure IV - 9

Behavior of Diffusion Runs - Series H
First Order Plot

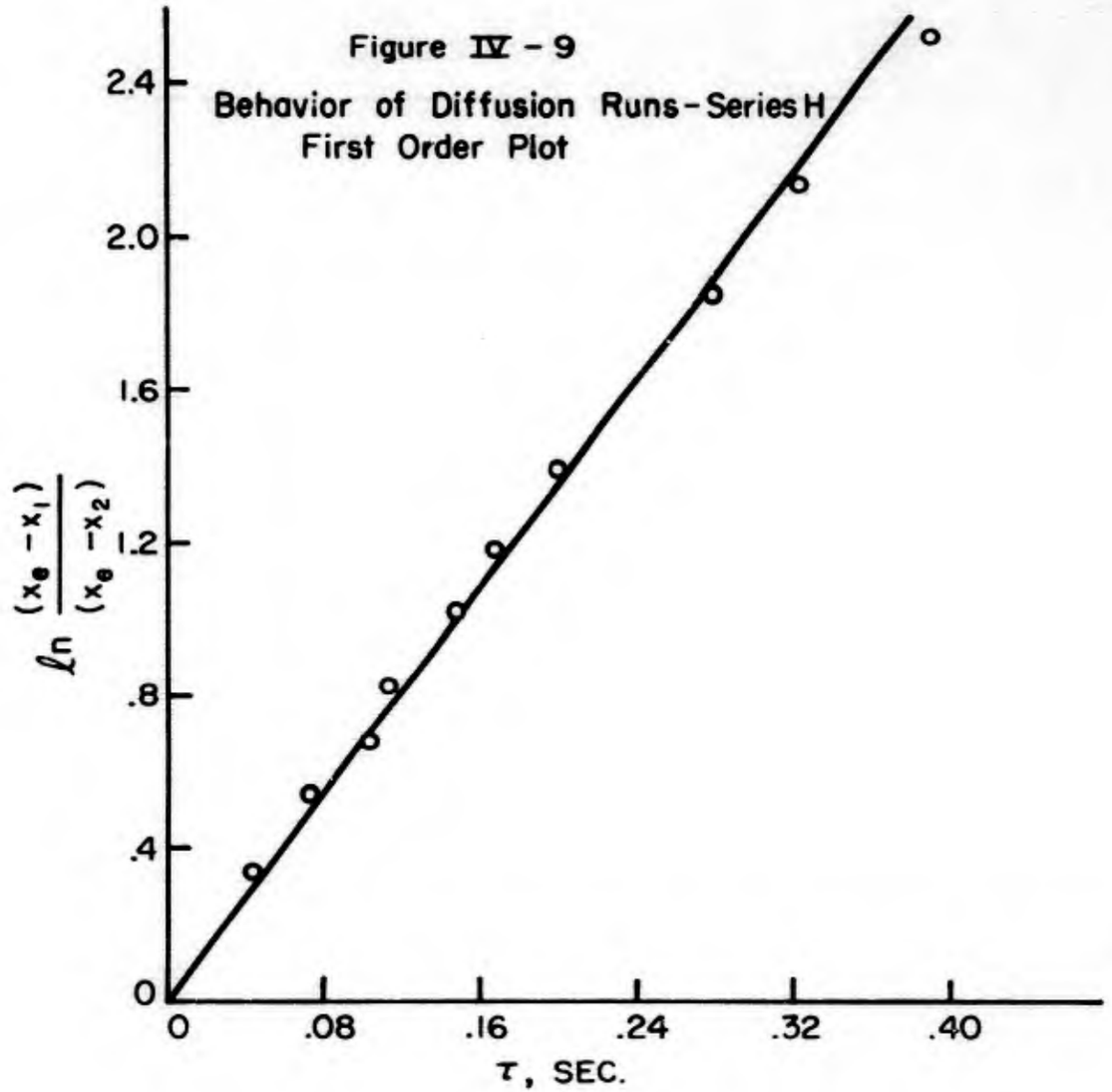

the Reynolds number of the fluid decreases, it will suffice to show that the pertinent equations show both types of diffusion to be negligible at the lowest Reynolds number attained.

The lowest Reynolds number reached during this part of the investigation was in Run H-7, in which a value of 10.1 was obtained. Also during this run, the overall first-order rate constant based on catalyst volume was 10.0 $sec^{-1}$. From the correlation presented by Levenspiel (8), a Peclet number of 230 is estimated as existing within the reactor. Since the value of $K_{RV}\tau$ during run H-7 was 2.53, the value of $(K_{RV})^2(\frac{D}{uL})$ is equal to 0.0275. Thus the deviation of the value of the quantity $(c_{pe} - c_{p2})$ from that which would be obtained if true plug flow prevailed is less than 3%. Simple calculations also show that the deviation of the quantity $\ln [(x_e - x_1)/(x_e - x_2)]$ is less than 2%, the deviation of the quantity $\left\{\ln [(x_e - x_2)/(x_e - x_1)]\right\}/(x_2 - x_1)$ is less than 1%, and deviation of the quantity $\tau/(x_2 - x_1)$ is less than 1%. Thus axial diffusion under the conditions of run H-7 predicts a decrease in rate of less than 2%, and that there will be no noticeable effect in the plots which are used to determine the reaction kinetics.

Table IV-II compares the predicted mass transfer coefficients based on the pellet volume with the first-order rate constant based on the pellet volume for Run H-7. The different correlations are in quite close agreement, deviating within a range of ± 30% from the median value. All of the values of the mass transfer coefficient are orders of magnitude larger than the first order reaction rate constant. The lowest of them predicts a deviation of the predicted from the observed reaction rate (difference between $k_p$ and $K_{ov}$) of less than 1%. It was concluded that these correlations predicted no observable effect of diffusion through the boundary layer surrounding the catalyst pellet.

## IV.7 Absence of Observable Diffusion Effects

Figures IV-1 through IV-8, which present the data obtained in this portion of the investigation, show no observable diffusion effects. If either axial diffusion or diffusion through the pellet boundary layer decreased the reaction rate, there should be a deviation from the straight-line behavior of the kinetics as portrayed in these figures in the range in which the Reynolds numbers are lowest, i.e., at low values of $\left\{\ln [(x_e - x_2)/(x_e - x_1)]\right\}/(x_2 - x_1)$ and high values of $\tau/(x_2 - x_1)$. There is no such deviation from the straight line

TABLE IV-II

COMPARISON OF MASS TRANSFER COEFFICIENTS WITH OVERALL REACTION RATE CONSTANTS

Catalyst: 00

Space time, sec. 0.389

Reynolds number of fluid: 10.1

| Equation: | (IV-2) | (IV-3) | (IV-4) | (IV-5) | (IV-6) |
|---|---|---|---|---|---|
| Coefficient of mass transfer per unit external area, $k_f$, cm/sec | 16.3 | 10.8 | 13.0 | 13.1 | 9.30 |
| Coefficient of mass transfer per unit volume of catalyst, $k_F$, $sec^{-1}$ | 2330 | 1550 | 1860 | 1870 | 1330 |
| Overall reaction rate constant, $K_{ov}$, $sec^{-1}$ | | | 10.0 | | |

behavior in these figures. The only deviation is at the other end of the line, in the region of high flow rates, where the energy evolved in the form of heat affects the rate of reaction. Thus it is concluded that there are no observable diffusion effects in these runs.

In Section II, there was a deviation from the straight line relationship at low Reynolds numbers, and it was considered possible that diffusion effects might be the cause of this deviation. However, in this part of the investigation, at Reynolds numbers lower than those encountered in the study reported in Section II, there was no deviation in the straight-line behavior of the kinetics. It was concluded that the most probable causes of the deviation of the observed values from the predicted in Section II were the precision of the data and the difficulty of the precise temperature control required.

As explained in the description of the experimental program, it was impossible to compare the different series of runs directly with one another, because the catalyst activities were not sufficiently reproducible.

Throughout this portion of the study, diffusion inside the catalyst particle was ignored. It was shown in Section III of this report that this effect was very small for Catalyst 00 when used in the 30-50 mesh size. An effectiveness factor of 0.94 was obtained for this catalyst, which meant that the decrease in rate was only 6% from that which would occur if the intraparticle diffusion was entirely negligible.

## IV.8 Conclusions

1. The available correlations for mass transfer through the boundary layer surrounding granules in a fixed bed predict that this type of diffusion should have a negligible effect on the rate of the ortho-para hydrogen shift over the ferric oxide gel catalyst when the granule size is 30-50 mesh.

2. The correlations for longitudinal diffusion predict that this type of diffusion should also have a negligible effect on the reaction rate when the catalyst granule is within the 30-50 mesh size range.

3. The reaction rate was well correlated by the expression:

$$r = \frac{k(c_{pe} - c_p)}{1 + k'c_p}$$

in which r is the rate of [illegible] of parahydrogen, [illegible] is the concentration of parahydrogen in the gas [illegible] the equilibrium gas phase concentration at the temperature of the [illegible] and k' are constants. This is the negative of the rate expression [illegible] for the change of parahydrogen to orthohydrogen, which confirms the [illegible] reported in Section II of this report as representing the actual mechanism [illegible] reaction.

4. There was no evidence of any type of diffusion [illegible] rate within the range studied. Thus the predictions of [illegible] both axial diffusion and diffusion through the pellet boundary [illegible] confirmed.

## NOTATION

$A$ = Cross-sectional area across which material is diffusing, sq cm

$c_b$ = Concentration of substance in gas, gm-moles/cc

$c_e$ = Equilibrium gas phase concentration of substance, gm-moles/cc

$c_H$ = Total concentration of hydrogen in gas, gm-moles/cc

$c_p$ = Concentration of parahydrogen in gas, gm-moles/cc

$c_{pb}$ = Concentration of parahydrogen in the bulk phase of the gas exterior to the catalyst pellet, gm-moles/cc

$c_{pe}$ = Equilibrium gas phase concentration of parahydrogen at the temperature of the reaction, gm-moles/cc

$c_{ps}$ = Gas phase concentration of parahydrogen at the exterior surface of the catalyst pellet, gm-moles/cc

$c_s$ = Gas phase concentration of substance at exterior surface of the catalyst pellet, gm-moles/cc

$d_p$ = Equivalent diameter of catalyst pellet, cm

$D$ = Effective longitudinal diffusivity of parahydrogen in bulk gas stream, sq cm/sec

$D_{H2}$ = Molecular diffusivity of hydrogen, sq cm/sec

$k$ = Reaction rate constant in ortho-para hydrogen shift rate equation, $sec^{-1}$

$k'$ = Reaction rate constant in ortho-para hydrogen shift rate equation, cc/gm-mole

$k_f$ = Mass transfer coefficient based on catalyst external surface area, cm/sec

$k_F$ = Mass transfer coefficient based on catalyst volume, $sec^{-1}$

$k_p$ = First-order reaction rate constant based on catalyst volume, $sec^{-1}$

$K_{ov}$ = Overall first-order reaction rate constant based on catalyst volume, $sec^{-1}$

$K_{RV}$ = Overall first-order reaction rate constant based on reactor volume, $sec^{-1}$

L = Length of the reaction zone, cm

N = Number of moles of substance diffusing across area, moles/sec

$N_{Pe}$ = Peclet number, uL/D, dimensionless

$N_{Re}$ = Reynolds number, $d_p u\rho/\mu$, dimensionless

$N_{Sc}$ = Schmidt number, $\mu/\rho D_{H2}$, dimensionless

$N_{Sh}$ = Sherwood number, $k_f d_p/D_{H2}$, dimensionless

r = Rate of production of parahydrogen, gm-moles/(cc)(sec)

$R_p$ = Radius of sphere which approximates catalyst pellet, cm

u = Superficial gas velocity in catalyst chamber, cm/sec

x = Mole fraction of parahydrogen in gas phase, dimensionless

$x_e$ = Equilibrium mole fraction of parahydrogen in gas phase at temperature of reaction, dimensionless

$\gamma$ = Fraction of catalyst chamber occupied by catalyst--is equal to (1 - void fraction)

$\epsilon$ = Void fraction in catalyst chamber

$\mu$ = Viscosity of hydrogen, poise

$\rho$ = Density of hydrogen, gm/cc

$\tau$ = Residence time of reactants in catalyst chamber, or space time, sec.

SUBSCRIPTS

1 = Measured at entrance to reaction zone

2 = Measured at exit from reaction zone

## REFERENCES


1. Bradshaw, R. D., and C. O. Bennett, A.I.Ch.E. Journal 7, 48 (1961).

2. Carberry, J. J., A.I.Ch.E. Journal 6, 460 (1960)

3. Corrigan, T. E., Chem. Eng. 65, No. 4, 199 (April, 1955)

4. Damköhler, G., in "Der Chemie-Ingenieur," Band III, A. Eucken and M. Jakob, ed., Akademische Verlagsgesellschaft, 1937, pp. 381-402

5. DeAcetis, J., and G. Thodos, Ind. Eng. Chem. 52, 1003 (1960).

6. Levenspiel, O., "Chemical Reaction Engineering," Wiley, 1962, p. 280

7. ibid., p. 32

8. ibid., p. 275

9. Wakao, N., T. Oshima and Sakae Yagi, Chem. Eng. (Japan) 22, 780 (1958) (quoted in N. Wakao, P. W. Selwood, and J. M. Smith, A.I.Ch.E. Journal 8, 478 (1962))

10. Yeh, G. C., J. Chem. Eng. Data 6, 526 (1961)

## APPENDIX IV-A

### Series: B

Reactor o.d., in: 0.250

Reactor i.d., in: 0.219

Total weight of catalyst in reactor, gms: 8.00

| Run No. | Flow rate of gas through reactor at reaction conditions, cc/sec | Parahydrogen composition in exit gas stream, % | $\ln \frac{x_e - x_1}{x_e - x_2}$ | $\tau$, sec* | $\frac{\ln \frac{x_e - x_2}{x_e - x_1}}{x_2 - x_1}$ | $\frac{\tau}{x_2 - x_1}$, sec | $N_{Re}$ |
|---|---|---|---|---|---|---|---|
| 1 | 26.6 | 0.473 | 1.86 | 0.240 | - 8.35 | 1.08 | 66.6 |
| 2 | 37.5 | 0.399 | 0.831 | 0.171 | - 5.58 | 1.15 | 93.7 |
| 3 | 39.8 | 0.324 | 0.329 | 0.161 | - 4.44 | 2.17 | 99.6 |
| 4 | 36.6 | 0.360 | 0.539 | 0.175 | - 4.90 | 1.59 | 91.5 |
| 5 | 33.8 | 0.433 | 1.18 | 0.190 | - 6.46 | 1.04 | 84.4 |
| 6 | 19.3 | 0.493 | 2.53 | 0.332 | -10.42 | 1.37 | 48.1 |
| 7 | 43.5 | 0.419 | 1.02 | 0.147 | - 6.05 | 0.870 | 108.8 |
| 8 | 44.0 | 0.379 | 0.671 | 0.146 | - 5.20 | 1.13 | 109.9 |
| 9 | 26.6 | 0.473 | 1.86 | 0.241 | - 8.35 | 1.08 | 66.4 |

*A catalyst bulk density of 1.25 gm/cc was assumed.

APPENDIX IV-A (cont.)

Series: C

Reactor o.d., in: 0.250

Reactor i.d., in: 0.219

Total weight of catalyst in reactor, gms: 2.00

| Run No. | Flow rate of gas through reactor at reaction conditions, cc/sec | Parahydrogen composition in exit gas stream, % | $\ln \frac{x_e - x_1}{x_e - x_2}$ | $\tau$, sec* | $\frac{\ln \frac{x_e - x_2}{x_e - x_1}}{x_2 - x_1}$ | $\frac{\tau}{x_2 - x_1}$, sec | $N_{Re}$ |
|---|---|---|---|---|---|---|---|
| 1 | 5.45 | 0.473 | 1.86 | 0.293 | - 8.35 | 1.32 | 13.6 |
| 2 | 13.0 | 0.399 | 0.831 | 0.123 | - 5.58 | 0.829 | 32.4 |
| 3 | 36.2 | 0.324 | 0.329 | 0.0441 | - 4.94 | 0.597 | 90.6 |
| 4 | 21.9 | 0.360 | 0.539 | 0.0730 | - 4.90 | 0.664 | 54.8 |
| 5 | 9.36 | 0.433 | 1.18 | 0.171 | - 6.46 | 0.935 | 23.4 |
| 6 | 7.92 | 0.448 | 1.39 | 0.202 | - 7.00 | 1.02 | 19.8 |
| 7 | 3.93 | 0.493 | 2.53 | 0.407 | -10.42 | 1.68 | 9.8 |
| 8 | 4.74 | 0.483 | 2.14 | 0.338 | - 9.19 | 1.45 | 11.8 |
| 9 | 10.9 | 0.419 | 1.02 | 0.146 | - 6.05 | 0.865 | 27.4 |
| 10 | 15.8 | 0.379 | 0.671 | 0.102 | - 5.20 | 0.787 | 39.4 |

*A catalyst bulk density of 1.25 gm/cc was assumed

APPENDIX IV-A (cont.)

Series: F

Reactor o.d., in: 0.219

Reactor i.d., in: 0.188

Total weight of catalyst in reactor, gms: 6.00

| Run No. | Flow rate of gas through reactor at reaction conditions, cc/sec | Parahydrogen composition in exit gas stream, % | $\ln \frac{x_e - x_1}{x_e - x_2}$ | $\tau$, sec* | $\ln \frac{\frac{x_e - x_2}{x_e - x_1}}{x_2 - x_1}$ | $\frac{\tau}{x_2 - x_1}$, sec | $N_{Re}$ |
|---|---|---|---|---|---|---|---|
| 1 | 18.9 | 0.473 | 1.86 | 0.255 | - 8.35 | 1.14 | 64.1 |
| 2 | 39.7 | 0.399 | 0.831 | 0.121 | - 5.58 | 0.811 | 135. |
| 3 | 40.9 | 0.344 | 0.440 | 0.117 | - 4.68 | 1.25 | 139. |
| 4 | 39.2 | 0.360 | 0.539 | 0.122 | - 4.90 | 1.11 | 134. |
| 5 | 32.5 | 0.433 | 1.18 | 0.148 | - 6.46 | 0.806 | 111. |
| 6 | 26.3 | 0.448 | 1.39 | 0.183 | - 7.00 | 0.923 | 89.4 |
| 7 | 12.3 | 0.493 | 2.53 | 0.391 | -10.42 | 1.61 | 41.8 |
| 8 | 15.3 | 0.483 | 2.14 | 0.313 | - 9.19 | 1.34 | 52.2 |
| 9 | 35.3 | 0.419 | 1.02 | 0.136 | - 6.05 | 0.804 | 120. |
| 10 | 37.8 | 0.379 | 0.671 | 0.127 | - 5.20 | 0.985 | 129. |

*A catalyst bulk density 1.25 gm/cc was assumed

APPENDIX IV-A (cont.)

Series: G

Reactor o.d., in: 0.219

Reactor i.d., in: 0.188

Total weight of catalyst in reactor, gms: 1.50

| Run No. | Flow rate of gas through reactor at reaction conditions, cc/sec | Parahydrogen composition in exit gas stream, % | $\ln \frac{x_e - x_1}{x_e - x_2}$ | $\tau$, sec* | $\frac{\ln \frac{x_e - x_2}{x_e - x_1}}{x_2 - x_1}$ | $\frac{\tau}{x_2 - x_1}$, sec | $N_{Re}$ |
|---|---|---|---|---|---|---|---|
| 1 | 4.71 | 0.473 | 1.86 | 0.255 | - 8.35 | 1.14 | 16.0 |
| 2 | 11.2 | 0.399 | 0.831 | 0.107 | - 5.58 | 0.720 | 38.0 |
| 3 | 33.6 | 0.324 | 0.329 | 0.358 | - 4.44 | 0.483 | 114. |
| 4 | 19.1 | 0.360 | 0.539 | 0.0629 | - 4.90 | 0.572 | 64.9 |
| 5 | 7.69 | 0.433 | 1.18 | 0.156 | - 6.46 | 0.555 | 26.1 |
| 6 | 6.68 | 0.448 | 1.39 | 0.242 | - 7.00 | 0.908 | 22.7 |
| 7 | 3.42 | 0.493 | 2.53 | 0.351 | -10.42 | 1.44 | 11.6 |
| 8 | 4.11 | 0.483 | 2.14 | 0.292 | - 9.19 | 1.25 | 14.0 |
| 9 | 9.31 | 0.419 | 1.02 | 0.129 | - 6.05 | 0.763 | 31.7 |
| 10 | 4.95 | 0.379 | 0.67 | 0.0803 | - 5.20 | 0.622 | 50.9 |

*A catalyst bulk density of 1.25 gm/cc was assumed

## APPENDIX IV-A (cont.)

### Series: H

Reactor o.d., in: 0.188

Reactor i.d., in: 0.156

Total weight of catalyst in reactor, gms: 1.00

| Run No. | Flow rate of gas through reactor at reaction conditions, cc/sec | Parahydrogen composition in exit gas stream, % | $\ln \frac{x_e - x_1}{x_e - x_2}$ | $\tau$, sec* | $\ln \frac{\frac{x_e - x_2}{x_e - x_1}}{x_2 - x_1}$ | $\frac{\tau}{x_2 - x_1}$, sec | $N_{Re}$ |
|---|---|---|---|---|---|---|---|
| 1 | 2.86 | 0.473 | 1.86 | 0.279 | - 8.35 | 1.25 | 14.0 |
| 2 | 7.05 | 0.399 | 0.831 | 0.114 | - 5.58 | 0.762 | 34.5 |
| 3 | 17.9 | 0.324 | 0.329 | 0.0446 | - 4.44 | 0.603 | 87.8 |
| 4 | 10.9 | 0.360 | 0.539 | 0.0737 | - 4.90 | 0.670 | 53.2 |
| 5 | 4.76 | 0.433 | 1.18 | 0.168 | - 6.46 | 0.919 | 23.3 |
| 6 | 4.00 | 0.448 | 1.39 | 0.200 | - 7.00 | 1.01 | 19.6 |
| 7 | 2.06 | 0.493 | 2.53 | 0.389 | -10.42 | 1.60 | 10.1 |
| 8 | 2.47 | 0.483 | 2.14 | 0.323 | - 9.19 | 1.39 | 12.1 |
| 9 | 5.43 | 0.419 | 1.02 | 0.147 | - 6.05 | 0.872 | 26.6 |
| 10 | 8.41 | 0.379 | 0.671 | 0.0951 | - 5.20 | 0.738 | 41.2 |

*A catalyst bulk density of 1.25 gm/cc was assumed

APPENDIX IV-A (cont.)

Series: J

Reactor o.d., in: 0.188

Reactor i.d., in: 0.156

Total weight of catalyst in reactor, gms: 4.00

| Run No. | Flow rate of gas through reactor at reaction conditions, cc/sec | Parahydrogen composition in exit gas stream, % | $\ln \frac{x_e - x_1}{x_e - x_2}$ | $\tau$, sec* | $\frac{\ln \frac{x_e - x_2}{x_e - x_1}}{x_2 - x_1}$ | $\frac{\tau}{x_2 - x_1}$, sec | $N_{Re}$ |
|---|---|---|---|---|---|---|---|
| 1 | 16.1 | 0.473 | 1.86 | 0.198 | - 8.35 | 0.890 | 79.0 |
| 2 | 38.3 | 0.399 | 0.831 | 0.0837 | - 5.58 | 0.561 | 187. |
| 3 | 52.9 | 0.364 | 0.565 | 0.0605 | - 4.96 | 0.531 | 259. |
| 4 | 19.6 | 0.360 | 0.539 | 0.163 | - 4.90 | 1.48 | 96.2 |
| 5 | 23.2 | 0.433 | 1.18 | 0.138 | - 6.46 | 0.753 | 114. |
| 6 | 12.4 | 0.448 | 1.39 | 0.258 | - 7.00 | 1.30 | 60.8 |
| 7 | 14.9 | 0.493 | 2.53 | 0.215 | -10.42 | 0.887 | 72.8 |
| 8 | 28.3 | 0.428 | 1.12 | 0.113 | - 6.30 | 0.635 | 139. |
| 9 | 16.8 | 0.473 | 1.86 | 0.191 | - 8.35 | 0.854 | 82.3 |

*A catalyst bulk density of 1.25 gm/cc was assumed

## APPENDIX IV-A (cont.)

### Series: K

Reactor o.d., in: 0.188

Reactor i.d., in: 0.156

Total weight of catalyst in reactor, gms: 4.00

| Run No. | Flow rate of gas through reactor at reaction conditions cc/sec | Parahydrogen composition in exit gas stream, % | $\ln \frac{x_e - x_1}{x_e - x_2}$ | $\tau$, sec* | $\frac{\ln \frac{x_e - x_2}{x_e - x_1}}{x_2 - x_1}$ | $\frac{\tau}{x_2 - x_1}$, sec | $N_{Re}$ |
|---|---|---|---|---|---|---|---|
| 1 | 16.3 | 0.473 | 1.86 | 0.196 | - 8.35 | 0.880 | 79.9 |
| 2 | 37.3 | 0.399 | 0.831 | 0.0857 | - 5.58 | 0.575 | 183. |
| 3 | 50.6 | 0.324 | 0.440 | 0.0632 | - 4.44 | 0.855 | 248. |
| 4 | 44.8 | 0.360 | 0.539 | 0.0714 | - 4.90 | 0.649 | 220. |
| 5 | 26.3 | 0.433 | 1.18 | 0.122 | - 6.46 | 0.666 | 129. |
| 6 | 14.8 | 0.448 | 1.39 | 0.216 | - 7.00 | 1.09 | 72.5 |
| 7 | 12.0 | 0.493 | 2.53 | 0.266 | -10.42 | 1.09 | 59.0 |
| 8 | 14.6 | 0.483 | 2.14 | 0.220 | - 9.19 | 0.944 | 71.3 |
| 9 | 30.2 | 0.419 | 1.02 | 0.106 | - 6.05 | 0.627 | 148. |
| 10 | 46.5 | 0.379 | 0.671 | 0.0687 | - 5.20 | 0.533 | 228. |

*A catalyst bulk density of 1.25 gm/cc was assumed

APPENDIX IV-A (cont.)

Series: L

Reactor o.d., in: 0.188

Reactor i.d., in: 0.156

Total weight of catalyst in reactor, gms: 2.00

| Run No. | Flow rate of gas through reactor at reaction conditions, cc/sec | Parahydrogen composition in exit gas stream, % | $\ln \frac{x_e - x_1}{x_e - x_2}$ | $\tau$, sec* | $\frac{\ln \frac{x_e - x_2}{x_e - x_1}}{x_2 - x_1}$ | $\frac{\tau}{x_2 - x_1}$, sec | $N_{Re}$ |
|---|---|---|---|---|---|---|---|
| 1 | 7.81 | 0.473 | 1.86 | 0.205 | - 8.35 | 0.919 | 38.3 |
| 2 | 16.3 | 0.399 | 0.831 | 0.0984 | - 5.58 | 0.660 | 79.7 |
| 3 | 36.5 | 0.324 | 0.329 | 0.0439 | - 4.44 | 0.593 | 179. |
| 4 | 23.9 | 0.360 | 0.539 | 0.0671 | - 4.90 | 0.610 | 117. |
| 5 | 11.7 | 0.433 | 1.18 | 0.137 | - 6.46 | 0.747 | 57.4 |
| 6 | 9.77 | 0.448 | 1.39 | 0.164 | - 7.00 | 0.827 | 47.9 |
| 7 | 5.34 | 0.493 | 2.53 | 0.300 | -10.42 | 1.23 | 26.1 |
| 8 | 6.05 | 0.483 | 2.14 | 0.264 | - 9.19 | 1.13 | 29.6 |
| 9 | 13.5 | 0.419 | 1.02 | 0.119 | - 6.05 | 0.702 | 66.1 |
| 10 | 19.0 | 0.379 | 0.671 | 0.0841 | - 5.20 | 0.652 | 93.2 |

*A catalyst bulk density of 1.25 gm/cc was assumed

## SECTION V

## THE ACTIVITY OF THE FERRIC OXIDE GEL CATALYST-- ITS DEPENDENCE ON PREPARATION, COMPOSITION, AND METHOD OF ACTIVATION

### V.1. Introduction

As part of the investigations into the the kinetics of the para-ortho hydrogen shift and the effects of the different types of diffusion on this reaction, many different batches of the ferric oxide gel catalyst were prepared. In these different batches, variations were made in method of preparation, composition and method of activation. This section reports the activities of these catalysts, and how these activities changed depending on differences in the preparation, composition, and activation.

A summary of what has been reported concerning the ferric oxide gel catalyst is first presented. Following this is a description of variations in method of preparation that were tried and their effect on catalyst activity. A short account is then given of some experiments for determining the effect of different additives in the ferric chloride solution, and of the effect of the purity of the ferric chloride solution. The last part of this section treats the effect of the method of activation on the catalyst activity. It is shown in this last section how the activity of the ferric oxide gel catalyst may be doubled over that previously reported by improvements in the method of activation.

### V.2. Experimental Apparatus

The experimental apparatus for measuring the activity of the catalyst was identical with that described in Section III of this report. For activating the catalyst at elevated temperatures, two different heaters were used. The first was an air heater, approximately three inches inside diameter and ten inches deep, wound with nichrome wire and insulated. Temperature was controlled manually, by adjusting a variac connected to the input to the heater. The temperature was read by a thermometer in the heater.

The second heater consisted of a constant temperature bath, approximately six inches inside diameter and nine inches deep, wound with nichrome wire and insulated. The bath liquid was Dow Corning #710 silicone fluid. Temperature was controlled by a Fenwall sealed thermoswitch, connected through a solenoid switch

and variac to the bath heater. Temperature control appeared to be accurate to plus or minus two degrees centigrade, and temperatures of 300°C were obtainable for brief periods of time without excessive fuming of the bath fluid. The bath was stirred by an agitator powered by a small explosion proof motor.

## V.3. Early Preparation and Activation

In 1956, Weitzel and Park (9) described the preparation and activation of the ferric oxide gel catalyst in these words: "Preparation of the iron hydroxide gel consists simply of adding a hydroxide to a solution of ferric salt. We add sodium hydroxide to ferric chloride (both in water solution), then wash the gelatinous brown precipitate with distilled water by decantation until practically all of the chloride ion has been removed. The material is then filtered and, after drying at room temperature, the filter cake is activated in air at 140°C. for 24 hours. Finally the material is broken up, run through a grinder, and graded through a set of sieves. Final activation in the test chamber consists of maintaining a pressure of one mm. Hg and a temperature of about 110°C. for 16-20 hours. The vacuum is broken with hydrogen while the catalyst is still hot."

In 1960, Eriksson (2), following the procedure then in use at the National Bureau of Standards, gave some further detail in the recipe for manufacturing the catalyst: "A 2.50 normal solution of sodium hydroxide (10 percent in excess by weight of the theoretical required) was added slowly, with mixing, to a 1.86 molal solution of ferric chloride (as hexahydrate equivalent). The temperature of the exothermic reaction was kept below 30°C. by means of a water bath. A reddish brown precipitate of ferric hydroxide was formed.

"Over a period of three days, the precipitate was washed thoroughly with cool distilled water, allowed to settle and then decanted. This washing technique was performed in a two liter beaker with one liter of distilled water added in batch fasion and initially stirred well. This technique was repeated twice within the three day period. After the final decantation, the wet cake was filtered through a No. 41 Whatman filter paper and allowed to dry overnight at 25°C.

"The filter cake was then oven dried at 120°C. overnight and the hard cake crushed to 30-50 mesh."

The catalyst activity at this time varied significantly from batch to batch. At times the dried catalyst appeared either reddish brown or yellowish brown in color, and it was found that none of these catalysts possessed activity comparable

to catalysts which were dark brown or black in color; Eriksson (2) reported the activity of one of these yellowish-brown catalyst as 194 minutes$^{-1}$, as compared with activities in excess of 1000 minutes$^{-1}$ for catalysts which were considered satisfactory at that time. He ascribed the poor activity to the presence of 2.89 weight percent sodium hydroxide in the dried catalyst; in catalysts with a satisfactory activity the amount of sodium hydroxide in the dried catalyst ranged from nil to 0.9 weight percent. He concluded that "the precipitating step should be carried out slowly with good mixing . . . and that the washing step should be thorough."

## V.4 Experiments in Method of Preparation

Several variations were tried on the method given by Eriksson and summarized above. A short series of experiments was carried out to determine the optimum amount of sodium hydroxide that should be added in the preparation of the catalyst. Some experiments were tried in order to find the optimum solution temperature for the precipitation of the catalyst. Finally, the catalyst was precipitated in a magnetic field, in order to find out if this had any effect on the catalyst activity.

### V.4.A The Addition of the Sodium Hydroxide Solution

Initally, it was attempted to duplicate the recipe given by Eriksson. Eight batches of catalyst were prepared, differing only in the details of the mixing of the solutions. All eight of these catalysts were either reddish-brown or yellowish-brown in color, with a fluffy texture. Because the experience reported by Eriksson had indicated that this was evidence of the presence of excess sodium hydroxide in the catalyst, resulting in extremely poor activity, these catalysts were not further tested.

In catalyst #9, the changes in the method of preparation involved both the strength of the sodium hydroxide solution and the amount added. Instead of a 2.50 molal sodium hydroxide solution as was used in the preparation of catalyst #1-8, a 2.06 molal solution was used in the preparation of catalyst #9. The strength of the ferric chloride solution was kept at 1.86 molal.

In the precipitation step, sodium hydroxide solution was added slowly to a beaker containing 31.5 ml of the ferric chloride solution. The temperature of the resulting mixture was kept below 30°C. Within the first ten minutes, 7 ml. of sodium hydroxide solution was added three times to the ferric chloride solution, for a total of 21 ml. of the sodium hydroxide solution added during the first ten minutes. Following each

addition of the 7 ml. of the sodium hydroxide solution, the mixture was stirred rapidly to break up the aggregates of ferric hydroxide which had formed. The mixture was then allowed to stand a few minutes before the addition of the next 7 ml. of sodium hydroxide solution. After 21 ml. of the sodium hydroxide solution was added in this manner, the remaining sodium hydroxide solution that was used was added continuously, through very slowly, from the burette. The mixture was stirred continuously. The addition of the remainder of the sodium hydroxide solution for a particular sample took approximately twenty minutes.

Differing amounts of sodium hydroxide solution were used in each of five samples of catalyst #9, in order to determine the effect of the amount of sodium hydroxide solution on the activity of the resulting catalyst. The amounts of sodium hydroxide solution used ranged from 70 ml. to 62 ml., with 2 ml. differences between the different samples.

The resulting precipitates were each washed five times with approximately 100 ml. of water each time. This took place over a period of two days. After the final washings, the ferric hydroxide gels were filtered and oven-dried over night at 120°C.

The results of this method of the addition of the sodium hydroxide solution, and of the effects of adding differing amounts of sodium hydroxide solution, are presented in Table V-I.

It may be seen from Table V-I that there is an optimum amount of sodium hydroxide that should be added in order to obtain a catalyst with the maximum activity. It may be noted that the pH of the liquid phase apparently may be used as an indicator of the amount of sodium hydroxide added. A catalyst precipitated from a mixture with a final pH of 4.9 gave the maximum activity.

V.4.B Neutralizing Excess Sodium Hydroxide with Hydrochloric Acid

The experiments reported in the preceding paragraphs indicated that the pH of the solution from which the catalyst was precipitated was critical. A brief series of experiments was carried out for the purpose of determing if reaching this pH after the catalyst had been precipitated could also be effective in producing an active catalyst. An excess of sodium hydroxide was added, and then, after the gel had precipitated, the excess sodium hydroxide was neutralized with hydrochloric acid. In one case it was neutralized with dilute hydrochloric acid; in the other case concentrated hydrochloric acid was added and the excess hydrochloric acid was back titrated with sodium hydroxide to a pH of 4.5.

TABLE V-I

EFFECT ON CATALYST ACTIVITY OF ADDITION OF DIFFERING AMOUNTS OF SODIUM HYDROXIDE SOLUTION

Catalyst #9

| Part | Volume $FeCl_3$ Solution,[1] ml. | Volume NaOH Solution,[2] ml. | NaOH in Excess of stoichiometric amount, % | Resulting pH of Mixture | Method of Activation | Activity of Resulting Catalyst,[3,4,5] $min^{-1}$ |
|---|---|---|---|---|---|---|
| A | 31.5 | 70 | 6.7 | 11.5 | 4 hrs. at 160°C under flowing $H_2$ | 362 |
| B | 31.5 | 68 | 3.7 | 9.5 | 16 hrs. at 160°C under flowing $H_2$ | 965 |
| C | 31.5 | 66 | 0.7 | 4.9 | 4 hrs. at 160°C under flowing $H_2$ | 1510 |
| D | 31.5 | 64 | -2.2 | 4.4 | 3 hrs. at 160°C under flowing $H_2$ | 1040 |
| E | 31.5 | 62 | -7.4 | | | |

Part E became a fine suspension after the fifth washing and could not be filtered.

Catalyst chamber used: 1/4 in. o.d.

Heater: Air Heater

Notes:

1. The $FeCl_3$ solution was prepared by dissolving 60.8 grams of ferric chloride hexahydrate ($FeCl_3.6H_2O$--MW: 270.2) in 121.6 ml. of distilled water.

TABLE V-I (cont.)

Notes:

2. The NaOH (MW-40.0) solution was prepared by dissolving 28.8 grams of NaOH in 350 ml. of distilled water.

3. The activity of the catalyst is the volume of hydrogen (measured at standard temperature and pressure) per minute per unit volume of catalyst required at 76°K to convert a mixture containing 75% orthohydrogen and 25% parahydrogen to a mixture containing 48% parahydrogen.

4. This activity assumes a bulk density of the catalyst of 1.25 gm/cc. In packing small quantities of catalyst into a small reactor, it has been found that the bulk density varies over a wide range, and is not reproducible for any given catalyst. The activities are threrfore evaluated on a weight basis, and the value of 1.25 gm/cc, which is the average which has been found over many measurements, is used. The activities are reported on a volume basis because this is the basis of most interest to designers.

5. The samples reported in this table were not classified as to particle size. They were finer than the 30-50 mesh normally used in these studies, and as a result the activities should not be compared directly with other activities.

In neither case, as is shown in Table V-II, did the resulting catalyst match the activity of approximately 1400 $min^{-1}$ which was being routinely obtained by the standard method of preparation used at that time. However, a comparison of Tables V-I and V-II shows that the activities of the catalysts reported in Table V-II are approximately what would be predicted from the final pH's of the solutions. It was concluded that back titration with HCl could be used to neutralize excess NaOH during the precipitation step.

V.4.C Agitation of the Solution

The mixing of the solution appeared to be an important factor in the preparation of the catalyst, good mixing apparently resulting in a more active catalyst. For this reason, some experiments were carried out with the solution agitated by nitrogen being bubbled through the solution. In Table V-III, it is seen that this apparently has no effect, either beneficial or otherwise, on the catalyst activity. One catalyst had an activity of 1210 $min^{-1}$, the other 1380 $min^{-1}$. These may be compared with the activity of 1400 $min^{-1}$ which was considered normal at that time.

V.4.D The Temperature of the Solution

In the manufacture of different catalysts, the practice had been to keep the temperature of the solution below 30°C., as specified by Eriksson. In order to verify the necessity or desirability of this temperature, several catalysts were made, keeping the solution temperature at different levels. The results of this investigation are reported in Table V-IV. At this time, the standard catalysts manufactured in the laboratory had an average activity of approximately 1400 $min^{-1}$. It can be seen from this table that the catalysts prepared at either a very low solution temperature or a very high solution temperature had an activity significantly lower. It was concluded that the temperature of 25-30°C. was probably very close to the optimum temperature for the precipitation of the catalyst.

V.4.E Precipitation of the Catalyst in a Magnetic Field

It was reported by Weitzel, Loebenstein, Draper, and Park (8) that some samples of hydrous ferric oxide exhibiting ferromagnetism were more active catalysts than those in which ferromagnetism was absent. It was reasoned that precipitation of the catalyst in the presence of a strong magnetic field might increase the ferromagnetism exhibited by the catalyst, and yield a more active catalyst.

TABLE V-II

EFFECT OF NEUTRALIZING EXCESS SODIUM HYDROXIDE WITH HYDROCHLORIC ACID

| Catalyst No. | NaOH in excess of stoichiometric amount, % | Method of Addition of HCl | Method of Activation | Catalyst Activity, * $min.^{-1}$ |
|---|---|---|---|---|
| 33 | 9.1 | Back titration of solution with dilute HCl to pH of 4.0 | 18 hrs. at 160°C under flowing $H_2$ | 512 |
| 24 | 12.5 | Addition of conc. HCl after washing step--neutralization with NaOH to pH of 4.5 | 4 hrs. at 160°C under flowing $H_2$ | 1020 |

Catalyst chamber used: 1/4 in. o.d.

Heater: Air Heater

*See notes (3) and (4) in Table V-I

TABLE V-III

EFFECT OF BUBBLING NITROGEN THROUGH THE SOLUTION

| Catalyst No. | Solution Temperature During Precipitation, °C | Method of Activation | Catalyst Activity, * $min.^{-1}$ |
|---|---|---|---|
| 28-A | 22 | 4 hrs. at 148°C under flowing $H_2$ | 1210 |
| 28-B | 22 | 6½ hrs. at 148°C under flowing $H_2$ | 1380 |

Catalyst chamber used: 1/4 in. o.d.

Heater: Air Heater

*See notes (3) and (4) in Table V-I

TABLE V-IV

EFFECT ON CATALYST ACTIVITY OF SOLUTION TEMPERATURE

| Catalyst No. | Temp. of Solution During Precipitation, °C | Method of Activation | Catalyst Activity, $min.^{-1}$ * |
|---|---|---|---|
| 29-A | 41 | | 1200 |
| 29-B | 50 | 4 hrs. at 160°C under $H_2$ | 1150 |
| 27-B | 53 | 4 hrs. at 145°C under $H_2$ | 784 |
| 27-A | 13 | 7 hrs. at 150°C under $H_2$ | 1265 |
| 30-B | 10 | 20 hrs. at 160°C under $H_2$ | 955 |
| 30-A | 8 | 4 hrs. at 160°C under $H_2$ | 705 |

Catalyst chamber used: 1/4 in. o.d.

Heater: Air Heater

*See notes (3) and (4) in Table V-I

In order to check this speculation, samples of the catalyst were precipitated in the field of a small permanent magnet of unknown field strength, and also in the field of an electromagnet under magnetic fields varying from 2000 gauss to 8000 gauss.

Table V-V shows the results of this study. When the catalyst was precipitated in the field of the permanent magnet, consistently good activities were obtained. When the catalyst was precipitated in the field of the electromagnet, activities were poor, with no relation to the field strength of the magnet. Unfortunately, a different apparatus was necessary when mixing the catalyst in the field of the electromagnet, and the mixing may not have been as thorough. In addition, only very small quantities could be prepared in the field of the permanent magnet, and so the mixing may have been usually good in this case. Thus, both the good and the poor results exhibited by these catalysts might be caused by the conditions under which precipitation took place. However, this is not certain, and since the catalysts precipitated in the field of the permanent magnet gave unusually good activities, further work in this direction may be rewarding.

## V.5 Effects of Differences in Solution Compositions

Several variations were made in the composition of the solutions from which the catalysts were prepared. Ferric nitrate was used instead of ferric chloride; the use of different bivalent ions in trace quantitites as promoters was attempted; a small quantity of hydrogen peroxide was added for the purpose of oxidizing any ferrous ion present; and reagent grade ferric chloride was used instead of the usual USP grade. The effects of each of these variations are treated in turn.

### V.5.A Use of Ferric Nitrate Solution

Ferric nitrate was used instead of ferric chloride in the manufacture of the catalyst. Otherwise the method of preparation was identical with that of Catalyst #9-C. The resulting catalyst (#26-B) after an activation of 16 hours at 158°C., had an activity of 571 $min^{-1}$. It was concluded that the use of ferric nitrate gave a catalyst inferior to that obtained when ferric chloride was used.

### V.5.B Use of Bivalent Ions as Promoters

The presence of impurities is known to increase the activity of many well known catalysts (3). Because the work of Weitzel, et. al., (8) reported that some samples

TABLE V-V

EFFECT OF THE PRECIPITATION OF THE CATALYST IN A MAGNETIC FIELD

| Catalyst No. | Magnet Used | Field Strength, Gauss | Method of Activation | Catalyst Activity, $min.^{-1}$ * |
|---|---|---|---|---|
| 12 | permanent | unknown | 5 hrs. at 160°C under flowing $H_2$ | 1650 |
| 13 | permanent | unknown | 3 hrs. at 160°C under flowing $H_2$ | 1400 |
| 14 | premanent | unknown | 4½ hrs. at 150°C under flowing $H_2$ | 1630 |
| 19-A | electromagnet | 8000 | 4 hrs. at 160°C under flowing $H_2$ | 770 |
| 19-B | electromagnet | 6000 | 4 hrs. at 160°C under flowing $H_2$ | 824 |
| 20-A | electromagnet | 4000 | 4 hrs. at 160°C under flowing $H_2$ | 765 |
| 20-B | electromagnet | 2000 | 4 hrs. at 160°C under flowing $H_2$ | 860 |

Catalyst chamber used: 1/4 in. o.d.

Heater: Air Heater

*See notes (3) and (4) in Table V-I

of hydrous ferric oxide exhibiting ferromagnetism were more active catalysts than those in which ferromagnetism was absent, substances were added to the ferric chloride solution that were believed most likely to promote the presence of ferromagnetism. It is known that ferromagnetism is promoted by the presence of double oxides composed of ferric oxide and the oxide of a bivalent element such as nickel, cobalt, iron, or copper (4).

The substances added to the ferric chloride solution were nickelous chloride, cobaltous chloride, ferrous chloride, and cupric chloride. These substances were added in different relative amounts, to determine the effect of the concentration of the bivalent ion on the activity of the resulting catalyst. All of the catalysts made with the presence of bivalent ions in the ferric chloride solution were prepared by the procedure used in the manufacture of Catalyst #9-C, with the exception of the addition of the solution containing the bivalent ion to the ferric chloride solution prior to the addition of the sodium hydroxide solution.

The results of this study are presented in Table V-VI. In no case did the addition of a bivalent ion increase the activity of the ferric oxide catalyst; the opposite effect was observed. In every case, the larger the amount of bivalent ion added, the poorer the activity of the resulting catalyst.

### V.5.C The Addition of Hydrogen Peroxide

Since the presence of bivalent ions in every case inhibited the activity of the ferric oxide gel catalyst, an attempt was made to remove the slightest trace of any bivalent ion present by oxidizing it to a higher valence state. Five drops of ten percent hydrogen peroxide solution were added to sixty milliliters of the 1.86 molal ferric chloride solution before the addition of the sodium hydroxide solution. With this exception, the preparation of the catalyst was identical with that of Catalyst #9-C. The catalyst obtained by this procedure (#22) had an activity of 814 $min^{-1}$, after activating it for four hours at 160°C under flowing hydrogen. It was concluded that the addition of hydrogen peroxide solution to the ferric chloride solution resulted in a catalyst with a poorer activity than that obtained without the addition of the oxidant.

### V.5.D Use of Reagent Grade Ferric Chloride

The presence of any impurity apparently had an inhibiting effect on the catalyst activity; therefore a catalyst was prepared using a purer grade of ferric chloride. Reagent grade ferric chloride was used in the manufacture of Catalyst #21-A instead

TABLE V-VI

EFFECT OF THE ADDITION OF BIVALENT IONS
TO THE FERRIC CHLORIDE SOLUTION

| Catalyst No. | Substance added to $FeCl_3$ Solution | Wt. % Added | Method of Activation | Catalyst Activity, $min.^{-1}$ * |
|---|---|---|---|---|
| 15-A | $NiCl_2$ | 0.005 | 4 hrs. at 150°C under flowing $H_2$ | 1080 |
| 15-B | | 0.05 | 3 hrs. at 150°C under flowing $H_2$ | 990 |
| 15-C | | 0.5 | 3 hrs. at 150°C under flowing $H_2$ | 950 |
| 16-A | $CoCl_2$ | 0.005 | 4½ hrs. at 150°C under flowing $H_2$ | 1010 |
| 16-B | | 0.05 | 48 hrs. at 160°C under flowing $H_2$ | 750 |
| 16-C | | 0.5 | 16 hrs. at 160°C under flowing $H_2$ | 643 |
| 17-B | $FeCl_2$ | 0.05 | 16 hrs. at 150°C under flowing $H_2$ | 856 |
| 18-B | $CuCl_2$ | 0.05 | 5 hrs. at 160°C under flowing $H_2$ | 855 |

Catalyst chamber used: 1/4 in. o.d.

Heater: Air Heater

*See notes (3) and (4) in Table V-I

of the USP grade of ferric chloride which was normally used. The activity of Catalyst #21-A, after activating it by heating it for 16 hours at 145°C under flowing hydrogen, was 1450 $min.^{-1}$. It was concluded that the use of reagent grade ferric chloride gave a very active catalyst but that the improvement over a catalyst prepared using the USP grade ferric chloride, if any, was slight.

## V.6 Method of Activation

The method of activation first recommended by Weitzel and Park (9) consisted of holding the catalyst at a pressure of one millimeter of mercury absolute and a temperature of 110°C for 16-20 hours. Subsequent to this, Keeler and Timmerhaus (5) stated that a temperature of 160°C would give a higher activity. Scott (7) showed that activation at a pressure of 50 microns of mercury absolute at a temperature of 120°C for eighteen hours and activation under flowing hydrogen at the same temperature for the same period of time gave essentially the same activity.

The method of activation was investigated in two stages; type of activation, and time and temperature of activation. Some effects of activation were measured, and some speculations are presented as to why one method of activation is superior to another.

The catalyst used in most of the activation studies was a standard commercial ferric oxide gel catalyst obtained from the Cryogenic Engineering Company, Denver, Colorado. It was from their batch 339-6, and is so designated in the catalyst numbers listed in the tables. The letters following are used to identify the different treatments given the catalyst in the laboratory at the University of Colorado. The other catalysts used in the activation study were prepared at the University.

### V.6.A Type of Activation

The experiments included many different conditions of activation; activation at varying pressures, activation using different gases and different gas flow rates, activation using different catalyst chambers, and activation using different heaters. Table V-VII compares the effects of the three different types of activation at 115-120°C for twelve hours. There is apparently no difference in the resulting activity of the catalyst when the activations are carried out under these conditions.

Tables V-VIII through V-XII show a significant set of phenomena connected with the catalyst activation. Table V-VIII indicates that at 250°C either nitrogen or hydrogen can be used for activation with apparently little resulting difference in catalyst activity. Table V-IX shows that activation under both vacuum and under hydrogen at 100 psig gave activities lower than that obtained from a catalyst activated under hydrogen at 10 psig. Table V-X shows that when a catalyst is activated in a reactor with a smaller diameter, it possesses a higher activity. Table V-XI shows that a catalyst activated in an oil bath has a higher activity than a catalyst activated in an air heater. Table V-XII shows that there is a optimum flow rate of hydrogen for producing a catalyst with the highest activity.

All of these results may be explained by one conclusion: the rate of temperature rise has a significant effect on catalyst activity. In all of the cases cited in the above tables, it is either certain or probable that the lower activity catalysts resulted from circumstances in which the rate of temperature rise was slower than the circumstances in which the higher activity catalysts were produced. When a certain temperature and duration at that temperature have been chosen as giving the highest activity obtainable, then it is important that this temperature be reached as rapidly as possible. Only when this is done will the maximum activity be produced.

V.6.B Temperature and Duration of Activation

In Table V-XIII are presented the maximum activities that have been obtained at different levels of temperature, together with the length of time spent at these temperatures. It is apparent from this table that, over the range of temperatures investigated, the higher the temperature of activation, the higher the possible activity obtained. It is also apparent that shorter times are required at the higher temperatures. Table V-XIV shows that catalyst deactivation has been noted when the catalyst has been held at high temperatures for extended periods of time. This table implies that as the temperature of activation goes up, the period of activation becomes more sensitive.

There were only two activations carried out at temperatures above 250°C. A five minute activation at 300°C for a period of five minutes resulted in a catalyst with an activity of only 1295 $min.^{-1}$. A two and a half minute activation at 275°C resulted in a catalyst with an activity of 2320 $min.^{-1}$. Further work is indicated in order to reach to optimum time and temperature of activation.

TABLE V-VII

EFFECT OF TYPE OF ACTIVATION AT 115-120°C

| Catalyst No. | Type of Activation | Catalyst Activity, Min.$^{-1}$ * |
|---|---|---|
| F-1 | none | 200 |
| F-1 | flowing $N_2$ | 1245 |
| F-1 | flowing $H_2$ | 1210 |
| F-1 | vacuum | 1205 |

Catalyst chamber used: 1/4 in. o.d.
Temperature of Activation: 115-120°C
Time of Activation: 12 hr.
Heater: Air Heater

TABLE V-VIII

EFFECT OF GAS USED FOR ACTIVATION AT 250°C

| Catalyst No. | Time of Activation, min. | Reactor Used | Temperature of Activation, °C. | Heater | Type of Activation | Catalyst Activity, min.$^{-1}$ * |
|---|---|---|---|---|---|---|
| 339-6E | 5 | 1/4"o.d. | 250 | Oil bath | flowing $H_2$ | 2250 |
| 339-6F | 5 | 1/4"o.d. | 250 | Oil bath | flowing $N_2$ | 2140 |

Catalyst chamber used: 1/4 in. o.d.
Temperature of activation: 250°C.
Time of activation: 5 min.
Heater: Oil Bath

*See notes (3) and (4) in Table V-I

TABLE V-IX

EFFECT OF ACTIVATION PRESSURE AT 250°C

| Catalyst No. | Type of Activation | Catalyst Activity, $min.^{-1}$ * |
|---|---|---|
| 339-6P | flowing $H_2$ at 100 psig | 2070 |
| 339-6S | flowing $H_2$ at 100 psig | 1935 |
| 339-6Q | vacuum | 1850 |
| 339-6R | vacuum | 1590 |
| 339-6T | flowing $H_2$ at 10 psig | 2580 |

| | |
|---|---|
| Catalyst chamber used: | 1/8 in. o.d. |
| Temperature of activation: | 250°C. |
| Time of activation: | 5 min. |
| Heater: | Oil bath |

*See notes (3) and (4) in Table V-I

TABLE V-X

EFFECT OF REACTOR SIZE ON CATALYST ACTIVITY

| Catalyst No. | Catalyst Chamber Used | Catalyst Activity,* $min.^{-1}$ |
|---|---|---|
| 339-6E | 1/4 in. | 2260 |
| 339-6L | 1/8 in. | 2790 |

| | |
|---|---|
| Temperature of activation: | 250°C |
| Time of activation: | 5 min. |
| Heater: | Oil bath |
| Type of activation: | Flowing $H_2$ at 10 psig |

*See notes (3) and (4) in Table V-I

TABLE V-XI

EFFECT OF TYPE OF HEATER ON CATALYST ACTIVITY

| Catalyst No. | Heater | Catalyst Activity,* $min.^{-1}$ |
|---|---|---|
| 339-6 | Air heater | 1510 |
| 339-6AN | Oil bath | 1825 |

| | |
|---|---|
| Catalyst chamber used: | 1/4 in. o.d. |
| Temperature of activation: | 150°C |
| Time of activation: | 4 hrs. |
| Type of activation: | Flowing $H_2$ at 10 psig |

*See notes (3) and (4) in Table V-I

TABLE V-XII

EFFECT OF HYDROGEN FLOW RATE DURING ACTIVATION ON CATALYST ACTIVITY

| Catalyst No. | Hydrogen Flow Rate,* $min.^{-1}$ | Catalyst Activity,** $min.^{-1}$ |
|---|---|---|
| 339-6-2A | 141 | 1720 |
| 339-6-2B | 450 | 2040 |
| 339-6-2C | 778 | 2010 |
| 339-6-2D | 1140 | 1820 |
| 339-6-2E | 2100 | 1710 |

| | |
|---|---|
| Catalyst chamber used: | 1/4 in. o.d. |
| Temperature of activation: | 250°C |
| Time of activation: | 8 min. |
| Heater: | Oil bath |
| Type of activation: | Flowing $H_2$ at 10 psig |

*Reported as the volume of hydrogen (measured at standard temperature and pressure) per unit volume of catalyst per minute. Also see note (3), Table V-I

**See notes (3) and (4), Table V-I

TABLE V-XIII

MAXIMUM CATALYST ACTIVITIES OBTAINED AT DIFFERENT TEMPERATURES

| Temperature of Activation, °C. | Time of Activation, min. | Catalyst No. | Heater | Type of Activation | Catalyst Activity,* $min.^{-1}$ |
|---|---|---|---|---|---|
| 21 | $10^4$ | F-3 | Air heater | vacuum | 943 |
| 100 | 180 | F-21 | Air heater | flowing $H_2$ | 1230 |
| 150 | 240 | 339-6AL | Oil bath | flowing $H_2$ | 2580 |
| 250 | 5 | 339-6L | Oil bath | flowing $H_2$ | 2850 |

*See notes (3) and (4) in Table V-I

TABLE V-XIV

LENGTH OF TIME REQUIRED BEFORE DETECTABLE DEACTIVATION IS NOTED

| Temperature, °C | Length of time at which detectable deactivation is noted. |
|---|---|
| 150 | 20 hrs. |
| 200 | 1 hr. |
| 250 | 15 min. |

The temperatures reported throughout this study of methods of activation are the temperatures of the air heater or constant temperature bath. It should be emphasized that these are not the temperatures of the catalyst pellets or any average temperature of the catalyst bed. Since it is apparent that both the rate of temperature rise and the temperature of the catalyst during activation are critical factors in producing a catalyst with the maximum activity, a thorough investigation of the temperatures in the catalyst bed during activation seems to be necessary if a higher activity catalyst is desired.

V.6.C Effects of Activation

There is a loss in weight in the catalyst during activation. There is considerable scatter in the data, but the average weight loss appears to approximate thirteen percent of the original weight of the catalyst. There is no apparent correlation between weight loss during activation and the activity of the resulting catalyst. The loss in weight is probably loss in moisture, since the catalyst is composed only of ferric oxide and water.

The effect of varying the rate of temperature rise has not been determined. It can only be speculated that this must have some effect on the structure of the catalyst, since the loss in moisture content of a catalyst with an activity of 1400 $min.^{-1}$ is approximately the same as the loss in a catalyst with an activity of 2800 $min.^{-1}$.

V.6.D Reproducibility of Catalyst Activity

The analytical method for determining the catalyst activity was very accurate. Three different checks of the same catalyst over the course of a day, with the analyst unaware that the activities were supposed to be the same, resulted in catalyst activities of 1990, 1970, and 1940 $min.^{-1}$, for a reproducibility within 3%.

It was frequently found, however, that it was impossible to produce a high activity catalyst every time. Using the 1/8 in. o.d. reactor, and activating the catalyst at 250°C. for five minutes in the oil bath, the highest activity obtained in this study was 2850 $min.^{-1}$. Activities of over 2700 $min.^{-1}$ were routine. At various times, however, the activities obtained from the same batch of catalyst, using the identical method of activation, were in the range of only 2100 $min.^{-1}$. It is suspected that the difficulty lay in the purity of the hydrogen that was being used.

Even though steps were taken to purify the hydrogen by passing it through a bed of silica gel held at liquid nitrogen temperatures, it is felt that more rigorous steps should be taken. This view results from the work of Chapin, Park, and Corrin (1), and that of McKinley and Schmauch (6), who show the extreme effects of trace contaminants on catalyst activity in this reaction.

## V.7 Conclusions

1. The method of preparation of the ferric oxide gel catalyst discovered by Weitzel and Loebenstein has been investigated, and it is found that the amount of sodium hydroxide added is a critical factor in producing an active catalyst. The stoichiometric amount is apparently the correct amount to add in the manufacture of the catalyst.

2. Back titration with HCl may be used to neutralize excess sodium hydroxide when precipitating the catalyst.

3. Bubbling nitrogen through the solution during preparation has no effect on the activity of the resulting catalyst.

4. Solution temperatures in excess of 40°C or less than 15°C result in a lower activity catalyst than when the solution temperature is kept within the 25-30°C range.

5. Precipitating the catalyst in a magnetic field resulted in a higher activity catalyst.

6. The addition of bivalent ions to the ferric chloride solution results in a decrease in the activity of the resulting catalyst. Apparently the ferric chloride solution must be as pure as possible.

7. Precipitating the catalyst from a ferric nitrate solution resulted in a low activity catalyst.

8. When activating the catalyst, it is important that the catalyst be brought to the temperature of activation as rapidly as possible. The faster the temperature rise within the catalyst bed, the higher is the activity of the resulting catalyst.

9. Within the range of temperatures that were investigated thoroughly, the higher the temperature of activation, the higher the activity of the resulting catalyst.

10. The higher the temperature of activation, the shorter the time required to produce a catalyst of the highest activity.

11. It is possible to produce in the laboratory repeatedly catalysts with activities in excess of 2700 $min.^{-1}$. The highest activity obtained thus far is a catalyst with an activity of 2850 $min.^{-1}$.

12. It has not been possible to produce high activity catalysts every time in the laboratory, in spite of identical activation conditions. It is suspected that more rigorous steps to purify the hydrogen are necessary to correct this.

## V.8 Recommendations

1. It is recommended that a comprehensive investigation be undertaken to ascertain the mechanism of the catalyst activation, in order that a catalyst with the maximum activity can be produced.

2. It is recommended that the variables in the preparation of the catalyst be further investigated, in particular the precipitation in a magnetic field, in order that a catalyst with the maximum possible activity can be produced.

## REFERENCES


1. Chapin, D. S., C. D. Park and M. L. Corrin, J. Phys. Chem. 64, 1073 (1960).
2. Eriksson, M. R., M. S. Thesis, University of Colorado, Boulder, Colorado, 1960.
3. Innes, W. B., in "Catalysis," Vol. 1, P. H. Emmett, ed., Reinhold, 1954, pp. 272-281.
4. Jastrzebski, Z. D., "Engineering Materials," Wiley, 1959, p. 351.
5. Keeler, R. N., and K. D. Timmerhaus, in "Advances in Cryogenic Engineering," Vol. 4, Plenum Press, 1960, pp. 302 and 304.
6. McKinley, C., and G. E. Schmauch, "Effect of Adsorbed Nitrogen on Catalytic Activity of Ortho-Parahydrogen Conversion Catalysts," paper presented at 1963 Cryogenic Engineering Conference, Boulder, Colorado, August 19-21, 1963.
7. Scott, L. E., M. S. Thesis, University of Colorado, Boulder, Colorado,1960.
8. Weitzel, D. H., W. V. Loebenstein, J. W. Draper, and O. E. Park, J. Research Natl. Bur. Standards 60, 221 (1958).
9. Weitzel, D. H., and O. E. Park, Rev. Sci. Instr. 27, 57 (1956).

BLANK PAGE